

Durham E-Theses

The influence of fluorine substitution on some enzyme mediated reactions

Bridge, Colin Francis

How to cite:

Bridge, Colin Francis (1997) *The influence of fluorine substitution on some enzyme mediated reactions*, Durham theses, Durham University. Available at Durham E-Theses Online:
<http://etheses.dur.ac.uk/4715/>

Use policy

The full-text may be used and/or reproduced, and given to third parties in any format or medium, without prior permission or charge, for personal research or study, educational, or not-for-profit purposes provided that:

- a full bibliographic reference is made to the original source
- a [link](#) is made to the metadata record in Durham E-Theses
- the full-text is not changed in any way

The full-text must not be sold in any format or medium without the formal permission of the copyright holders.

Please consult the [full Durham E-Theses policy](#) for further details.

The Influence of Fluorine Substitution on some Enzyme Mediated Reactions

Colin Francis Bridge, B.Sc. (Hons)
Van Mildert College

Ph.D. Thesis
University of Durham

The copyright of this thesis rests
with the author. No quotation
from it should be published
without the written consent of the
author and information derived
from it should be acknowledged.

July 1997



23 JAN 1998

Copyright

The copyright of this work rests with the author. No quotation from it should be published without prior consent. Information derived from this thesis should be acknowledged.

Declaration

The work contained in this thesis was carried out in the Department of Chemistry at the University of Durham between October 1993 and September 1996. All the work is my own, unless otherwise indicated. It has not previously been submitted for a degree at this or any other university.

**This thesis is dedicated to the memory of
my friend and colleague Andrew Ridge
who died on the 18th October 1995.**

... Donkey!!!!

**Was many years ago when I left home and came this way
I was a young man full of hopes and dreams
But now it seems to me that all is lost and nothing gained
Sometimes things aren't what they seem.**

A. Smith

Stranger in a Strange Land

Acknowledgments

First and foremost many thanks go to my supervisor, Dr. David O'Hagan. Without his ideas, help, advice and encouragement, this work would not have been possible.

Special thanks to Jeff for proof reading and editing this thesis.

Thanks also go to the other members of the O'Hagan group past and present: Dave B, Sarah, Nikki, Naveed, Ruhul, Adam, Mustafa, Jens, Caragh, Chi, Ninja, Manju and my project student Ed for his help with the transketolase.

The other workers in CGI also deserve a mention for creating such an enjoyable atmosphere to work in: Jenny, Alison, Craig, Lee, Phil. Special thanks go to Dr. Patrick Steel for those weekend rounds of golf and Andy Byerley; cheers, mate.

Thanks also to Steve, Chez, Andy 'the boy lard' Green, all the Drobbers and Grad-Soc. football team for making the last three years so enjoyable.

Dr. Kevin Reynolds and Kimberlee Wallace are thanked for providing samples of the reductase enzyme and analysis of the kinetic results.

Dr. Mike Crampton and Ian Robotham are thanked for their assistance with the kinetic analysis of the fluoropenicillanates.

Dr. N. Turner and A. Humphrey are thanked for providing samples of transketolase.

Special thanks go to: Alan Kenwright, Ian McKeag, Julia and Barry Say and Ray Matthews for their help with NMR experiments; Jean, Hazel, Maureen and Brenda for keeping the lab tidy and making those all important cups of tea. Jimmy and Joe for help in the stores; Tom for his help; George for his cheerful conversation on a bleak winters morn; Ray and Gordon, the glass-blowers, for their essential help not only in repairing the glassware but for whiling away many an hour reminiscing about when Sunderland were good; Lenny Lauchlan for help with HPLC and GC experiments, for running a fantastic five-a-side league and always being prepared to talk footy; Mike Jones and Lara Turner for mass spec; the EPSRC high-res mass facility in Swansea and all the other members of staff who have given invaluable advice.

Funding from the EPSRC is gratefully acknowledged.

A special mention goes to my friends from Mildert.

Finally, many, many thanks go to my Dad, Mum, Pauline and Sarah, who despite the problems of recent years have always been there to support me throughout my six years in Durham.

Abbreviations

AIBN	: azaisobutyronitrile
6-APA	: 6-aminopenicillanic acid
Bn	: benzyl
bp	: boiling point
6-BPA	: 6 β -bromopenicillanic acid
Bu	: butyl
CCDB	: Cambridge Crystallographic Database
CCHR	: Cyclohexylcarbonyl-CoA reductase
CI	: Chemical Ionization
d	: doublet
DAST	: diethylaminosulfur trifluoride
ee	: enantiomeric excess
EI	: electron impact
Et	: ethyl
G-3-P	: glycerol-3-phosphate
GC	: gas chromatography
GC-MS	: gas chromatography-mass spectrometry
HLADH	: horse liver alcohol dehydrogenase
HOMO	: highest occupied molecular orbital
HPLC	: high performance liquid chromatography
IR	: infra red
K_m	: Michaelis constant
LAPS	: lipase from <i>Pseudomonas cepacia</i>
LDH	: lactate dehydrogenase
LUMO	: lowest unoccupied molecular orbital
m	: multiplet
Me	: methyl
mp	: melting point
MS	: mass spectrometry
NADPH	: nicotinamide-adenine dinucleotide
NBS	: <i>N</i> -bromosuccinimide
NMR	: nuclear magnetic resonance

PBP	: penicillin binding protein
Ph	: phenyl
ppm	: parts per million
q	: quartet
s	: singlet
t	: triplet
TBAF	: tetrabutylammonium fluoride
TBABF	: tetrabutylammonium bifluoride
THF	: tetrahydrofuran
TK	: transketolase
TLC	: thin layer chromatography
TPP	: thiamine pyrophosphate
UV	: ultraviolet

Abstract

The Influence of Fluorine Substitution on some Enzyme Mediated Reactions

Colin Francis Bridge

Ph.D. 1997

The replacement of a hydrogen or hydroxy group with a fluorine atom is a popular strategy to alter the activity of biologically important molecules, as their similar sizes mean that such a replacement has little steric impact. The effect of fluorine substitution in a number of enzyme mediated processes has been investigated.

3-Fluorocyclohex-1-enylcarbonyl-CoA has been synthesised and the reaction with cyclohexenylcarbonyl-CoA reductase investigated. The fluorinated substrate has a comparable K_m value to that of the natural substrate but a V_{max} that is five times greater. A change in the rate-determining step of the reduction was also observed upon fluorine incorporation. The enzyme showed a small but significant stereochemical preference for the production of the axial isomer, consistent with an Anh-Eisenstein model for the transformation.

The 6 α and 6 β isomers of benzyl fluoropenicillanate were synthesised and their methoxide-mediated hydrolyses were investigated. Competitive hydrolysis, using ^{19}F NMR spectroscopy, demonstrated that the β isomer was hydrolysed preferentially. A full kinetic analysis was undertaken, which furnished the rate and equilibrium constants.

Monofluorinated enamines were treated *in situ* with a range of Michael acceptors to afford a variety of novel substituted α -fluoro ketones.

2-Fluorohexanal was synthesised from methyl hexanoate and was demonstrated to be a substrate for the enzyme transketolase with hydroxypyruvate. The enzyme reaction was monitored by ^{19}F NMR spectroscopy. The enzyme showed a diastereoselectivity of 9:1 in the condensation of the aldehyde and hydroxypyruvate, and a self-condensation product was also produced.

The enzymatic oxidation of the mono- and di-fluoromethylenephosphonate analogues of glycerol-3-phosphate was investigated at neutral pH using a co-factor recycling protocol. The reactions allowed for the first time the identification of the products of oxidation and demonstrated the lability of fluoride *via* non-enzymatic elimination and stoichiometric defluorination.

Contents

Page

Chapter One

An Introduction to the Effects of Fluorine Substitution in Bio-organic Chemistry

1.1	Introduction	2
1.2	Historical perspective	4
1.3	Fluorine in biological chemistry	6
1.4	Fluorinated substrate analogues	9
1.4.1	β -Fluorinated α -amino acids	9
1.4.2	Fluoroacetate	10
1.4.3	Aromatic amines	11
1.5	Fluorine as a hydrogen bond acceptor	12
1.6	Stereoelectronic effects	14
1.6.1	The <i>gauche</i> and <i>cis</i> effects	14
1.6.2	The <i>cis</i> effect in enzyme chemistry; citrate synthase	15
1.6.3	The fluorine anomeric effect	17
1.6.4	The Anh–Eisenstein effect	18
1.6.5	The Anh–Eisenstein effect in enzyme reactions	21
1.7	^{19}F NMR Spectroscopy	25
1.8	Aims and objectives	26
1.9	Fluorinating reagents	27
1.9.1	Sulfur tetrafluoride (SF_4)	27
1.9.2	Diethylaminosulfur trifluoride (DAST)	28
1.9.3	Hydrogen fluoride	30
1.9.4	Metal fluorides	30
1.9.5	Tetraalkylammonium fluorides	31

Chapter Two

An Investigation into the Anh–Eisenstein Effect In an Enzymatic Transformation

2.1	Introduction	33
2.1.1	NAD(P)H-dependent alcohol dehydrogenases	35
2.1.2	Enoyl reductases	38
2.2	Cyclohex-1-enylcarbonyl-CoA reductase (CHCR)	40
2.3	Exploring Anh–Eisenstein stabilisation	43
2.3.1	3-Fluorocyclohex-1-enylcarbonyl-CoA 41	44
2.3.2	6-Fluorocyclohex-1-enylcarbonyl-CoA	45
2.3.3	¹⁹ F NMR spectroscopy of fluorocyclohexanes	46
2.4	Target compounds	49
2.5	Synthesis of fluorocyclohexenes	50
2.5.1	Synthesis of 3-fluorocyclohex-1-enecarboxylic acid 39	51
2.5.2	Synthesis of 6-fluorocyclohex-1-enecarboxylic acid 40	53
2.5.3	Synthesis of thio and CoA esters	55
2.6	Kinetic studies with fluorinated substrate	57
2.6.1	Determination of K_m and V_{max}	58
2.6.2	Kinetic analysis: results and discussion	59
2.7	¹⁹ F NMR study of the reduction catalysed by CHCR	62
2.8	Conclusions	65

Chapter Three

The Synthesis and Hydrolysis of C-6 Fluorinated Penicillins

3.1	Introduction	67
3.2	Mode of action of β -lactam antibiotics	68
3.3	Inhibition of β -lactamases	71
3.3.1	Penicillanic acid sulfone 72	74
3.3.2	6 β -Bromopenicillanic acid 73	75
3.3.3	6 α -(Hydroxymethyl)penicillanic acid 77	76

3.4	Fluorinated penicillins and stereoelectronic effects	77
3.5	Biological activity of fluorinated penicillins	79
3.6	Synthesis of 6-fluoropenicillins	80
3.6.1	Synthesis of Pom 6 α -fluoropenicillanate	82
3.6.2	Synthesis of 6 α -fluoropenicillanic acid	84
3.6.3	Synthesis of benzyl 6 β -fluoropenicillanate	87
3.7	Enzymatic hydrolysis of 6 α -fluoropenicillanic acid	91
3.8	Sodium methoxide mediated hydrolysis of 6 α - and 6 β -fluoropenicillanates	93
3.8.1	¹⁹ F NMR spectroscopic study of hydrolysis	94
3.8.2	Competitive hydrolysis study	95
3.8.3	Kinetic analysis of hydrolysis	97
3.8.4	Kinetic results	99
3.8.5	Discussion of kinetic analysis	103
3.9	Conclusions	105

Chapter Four

The Synthesis of α -Fluoro Ketones by 1,4-Additions of Monofluorinated Enamines to Michael Acceptors

4.1	Introduction	108
4.2	Synthesis of fluorinated ketones	113
4.3	Stork enamine chemistry	116
4.4	Synthesis of α -fluoroacetophenones and enamines	118
4.5	Alkylation of fluoroenamines	121
4.6	Asymmetric induction <i>via</i> Stork enamine methodology	123
4.7	Potential uses of the methodology	125
4.7.1	Fluorinated lactones	125

Chapter Five

Preliminary Studies into the Effect of Fluorine with Transketolase and Glycerol-3-Phosphate Dehydrogenase

Part A. Preliminary Studies with Transketolase

A5.1 Introduction	127
A5.2 Reaction of an α -fluoro aldehyde with transketolase	129
A5.3 Aims of investigation	130
A5.4 Synthesis of 2-fluorohexanal	131
A5.5 Results and discussion	133
A5.5.1 Results from NMR data for enzyme and control reaction	133
A5.6 The chemistry of the enzyme reactions	136
A5.6.1 Formation of diastereoisomeric products	136
A5.6.2 Formation of the self-condensation product	137
A5.6.3 Elimination of fluoride	137
A5.7 Conclusions and future work	139

Part B. The enzymatic oxidation of mono- and di-fluoromethylenephosphonate analogues of glycerol-3-phosphate

B5.1 Introduction	140
B5.1.1 Coupled enzyme co-factor recycling	144
B5.2 Enzymatic oxidation of CF_2 -phosphonate 173	145
B5.3 Enzymatic oxidation of CHF-phosphonate	148
B5.4 Conclusions	149

Chapter Six

Experimental

6.1	General	152
6.2	Experimental to Chapter Two	153
6.3	Experimental to Chapter Three	162
6.4	Experimental to Chapter Four	173
6.5	Experimental to Chapter Five	183
6.6	General protocol for enzyme assays	186

Chapter Seven

Appendices

7.1	Appendix 1	189
7.1.1	Derivation of equation (3.1)	189
7.1.2	Stopped-flow spectrometry	190
7.2	Appendix 2	192
7.2.1	Requirements for the Board of Studies	192
7.2.2	Colloquia, lectures and seminars from invited speakers	192
7.2.3	First year induction courses	200
7.2.4	Research conferences attended	200
7.2.5	Seminars, colloquia and poster presentations	201
7.2.6	Papers published	201

References

References	203
------------	-----

Chapter One

An Introduction to the Effects of Fluorine Substitution in Bio-organic Chemistry

An Introduction to the Effects of Fluorine Substitution in Bio-organic Chemistry

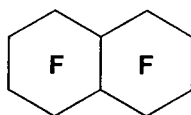
1.1 Introduction

As the thirteenth most abundant element in the Earth's crust,¹ surprisingly, natural products that contain fluorine are rare and in the cases where they are found very little is known about their origin or the enzymatic processes for generating the C–F bond. Only ten naturally occurring organofluorine metabolites have been identified,² five of which are homologous fatty acids from the bacterium *Dichapetalum toxicarium*. Potassium monofluoroacetate, the most common fluorinated natural product, is present in the South African plant *Dichapetalum cymosum* and in more than thirty other tropical plants in South America, Africa and Australia.³ Most organofluorine compounds are therefore 'unnatural' or anthropogenic in origin.

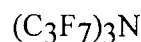
Fluorinated compounds can more generally be divided into two categories; firstly, perfluorinated or highly fluorinated derivatives, *i.e.* where all or most of the hydrogens are replaced by fluorine, and secondly, lightly fluorinated compounds which typically contain only one fluorine. The molecules within these two broad groups generally find quite different applications.

Perfluorocarbon (PFC) chemistry is a highly specialised area in industry with strong biomedical and technological connections. PFCs are characterised by exceptional chemical stability, high oxygen solubility and low surface tension, and are of medical interest because they are not metabolised in the human body. Perfluorooctane (C₈F₁₈), used in vitreo-retinal surgery, and perfluorodecalin (FDC), or notional derivatives thereof, *e.g.* perfluorotripropylamine (FTPA) and perfluoro-octyl bromide (PFOB), are examples of PFC compounds with important biomedical applications. Fluoropolymers, *e.g.* poly(tetrafluoroethylene) (PTFE) and poly(vinylidene fluoride) (PVDF), provide further examples of the increase in the use of PFCs in technology and medicinal applications.

(i) Blood substitutes



Perfluorodecalin



Perfluorotripropylamine

(ii) Oxygen transport/X-ray contrast agent



Perfluorooctyl bromide

(iii) Inhalation anaesthetics



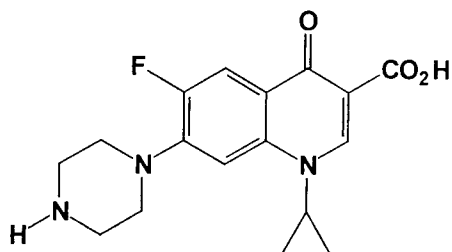
Isoflurane



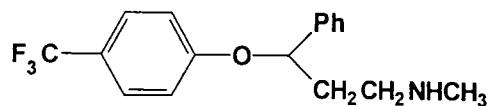
Halothane

Selective fluorination has become an extremely effective tool for modifying reactivity. It has been known for some time that the introduction of fluorine can alter the chemical and physical properties of organic compounds. Analogues of biologically important compounds, prepared by the replacement of a hydrogen or hydroxy group by a fluorine, can have useful modifications to their biological selectivity and activity.⁴ The importance of organofluorine-containing compounds is highlighted by the growing number of new drugs containing fluorine and the ever increasing number of publications. A number of useful reviews have been written on the subject of organofluorine compounds.⁵

Two of the current top twenty most successful drugs are fluoro-pharmaceuticals. One of these, the broad spectrum antibiotic ciprofloxacin **1** (Bayer's Cipro), with sales in the region of \$1 billion, is the leading member of a chemical class of antibiotics, the 6-fluoroquinolones. The second drug is the antidepressant fluoxetine **2** (Lilly's Prozac).



1 (Antibacterial)



2 (Antidepressant)

The range of other therapeutic classes where fluorinated compounds have found utility demonstrates the effectiveness that fluorine substitution can have.

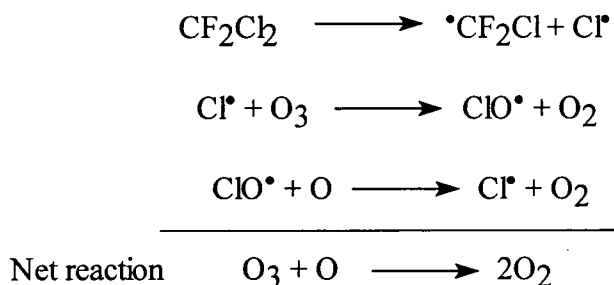
- anti-psychotics (*e.g.* butyrophenones and phenothiazines typified by haloperidol and trifluoroperazine).
- other CNS agents, including the sedatives flurazepam and flunitrazepam.
- anti-cancer agents (5-fluorouracil).
- corticosteroids (*e.g.* the recently introduced asthma inhaled steroid fluticasone).
- non-sedating antihistamines such as astemizole.

1.2 Historical perspective

Although hydrogen fluoride was discovered in 1771 by Scheele,⁶ molecular fluorine was not prepared until 1886 by Moissan.⁷ The work of the Belgian chemist Swarts⁸ in the early 1890s on the preparation of fluorinated materials by metal fluoride-promoted HF exchange heralded the beginning of modern organofluorine chemistry. Swarts subsequently prepared trifluoroacetic acid in 1922. During the 1930s Midgley and Henne prepared a range of fluorocarbons,⁹ and pioneered their use as thermally and chemically stable refrigerants and lubricants. Fluorinated chlorocarbons (CFCs) were developed in the 1930s by the General Motors Research Laboratories in a search for a non-toxic, non-flammable refrigerant to replace the then in use SO₂ and NH₃. The CFC CF₂Cl₂ is a typical example and is identified by the notation CFC-12.[†] In addition to their use as refrigerants their chemical inertness has made CFCs valuable as aerosol propellants, blowing agents for plastic foam production, and as solvents. The two most

[†] CFC is followed by a coded two or three digit number. The hundreds unit is the number of carbon atoms minus one, the tens is the number of hydrogen atoms plus one, the units is the number of fluorine atoms, and the residue is assumed to be chlorine. If the first digit is zero it is dropped. Thus CFC-11 is CFC₁Cl₃, CFC-12 is CF₂Cl₂ and CFC-115 is CF₃CF₂Cl.

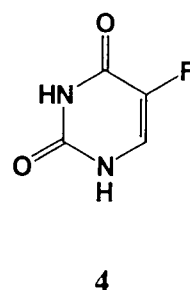
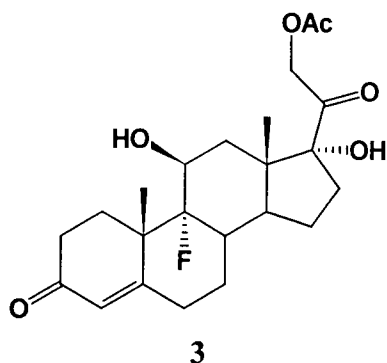
common CFCs are CFC-11 and CFC-12, with an estimated 3.1×10^8 and 4.5×10^8 kg respectively manufactured in 1981. These CFCs, notably the chlorofluoromethanes (CFMs) used as aerosol propellants, have been released into the atmosphere where, due to their high chemical stability, they accumulate in the stratosphere (CF_2Cl_2 atmospheric lifetime 107.8 years). Once there they dissociate under the influence of solar radiation to provide chlorine atoms which catalyse the destruction of ozone.



With the environmental implications of the destruction of the ozone layer, the production and use of CFCs have been reduced under the Montreal Protocol, to be replaced by HFCs which are 'ozone friendly'. A key replacement, H134a ($\text{CF}_3\text{CH}_2\text{F}$), manufactured by Dupont and ICI is however required by the Protocol to be phased out by *ca.* 2005.

The biological effects of introducing fluorine into organic molecules were first studied during World War II by Saunders at Cambridge and Schrader in Germany.¹⁰ The revelation by Marais in 1943¹¹ that the toxicity of the South African plant *Dichapetalum cymosum* was due to monofluoroacetate provided the impetus for studies on the toxicology and pharmacology of organofluorine compounds more generally. The first significant report of the use of selective fluorination to modify biological activity came from Fried in 1954, when 9 α -hydrocortisone acetate was monofluorinated to 9 α -fluorohydrocortisone acetate **3**.¹² The fluorine in this case is judged to increase the acidity of the geminal hydroxy group, strengthen hydrogen bonding and electronically retard *in vivo* oxidation, thus adding to the *in vivo* half-life of this corticosteroid.

In 1957 Heidelberger^{4e} described the results of initial clinical trials of 5-fluorouracil (5FU) **4** in patients with advanced cancer. This chemotherapeutic agent is a frequently cited example of a fluorinated antimetabolite, which is an effective cytotoxic agent that inhibits the enzyme thymidylate synthetase¹³ and is much used in cancer chemotherapy. Since the 1950s selective fluorination for the purpose of modifying biological activity has been carried out routinely by medicinal and bio-organic chemists.



1.3 Fluorine in biological chemistry

Hydrogen atom or hydroxy group substitution by fluorine in enzyme substrate analogues has been widely practised in various areas of medicinal and bio-organic chemistry. The attractiveness and utility of fluorine as a substituent in a biologically active molecule results from the profound electronic effects that may result on fluorination as well as the fact that fluorine is not a sterically demanding substituent. The van der Waals radius of fluorine (1.47 Å) lies between that of oxygen (1.57 Å) and hydrogen (1.20 Å).¹⁴ Fluorine therefore has a close isosteric relationship to oxygen and is significantly larger than hydrogen. This is not often appreciated as the old Pauling value of 1.35 Å is often cited as the accepted radius of fluorine.¹⁵ Comparison of the van der Waals volume of a methyl group (19.6 Å³), using a half sphere approximation, with a trifluoromethyl group (42.6 Å³) shows that the CF₃ group is sterically more akin to an isopropyl group.¹⁶

Table 1.1 summarises some of the physical properties of hydrogen, fluorine and oxygen.

Table 1.1 Comparison of size and electronegativity for hydrogen, fluorine and oxygen

Element	van der Waals radius/Å	C–X Bond length /Å	Electronegativity	Bond energy to carbon/kcal mol ⁻¹
H	1.20	1.09	2.1	100
F	1.47	1.39	4.0	107
O	1.57	1.43	3.5	66.5

Despite this increase in size, the steric impact of a *single* fluorine is never too great and the binding of monofluorinated analogues to target proteins is not normally

impaired. For example, the steric impact of fluorine substitution has been studied using aryl fluorines with lipases.¹⁷ A series of partially fluorinated benzhydrol acetates **5** were presented to the lipase from *C. cylindracea*. The reactions were terminated after 40% conversion and the %ee of the resultant alcohols determined (Table 1.2).

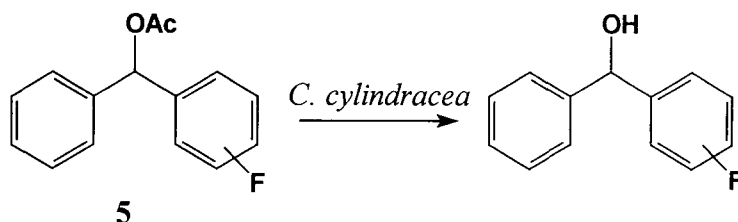


Table 1.2 Enantiomeric excess (% ee) of recovered alcohol

Fluorine substitution of benzhydrol acetate	Ee of alcohol at 40% conversion (%)
2-fluoro	10
4-fluoro	0
2,5-difluoro	57
2,6-difluoro	52
3,5-difluoro	24

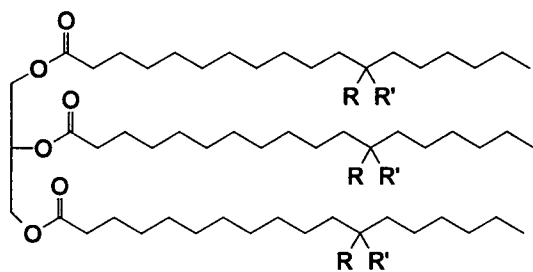
Mono-substitution at the *para* position (4-fluoro) resulted in a racemic alcohol, and clearly no distinction was made by the enzyme between the two aryl groups. Substitution, however, at the *ortho* position (2-fluoro), closest to the reaction centre, resulted in some resolution, although the effect was small. The enantioselectivity was however increased significantly by the introduction of a second fluorine atom. The experiments showed that certain enzyme–substrate combinations will distinguish between hydrogen and fluorine on steric grounds.

Table 1.1 also shows some other significant differences between a hydrogen and fluorine atom. The high electronegativity of fluorine compared to hydrogen (*c.f.* 4.0 to 2.1) can dramatically alter the electronic profile of a substrate. Fluorine also forms the strongest bond to carbon and thus it renders the substituent relatively resistant to metabolic transformations. The formation of a C–F bond may also increase the lipophilicity of the molecule, particularly as the CF₃ group is one of the most lipophilic groups known. CF₃ substitution renders organofluorine compounds more fat-soluble than their non-substituted counterparts, a feature that makes systematic fluorine substitution a useful tool in optimising the absorption properties of a drug. For

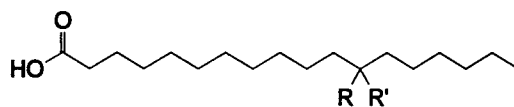
example, almost all of the clinically useful quinolone antibacterial agents (e.g. 1 ciprofloxacin) contain a fluorine at the C-6 position due in part to a 1–70-fold increase in cell penetration compared to derivatives with no substitution at the C-6 position.¹⁸ Finally, fluoride is a moderately good leaving group, and may be eliminated at or near to the enzyme active site leading to covalent attachment of the substrate to the enzyme.

If the substitution of a single hydrogen has little steric impact the replacement of a methylene for a difluoromethylene group (CH_2 for CF_2) can however induce much more dramatic steric and geometric effects. In a recent study, the physical properties of the tristearins **6** and **7**, containing one and two fluorine atoms at C-12, were examined.¹⁹

The substitution of one fluorine atom at C-12 was seen to have little effect on the observed melting point and other physical properties. The introduction, however, of a second fluorine lead to a significant lowering of the melting point (72 vs. 58 °C) and changes in the other observed physical properties. The stability of the Langmuir films of the corresponding fluorinated stearic acids **8–10** was also investigated. 12-Fluorostearic acid **9**, like stearic acid **8**, formed a stable monolayer on the surface of the aqueous subphase. 12,12-Difluorostearic acid **10**, however, formed a monolayer that was unstable and susceptible to collapse and reorganisation at comparable surface pressures. The observations were indicative of significant conformational disorder as a result of the difluoromethylene group.



$\text{R} = \text{R}' = \text{H}$ mp 72 °C
6 $\text{R} = \text{H}, \text{R}' = \text{F}$ mp 73 °C
7 $\text{R} = \text{R}' = \text{F}$ mp 58 °C

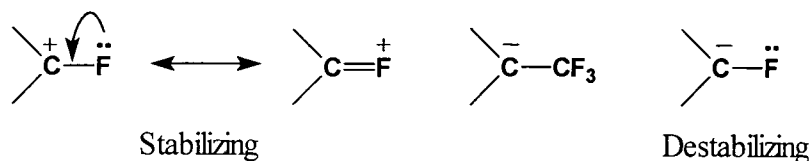


8 $\text{R} = \text{R}' = \text{H}$
9 $\text{R} = \text{H}, \text{R}' = \text{F}$
10 $\text{R} = \text{R}' = \text{F}$

A similar lowering in the melting point upon the introduction of a CF_2 group has been observed in diacylphosphatidylcholines²⁰ and the phenomenon, whereby a CF_2 group increases the conformational flexibility of a hydrocarbon chain, appears to be general.

Important differences in the chemical reactivity commonly arise on fluorine substitution due to the difference in electronegativity and the increased C–F bond

strength. The effects may be briefly summarised as follows.²¹ Fluorine stabilises α -cations by the interaction of the vacant p-orbital of the carbocation with the filled orbitals of the fluorine. Fluorine bonded directly to a carbanionic centre is generally destabilising, but when not bonded directly, as in trifluoromethyl-substituted carbanions, it can be stabilising.



1.4 Fluorinated substrate analogues

1.4.1 β -Fluorinated α -amino acids

The ability of fluorine to act as a leaving group in addition-elimination processes has been exploited in the development of ‘suicide’ substrates for enzymes. Selectively fluorinated β -fluorinated α -amino acids have been widely explored as mechanistic based inhibitors^{4d,15,22} for decarboxylases, racemases and transaminases. These enzymes are all pyridoxal phosphate (PLP) linked enzymes which generate an α -carbanion equivalent during catalysis. An example of such an application is the use of fluoroalanine²³ as an inhibitor of the enzyme alanine racemase. Fluoroalanine differs little sterically from alanine which enables the enzyme to accept the fluorinated analogue as a substrate.

The PLP binds to the enzyme through a lysine residue *via* an imine which then transaminates with the amino acid. The enzymatic inactivation is thought to be dependent upon loss of fluoride from the intermediate Schiff base **11** formed between pyridoxal phosphate and the fluoromethyl amino acid. Loss of fluoride generates a reactive Michael type acceptor **12** which can add an enzyme-bound nucleophilic functional group (*e.g.* $-\text{NH}_2$, $-\text{OH}$, $-\text{CO}_2^-$, $-\text{SH}$). The covalently bound enzyme is then no longer free to bind any additional substrate. (Fig 1.1).

The *E. coli* enzyme processes either enantiomer of β -fluoroalanine with a partition ratio of about 800 eliminative turnovers to pyruvate for every Michael attack and alkylative inactivation.²³ Other fluorinated amino acids have been assimilated

biochemically into proteins²⁴ and used to study structural changes that result from ligand binding or interaction with other macromolecules.

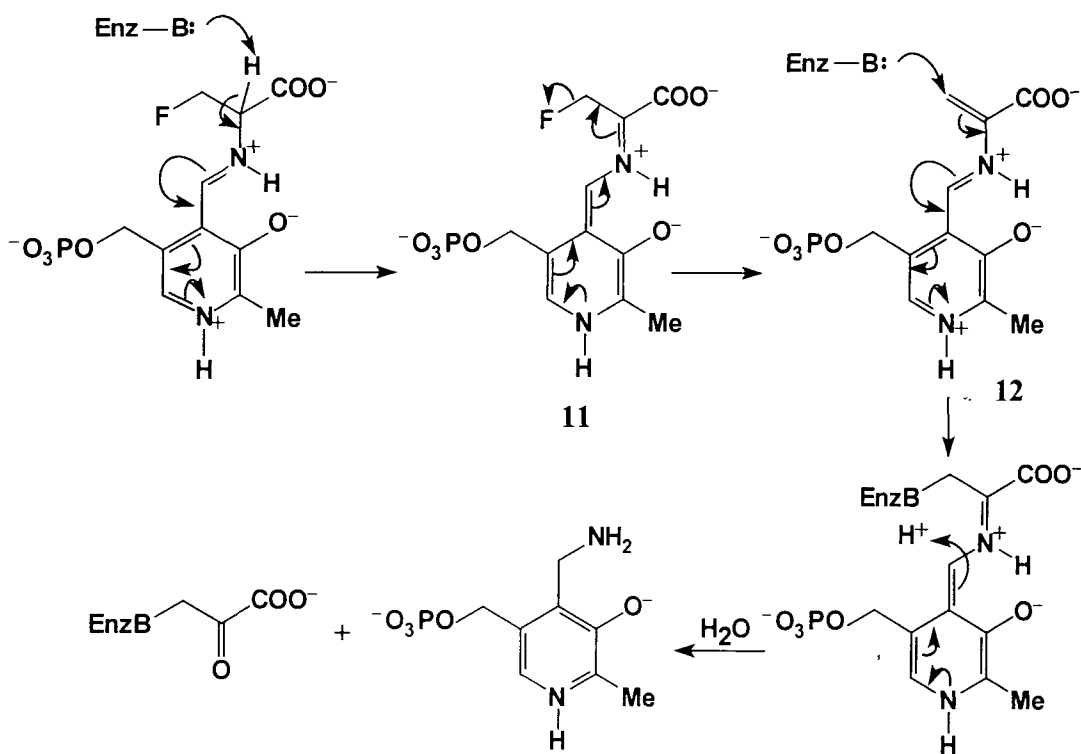


Fig. 1.1 Mechanism of inhibition of alanine racemase by fluoroalanine

1.4.2 Fluoroacetate

Fluoroacetate **13** is the most common of the ten occurring natural products that contain fluorine and has now been identified in over 30 plant species on four continents.² Fluoroacetate is toxic to all cells when activated to fluoroacetyl-CoA **14** and is an excellent acetyl-CoA **15** mimic for citrate and malate synthases. The toxicity arises because fluoroacetyl-CoA leads to the inhibition of the citric acid (Krebs') cycle, a central pathway responsible for generating metabolic energy. Peters showed that fluoroacetyl-CoA competes with acetyl-CoA for the enzyme citrate synthase, where it reacts with oxaloacetate and is involved in the 'lethal synthesis' of (2*R*,3*R*)-fluorocitrate **16** instead of citrate (Fig. 1.2). It is an interesting quirk that citrate synthase mediates the formation of the only toxic stereoisomer of the four possible forms. This fluorocitrate isomer is a powerful competitive inhibitor of the next enzyme on the pathway, aconitase, and this in turn induces inhibition of respiration. There is also evidence that

fluorocitrate can bind irreversibly to a protein responsible for transporting citrate into mitochondria, the site of a cell's energy production, and thus disrupt citrate transport.

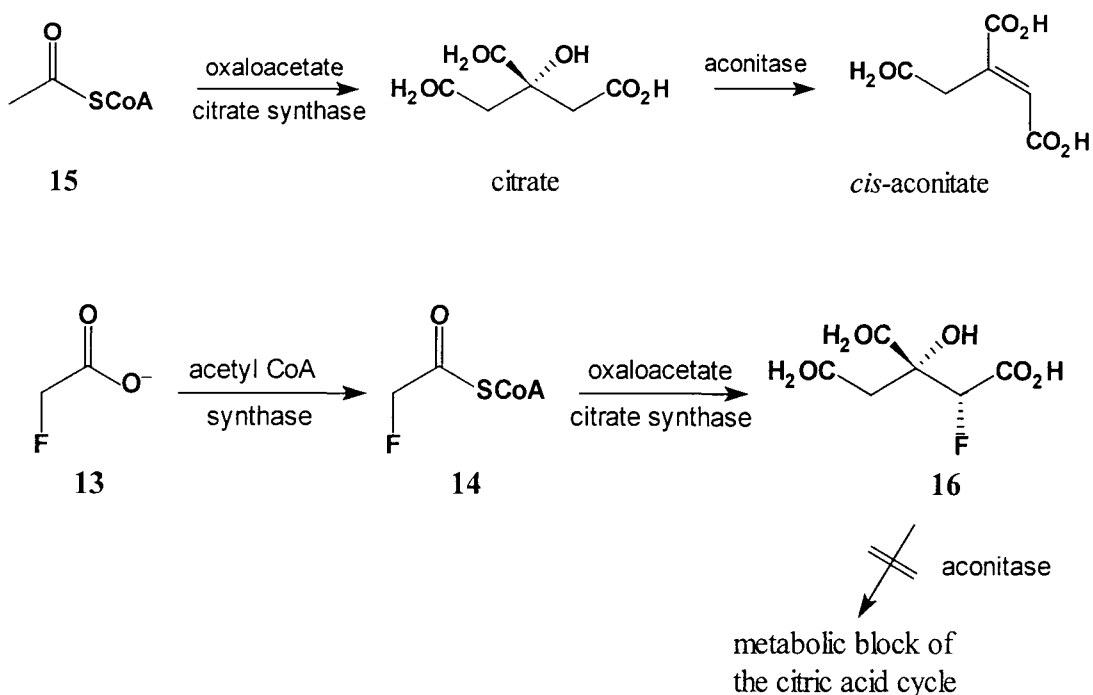
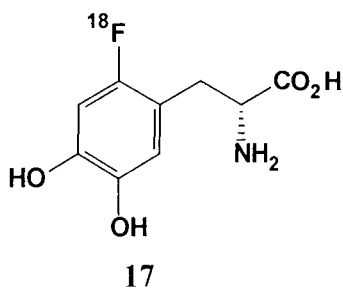


Fig. 1.2 The 'lethal synthesis' pathway for the inhibition of the Krebs' cycle

1.4.3 Aromatic amines

Fluorine has a useful short-lived isotope, ^{18}F (half life 110 min), which decays by positron emission. Positron emission tomography (PET) using ^{18}F has become increasingly important in identifying the binding sites of selective drug molecules, particularly those acting on the brain. One application of ^{18}F PET is the brain imaging of Parkinson's disease patients using the fluorinated amine 6 α -[^{18}F]fluoro-L-dopa **17**.



The use of fluorine to modify and probe the reactivity of organic compounds has also been extended to carbohydrates,^{25,26} prostaglandins,²⁷ steroids,¹² acids and esters.²¹

1.5 Fluorine as a hydrogen bond acceptor

Despite the good size correlation between fluorine and oxygen the ability of fluorine to act as a hydroxy mimic is less clear. For fluorine to be a successful hydroxy mimic in bio-organic chemistry it must replace the hydrogen bond acceptor ability of the hydroxy oxygen. Clearly fluorine cannot replace the hydrogen bonding donor role as it is devoid of the hydroxy group's acidic hydrogen (Fig. 1.3).

Hydrogen bonding, particularly when considering enzyme–substrate binding interactions, is important in bio-organic chemistry. The higher electronegativity and lower polarisability of fluorine however, weaken its electrostatic influence in comparison to oxygen. This compromises its hydrogen bonding ability, and in turn effects the ability of fluorine to act as a hydroxy group mimic.

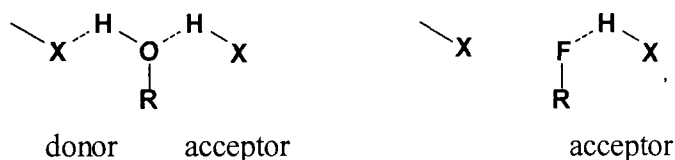
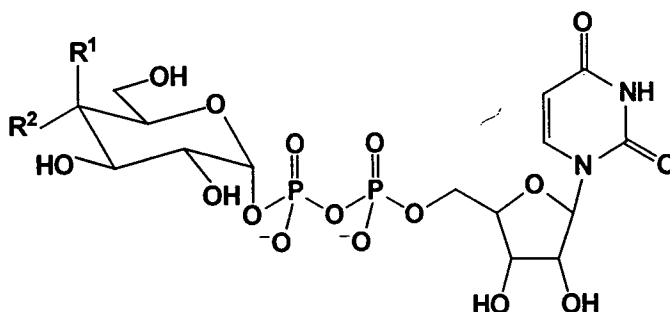


Fig. 1.3 OH can act as a hydrogen bond donor or acceptor, fluorine can only act as an acceptor

Theoretical calculations have estimated the strength of an $F\cdots H$ hydrogen bond to be between 2 and 3.0 kcal mol⁻¹ with an upper value of 3.2 kcal mol⁻¹ in the *cis*-enol tautomer of fluoroacetaldehyde.²⁸ This can be compared to an $O\cdots H$ hydrogen bond which is typically between 5–10 kcal mol⁻¹.²⁹ In strength, therefore, $F\cdots H$ hydrogen bonds are more comparable to $O-H\cdots\pi$ interactions.³⁰ Consistent with this the electrostatic influence of fluorine is approximately half that of oxygen.³¹ Thus the greater electronegativity and lower polarisability of fluorine over oxygen suppresses its electrostatic influence and renders it a poorer hydrogen bond acceptor.

Studies of organofluorine compounds in the Cambridge Crystallographic Data Centre database have revealed only a few situations where fluorine is involved in short contacts to acidic hydrogens.³² Acidic hydrogens show an overwhelming preference for an oxygen or nitrogen acceptor in preference to fluorine. Theoretical and crystallographic evidence force the conclusion that fluorine is a poor hydrogen bond

acceptor with only moderate capacity to replace oxygen (or nitrogen) in this role. Nonetheless, in the desolvated and preorganised binding site of a receptor or enzyme, a fluorine atom substituted for a hydroxy group should be inclined towards the acidic hydrogen bond donor, particularly if there are other peripheral stabilising interactions present. In such a case an F...H hydrogen bond may contribute up to half the energy of the original O...H hydrogen bond to the overall binding energy.



18 R¹ = H, R² = F UDP FGal

19 R¹ = F, R² = H UDP FGal

In this context the fluorodeoxysugars **18** and **19** emerge as good substrate analogues for the appropriate enzymes.³³ Support for an F...H hydrogen bond controlling the enzymatic transformation was provided by Chapeau.³⁴ UDP-4-Deoxy-4-fluoroglucose **18** and UDP-4-deoxy-4-fluorogalactose **19** were tested as substrates for the enzyme UDP-D-glucose dehydrogenase. It was found that **18** was an excellent substrate for the enzyme whereas the diastereoisomeric C-4 epimer **19** was not a substrate but a competitive inhibitor. The configuration of the fluorine at C-4 therefore appears crucial in securing the correct reactive conformation of the substrate on the enzyme surface for reaction at the remote C-6 centre. The example suggests that fluorine is replacing OH, possibly as a hydrogen bond acceptor, however other examples are rare and more often than not the substitution proves detrimental.^{35,36} Such examples could be due to the hydrogen bond donor finding an alternative acceptor to fluorine with corresponding adverse effects on the binding interaction of the substrate and enzyme.

1.6 Stereoelectronic effects

The active site of an enzyme provides an attractive environment in which geometric and stereoelectronic effects that emerge as a consequence of fluorine substitution can be probed. Stereoelectronic effects are significantly effected by indiscriminate solvent interactions in solution and are generally considered to be low energy phenomenon. The dielectric constant of water, at 78.5,³⁷ can be compared to estimates of 15–20 for that of an enzymatic environment. The enzyme active site is therefore significantly less polar than aqueous solvent. Once bound, the substrate is largely desolvated, and exposed to either the co-factor, enzyme or second substrate without the presence of any intervening solvent. Additionally, the ability of enzymes to restrict the conformational freedom of bound substrates may maximise a stereoelectronic effect if a particular conformation is adopted.

1.6.1 The *gauche*^{38,39} and *cis*⁴⁰ effects

For butane, and most other molecules of the form YCH_2-CH_2Y and YCH_2-CH_2X , the most stable conformation is that of the *anti* conformer. However, molecules that contain small, electronegative atoms like fluorine, e.g. 1,2-difluoroethane,⁴¹ are known to exist predominantly in the *gauche* form (Fig. 1.4).

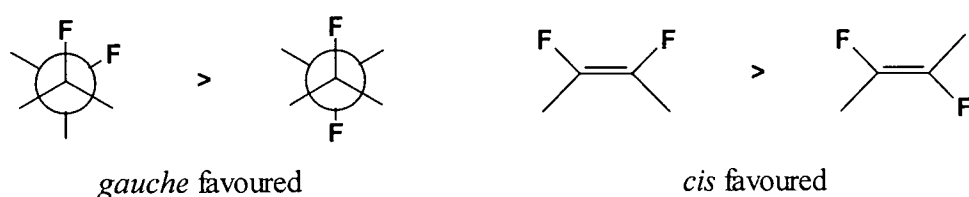


Fig. 1.4 The *gauche* and *cis* effects favour a *syn* relationship between vicinal fluorines

The *gauche* effect is ascribed to nuclear electron attractive forces between the groups or unshared pairs of electrons.⁴² This attractive interaction will be maximal for the *syn* eclipsed conformation, however the *syn* conformation will suffer from repulsive H–H eclipsing interactions and so the *gauche* conformation is adopted as a compromise. For molecules such as 1,2-difluoroethene, the *cis* geometric isomer is 1–2 kcal mol⁻¹

more stable than the *trans* isomer. This is known as the *cis* effect and is probably related in origin to the *gauche* effect.

1.6.2 The *cis* effect in chemistry; citrate synthase

The action of fluoroacetate with citrate synthase has been discussed previously in section 1.4.2. The high stereospecificity of the formation of only one of the four possible stereoisomers of 4-fluorocitrate is of interest, particularly as a related reaction mediated by malate synthase does not show the same level of stereochemical discrimination.

During the condensation of fluoroacetyl-CoA with oxaloacetate (Fig. 1.5), citrate synthase abstracts with a high level of selectivity ($\Delta G > ca. 3 \text{ kcal mol}^{-1}$) only the *pro*-2*S* hydrogen atom. The condensation proceeds with inversion of configuration at this centre and attack is to the *si*-face of the α -carbonyl of oxaloacetate.

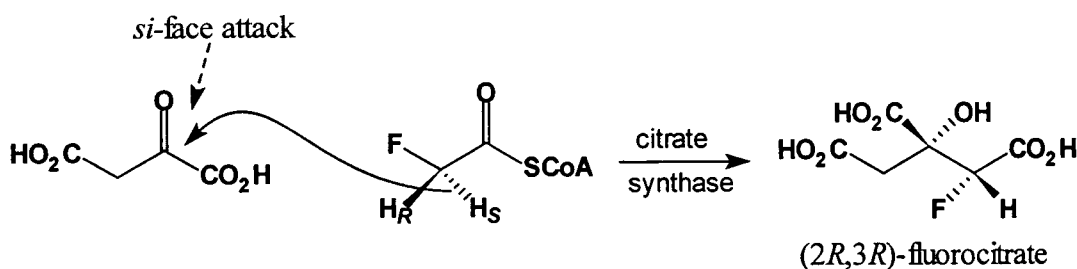


Fig. 1.5 Condensation of oxaloacetate and fluoroacetyl-CoA

Malate synthase can also employ fluoroacetyl-CoA as a substrate and mediates the condensation with glyoxal to generate two diastereoisomers (*2R,3R*) and (*2R,3S*) of 3-fluoromalate **20** in an approximate 3:4 ratio (Fig. 1.6).^{43,44} Malate synthase therefore, unlike citrate synthase, does not control the stereochemistry of the new chiral centre generated as a consequence of fluorine substitution.

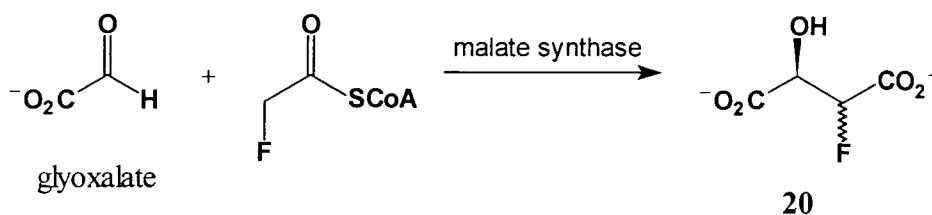


Fig. 1.6 3-Fluoromalate formation with malate synthase

The rate determining step for both enzymes is the abstraction of the proton from acetyl-CoA (citrate synthase⁴⁵ $k_H/k_D = 1.94$, malate synthase⁴⁶ $k_H/k_D = 3.9$). When fluoroacetyl-CoA is the substrate the enzyme bound enol or enolate can have *E* or *Z* geometries.

The relative energies of the enols and enolates were calculated by computational modelling.⁴⁷ High level *ab initio* calculations of a model system, $FCH_2C(O)SH$, showed a significant difference (*ca.* 4 kcal mol⁻¹) in the relative energies of the neutral *E* and *Z* enols. This difference was significantly reduced (*ca.* 1.8 kcal mol⁻¹) when the charged enolate intermediates were modelled (Fig. 1.7).

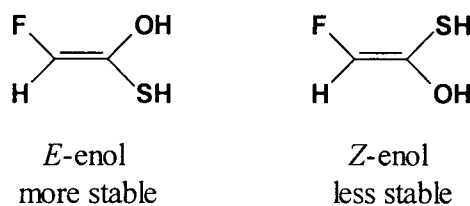


Fig. 1.7 Enols formed from $FCH_2C(O)SH$

It would therefore appear that in the case of citrate synthase, the enolate as it is formed is protonated to an enol in the more stable *E* geometry to give the resultant (2*R*,3*R*)-fluorocitrate product (Fig. 1.8). The preference for the *E* isomer is consistent with the *cis* effect where the harder fluorine and oxygen atom pair. This is preferred over the hard/soft interaction between fluorine and sulfur. By analogy malate synthase is predicted to have a more enolic intermediate giving less control over the stereochemistry of the product.

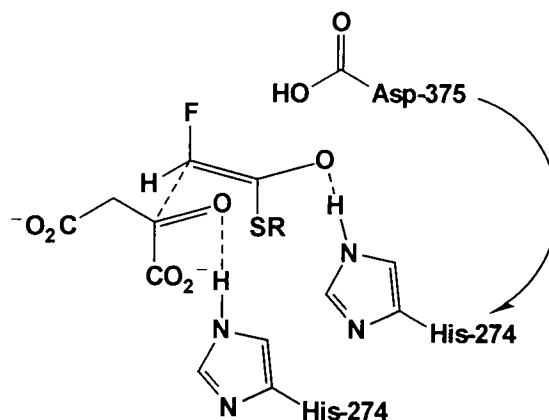


Fig. 1.8 Proposed intermediate for formation of enol and aldol condensation

1.6.3 The fluorine anomeric effect

The *anomeric effect*⁴⁸ is a common phenomenon in carbohydrate chemistry where a polar group, usually OH, prefers the axial conformation over the sterically preferred equatorial position (Fig. 1.9). This observation extends more generally to X–C–Y systems where X has non-bonding electrons and Y is an electronegative group/atom, *e.g.* O–C–F and N–C–F systems.⁴⁹

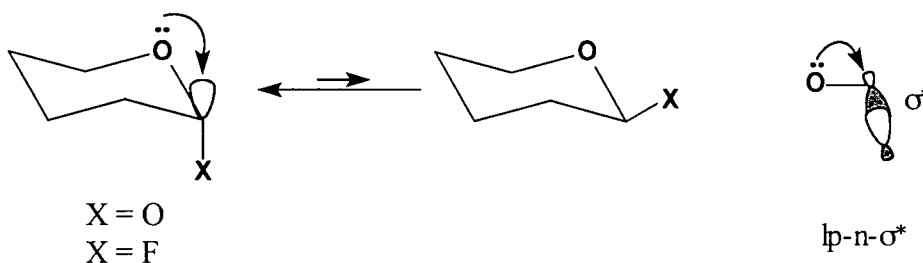


Fig. 1.9 Molecular orbital representation of the anomeric effect

The most accepted molecular orbital explanation for the anomeric effect suggests that the lone pair on oxygen lying antiperiplanar to the C–X bond donates electron density into the adjacent σ^*_{C-X} orbital in a stabilising hyperconjugative interaction, as shown in Fig. 1.9. This interaction is proportional to the overlap (*i.e.* relative orientation) of the participating orbitals and is inversely proportional to the energy gap between them.⁵⁰ Theoretical studies for understanding the role and nature of stereoelectronic effects in O–C–F and N–C–F systems do not go beyond the smallest

molecules, namely fluoromethanol (HOCH_2F),⁴⁹ fluoromethyl methyl ether (MeOCH_2F)^{51,52} and fluoromethylamine ($\text{H}_2\text{NCH}_2\text{F}$).⁵³ These studies show a preference for the *gauche* conformer over the *anti* with an energy stabilisation of $6.0 \text{ kcal mol}^{-1}$. The structural trends associated with the anomeric effect, a shortening of the C–O bond, lengthening of the C–F bond and opening of the O–C–F bond angle, are observed in X-ray structure data of the appropriate compounds and is consistent with the hyperconjugation hypothesis.

1.6.4 The Anh–Eisenstein effect

The search for an understanding of the underlying reasons for π -facial selectivity in the addition of nucleophiles to double bonds, especially carbonyls, has generated more models and hypotheses than any other subject in the field of stereoselective synthesis. The most widely accepted model for explaining π -facial stereoselectivity in nucleophilic addition reaction to cyclic and chiral acyclic carbonyl compounds is that based on the Felkin-type transition structure (Fig. 1.10).⁵⁴ In Felkin's model, the favoured transition state structures have a conformation where the bulkiest of the α ligands (L) takes up a perpendicular relationship to the plane of the carbonyl group and is *anti* to the incoming nucleophile. Steric and torsional repulsions are then at a minimum. The major stereoisomer results from the conformation in which the medium sized group (M) occupies the sterically less congested inside position *gauche* to the carbonyl.

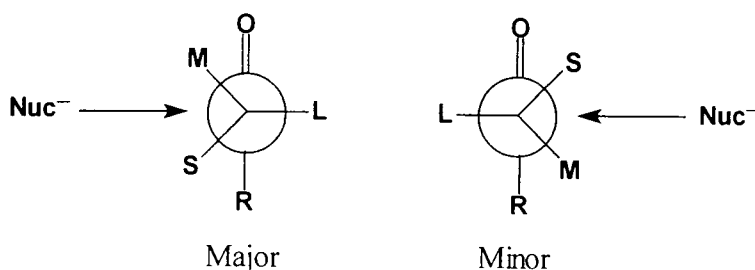


Fig. 1.10 Felkin model for nucleophilic addition to carbonyl ($L > M > S$)

A particular problem with this model lies with the correct identification of the 'large' group (L), because the attribute 'large' incorporates not only obvious steric factors, but also electronic factors. Anh and Eisenstein have undertaken a theoretical

study of the various models, using the reaction of hydride attack on 2-chloropropanal.⁵⁵ *Ab initio* calculations found that the conformations assumed by the Felkin model were energetically the most favoured, with hydride approaching antiperiplanar to the most electronegative atom, chlorine, on C-2.

The principal of stereoelectronic control states that, 'all other things being equal reactions will proceed along paths corresponding to the most favourable molecular orbital attack'. Validation of the Anh–Eisentein model comes from consideration of the molecular orbitals involved. The low relative energy of the Felkin transition state arises from the antiperiplanarity of the C1–H⁻ and C2–L bond. The principal molecular orbital (MO) interaction occurring is that between the HOMO of the nucleophile and the LUMO (π^*_{CO}) orbital of the substrate. Although overlap would be maximised by a perpendicular approach of the nucleophile, there are destabilising interactions arising from the out-of-phase overlap with the oxygen atom and the four electron interaction with the HOMO of the substrate. These are reduced by increasing the angle of attack of the nucleophile corresponding to the Bürgi–Dunitz trajectory (Fig. 1.11).⁵⁶

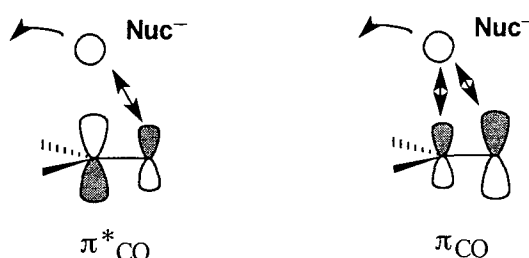


Fig. 1.11 Non-perpendicular attack as a result of stereoelectronic control

As the principle interaction is the π^*_{CO} with the nucleophile's HOMO any effect which lowers the energy of π^*_{CO} will increase this interaction and stabilise the transition state. When C1–H⁻ and C2–L bonds are antiperiplanar there is a good overlap between π^*_{CO} and σ^*_{C2-L} which leads to a stabilisation of the former. However, this good overlap also occurs for a synperiplanar attack but this stereochemistry is disfavoured for two reasons: (i) *anti* attack with respect to L leads to an in phase overlap between H⁻ and σ^*_{C2-L} ($n-\sigma^*$) at C2, *syn* attack leads to an out-of-phase overlap (Fig. 1.12); and (ii) *syn* attack implies an eclipsing of C1–H⁻ and C2–L bonds.

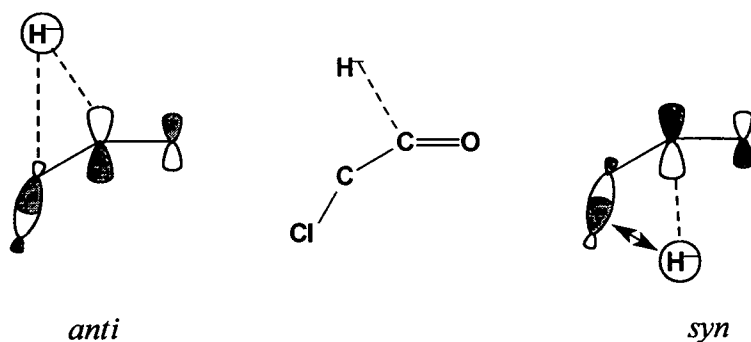


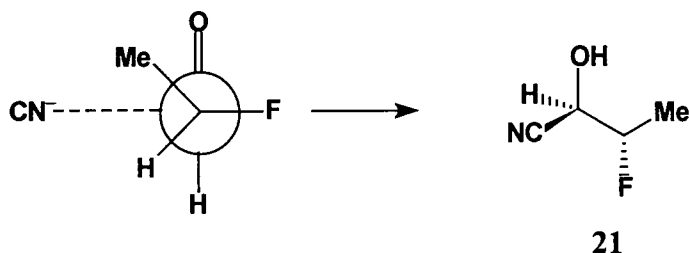
Fig. 1.12 Secondary interactions for anti- and syn-periplanar attacks

In summary, the electronic factors attributed to L, in the context of frontier orbital theory, arise from stabilising two-electron interactions in the transition structure. These are thought to be dominated either by mixing the filled σ_{HOMO} of the forming nucleophile-carbon bond with the vacant σ^*_{LUMO} of the C-L bond (Anh-Eisenstein model),⁵⁵ or by mixing the vacant σ^* MO of the forming bond with the filled σ MO of the C-L bond (Cieplak model).⁵⁷

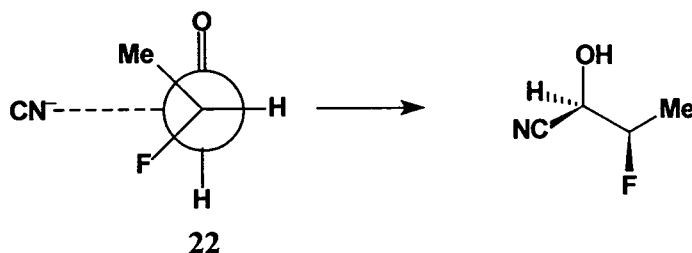
Steric factors aside therefore, the Anh-Eisenstein model assigns the best acceptor ligand to 'L', whereas the Cieplak model assigns the best donor ligand to 'L'.

In a further theoretical study, Wong and Paddon-Row sought to tackle which electronic model was the more realistic using an *ab initio* MO study of nucleophilic attack on a chiral carbonyl system with fluorine as one of the substituents on the α -carbon.⁵⁸ The study specifically concentrated on the addition of a cyanide nucleophile to 2-fluoropropanal.

The results of the study showed that the lowest energy transition state was achieved when the best acceptor, fluorine, was antiperiplanar to the attacking cyanide nucleophile, and the methyl group occupied the inside position to give the product **21** which agrees with the Anh-Eisenstein model.



The transition state structure for **21** is 12.4 kJ mol⁻¹ more stable than the Cieplak transition structure **22**, in which the C–H bond is antiperiplanar; this gives rise to the corresponding diastereoisomer of **21**.



The greatest amount of charge transfer to the aldehyde was observed when the C–F bond was antiperiplanar. This is in accord with the stabilisation of electron rich transition states by an electron-withdrawing antiperiplanar C–F bond. The results of the study concluded that the electronic component to the determinant of π -facial stereoselectivity in the nucleophilic addition to α -halogenated carbonyl groups is better represented by the Anh–Eisenstein model. However it should be noted that the preference for the C–F to adopt the antiperiplanar conformation could be contributed in part to adverse dipole or electrostatic effects which are reduced by *anti* attack.

The origins of both the fluorine anomeric effect and the Anh–Eisenstein effect therefore lie in the ability of the σ^* LUMO orbital of the C–F bond to accept electron density, from either the heteroatom in the former or attacking nucleophile in the latter case.

1.6.5 The Anh–Eisenstein effect in enzyme reactions

There is now considerable interest in the use of enzymes to produce optically active compounds either by means of a kinetic resolution or stereospecific chemical transformation (*e.g.* reductions, oxidations, epoxidations). This interest extends to the preparation of homochiral fluorinated compounds. A recent publication by Haufe⁵⁹ reported the first example of enzymatic esterifications of monofluorinated alcohols in organic media. Racemic ω -fluoro-(ω -1)-hydroxyalkanoates were resolved by the lipase of *Pseudomonas cepacia* (LAPS) in toluene at room temperature (Fig. 1.13).

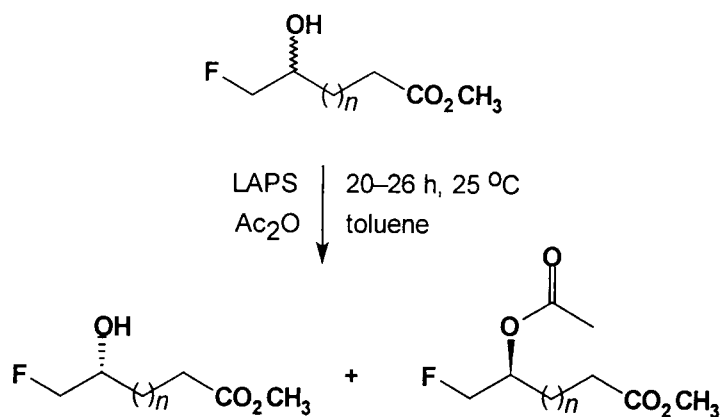


Fig. 1.13

Hydrolases in general have been used to effect kinetic resolutions of racemic esters, primarily in the enantioselective hydrolysis of mono- and di-esters with chiral centres on the carboxylate part of the molecule.⁶⁰ Lipases have been used to effect kinetic resolutions of chiral alcohols *via* enantioselective hydrolysis of their esters, but it is their application to the hydrolysis of racemic esters with chirality on the carboxylate moiety that has been more widely exploited.⁶¹ The availability and low cost of lipases make them a very attractive class of catalyst for effecting kinetic resolutions in industrial applications.

Pig Liver Esterase (PLE) is one of the most useful enzymes for the preparation of valuable chiral synthons. However, its applications in asymmetric synthesis has been hampered by its seemingly unpredictable specificity. This disadvantage has been overcome by the development of active-site models which can account for the structural and stereoselectivity of PLE-hydrolases reported and is of predictive value for new substrate structures.⁶² The model depicted in Fig.1.14 is comprised of four binding regions. The two hydrophobic pockets, which interact with the aliphatic or aromatic hydrocarbon portions of the substrate, are designated H_L and H_S. Two more polar cavities at the front P_F and P_B can accommodate electron-rich functions and act as hydrogen bond acceptors. The ester group to be hydrolysed must locate in the serine nucleophile region (dotted circle).

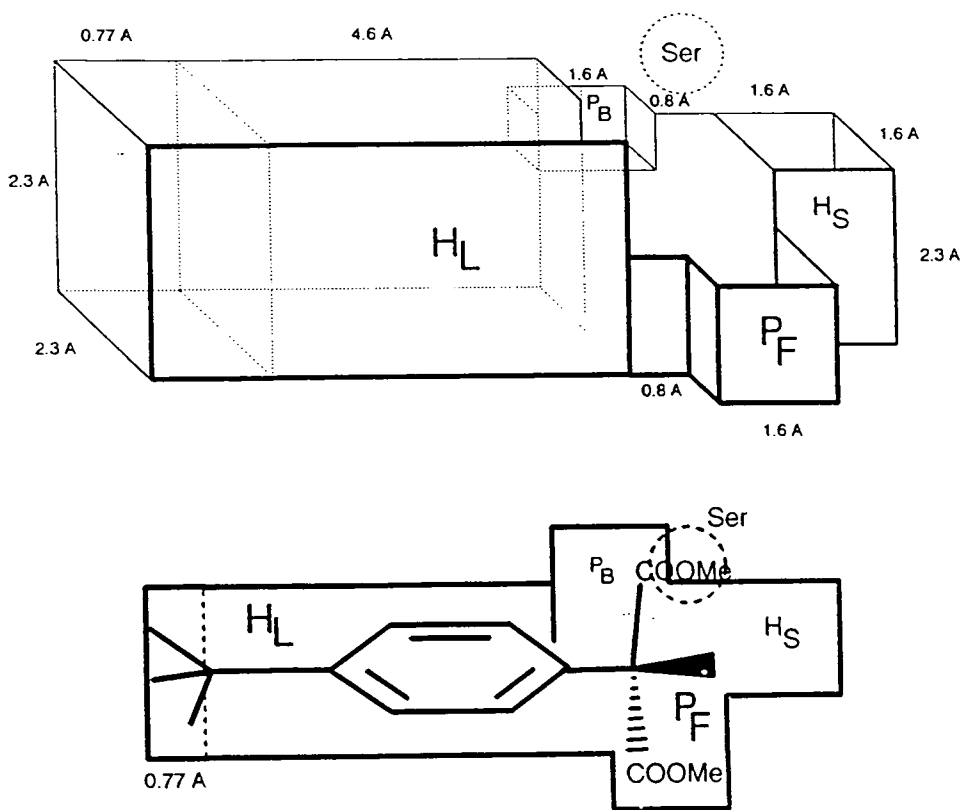


Fig. 1.14 Active site model of pig liver esterase⁶²

The active site of a lipase is therefore generally considered to accommodate a particular substrate on the basis of fit and electronic compatibility to the surface of the protein. This gives rise to the preferential binding and subsequent hydrolysis of one enantiomer over the other.

Despite this recent rapid development in the use of enzymes in organic synthesis only a few successful examples of enzymatic hydrolysis of monofluorinated compounds have been found. In this context the lipase resolution in high enantiomeric excess of α -fluoro esters **23** and **25** (Fig. 1.15) are remarkable.^{63,64}

In the first example racemic ethyl 2-fluorohexanoate **23** was resolved into its component enantiomers using a lipase from *Pseudomonas fluorescens* (P30).⁶³ The reaction was allowed to proceed to 60% conversion, at which point the isolated residual ester was judged to be solely the *R* enantiomer **24** in 99% ee. In the second example the Amano MY lipase from *Candida cylindracea* exclusively hydrolysed the *pro-S* ester group of the prochiral compound 2-fluoromalonnate **25**, to give **26** with a 99% ee.⁶⁴

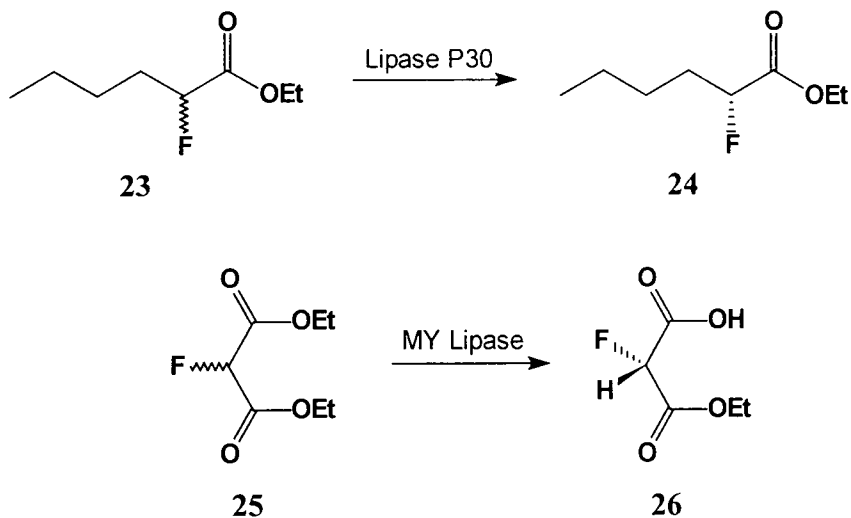


Fig. 1.15 Lipase hydrolysis of α -fluorinated esters

These levels of stereoselectivity are difficult to rationalise on the basis of a spatial active site model. In each case the lipase makes a complete distinction between the fluorine and hydrogen atoms. As already discussed, the steric influence of fluorine over hydrogen is predicted to be too small to lead to such high levels of selectivity. It has therefore been proposed⁶⁵ that the high selectivity displayed in these lipase resolutions arises due to an Anh–Eisenstein type stabilisation in the transition state.

In a lipase-mediated hydrolysis a serine alkoxide nucleophile at the enzyme active site attacks at a predesignated face of the ester carbonyl group. The two enantiomers of the α -fluoro ester substrate will then give rise to two different diastereoisomeric transition states (Fig. 1.16).

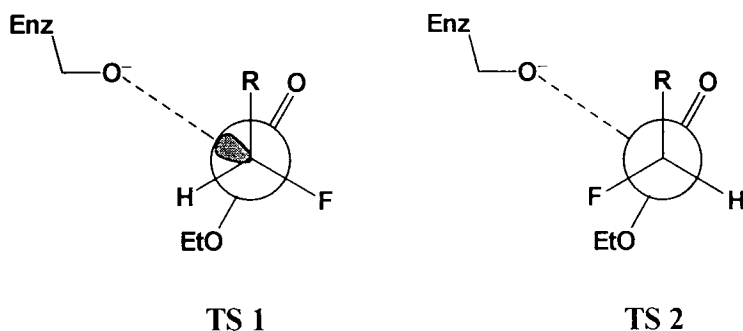


Fig. 1.16 Diastereoisomeric transition states formed by alkoxide attack on α -fluoro esters

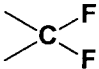
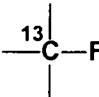
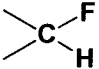
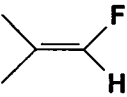
Following the Felkin model the nucleophile can approach either *anti* to the C–F bond (TS 1) or *gauche* (TS 2) to the C–F bond. Clearly, from previous analysis of nucleophilic attack at carbonyl groups with a fluorine at the α -carbon, the preferred transition state geometry will be as shown in TS 1 where the incoming nucleophile is antiperiplanar to the C–F bond. The situation was modelled at an *ab initio* level, using MeO^- as the nucleophile (serine hydroxide surrogate) and methyl 2-fluoropropionate as the substrate ester. The results of the study revealed a significant discrimination in the energies of the two transition states with TS 1 lower in energy than TS 2 by 2.8 kcal mol⁻¹. The calculated entropy difference between the two transition states of 0.4 cal K⁻¹ mol⁻¹ gave a free energy difference at 300 K of 2.5 kcal mol⁻¹. An energy difference of this magnitude would correspond to a ratio between TS 1 and TS 2 of *ca.* 100:1, which can fully account for the observed high enantioselectivities (99% ee).

Implicit in these resolutions is the ability of the enzyme to hold the substrate in a conformation which can accommodate the stereoelectronic effect as the reaction moves towards a transition state. Depending on the bound conformation of the ester substrates, differing lipases will show varying abilities to resolve the α -fluoro esters.

1.7 ¹⁹F NMR Spectroscopy

Since the first attempts to detect fluorine NMR signals over fifty years ago, ¹⁹F NMR spectroscopy has evolved into a powerful analytical tool routinely used for the elucidation of chemical structures.⁶⁶ With a 100% natural abundance and a large magnetic moment, the ¹⁹F isotope presents no problems in sensitivity. Like a proton, ¹⁹F has a spin quantum number of $I = \frac{1}{2}$ making coupling patterns easy to deduce. The range of chemical shifts is very wide, around 800 ppm, however most resonances of a carbon–fluorine environment occur within a 300 ppm range. Strong coupling (Table 1.3) to other nuclei results in long range effects that influence both the ¹⁹F NMR spectrum and that of the other nuclei. At 2.35 T, fluorine resonances are at 94 MHz: the range of δ values in common environments is around 300 ppm, so the spread of frequencies is approximately 30 000 Hz. This range is far greater than for any other commonly studied NMR nucleus. ¹⁹F NMR spectra are routinely referenced to CFCl_3 as 0 ppm, with the usual convention that positive δ means higher frequency than CFCl_3 .

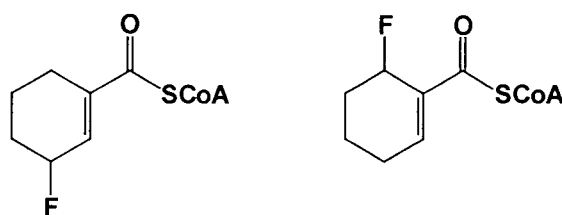
Table 1.3 Representative ^{19}F NMR coupling constants⁶⁷

System	Type	Typical J value/Hz	System	Type	Typical J value/Hz
	$^2J_{\text{FF}}$	150–270		$^1J_{\text{CF}}$	160–370
	$^2J_{\text{HF}}$	45–65	$^{13}\text{C}-\text{C}-\text{F}$	$^2J_{\text{CF}}$	30–45
	$^2J_{\text{HF}}$	70–90	$^{13}\text{C}-\text{C}-\text{C}-\text{F}$	$^3J_{\text{CF}}$	5–25

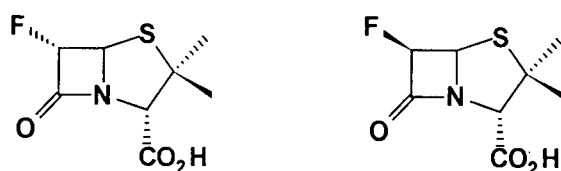
1.8 Aims and objectives

The objectives of the project were to further probe the effects of fluorine substitution in a range of enzymatic transformations. This would involve the synthesis of a number of regio- and stereo-specifically fluorinated compounds which would, by a series of techniques, be studied through the course of given enzyme reactions. Suitable fluorinated substrate analogues for various enzymatic transformations are outlined below.

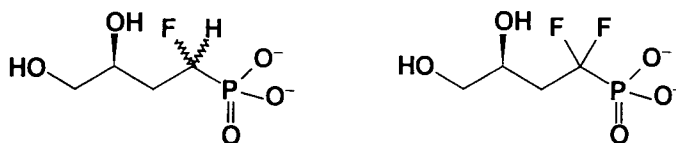
(i) Cyclohex-1-enecarbonyl-CoA reductase (enoyl reductase)



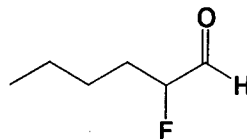
(ii) β -Lactamase



(iii) Glycerol-3-phosphate dehydrogenase



(iv) Transketolase



For each transformation the fluorinated analogue of the natural substrate is employed to explore any kinetic differentiation or stereoelectronic control exhibited by the enzyme.

1.9 Fluorinating reagents

With the need to prepare a number of fluorinated compounds it is useful to briefly review some of the methods employed for fluorination of organic compounds, with a particular emphasis on those methods employed in this thesis. The preparation of organofluorine compounds remains a difficult area, especially when incorporation of fluorine is required in a regio- or stereo-selective manner. Since fluorine itself is so reactive and difficult to control, alternative methods of incorporating fluorine into organic molecules are required. The great importance of selectively fluorinated molecules has unsurprisingly given rise to numerous methods for fluorine insertion and a number of reviews have been published covering fluorination techniques.^{68,69} Fluorinating reagents are classified into groups according to their mode of action, *i.e.* nucleophilic, electrophilic or free radical fluorine transfer. The methods discussed here and used throughout the project are all of the nucleophilic type.

1.9.1 Sulfur tetrafluoride (SF_4)

Sulfur tetrafluoride (SF_4) was first introduced by Dupont in 1960 and many reviews have described its applications.^{70,71} The main uses of SF_4 are outlined in Fig. 1.17.

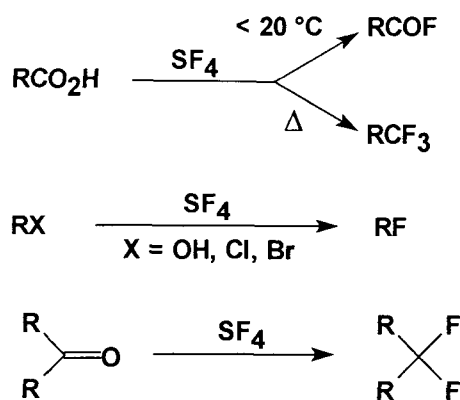


Fig. 1.17 Major functional group interconversions using SF₄

Sulfur tetrafluoride is usually used in conjunction with a Lewis acid or with liquid HF, which act catalytically and reduce reaction temperatures and times. However, the major drawbacks of SF₄ are its volatility (bp -38 °C) and its toxicity, which is comparable to phosgene. Reactions also require the use of sealed, stainless steel vessels which make the reagent relatively difficult to handle.

1.9.2. Diethylaminosulfur trifluoride (DAST)

Diethylaminosulfur trifluoride (DAST), which was first prepared by Middleton, has become the most widely used fluorinating reagent.⁷² Its success is due to the fact that it can mimic the chemistry of SF₄ while avoiding the problems of high pressure and toxicity. It is a commercially available liquid that is relatively easy to handle (bp 46–47 °C at 10 mmHg), and can be stored for long periods without significant decomposition. Among the major uses of DAST are the fluorination of alcohols to monofluorinated species and the conversion of aldehydes and ketones to *gem*-difluorides.⁷³

Mechanistically, the reaction of DAST with hydroxy groups proceeds *via* nucleophilic attack by the hydroxy group on to sulfur generating the intermediate **27**. Nucleophilic attack of fluoride to the intermediate gives the product, generally with overall inversion of stereochemistry (Fig. 1.18).

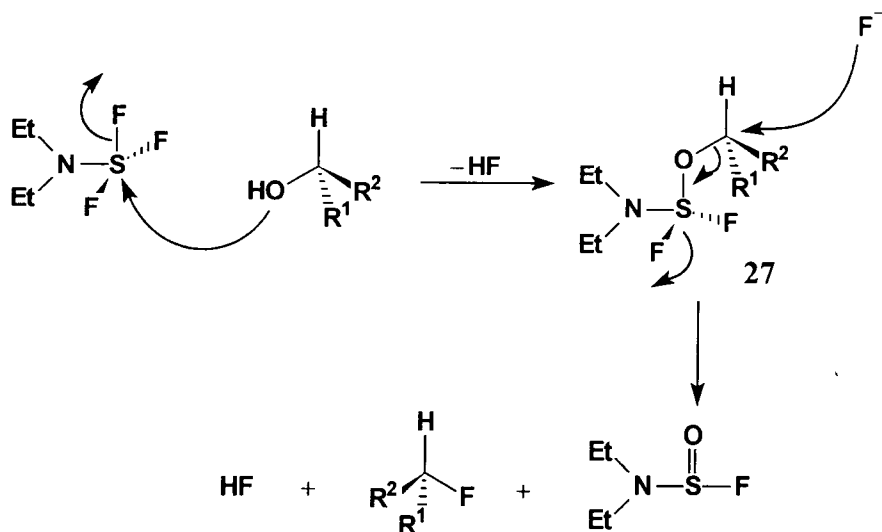
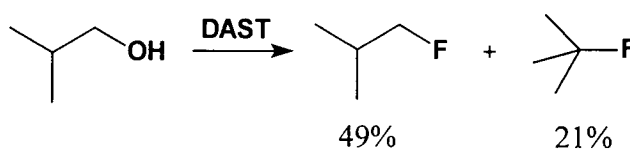
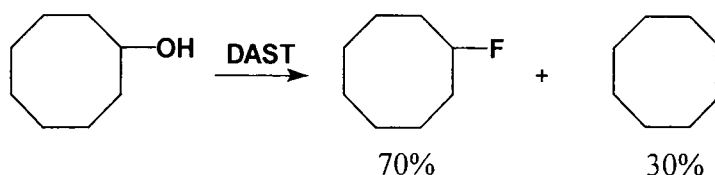


Fig. 1.18 Mechanism of fluorination of alcohols with DAST

Although reactions usually occur with stereochemical inversion, reactions where stereochemistry is retained are known, as well as $\text{S}_{\text{N}}\text{i}$ type mechanisms. Two problems that can occur when replacing OH groups with DAST are carbonium ion type rearrangements and dehydration to give alkenes. The carbonium ion rearrangements are however less likely to occur with DAST than with other known fluorinating reagents. For example, fluorination of isobutyl alcohol with DAST gave more than a 2:1 ratio of isobutyl fluoride to *tert*-butyl fluoride, whereas fluorination with $\text{SeF}_4 \cdot \text{pyridine}$ is reported to give only the rearranged *tert*-butyl fluoride.⁷⁴



Dehydration (elimination) is also less of a problem with DAST. For example, cyclooctanol reacts with DAST to give a 70:30 ratio of cyclooctyl fluoride to cyclooctene, whereas $\text{Et}_2\text{NCF}_2\text{CHClF}$ gives only cyclooctene.⁷²



1.9.3 Hydrogen fluoride

Anhydrous hydrogen fluoride is one of the classical fluorinating reagents, but though cheap and readily available its volatility (bp 19.6 °C) and corrosiveness provide obstacles to its utility. The introduction of pyridinium poly(hydrogen fluoride), (HF)_xpy, a stable liquid of approximate composition 30% pyridine–70% HF, by Olah in 1973 has allowed numerous new applications for the use of HF.⁷⁵ The reagent is commercially available, does not lose HF below 50 °C, and is relatively easy to handle. It has proved to be an extremely versatile reagent which can be used to fluorinate a range of reagents including fluorination of alkenes and alkynes, isocyanates, alcohols, diazoalkenes and diazoketones and acid chlorides (Fig. 1.19).⁷⁶

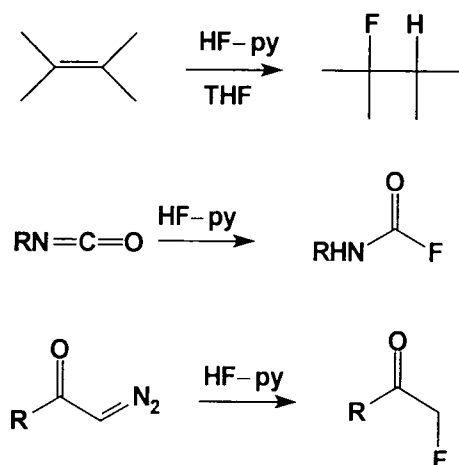


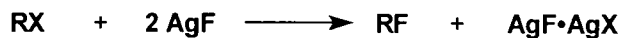
Fig. 1.19 Functional group interconversions with HF–pyridine

1.9.4. Metal fluorides

Nucleophilic displacement of a halide by fluoride is amongst the cheapest and most widely employed methods for the introduction of fluorine. Among the most common reagents are KF, CsF, KF–HF and AgF, which are generally used in the displacement of tosylates, mesylates and triflates.^{4d} Anhydrous polar solvents (*e.g.* MeCN, DMF) are usually required to obtain a high concentration of dissolved fluoride, as water reduces the nucleophilicity of fluoride.

Silver fluoride is a commercially available solid which was used by Swarts in his synthesis of methyl fluoroacetate.^{8b} It is a popular reagent because of its high selectivity and low basicity (compared to alkali metal fluorides) which minimises elimination

reactions. Its main use is in selective halogen exchange reactions, e.g. $\text{RI} \rightarrow \text{RF}$. However, its disadvantages are its high cost (5 g = £35) and that two equivalents of reagent are required to generate one equivalent of fluorinated product.



1.9.5 Tetraalkylammonium fluorides

Tetraalkylammonium fluorides overcome the problems of alkali metal fluorides by providing (i) a soluble source of F^- and (ii) replacing the M^+ ion with a bulky organic cation, thereby reducing ion-pairing and enhancing the nucleophilicity of F^- . The most common reagent of this class is 'anhydrous' tetrabutylammonium fluoride (TBAF). TBAF is commercially available, however it suffers from being extremely hygroscopic and its major disadvantage is that the presence of varying amounts of water often produce erratic results. However, wet TBAF has been successfully used to prepare fluorinated compounds. Tetrabutylammonium hydrogen bifluoride ($\text{Bu}_4\text{N}^+\text{HF}_2^-$) (TBABF) has been used as an improved source of 'naked' fluoride ion.⁷⁷ TBABF has been used in the halofluorination of alkenes by treatment of the alkene with NBS and TBABF in dichloromethane.⁷⁸ However, unlike reaction with TBAF–NBS mixture which gives high yields of the bromo–fluoro product, a major side product with TBABF–NBS was the formation of vicinal dibromides (Fig. 1.20).

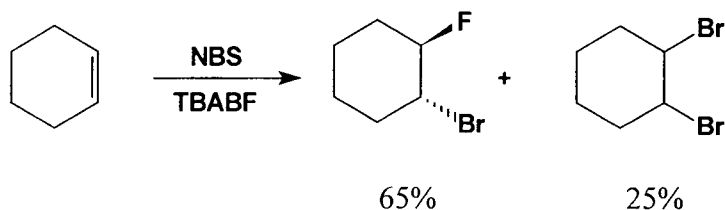


Fig. 1.20 Halofluorination of alkene using NBS–TBABF

Chapter Two

An Investigation into the Anh–Eisenstein Effect in an Enzymatic Transformation

An Investigation into the Anh–Eisenstein Effect in an Enzymatic Transformation

2.1 Introduction

In 1961 the International Union of Biochemistry adopted a systematic scheme for the classification of the known enzymes. The six main classes of enzyme were established as the oxidoreductases, transferases, hydrolases, lyases, isomerases and ligases.⁷⁹ The action of the oxidoreductases (group I) is the catalysis of oxidation-reduction reactions, of which the most common is the interconversion of alcohols to aldehydes or ketones (E.C. 1.1.1.1 alcohol dehydrogenase) (Fig. 2.1).

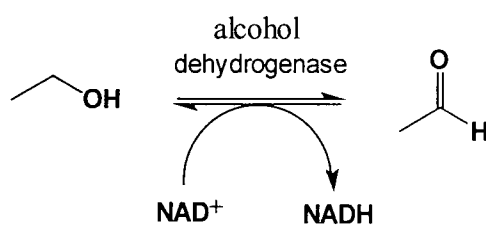


Fig. 2.1

In order for enzymes to be catalytically active many require additional co-factors. These co-factors may be as simple as metallic cations or as elaborate as complex organic molecules known as co-enzymes. When co-factors are required, the enzyme must include additional binding sites. An enzyme that lacks an essential co-enzyme is known as an apoenzyme, while the complex between enzyme and co-enzyme is termed the holoenzyme.

Nicotinamide adenine dinucleotide and its reduced form (NAD⁺ and NADH) serve as co-enzymes in a large number of enzymatic redox reactions, and form one of two co-enzyme forms of nicotinamide. The other is nicotinamide adenine dinucleotide phosphate (NADP⁺ and NADPH), which differs by the presence of a phosphate group at C-2' of the adenosyl moiety (Fig. 2.2). The NAD(P)H dependent enzymes include dehydrogenases, transhydrogenases, oxidases and enoyl reductases.⁸⁰

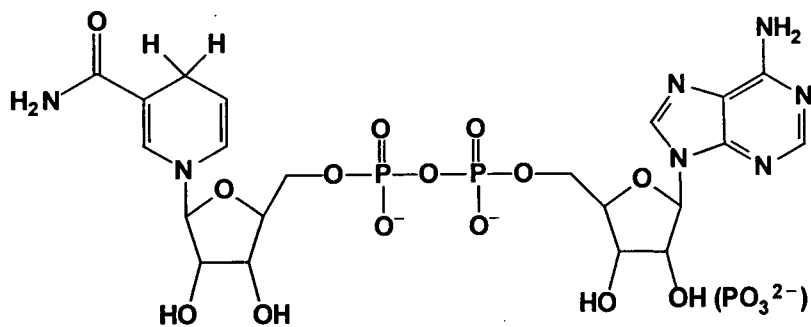


Fig. 2.2 Structure of NADH (and NADPH) co-enzyme

The function of the NAD(P)H co-enzyme is to either accept a hydride (H^-) from a substrate (oxidation) or to donate hydride to a substrate (reduction). This hydride transfer takes place between the substrate and the pyridinium cation or, conversely, the 1,4-dihydropyridine in the nicotinamide moiety and the carbonyl substrate, and is a readily reversible process (Fig. 2.3).

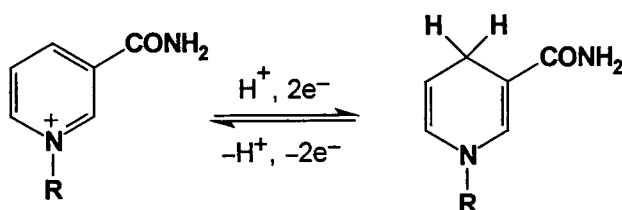


Fig. 2.3 Interconversion of NAD^+ (NADP^+) and NADH (NADPH)

The essential characteristics of NAD(P)H-dependent enzymes can be summarised as follows: (i) the reactions take place with the ternary (apoenzyme-co-enzyme-substrate) complexes; (ii) the transfer of the hydride is direct and apparently involves no exchange with solvent proton; (iii) the reactions are stereospecific with respect to both the co-enzyme and the substrate.⁸⁰ Once formed, the NADH diffuses or is transported to the terminal electron-transfer sites of the cell and is re-oxidised by terminal electron acceptors (O_2 in aerobic organisms) with the concomitant formation of ATP.

2.1.1 NAD(P)H-dependent alcohol dehydrogenases

Among the enzymes that utilise NAD(P)H as a co-enzyme are a number of dehydrogenase activities which include alcohol dehydrogenase, glutamate dehydrogenase and glyceraldehyde-3P-dehydrogenase. Many alcohol dehydrogenases such as horse liver alcohol dehydrogenase (HLADH) have been identified which catalyse the redox conversion of carbonyls and alcohols. Such enzymes have been the subject of extensive kinetic and mechanistic studies and have been widely exploited in biotransformations.⁸¹ These enzymes are readily available, and accept a broad range of substrates. The chemical mechanism by which NAD⁺ is reduced to NADH is shown in Fig. 2.4.

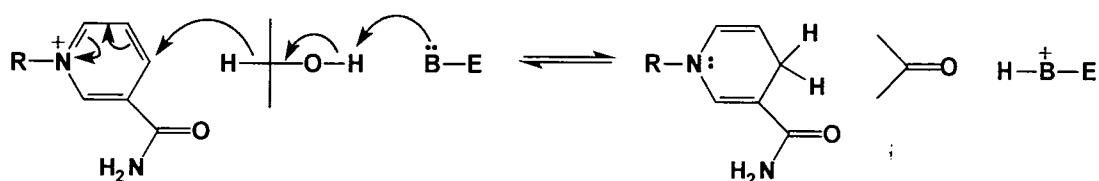
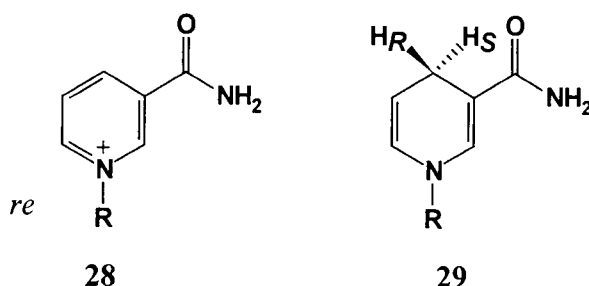


Fig. 2.4

NAD(P)⁺ functions as a co-enzyme in redox reactions by reversibly accepting hydrogen at the 4-position of the nicotinamide ring (Fig. 2.3). The C-4 position in the dihydronicotinamide ring is prochiral and thus the faces of the nicotinamide ring **28** and the C-4 protons of the dihydronicotinamide ring **29** may be assigned by the *re* and *si* convention.



In a series of historically important experiments, Westheimer, Vennesland and co-workers demonstrated that the hydrogen transfer between substrate and NAD⁺ was direct and stereospecific.^{82,83} The experiments with alcohol dehydrogenase were the earliest to show the high stereospecificity of enzymatic action at prochiral centres

involving chemically equivalent hydrogen atoms and were achieved by tracing deuterium through the course of the transformations. Yeast alcohol dehydrogenase transfers 1 mol of deuterium from $\text{CH}_3\text{CD}_2\text{OH}$ to NAD^+ . When the formed NADD was incubated with unlabelled acetaldehyde, all the deuterium was lost from the NADD and incorporated back into the alcohol formed. The deuterium or hydrogen was transferred stereospecifically to one face of the NAD^+ and then transferred back from the same face. A non-specific transfer to both faces would have led to the transfer of 50% of the deuterium back to the acetaldehyde (Fig. 2.5).

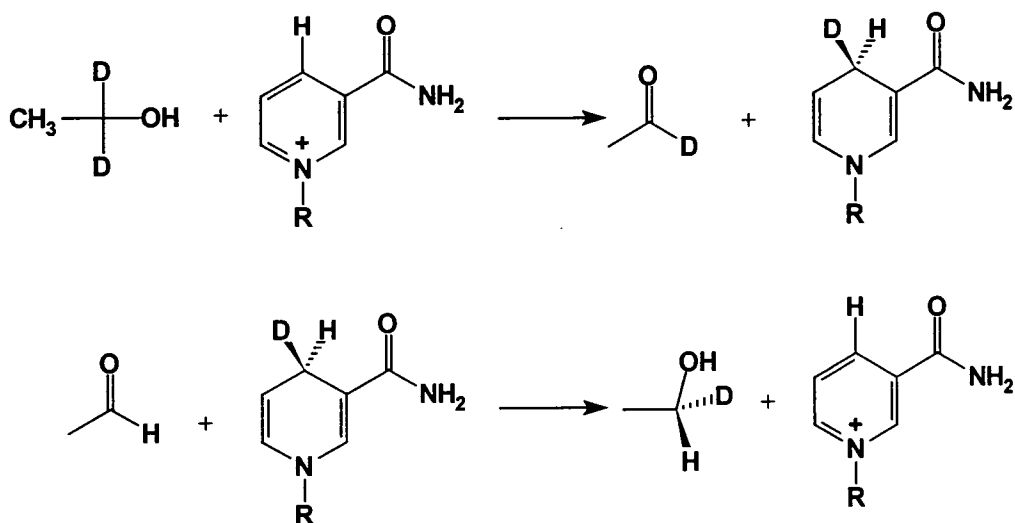
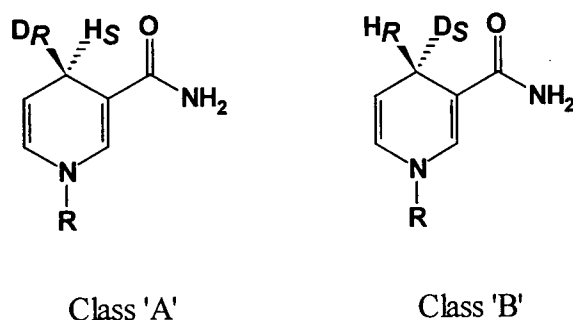


Fig. 2.5

Through the use of deuteriated substrates it has been determined that some dehydrogenases will transfer hydrogen to one face of the ring preferentially, while others will transfer to the opposite face. The enzymes have therefore been classified as 'A' or 'B' on this basis (Table 2.1).



The enzymes in class 'A' transfer the *pro-4R* hydrogen from NAD(P)H to a substrate, whereas those in class 'B' transfer the *pro-4S* hydrogen. Crystal structures of the dehydrogenases show that for the class 'A' enzymes the NAD⁺ binds with the nicotinamide ring in the *anti* conformation about the glycoside bond, where the class 'B' enzymes bind in the *syn* conformation.⁸⁴

Table 2.1 The co-enzyme specificity of some dehydrogenases⁸⁵

Dehydrogenase	Co-enzyme	Stereospecificity class
Glutamate	NAD ⁺ or NADP ⁺	B
Glucose-6-phosphate	NADP ⁺	B
3-Glycerol phosphate	NAD ⁺	B
Glyceraldehyde-3P	NAD ⁺	B
Alcohol	NAD ⁺	A
Lactate	NAD ⁺	A
Isocitrate	NADP ⁺	A

The specificity shown by the enzyme is thought to arise as a natural consequence of the fact that enzymes are asymmetric molecules that form highly stereoselective complexes with their substrates. The enantiomeric specificity of HLADH has been widely exploited for the resolution of racemic alcohols and ketones.⁸⁶

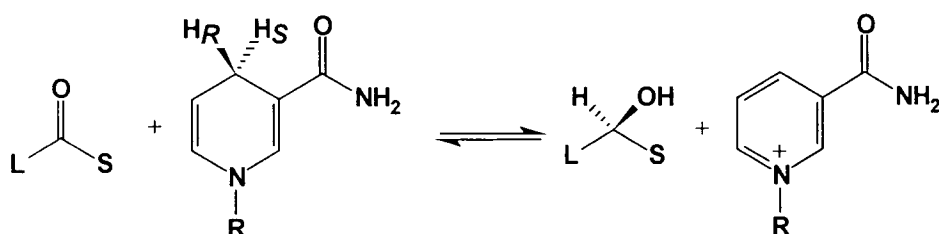


Fig. 2.6 Stereochemical course of most ADH-catalysed reactions

The stereochemical course for most ADH catalysed reductions is known to involve attack at the *re* face of the carbonyl by the *pro-4R* hydrogen giving an alcohol with the *S* configuration (Fig. 2.6). This observation has been formulated as Prelog's rule.⁸⁷

The major practical problem with the use of enzymes in organic synthesis is the expense of co-enzymes like NAD(P)H. The co-enzymes are much more expensive than the most expensive competitive selective chemical reducing agent. This economic problem can be overcome by using catalytic quantities of the co-enzyme and recycling it *in situ* to the active form. Recycling can be achieved in three ways; non-enzymatically, *e.g.* with sodium dithionite ($\text{Na}_2\text{S}_2\text{O}_4$),⁸⁸ enzymatically by a coupled enzyme system or enzymatically by a coupled substrate system. The first extensively-used method employed coupled substrates using only one enzyme which catalyses the desired redox reaction as well as the recycling reaction.⁸⁹ This is achieved by the addition of a second compound which is a good substrate for the enzyme but in the opposite direction (Fig. 2.7).

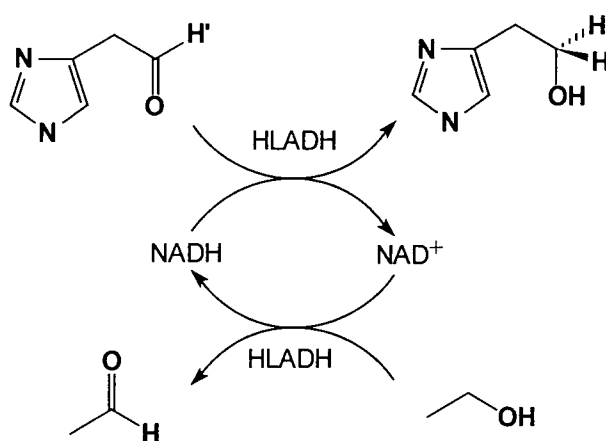


Fig. 2.7 Coupled-substrate NADH regeneration⁹⁰

In coupled enzyme recycling methods an auxiliary enzyme system is used to regenerate the active co-enzyme. This auxiliary enzyme may be one single enzyme or a multi-enzyme system. It was the work of Whitesides who first demonstrated that NAD(P)H could be recycled in up to mole quantities using a coupled enzyme system^{91,92} and this will be discussed further in Chapter 5.

2.1.1 Enoyl reductases

In contrast to the alcohol dehydrogenases, NAD(P)H-dependent enoyl thioester reductases have received limited study, even though such enzymes play a key role in processes such as fatty acid and polyketide biosynthesis.⁹³ In the biosynthesis of fatty acids the enoyl reductase is the enzyme responsible for catalysing the final reaction in

the cycle of condensation–reduction–dehydration–reduction sequence that results in the lengthening of the fatty alkyl chain by one CH_2CH_2 unit.⁹⁴

Interestingly, up until the final stage of the cycle it appears that the individual enzymes of the fatty acid synthetase (FAS) operate with a universal stereo-integrity. However, the stereochemical course of the final reduction by the enoyl reductase appears to vary in different organisms. Within the final reduction by the enoyl reductase there are three stereochemical issues to be addressed. Firstly, which of the hydrogens, *pro-4R* or *pro-4S*, in NADPH is delivered to the alkene. Secondly, to which face of the alkene at C-3 is the hydrogen transferred. Finally, to which face does protonation from the medium occur at C-2. *trans*-2-Enoyl reductases from different sources are known to utilise different prochiral hydrogens of NAD(P)H and present to them to varying faces of the double bond (Fig 2.8).

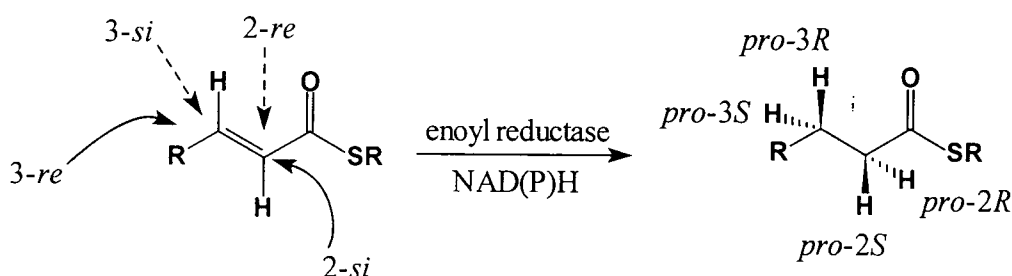


Fig. 2.8 Stereochemistry of enoyl reductases

The reductase from *E. coli*, for example, is known to present the *pro-4S* hydrogen of NADPH, and adds hydrogens suprafacially to the *2re,3si* face of the double bond. Yeast also transfers the *pro-4S* hydrogen of NADPH but instead adds hydrogens antarafacially in a *2si,3si* mode. Some of the available stereochemical data on this transformation is summarised in Table 2.2.⁹⁵

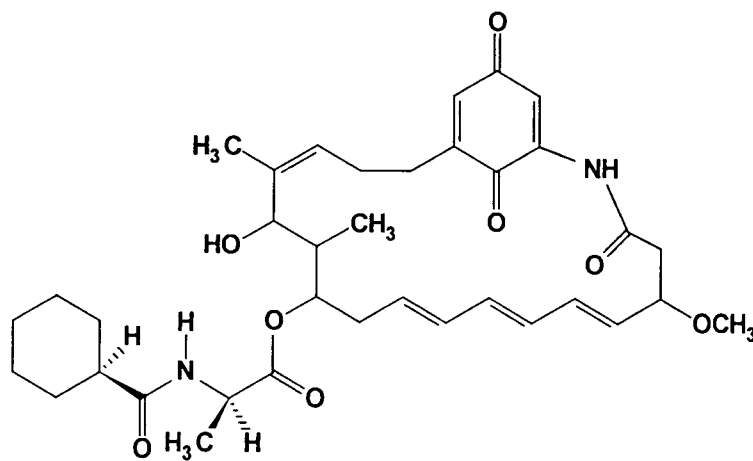
Table 2.2 Stereochemistry of various *trans*-2-enoyl reductases

Source	NAD(P)H	C-2	C-3	Classification
<i>E. coli</i>	<i>pro-4S</i>	<i>re</i>	<i>si</i>	bacteria
<i>A. nidulans</i>	—	<i>re</i>	—	blue-green algae
<i>B. ammoniagenes</i>	<i>pro-4S</i>	<i>si</i>	<i>si</i>	bacteria
<i>S. cerevisiae</i>	<i>pro-4S</i>	<i>si</i>	<i>si</i>	yeast
Rat Liver	<i>pro-4R</i>	<i>si</i>	<i>re</i>	mammal
<i>A. cinerariae</i>	—	<i>si</i>	—	fungi

The stereochemical outcome at C-2 of a number of fungal strains (*A. cinerariae* and *C. cladosporioides*) which produce polyketide secondary metabolites has also been investigated.⁹⁵ The enoyl reductase of fungal polyketide synthase presents hydride to the *re* face at C-2, whereas *in the same organism* the corresponding enzyme from the FAS presents hydride to the *si* face at C-2. This observation suggests that the polyketide synthase and FAS have different evolutionary origins.

2.2 Cyclohex-1-enylcarbonyl-CoA reductase (CHCR)

Ansatrienin A (mycotrienin I) **30** is an antibiotic metabolite that has been isolated from *Streptomyces collinus*⁹⁶ and *Streptomyces rishiriensis*⁹⁷ and shows pronounced activity against fungi and yeasts.



The structure of the antibiotic is unusual in that it contains a cyclohexanecarboxylic acid moiety which is attached *via* an alanine residue to the ansa ring system. Biosynthetic studies have revealed that the cyclohexanecarboxylic acid moiety is derived intact from the seven carbon atoms of Shikimic acid **31**.^{98,99} The cyclohexanecarboxylic acid of **30** was also found to have exclusively an *S* configuration at C-1 of the cyclohexane ring upon incorporation of [2-¹³C]Shikimic acid. Furthermore, evidence that the pathway to cyclohexanecarboxylic acid passes through a cyclohex-1-enecarboxylic acid intermediate **34** was obtained with the detection of an ansatrienin analogue (ansatrienin A4) which contains a cyclohex-1-ene rather than a cyclohexane moiety.⁹⁸ Conversion to the cyclohex-1-enecarboxylic acid moiety is accompanied by migration of the original double bond in the ring. The final process apparently involves the reduction of the double bond by addition of hydrogen to the *re*-face of C-1 (Fig. 2.9).

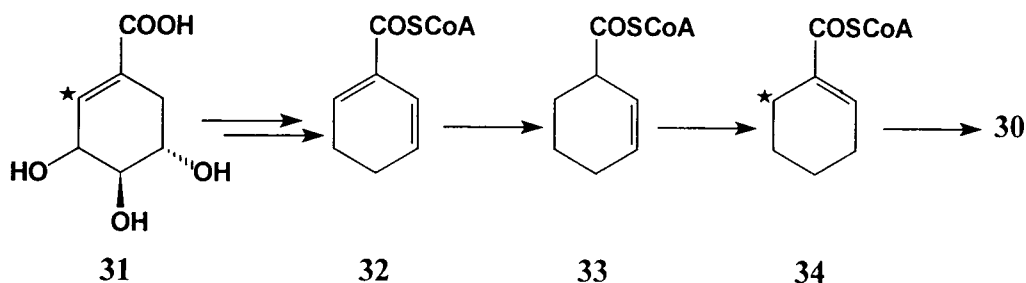


Fig. 2.9 Incorporation of [2-¹³C]Shikimic acid into ansatrienin **30**

The unique pathway from Shikimic acid to the cyclohexanecarboxylic acid **35** would appear to progress through a series of alternating dehydrations and reductions. The last three steps of the pathway involve a reduction of the α,β -double bond of cyclohexa-1(6),2-dienylcarbonyl-CoA **32** to produce cyclohex-2-enylcarbonyl-CoA **33**. This then undergoes an isomerisation of the double bond into conjugation with the carbonyl group to give cyclohex-1-enylcarbonyl-CoA **34**. Finally, the alkene is reduced by an enoyl reductase activity to give the cyclohexanecarboxylic acid moiety which is incorporated into **30**.

Reynolds and co-workers have isolated the NADPH enoyl reductase activity from *Streptomyces collinus*.^{100,101} This was the first isolation of an enoyl-reductase activity involved in a secondary metabolic process. The purified enzyme catalyses the conversion of cyclohex-1-enylcarbonyl-CoA **34**, to the corresponding thioester of cyclohexanecarboxylic acid **35**. The enzyme has recently been cloned, over-expressed

in *E. coli*, purified to homogeneity and has been named cyclohex-1-enylcarbonyl-CoA reductase (CHCR).¹⁰²

This reductase is a dimer with subunits of identical M_r (36 000). It exhibits a K_m of $1.5 \pm 0.3 \mu\text{M}$ for NADPH and $25 \pm 3 \mu\text{M}$ for cyclohex-1-enylcarbonyl-CoA and it is most active at 30 °C at a pH optimum of 7.5, with a rapid fall-off in activity at pH values above 7.5. Like other previously studied enoyl reductases it is inhibited by thiol reagents, and divalent cations (only if preincubated without co-factor). The enzyme is also highly specific for NADPH as the co-factor, with no measurable activity being observed with NADH. Unlike some other enoyl reductases, which have been shown to be active with the *N*-acetylcysteamine derivatives of the carboxylic acids,⁹⁴ the enzyme showed no activity with either the free acid or *N*-acetylcysteamine derivatives and was only active when the cyclohex-1-enecarboxylic acid was activated as the CoA thioester.

The stereochemical course of the reduction step has been evaluated by Reynolds.¹⁰⁰ The reduced cyclohexanecarbonyl-CoA produced after an incubation of **34** in $^2\text{H}_2\text{O}$ was hydrolysed, and converted into its corresponding methyl ester. The methyl cyclohexanecarboxylate obtained was found to be 77% monodeuteriated at C-1 by GC-MS analysis. In order to determine the stereochemical course of hydrogen incorporation at C-2, [(4*R*)- ^2H]NADPH and [(4*S*)- ^2H]NADPH were synthesised and used in the reduction. Deuterium incorporation was only seen with [(4*S*)- ^2H]-labelled NADPH.

Thus the stereochemical course of the reduction of **34** to **35** catalysed by cyclohex-1-enylcarbonyl-CoA reductase proceeds by transfer of the *pro*-4*S* hydrogen of NADPH to the *si* face of the β carbon (C-2) and hydrogen incorporation at the α carbon (C-1) from the medium (H_2O) in an *anti* mode (Fig. 2.10).

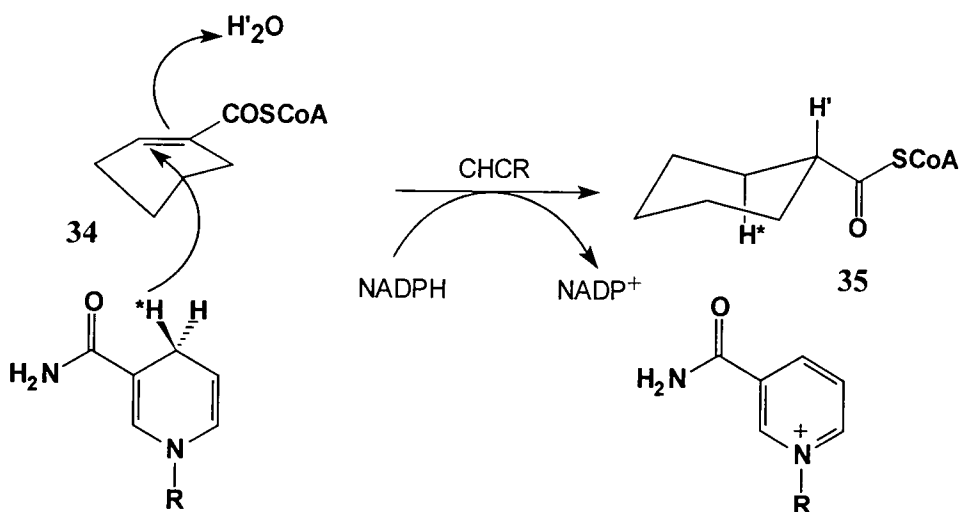
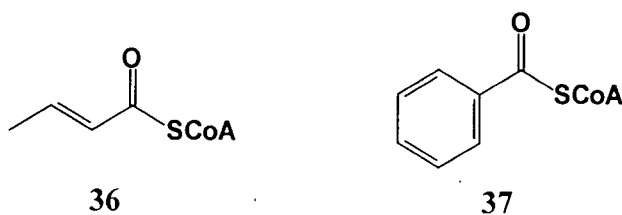


Fig. 2.10 Stereochemical course for the conversion of **34** to **35** catalysed by cyclohex-1-enylcarbonyl-CoA reductase

This enzymatic system attracted our attention as the product of the reduction **35** contains a cyclohexane ring. The cyclohexane ring has long occupied a central place in the study and development of stereoelectronic theory, and therefore this enoyl reductase offered a unique and highly attractive system with which to probe the stereoelectronic effect of a fluorine atom in an enzymatic transformation.

2.3 Exploring Anh–Eisenstein stabilisation

Reynolds has shown that CHCR will accept some novel substrates. The enzyme was shown to display similar levels of activity for cyclohexa-1(6),2-dienylcarbonyl-CoA **32** and cyclohex-1-enylcarbonyl-CoA. Analysis of the incubation of **32** with CHCR revealed that the product was exclusively cyclohex-2-enylcarbonyl-CoA **33**. The enzyme also reduced *trans*-hexenoyl-CoA but it showed no activity with crotonyl-CoA **36**, benzoyl-CoA **37** or cyclohex-2-enylcarbonyl-CoA. However, low levels of reduction were observed for cyclohexa-1,3-dienylcarbonyl-CoA (13%) and cyclohexa-1,4-dienylcarbonyl-CoA (28%).¹⁰¹



The introduction of fluorine onto the cyclohexene ring system would allow further probing of the substrate specificity of the enzyme, but more importantly, the stereoelectronic effect of a fluorine atom in an enzymatic transformation could be tested with the reductase. In the previously cited examples of lipase resolutions with fluorinated substrates, the fluorine atom was placed on the α carbon of the sp^2 carbon centre under nucleophilic attack. It was then possible to explain the high levels of stereoselectivity by an Anh–Eisenstein stabilising interaction.

Similarly, substitution of a single fluorine atom at either the allylic C-3 or C-6 positions in the cyclohex-1-enylcarbonyl-CoA substrate might induce the same effect. This substitution, as discussed in Chapter 1, would be expected to impart only a small steric perturbation on the ring because of the similar sizes of fluorine and hydrogen, but it may induce significant changes in the electronic character of the substrate.

Clearly, in the fluorinated substrate analogue the fluorine atom may occupy either an axial or equatorial position in the substrate. If the approach of the incoming hydride nucleophile is considered with respect to the fluorine on the α -carbon then two diastereoisomeric transition states emerge (Fig. 2.11).

2.3.1 3-Fluorocyclohex-1-enylcarbonyl-CoA 41

It can be envisaged that for the 3-fluorocyclohex-1-enylcarbonyl-CoA substrate the (3*R*) pseudo-axial fluorine would give the lower energy transition state. In this case approach to the double bond at C-2 is antiperiplanar to the fluorine, allowing an Anh–Eisenstein $n-\sigma^*$ stabilising interaction to occur (Fig. 2.11). This stabilisation is not, however, possible if the fluorine occupies a pseudo-equatorial position (3*S*). It would therefore be anticipated that the enzyme will show a kinetic discrimination in favour of the (3*R*) isomer over the (3*S*) if such a stereoelectronic effect operates.

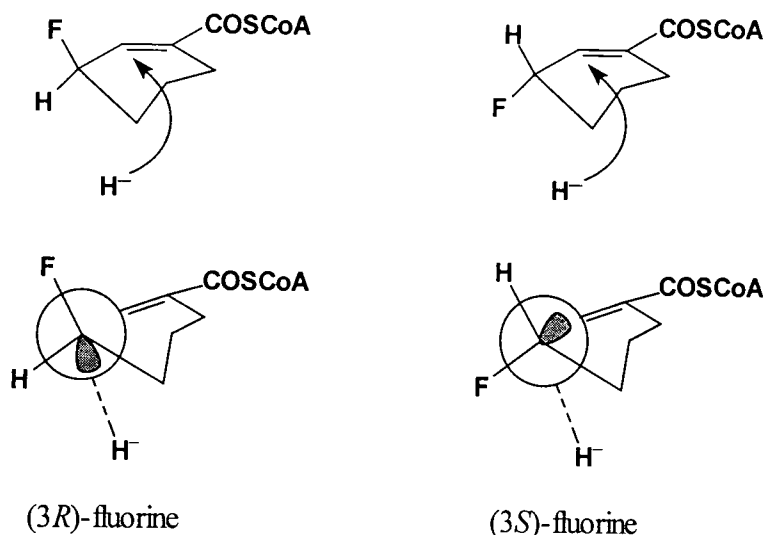


Fig 2.11 Schematic representation of the transition states for hydride delivery to **41**

2.3.2 6-Fluorocyclohex-1-enylcarbonyl-CoA

If the reaction is interpreted such that in the course of the reduction an anion develops at C-1, a fluorine at C-6 may also stabilise this anion by an Anh–Eisenstein interaction. In this case the anion may be stabilised *at the transition state* by an axially orientated fluorine, and much less significantly by an equatorial fluorine at C-6 (Fig. 2.12). At the outset a comparison of rates for the C-3 and C-6 fluorinated substrates appeared valid and attractive to determine if discrimination between an early or late transition state could be evaluated.

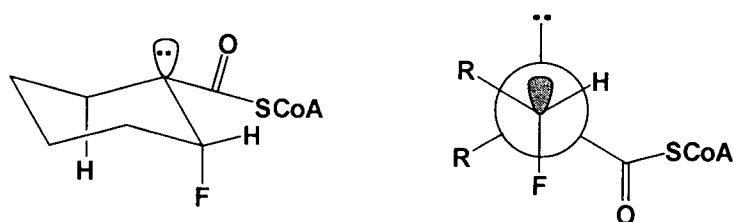


Fig. 2.12 Schematic representation of stereoelectronic stabilisation of an anion at C-1 by an axial fluorine at C-6

2.3.3 ^{19}F NMR spectroscopy of fluorocyclohexanes

It is well established that axial and equatorial fluorines on a cyclohexane ring can easily be distinguished by ^{19}F NMR spectroscopy. Roberts' work, using ^{19}F NMR spectroscopy as an aid to conformational analysis with *gem*-substituted difluorocycloalkanes, illustrated how at low temperatures the axial and equatorial fluorines are easily distinguishable.¹⁰³

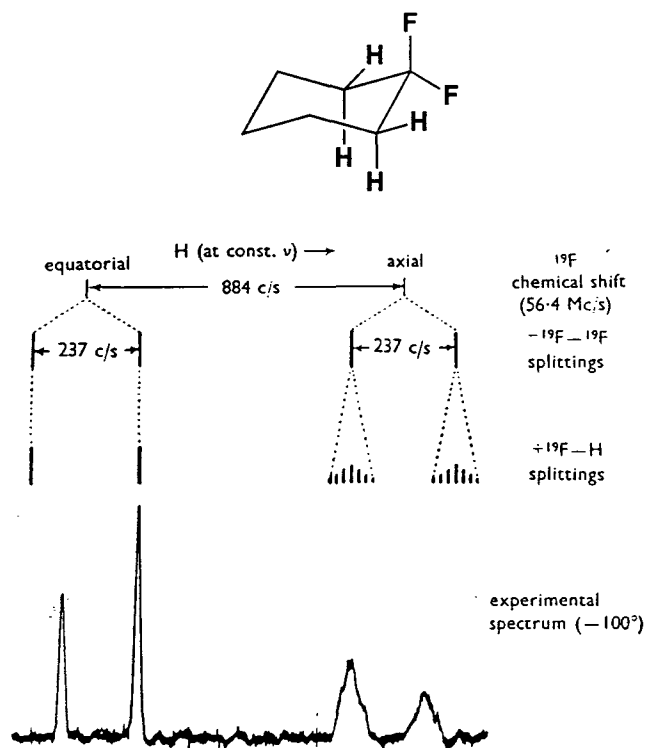


Fig. 2.13 Chemical shift and spin-spin splitting in ^{19}F NMR spectrum of 1,1-difluorocyclohexane at -100°C

The observed ^{19}F NMR spectrum at -100°C (Fig. 2.13) showed a chemical shift difference between the two fluorines of 884 Hz at 56.4 MHz, a fluorine-fluorine splitting of 237 Hz and finally fluorine-hydrogen splittings which were assumed to only involve the four vicinal hydrogens. With the axial fluorines coupling more strongly with the adjacent hydrogens it was possible to assign the axial and equatorial fluorines in the spectra.

Cantacuzène also used ^{19}F NMR with a number of substituted cyclohexane rings to show how the axial and equatorial fluorines were readily identifiable. One specific

example used the cyclohexane derivative **38** in which the two fluorine resonances were observed to be 4 ppm apart and, as for 1,1-difluorocyclohexane, were easily assignable by their ^{19}F - ^1H coupling patterns.¹⁰⁴

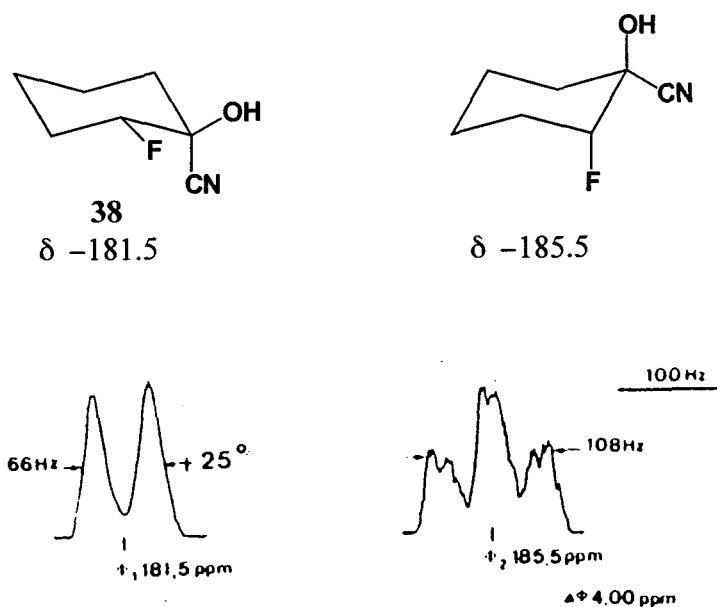


Fig. 2.14 Observed ^{19}F NMR spectra of **38** at $-100\text{ }^\circ\text{C}$

With the ease of assignment of the axial and equatorial fluorines in a cyclohexane ring it was envisaged that any kinetic preference exercised by the enoyl reductase (CHCR) should therefore be assayable directly by ^{19}F NMR spectroscopy. This could be achieved by analysis of the reaction and determining the relative rates of accumulation of both axial and equatorial products. This assay meant it was unnecessary to produce the fluorinated substrates in a homochiral form; they could be used as a racemate in a competitive reaction using ^{19}F NMR spectroscopy to monitor the products of the reduction.

Implicit in this analysis using ^{19}F NMR spectroscopy, however, is the anticipated conformational preference for the product with the thioester group occupying the equatorial position at C-1. This preference should ensure little interconversion of the products upon their formation in the enzymatic reduction. It is therefore anticipated that the (3*R*)-3-fluorocyclohex-1-enylcabonyl-CoA will give predominantly the axially orientated product upon reduction and likewise the (3*S*) isomer will give the equatorial product.

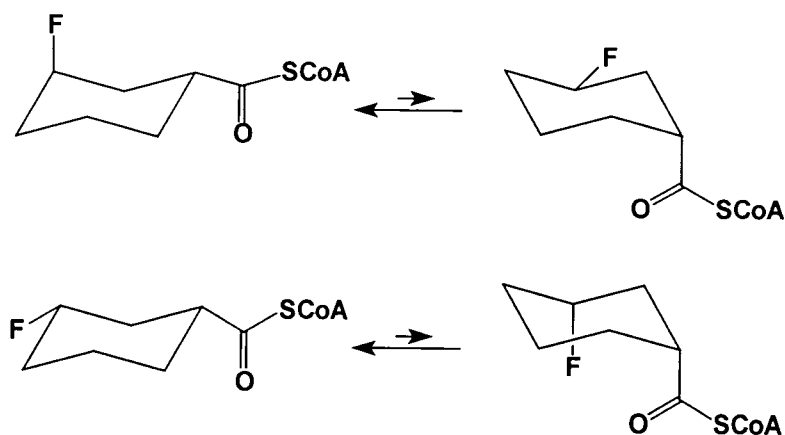


Fig. 2.15 Interconversion of axial and equatorial products

Conformational free energy differences, or 'A values', give the energy difference between axial and equatorial conformers for monosubstituted cyclohexanes.²⁰ Some values are listed in Table 2.3.

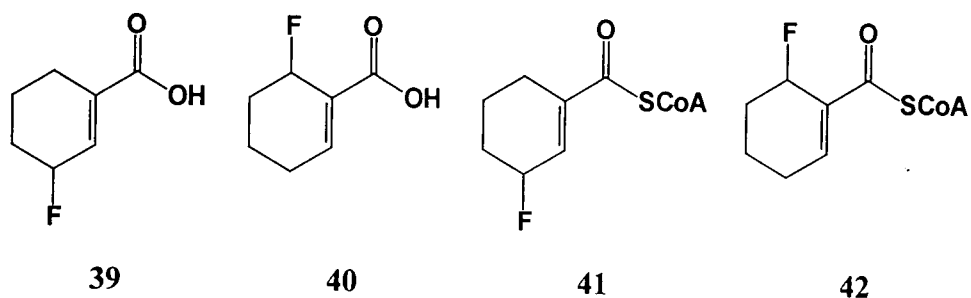
Table 2.3 Conformational free energy differences for monosubstituted cyclohexanes

Substituent	$-\Delta G^0/\text{kcal mol}^{-1}$
F	0.25–0.42
CH ₃	1.74
CO ₂ CH ₃	1.2–1.3
COF	1.4–1.7
C(CH ₃) ₃	4.7

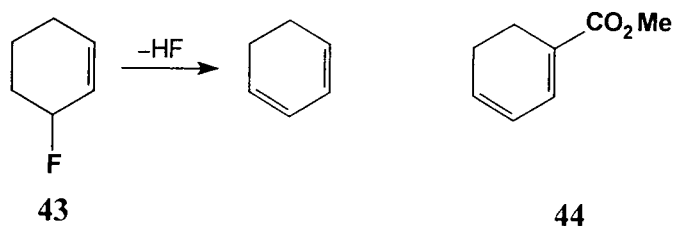
The values demonstrate that for a thioester a value of approximately 1.4 kcal mol⁻¹ may be anticipated. This, together with the small value for fluorine, should prevent any interconversion of the isomers; particularly unfavourable would be the diaxial species formed by the 'ring flip' of the equatorial product. However, any small interconversions should cancel out and would not be anticipated to effect the observed outcome of the reduction.

2.4 Target compounds

For this study it was necessary to synthesise 3-fluorocyclohex-1-enylcarbonyl-CoA **41** and 6-fluorocyclohex-1-enylcarbonyl-CoA **42**. The synthetic targets were the corresponding free carboxylic acids **39** and **40** which would be activated in due course to their CoA esters.

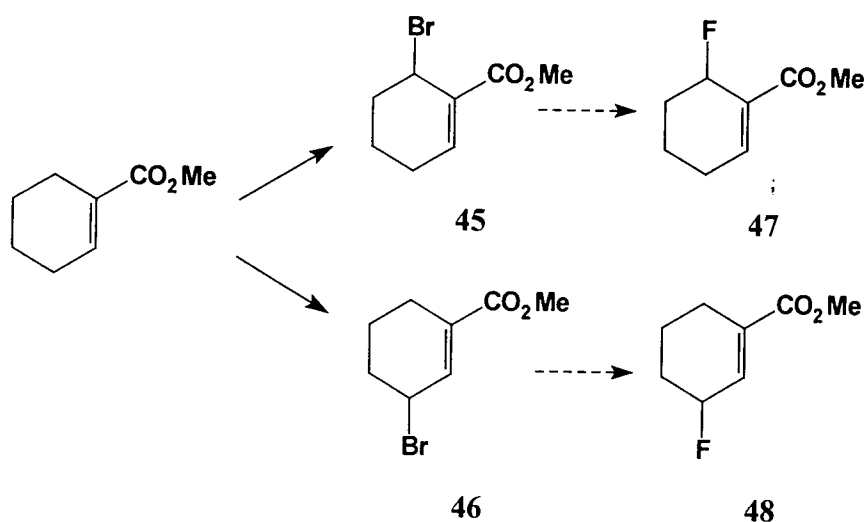


The mono-fluorinated cyclohexenes had not previously been synthesised and thus a synthetic route to the compounds had to be developed. Hudlicky has reported a synthesis of 3-fluorocyclohex-1-ene **43** but found it was unstable and rapidly decomposed at room temperature with the elimination of HF.¹⁰⁵ The eliminated HF reacted strongly with glass and blue-green decomposition products containing cyclohexa-1,3-diene were detected. In view of this observation we were concerned that we may also experience difficulties with HF elimination during the course of the preparation of **41** and **42**. The expected products of HF elimination from compounds like **39–42** would be the corresponding cyclohexa-1,3-dienes. The data provided by Delany in the synthesis of methyl cyclohexa-1,3-diene **44** could be used to assess if any HF elimination was occurring to afford the cyclohexa-1,3-dienes.¹⁰⁶



2.5 Synthesis of fluorocyclohexenes

Initial preparative routes to the target compounds were based around a halogen exchange reaction replacing bromine with fluorine. The requisite 3- and 6-brominated isomers **45** and **46** were produced by the allylic bromination of commercially available methyl cyclohex-1-enecarboxylate with *N*-bromosuccinimide (NBS) and AIBN.^{107,108} The reaction gave a mixture of the two regioisomers (*ca.* 1:1 ratio), but in low overall yields, producing only small amounts of product (50 mg) for further reaction. The two regioisomers were separable by column chromatography and were assigned by COSY ¹H NMR spectroscopy.



The halogen exchange was initially attempted using silver fluoride in wet acetonitrile.¹⁰⁹ Product analysis by ¹⁹F NMR spectroscopy did not indicate any incorporation of organic fluorine. Further analysis of the product was consistent with the formation of the 6-hydroxy compound **49**, presumably *via* a silver ion-assisted displacement of the bromine either directly or by an S_N2' process (Fig. 2.16). Further attempts using antimony trifluoride in refluxing benzene and THF also proved to be ineffective methods for the replacement of the bromine with a fluorine atom.⁶

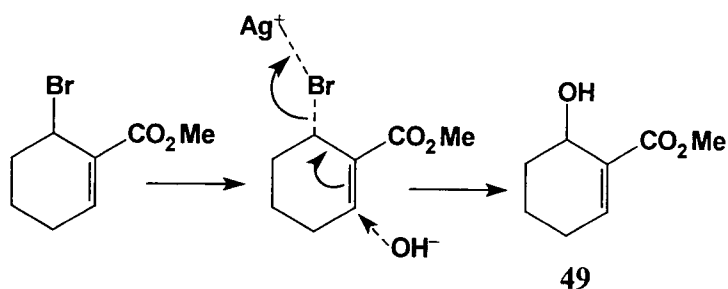


Fig. 2.16

2.5.1 Synthesis of 3-fluorocyclohex-1-enecarboxylic acid **39**

It became attractive to generate the appropriate methyl 3-hydroxycyclohex-1-enecarboxylate **51** such that an attempt could be made to fluorinate it using DAST.⁷² The proposed route outlined in Fig. 2.17 again began with the readily available methyl cyclohex-1-enecarboxylate. This was initially oxidised to give the α,β -unsaturated ketone compound **50** which could be subsequently reduced to afford the desired allylic alcohol **51**.

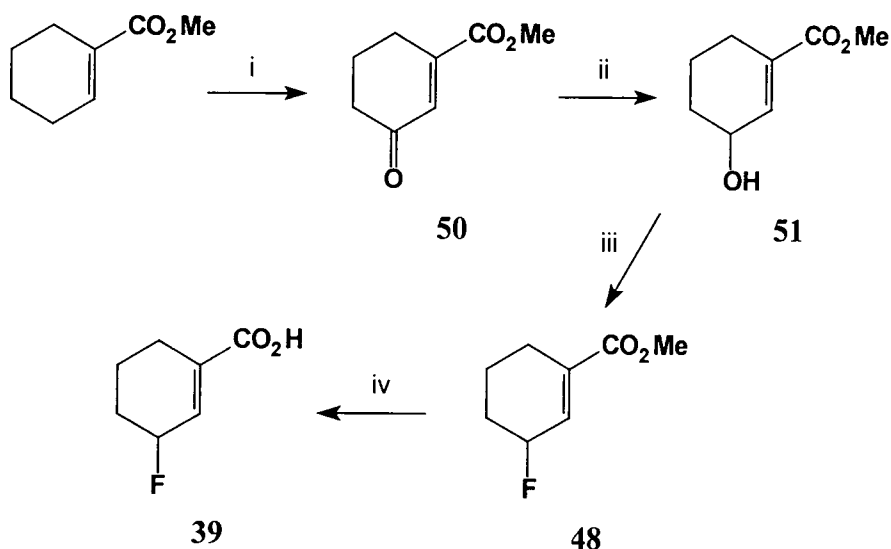


Fig. 2.17 Reagents: i, CrO_3 , AcOH, Ac_2O , benzene, 56%; ii, NaBH_4 , $\text{CeCl}_3 \cdot 7\text{H}_2\text{O}$, MeOH, 80%; iii, DAST, CH_2Cl_2 , 69%; iv, 5% KOH in MeOH, 77%

The allylic oxidation was achieved using 3 equiv. of chromium trioxide in an oxidising solution of acetic acid and acetic anhydride in benzene.^{110,111} This generated the desired 3-oxo product **50** in 56% yield.

The regioselective 1,2 reduction of the α -enone **50** was achieved following the conditions of Luche, using NaBH_4 in conjunction with $\text{CeCl}_3 \cdot 7\text{H}_2\text{O}$ in methanol.¹¹² After significant experimentation Luche determined that the optimal conditions for yield and regioselectivity were a 1 equiv. of NaBH_4 for each mole of substrate in a 0.4 M methanolic solution of $\text{CeCl}_3 \cdot 7\text{H}_2\text{O}$. Under these conditions the reduction of **50** proved successful and the desired allylic alcohol **51** was recovered in 80% yield after purification. When the reduction was attempted in the absence of the $\text{CeCl}_3 \cdot 7\text{H}_2\text{O}$ concomitant 1,2 and 1,4 reduction was observed with none of the desired product being isolated. Luche considered the major role of the Ce^{3+} in the regioselective reduction to be the catalysis of BH_4^- decomposition by the solvent to afford alkoxyborohydrides. The substitution of hydrides in BH_4^- increases the hardness of the reagent and enhances the attack at the hard C-2 carbon of the conjugate enone (Fig. 2.17).

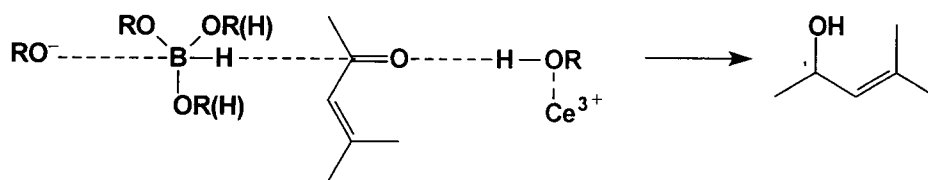


Fig. 2.18 Luche's mechanistic interpretation of 1,2 reduction with Ce^{3+}

With the allylic alcohol in hand the fluorination was attempted. Despite the potential for elimination, fluorination with DAST proved straightforward, affording the desired allylic fluorine compound **48** in 69% yield, an overall yield of 31% from methyl cyclohex-1-enecarboxylate. This route proved relatively straightforward and enabled several grams of **48** to be prepared in a satisfactory state of purity.

The final stage of the synthesis required the conversion of the methyl ester **48** to the free carboxylic acid **39**. With the anticipated potential problem of base-induced elimination of HF, the initial methods of hydrolysis which were considered all avoided the use of base. Initially enzymatic hydrolysis under neutral conditions was explored. Pig liver esterase, wheatgerm lipase and the *Candida cylindracea* lipase were all employed to try to effect hydrolysis. The course of the enzyme reactions were followed over time by ^{19}F NMR spectroscopy directly on the reaction solutions. Although the NMR analysis showed progressive changes, no free carboxylic acid could be isolated. It was also clear by ^{19}F NMR spectroscopy that fluorine was lost as fluoride on work up.

The second reagent explored for the hydrolysis of the ester was trimethylsilyl iodide (TMSI), which can also hydrolyse esters under neutral conditions.^{113,114} After work up, ¹⁹F NMR analysis of the product did not show the presence of any organofluorine compounds. This may be due to silicon's high affinity for fluorine resulting in the formation of trimethylsilyl fluoride.

Base hydrolysis of the ester was attempted using a 5% solution of KOH in methanol. The reaction could easily be monitored by TLC and after 1 h the starting material had been consumed. The reaction was acidified and the products extracted into diethyl ether. Upon removal of the solvent a white solid formed which proved to be the desired 3-fluorocyclohex-1-enecarboxylic acid **39**. The compound was unstable at room temperature, thus in order to prevent decomposition- it was necessary to store the material at -20 °C. Nonetheless the compound could be readily prepared and was used on several occasions throughout the programme.

2.5.2 Synthesis of 6-fluorocyclohex-1-enecarboxylic acid **40**

In an attempt to synthesise the 6-fluoro analogue of cyclohex-1-enylcarbonyl-CoA, an analogous strategy to that used for the 3-fluoro isomer was implemented. Thus the allylic alcohol **53** became the substrate required for fluorination. The commercially available ethyl 2-oxocyclohexanecarboxylate was readily converted into the β -dicarbonyl derivative **52** by selenation using a 1:1 complex of phenylselenenyl chloride and pyridine. This was followed by an *in situ* oxidation using 30% hydrogen peroxide which afforded **52** in 95% yield (Fig 2.19).¹¹⁵ This method for the formation of unsaturated β -dicarbonyls works particularly well in compounds where the β -dicarbonyl compound exists substantially in its enolised form.¹¹⁵

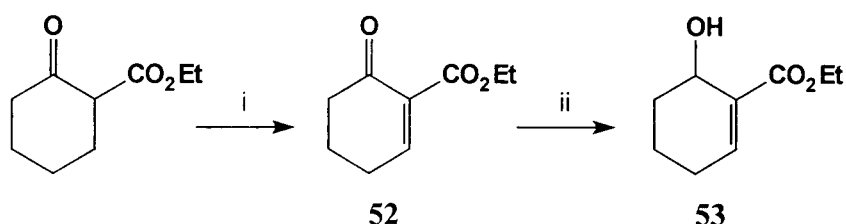


Fig. 2.19 Reagents: i, PhSeCl-pyridine, CH₂Cl₂, H₂O₂, 95%; ii, NaBH₄, CeCl₃·7H₂O

With the unsaturated β -dicarbonyl compound **52** in hand the selective reduction was attempted with NaBH_4 and $\text{CeCl}_3 \cdot 7\text{H}_2\text{O}$ to obtain the allylic alcohol **53**. However in this case, even with the $\text{CeCl}_3 \cdot 7\text{H}_2\text{O}$, the double bond was significantly reduced by a 1,4 hydride addition. ^1H NMR analysis of the crude product from the reduction showed that all the alkene had been reduced, and there was a concomitant increase in the complexity of the CH_2 region. It appeared that in this case 1,4 addition was unhindered and occurred rapidly, whereas in the case of the 3-oxo isomer **50**, attack of the hydride in a 1,4 manner is controlled by the addition of the lanthanoid.

An alternative method was attempted which formed **53** directly in a one pot reaction.¹¹⁶ The reaction is a bis-aldolisation using commercially available aqueous 25% glutaraldehyde and triethyl phosphonoacetate. The Wittig–Horner reaction under weak basic conditions gave rise to two products, the desired 6-hydroxy compound **53** and the dienic diester **54**, which are obtained from the concurrent bis-aldolisation and elimination processes on the first aldol intermediate (Fig. 2.20).

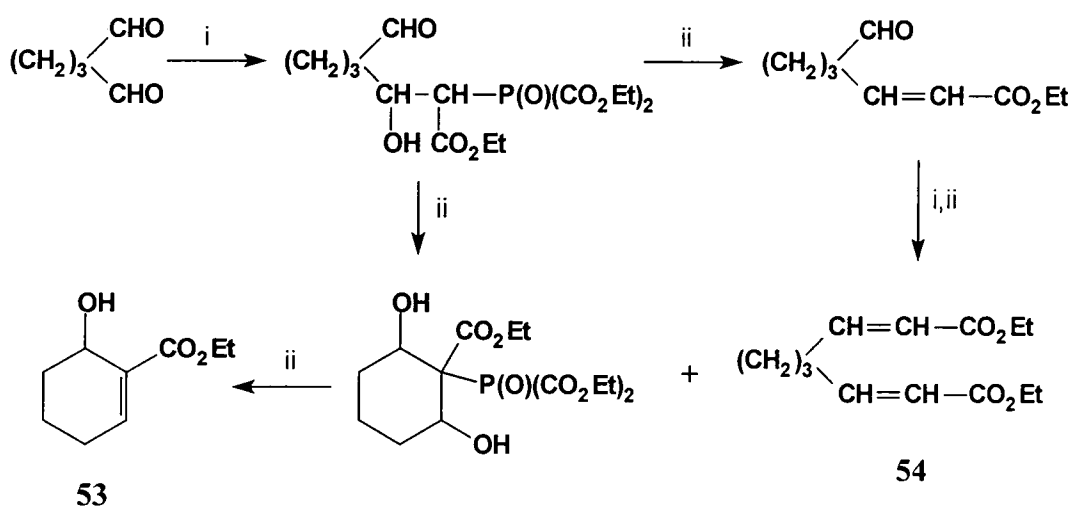


Fig 2.19 Reagents: i, $(\text{EtO})_2\text{P}(\text{O})\text{CH}_2\text{CO}_2\text{Et}$; ii, K_2CO_3

The two products of the reaction were easily separated by distillation and the reaction was amenable to scale-up, allowing the production of several grams of material. Fluorination using DAST generated the desired 6-fluoro ethyl ester **55**, which was purified, giving satisfactory analytical data.

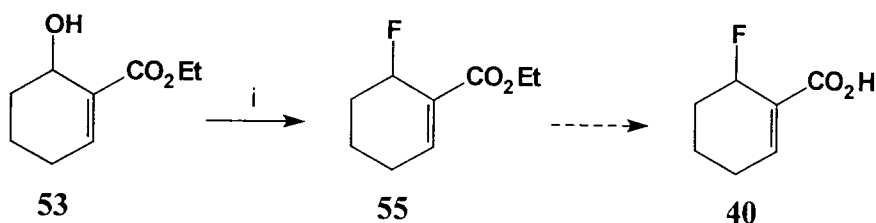


Fig. 2.21 Reagents: i, DAST, CH_2Cl_2 , 69%

Activation to the CoA ester again initially required the hydrolysis of the ester to the free acid and it was at this stage that an insurmountable problem arose. In order to hydrolyse the ester the same methods as used previously were attempted. However, no method was found to hydrolyse the ester and all the methods employed resulted in the loss of organofluorine material as determined by ^{19}F NMR spectroscopy. Analysis of the product from the TMSI reaction appeared to show the formation of an iodo species, possibly by an $\text{S}_{\text{N}}2'$ reaction involving I^- as a nucleophile. Methanolic KOH hydrolysis resulted in some transesterification, as well as loss of fluorine with the formation of the methyl ether. To prevent the transesterification the methyl ester **47** was prepared using trimethyl phosphonoacetate in the Wittig–Horner reaction with glyceraldehyde. Subsequent hydrolysis with methanolic KOH was, however, unsuccessful with loss of organic fluorine. Acidic hydrolysis using THF–HCl mix gave the same unsuccessful result. At this stage it also became a concern that, even if it were possible to synthesise the free acid **40**, it may not prove possible to activate it as the CoA ester. Formation of the thioester would require the addition of a sulfur nucleophile to an activated mixed anhydride (Fig. 2.22); however, with all the previous examples of nucleophiles (H^- , I^- and MeO^-) which had apparently undergone $\text{S}_{\text{N}}2'$ type reactions eliminating fluorine, it was quite likely that this would occur in the formation of the CoA ester.

2.5.3 Synthesis of thio and CoA esters

In order to carry out the enzyme studies with the CHCR it was necessary to activate **39** as its CoA ester. This could be achieved by two methods.

The first involved reaction of the acid with triethylamine and ethyl chloroformate to produce a mixed anhydride **56**. The mixed anhydride is then coupled to CoASH to give the desired thio ester **41** (Fig. 2.22).¹¹⁷ An alternative method

involves reaction with carbonyldiimidazole to form a reactive *N*-acylimidazole intermediate which is coupled to CoASH.

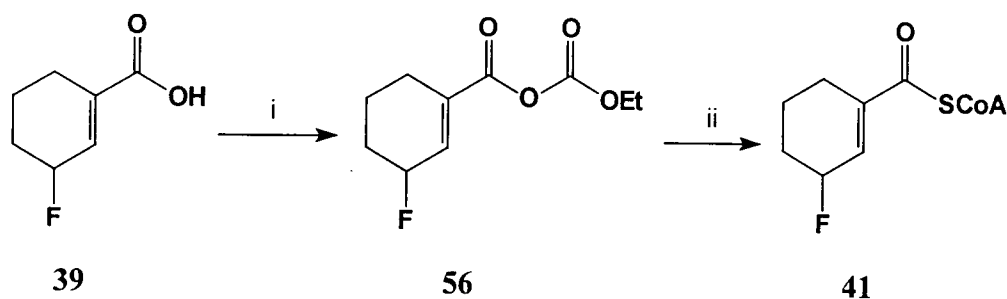


Fig. 2.22 Reagents: i, Et₃N, ClCO₂Et; ii, CoASH

The coupling reaction was initially modelled using *N*-propionylcystamine 58, which is an analogue of co-enzyme A as it bears structural similarities to the terminus of the co-factor. Often the esters formed by *N*-propionylcystamine can be used as enzyme substrates, however it is known that in this case the cyclohex-1-enylcarbonyl-CoA reductase does not accept *N*-acetylcystamine derivatives as substrates.

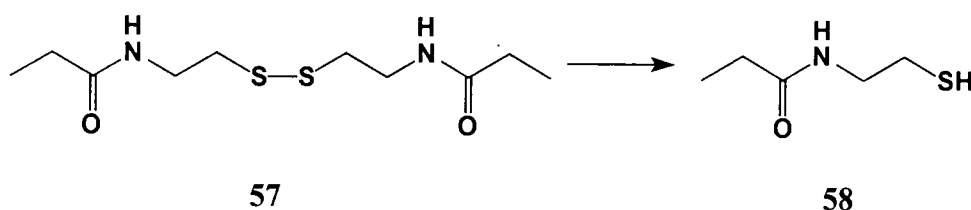
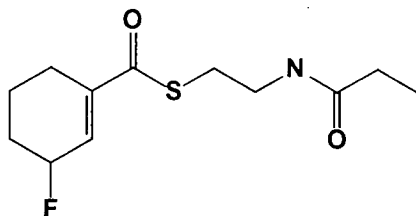


Fig. 2.23

N-propionylcystamine was synthesised from cystamine dihydrochloride and propionyl chloride, which form the disulfide dimer *N,N'*-dipropionylcystamine 57. The disulfide is reduced using 3% sodium amalgam to give 58 as a colourless oil. This material was then efficiently coupled to 39 using triethylamine and ethyl chloroformate to afford the *N*-acetylcystamine derivative 59 as a colourless oil. ¹⁹F NMR spectral analysis of this thioester derivative showed a chemical shift of $\delta -172$, compared with that of the free acid of $\delta -173.3$. Thus the compound provided a model for optimising the activation to the co-enzyme A ester and a useful ¹⁹F NMR reference.



59

In the event the co-enzyme A ester **41** was prepared by the ethyl chloroformate-triethylamine method. The product of the reaction was a white powder generated after freeze-drying the reaction mixture. This material was used directly in the enzyme studies as attempts to purify **41** by HPLC proved unsuccessful due to apparent decomposition. ^{19}F NMR analysis of **41** showed a single peak at $\delta -170$ with fluoride evident, indicating some fluoride release.

2.6 Kinetic studies with fluorinated substrate

Initial experiments carried out demonstrated that the 3-fluorocyclohex-1-enecarbonyl-CoA **41** was a substrate for the enzyme. A series of control experiments showed that the presence of both enzyme and co-factor were required for any reduction of the substrate to take place. ^{19}F NMR analysis of the reaction products demonstrated that the two expected products were clearly visible and could be readily assigned to the axial and equatorial isomers by reference to the ^1H - ^{19}F coupling constants and the examples previously cited.

A kinetic analysis was undertaken to determine the K_m and V_{max} values of the enzymatic reduction, for comparison with those of the natural substrate **34**. The reactions were carried out in 1 ml cuvettes in a potassium phosphate buffer solution (pH 7.3), and were monitored by following the rate of depletion of NADPH spectrophotometrically at 340 nm. The data obtained were used to evaluate the effectiveness of the enzyme to reduce the fluorinated substrate. A kinetic analysis of the fluorinated substrate **41** was carried out independently both in Durham and at the University of Baltimore.

2.6.1 Determination of K_m and V_{max}

K_m and V_{max} are two experimentally measurable kinetic parameters that may be defined as follows.

V_{max} is the maximum initial velocity of the enzyme catalysed reaction under the given conditions, and is the limiting value that v_0 approaches as $[S] \rightarrow \infty$. The value of V_{max} is measured in units of quantity of substrate per unit time for a given concentration of enzyme.

K_m is the Michaelis constant. It can be defined only in experimental terms and equals the value of $[S]$ at which v_0 equals $1/2V_{max}$. The value of K_m is measured in units of concentration.

The Michaelis equation, which relates v_0 (initial velocity) and $[S]$, is normally written as:

$$v_0 = \frac{V_{max} [S]}{[S] + K_m}$$

A plot of v_0 versus $[S]$ gives a hyperbolic graph from which the values of K_m and V_{max} can be read. However in practice it can often prove difficult to draw accurate hyperbola, and to supply sufficiently high concentrations of S to ensure the attainment of V_{max} . These difficulties are overcome by the Lineweaver–Burk equation, which makes use of the fact that the reciprocal of the equation of a rectangular hyperbola is the equation of a straight line.

$$\frac{1}{v_0} = \frac{1}{V_{max}} + \frac{K_m}{V_{max}} \cdot \frac{1}{[S]}$$

Therefore, if $1/v_0$ is plotted against $1/[S]$, a straight line is obtained whose slope is K_m/V_{max} , whose intercept on the y-axis equals $1/V_{max}$, and whose intercept on the negative side of the x-axis equals $-1/K_m$.

In the case of the enoyl reductase activity two substrates have to be considered, the cyclohex-1-enylcarbonyl-CoA and the co-factor NADPH. To perform initial velocity studies with a two substrate system, values of v_0 are measured using different concentrations of one substrate in the presence of a series of fixed concentrations of the

second. In this way, a family of plots is obtained of $1/v_0$ against $1/[S]$ using different fixed concentrations of NADPH. The kinetic parameters, though, cannot be determined from primary reciprocal plots obtained at arbitrary concentrations of fixed substrate (even if this is thought to be saturating). The values of K_m and V_{max} are obtained from secondary plots of (i) the intercepts, and (ii) the slopes of the primary reciprocal plots against the reciprocal of the concentration of the fixed substrate (Fig. 2.24).

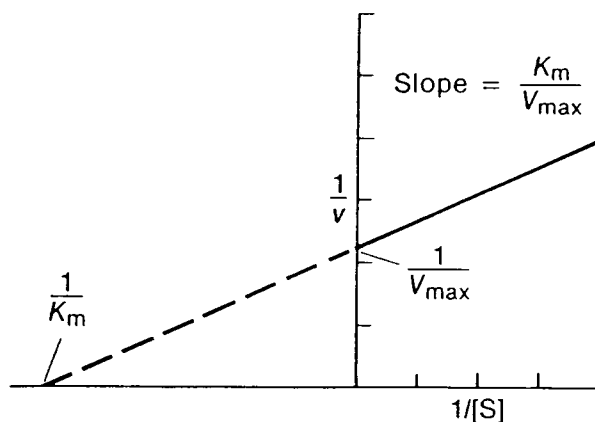


Fig. 2.24 Determination of K_m and V_{max} via Lineweaver–Burk plots

2.6.2 Kinetic analysis: results and discussion

The K_m and V_{max} values were obtained for the enzymatic reduction of the natural substrate cyclohex-1-enylcarbonyl-CoA **34** with purified CHCR using NADPH and [4S- ^2H]NADPH (Table 2.4).¹¹⁸ The results showed a significant decrease in the observed value of V_{max} for the reduction when using [4S- ^2H]NADPH as the co-factor. This observation is indicative of a primary isotope effect such that $k_H/k_D = 3.0$, demonstrating that hydride (or deuteride) delivery is the rate limiting step of the reduction in the case of the natural substrate **34**. Similar primary isotope effects ($k_H/k_D = 3-5$) have previously been observed in NAD(P)⁺-dependent alcohol dehydrogenases where hydride (deuteride) transfer between the substrate and nucleotide co-factor is the rate limiting step of the reaction.¹¹⁹ The observed values of K_m for **34** were unaffected by the choice of co-factor. The co-factor K_m values, however, showed a significant decrease when [4S- ^2H]NADPH was employed. Such a decrease is unlikely to be due to an isotope effect on binding. The observation of an isotope effect on K_m under conditions where

there are substantial isotope effects on V_{\max} more likely indicates a Michaelis constant that is a steady state rather than a dissociation constant.

The steady state assumption by Briggs and Haldane assumes that in an enzyme reaction of the form outlined in Fig. 2.25 the concentration of the enzyme–substrate complex [ES] remains constant, which in turn gives rise to eqn. (2.1).

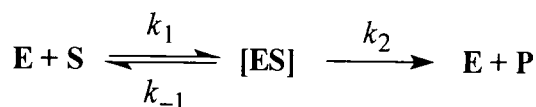


Fig. 2.25

$$K_m = \frac{k_{-1} + k_2}{k_1} \quad (2.1)$$

This is in contrast to the rapid equilibrium assumption in which it is assumed that the rate of dissociation of [ES] (k_2) is much smaller than k_{-1} such that its value is negligible which gives rise to eqn. (2.2).

$$K_m = \frac{k_{-1}}{k_1} \quad (2.2)$$

Table 2.4 Kinetic analysis of the reaction catalysed by CHCR using NADPH and NADP^2H . Substrate concentrations ranged from 3–100 $\mu\text{mol dm}^{-3}$. Data were analysed by Lineweaver–Burk plots and non-linear regression (latter values in brackets).

Substrate	Substrate $K_m / \mu\text{M}^{-1}$	Cofactor $K_m / \mu\text{M}^{-1}$	$V_{\max} / \text{U mg}^{-1} \text{ protein}$
Cyclohex-1-enylcarbonyl-CoA	22±3 (25±1)	9.0±1 (9.5±1)	6.3±0.6 (7.5±0.5)
3-Fluorocyclohex-1-enylcarbonyl-CoA	23±3 (26±4)	3.8±0.5 (3.6±0.9)	1.9±0.3 (2.5±1.0)
3-Fluorocyclohex-1-enylcarbonyl-CoA	28±2 (44±4)	13.5±3 (16±3)	29±4.6 (36±5)
3-Fluorocyclohex-1-enylcarbonyl-CoA	22±5 (14±4)	17±4 (28±4)	28±4.6 (27±1)

Table 2.4 shows the obtained values for the parameters of K_m and V_{\max} . The data was initially analysed by Lineweaver–Burk plots and then by non-linear regression (figures in parenthesis). The substrate K_m values are averages obtained from analyses

conducted at 50 and 100 mmol dm⁻³ co-factor concentrations while co-factor K_m were conducted at 100 and 200 mmol dm⁻³ substrate concentrations.

The observed V_{\max} for the reaction catalysed by CHCR with 3-fluorocyclohex-1-enylcarbonyl-CoA **41** was almost five times greater than that observed with the natural substrate. A rate enhancement of this magnitude by addition of a fluorine substituent in an enzyme catalysed reaction is unprecedented.¹²⁰ It is presumed that the increase arises due to the electronegativity of the fluorine atom at C-3 lowering the energy barrier for hydride delivery to C-2. Previously studied NAD⁺-dependent yeast alcohol dehydrogenases have shown an increase in the rate of hydride transfer to aldehydes with electron-withdrawing groups.¹¹⁹ However, all the substituted benzaldehyde derivatives were converted at a much slower rate than the natural acetaldehyde substrate.

The determined K_m value for **41** was initially similar to that of **34** by Lineweaver–Burk analysis. However when the data was analysed by non-linear regression the value inexplicably rose to 44 μM^{-1} . However **41** still emerges as an excellent substrate for the enzyme. The cofactor K_m values for NADPH were higher for the fluorinated substrate and those determined for [4S-²H]NADPH were almost seven times greater with **41**. These increases, accompanied by an increased reaction rate suggest that the Michaelis constant for the nucleotide co-factor is a steady state rather than a dissociation constant.

The observed V_{\max} values for the fluorinated substrate with NADPH and [4S-²H]NADPH were significantly closer ($k_H/k_D \approx 1.3$) than those for the natural substrate, indicating that hydride (deuteride) is no longer the rate determining step of the reduction and is at best only partially rate limiting. The fluorine substituent at C-3 has presumably lowered the energy barrier for hydride delivery sufficiently to allow another step in the catalytic cycle to contribute to the overall rate. The energy profile diagram in Fig. 2.26 schematically represents the lowering in energy of the hydride delivery step.

Experiments carried out in D₂O rather than H₂O gave no change in the observed value of V_{\max} . This demonstrated that protonation from the solvent is not the rate limiting step of the reduction of **41**. Consequently, the rate limiting step for the reduction of **41** by CHCR is either substrate–cofactor binding or product–cofactor release. The rate limiting step for NAD⁺-dependent horse liver alcohol dehydrogenase, which has a $k_H/k_D = 1$ for the hydride step, is the release of the NAD⁺ co-factor.¹²¹ As hydride transfer is rate limiting for the reduction of the natural substrate but not **41**, the

difference in the V_{\max} values for the reduction of these substrates with $[4S-^2H]NADPH$, approximately 15-fold, is even more dramatic than with NADPH.

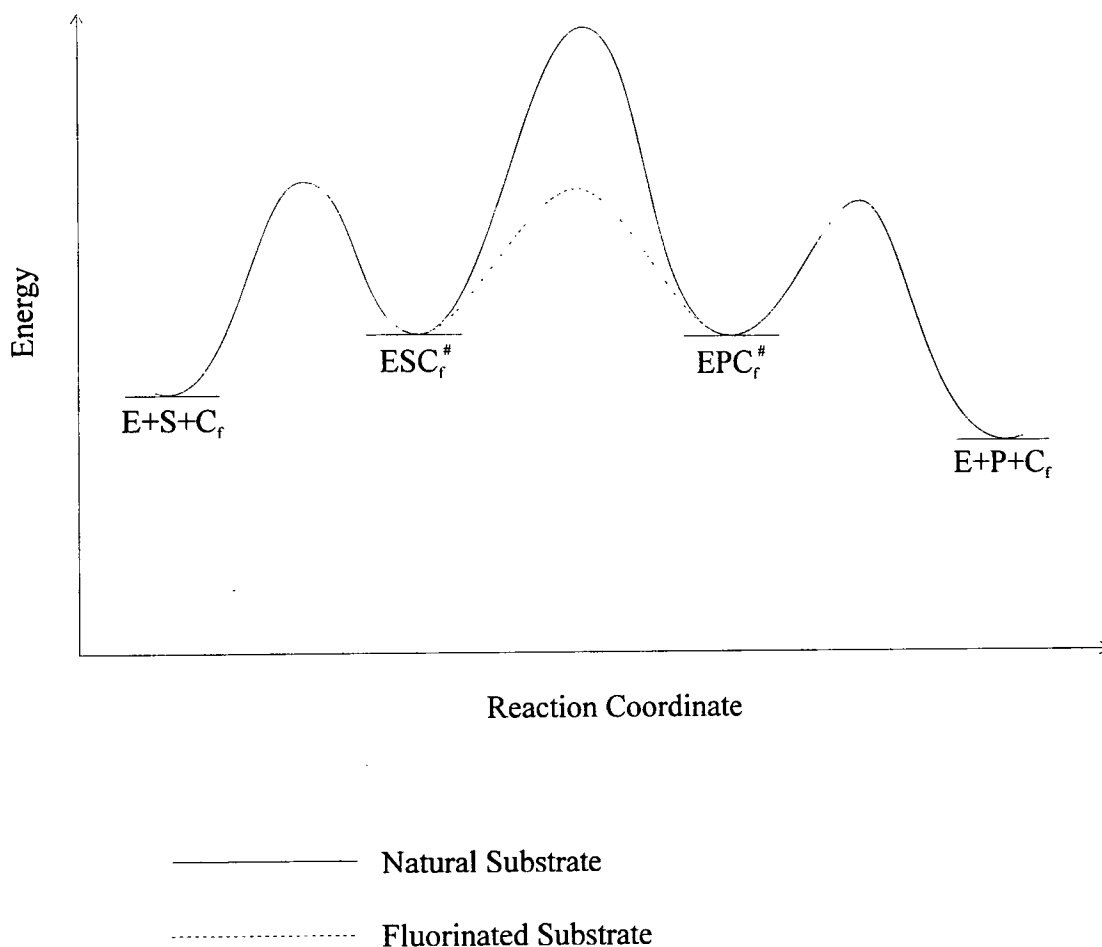


Fig. 2.26

2.7 ^{19}F NMR study of the reduction catalysed by CHCR

As previously described in section 2.3, ^{19}F NMR spectroscopy was used to determine whether any kinetic differentiation was made between the two diastereoisomers of **41** upon reduction by the CHCR enzyme. The chemical shifts of the axial and equatorial fluorines can be clearly distinguished by ^{19}F NMR spectroscopy and by using proton decoupling $^{19}F\{^1H\}$ the signal/noise ratio can be increased while simplifying the observed spectra.

Analysis by ^{19}F NMR spectroscopy of the products from initial reactions of **41** with CHCR revealed the disappearance of the substrate signal at $\delta -171.0$ accompanied by a concomitant increase in two signals at $\delta -168.5$ and -182.5 (Fig 2.27). These

peaks were assigned to the formation of (1*R*,3*S*)-3-fluorocyclohexylcarbonyl-CoA (equatorial fluorine) and (1*R*,3*R*)-3-fluorocyclohexylcarbonyl-CoA (axial fluorine) respectively. The assignments, based on literature precedent for fluorinated cyclohexanes, were reinforced by analysis of the ^1H - ^{19}F coupling constants in the ^{19}F NMR spectrum. The equatorial product (δ -168.5) gave a broad doublet ($J = 47$ Hz) while the axial isomer (δ -182.5) gave a more complex doublet of broad triplets ($J = 47$ and 30 Hz).

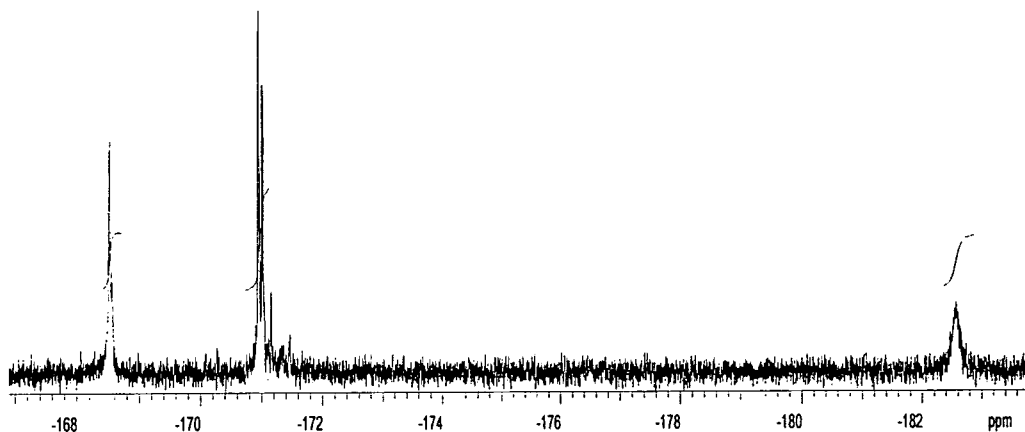


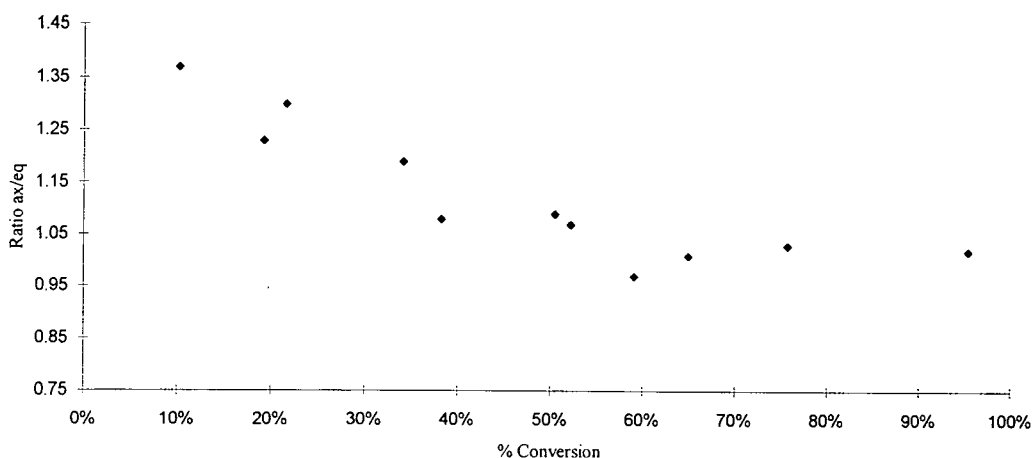
Fig. 2.27

When the enzyme reaction of **41** with CHCR was allowed to run to completion the intensity of the two new product signals was determined to be equal by integration of the signals in the ^{19}F NMR spectrum.

In order to determine whether the enzyme demonstrated any stereochemical preference, experiments were performed under conditions which controlled the extent of conversion of substrate to product. This was achieved by limiting the amount of NADPH co-factor added. When the reactions were complete, as determined spectrophotometrically, the aqueous solutions were freeze-dried, analysed by high field $^{19}\text{F}\{^1\text{H}\}$ NMR spectroscopy and the relative ratio of axial to equatorial product calculated by integration of the respective signals. The results are given in Table 2.5.

Table 2.5 Relative rates of formation of axial and equatorial product from the reduction of 3-fluorocyclohex-1-enylcarbonyl-CoA

Axial (%)	Equatorial (%)	Conversion (%)	Ratio axial:equatorial
5.9	4.3	10.2	1.37
10.6	8.6	19.2	1.23
12.2	9.4	21.6	1.30
18.5	15.6	34.1	1.19
19.8	18.4	38.2	1.08
26.3	24.2	50.5	1.09
27.0	25.2	52.2	1.07
29.1	30.0	59.1	0.97
32.6	32.4	65.0	1.01
38.4	37.3	75.7	1.03
48.6	46.8	95.4	1.03



The results from these experiments show that in the early stages of the reduction the axial product predominates. The enzyme appears to exhibit a small but significant discrimination between the two diastereoisomers of the fluorinated substrate **41**, with an observed value of 1.37 for the ratio of axial–equatorial product at approximately 10% conversion. This ratio is seen to decrease, as is expected, as the conversion approaches 50% and progresses towards completion, and ultimately the ratio becomes 1:1. The experiments were repeated on three occasions and each time a comparable result emerged. Thus we are forced to conclude that the enzyme reaction shows a small but significant kinetic preference for the production of the axial over the equatorial product

in the early stages of the reaction. This observed discrimination could have two origins, either a binding effect or a kinetic preference.

If the discrimination arose due to a differential binding of the substrates, the K_m values would be significantly different for the two isomers, with the experimentally observed K_m value emerging as an average of the two. The closeness of the experimentally determined values for K_m of the natural and fluorinated substrate is inconsistent with a differential binding effect. On the other hand, the experimental observation for the preference of the axial over the equatorial product was predicted and is consistent with the Anh–Eisenstein effect operating.

2.8 Conclusions

The fluorinated analogue **41** of cyclohex-1-enecarbonyl-CoA was shown to be a good substrate for the CHCR enzyme. The results from the kinetic and ^{19}F NMR spectroscopic studies can be summarised as follows.

(i) Introduction of the fluorine at C-3 increased the V_{max} of the reaction by *ca.* 5 times.

(ii) A kinetic isotope effect of 3 for the natural substrate was reduced to 1.3 on fluorine substitution, demonstrating a change in the rate determining step of the reduction.

(iii) ^{19}F NMR analysis showed that the enzyme exhibited a small preference for the axial over the equatorial fluorine in the early stages of the reduction, indicative of a kinetic preference with a stereoelectronic origin.

Chapter Three

The Synthesis and Hydrolysis of C-6 Fluorinated Penicillins

The Synthesis and Hydrolysis of C-6 Fluorinated Penicillins

3.1 Introduction

Sir Alexander Fleming's historical observations of the antibacterial properties of a culture of the fungus *Penicillium notatum* in 1929 marks the starting point of research into the penicillin antibiotics. By 1940 a research team at Oxford, led by Abraham, Chain and Florey, had isolated penicillin [later known as penicillin G (**60**)] for the first time in reasonably pure form.

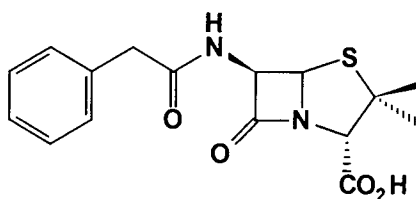
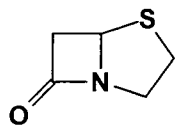


Fig. 3.1 Benzylpenicillin **60** (Penicillin G)

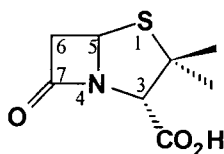
Abraham and Chain also in 1940 reported that bacteria contained an enzyme capable of destroying the biological activity of penicillin which they termed penicillinase. Indeed soon after benzylpenicillin **60** was introduced into the clinic at the end of World War II, the emergence of resistant strains of pathogenic micro-organisms threatened its efficacy as an antibiotic. Many enzymes of this type have now been characterised, generally termed β -lactamases they are the commonest cause of bacterial resistance to β -lactam antibiotics.

The first proposal that penicillin contained a β -lactam moiety was made in 1943,¹²² however this was not generally accepted until the X-ray structural determination by Hodgkinson had been completed,¹²³ which established the fused bicyclic β -lactam-thiazolidine nucleus and the relative stereochemistry of the penicillin molecule.

The penam **61** and penicillanic acid **62** nomenclature systems were first proposed in 1953 by Sheehan.¹²⁴



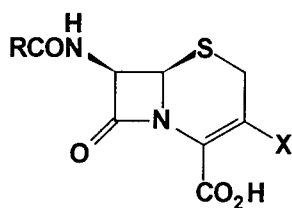
61



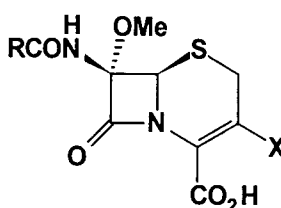
62

Penicillin was the first naturally occurring antibiotic to be characterised and used in clinical medicine. There were however a number of serious shortcomings evident in the early penicillins, in that they exhibited only weak activity when administered orally, their spectrum of antibacterial activity was very limited (particularly against Gram-negative bacteria) and their *in vivo* half-lives were short owing to rapid renal excretion.

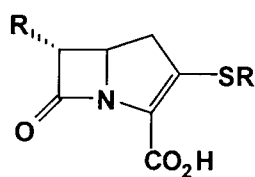
Until 1970, penicillins and the structurally related cephalosporins were the only examples of naturally occurring β -lactam antibiotics. The discovery of 7 α -methoxycephalosporins from *Streptomyces* in 1971 stimulated the search for novel β -lactam antibiotics of microbial origin.¹²⁵ Today a large family of antibiotics exist which possess a β -lactam ring. These include the penicillins, the cephalosporins **63**, the cephamycins **64**, the carbapenams **65** and the monobactams **66**.¹²⁶



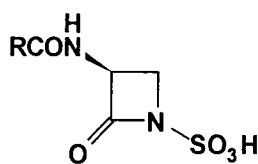
63



64



65



66

3.2 Mode of action of β -lactam antibiotics

β -Lactams exert their lethal action only on growing bacterial cells. Within a short time of adding penicillin to a bacterial culture, small bulges form, which with time cause the cell to rupture, resulting in the death of the cell. These effects are accompanied by the covalent binding of the antibiotic to cellular proteins, called penicillin binding proteins

(PBP).¹²⁷ The PBPs are located on the inner membrane and, to reach these, the antibiotic has to cross a variety of chemical and physical barriers (Fig. 3.2).¹²⁸

When a β -lactam antibiotic attacks a Gram-negative bacterium, *e.g.* *E. coli*, it must initially cross the outer membrane by passive diffusion through channels formed by the 'porin' proteins. The antibiotic then crosses the cell wall, which is a cross-linked peptidoglycan network upon which the structural integrity of the cell depends. Finally the β -lactam must cross the periplasm on its way to the PBPs on the inner membrane. The periplasm may contain many thousands of β -lactamase enzymes. For example, an *E. coli* cell carrying the plasmid RP4 contains around 65 000 molecules of β -lactamase in the periplasm, which may catalyse the hydrolysis of the penicillin **67** to the harmless monocyclic penicilloic acid product **68**.

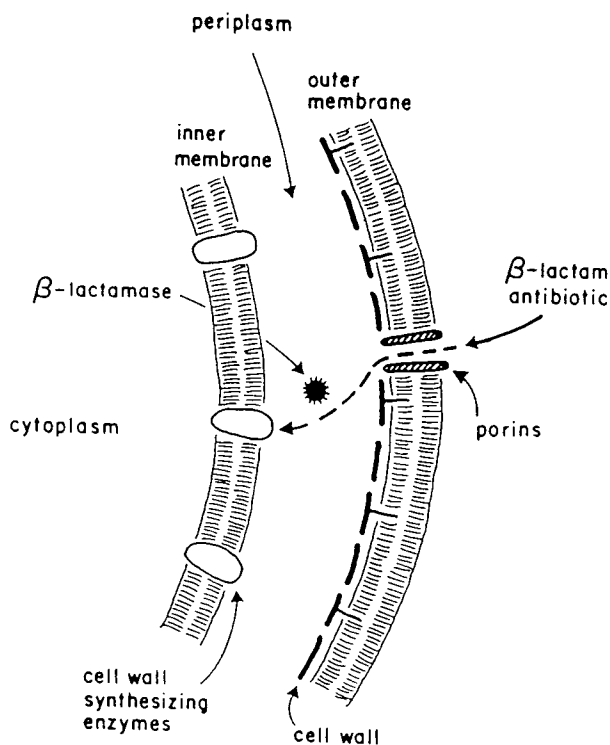


Fig. 3.2 Passage of a β -lactam antibiotic through cell of a Gram-negative bacteria

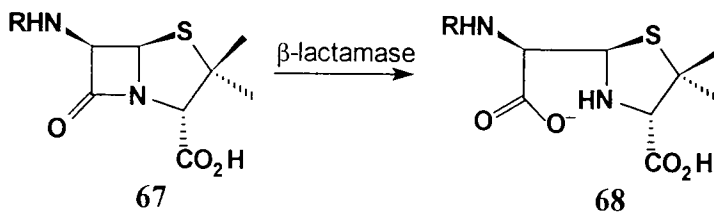


Fig. 3.3

The β -lactam antibiotics that survive the crossing to the inner membrane exert their antibacterial activity by disrupting bacterial cell wall biosynthesis. This is accomplished by specifically inhibiting the transpeptidases which cross-link peptidoglycan chains in the final stages of the biosynthetic sequence. The enzyme formally cleaves a D-alanyl-D-alanyl bond at the terminus of one peptidoglycan chain with the formation of a new amide linkage between the remaining D-alanine and the terminal glycine of a pentaglycine sequence of a second peptidoglycan chain.¹²⁹ Tipper and Strominger first proposed that the penicillins are substrate analogues of the D-alanyl-D-alanyl moiety cleaved by the transpeptidase.¹³⁰

Seven PBPs have been identified, numbered Ia, Ib, II, III, IV, V and VI in order of decreasing molecular weight, and are a mixture of transpeptidases and carboxypeptidases, with the latter predominating. PBPs Ia, Ib, II and III are transpeptidases, some or all of which are essential for cell survival. It is assumed that the β -lactams inhibit both the transpeptidases and carboxypeptidases by similar mechanisms (Fig. 3.4).

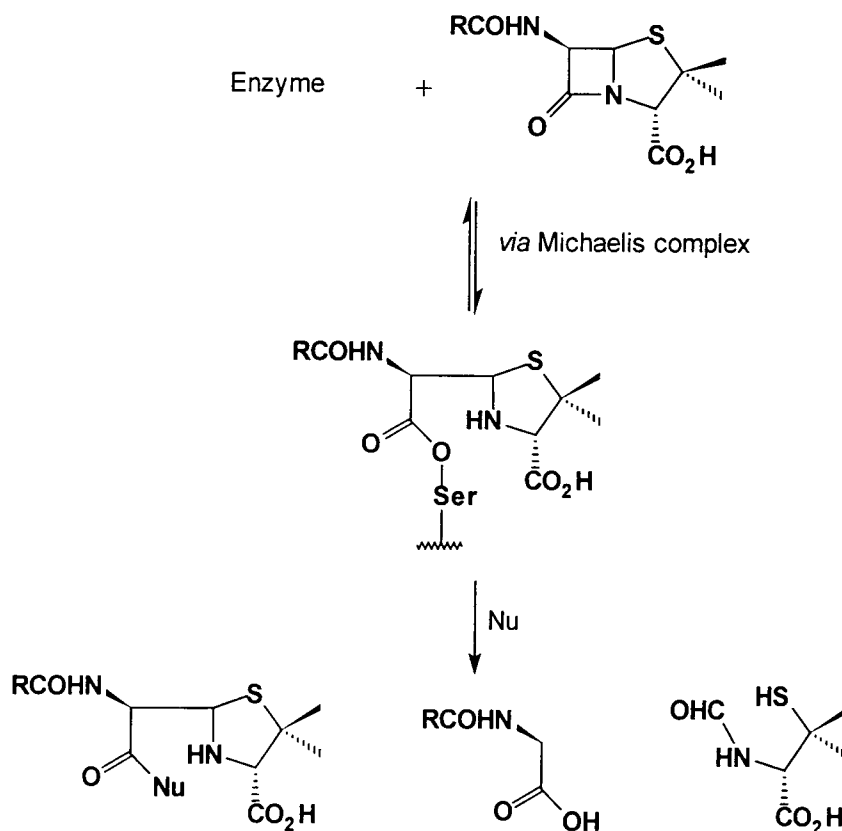


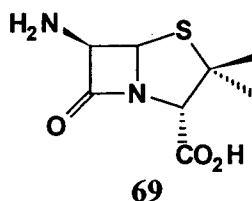
Fig. 3.4 Interaction of penicillins with bacterial β -lactamases and carboxypeptidases
(Nu = water, amino acid, alcohol)

Following initial formation of the Michaelis complex, a second complex forms where, through acylation of a serine residue, the penicillin becomes covalently bound to the enzyme.¹³¹ The enzyme is regenerated in the case of the lactamase, by transfer of the penicilloyl moiety to water with the formation of penicilloic acid (Nu = OH). With the penicillin sensitive enzymes hydrolytic regeneration usually occurs concomitant with cleavage of the 5,6-bond to afford an acylated glycine and *N*-formylpenicillamine. The rate of formation and stability of the acylated complex determines lactamase resistance and anti-bacterial activity. The rate of breakdown of the penicilloylated enzyme can be very slow, for example, under physiological conditions the half-life of the benzylpenicillin-carboxypeptidase complex from *Streptomyces* R39 is 70 h.¹³² The newer lactamase resistant antibiotics are resistant because they are poor substrates for lactamases, yet retain their inhibition properties for the penicillin sensitive-enzymes.

There are several ways by which a bacterial population may become resistant to the action of β -lactam antibiotics. Firstly the target enzymes become less susceptible to acylation and inactivation. Secondly, changes in the outer membrane permeability may limit the access of the antibiotic to the periplasm. Finally, and most commonly, a β -lactamase may result in the hydrolytic destruction of the antibiotic in the periplasm before it can reach its target.

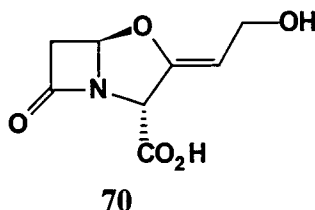
3.3 Inhibition of β -lactamases

Any compound that prevents or slows down enzyme catalysis is an enzyme inhibitor. A compound that prevents enzyme activity for an extended period of time is an irreversible inhibitor. The destructive action of a β -lactamase may be overcome in two ways. Firstly, by altering the structure of the β -lactam, rendering it insensitive to hydrolysis by the β -lactamase while retaining its antibiotic potency. Secondly, by using a reagent that disables the β -lactamase, in association with a β -lactam antibiotic that would otherwise be rapidly hydrolysed by the enzyme. The first approach became possible when the deacylated penam, 6-aminopenicillanic acid (6-APA) **69** was produced both microbiologically¹³³ and by *de novo* synthesis.¹³⁴



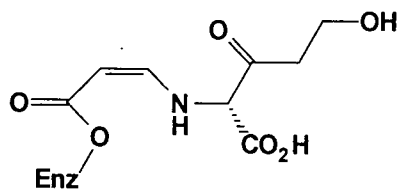
The availability of **69** allowed the semi-synthesis of an immense number of acylated penams and cepams varying in their *N*-acyl side chains. It was, however, often found that the molecules more resistant to the β -lactamase were also less effective antibiotics.

The second approach, inactivating the β -lactamase, was pursued, with the first success coming in 1976 with the isolation of clavulanic acid **70** from *Streptomyces clavuigerus* by workers at Beecham Pharmaceuticals.¹³⁵



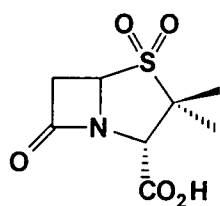
Clavulanic acid differed from the previously studied β -lactams in that it was a weak anti-bacterial agent but an irreversible inhibitor of β -lactamases. It was capable of protecting susceptible β -lactam antibiotics against the hydrolytic action of bacterial β -lactamases. A combination of amoxicillin and clavulanate ('Augmentin') is currently in clinical use. Mechanistic investigation into the interaction of **70** with the β -lactamases demonstrated it was a 'suicide' or 'mechanism-based' inhibitor. The enzyme recognises it as a potential substrate yet leads, in a diversion from the normal course of the hydrolytic reaction, to inhibition and/or inactivation of the enzyme. Penicillin G is a typical example of a compound which is a good inhibitor of the transpeptidases, but is also a good substrate for the β -lactamases. Ceftazidime and cefoxitin, on the other hand, are good inhibitors of the transpeptidases and poor substrates for the β -lactamases.

Fisher suggested that clavulanic acid's inhibitory action arises from initial acylation of the enzyme followed by a β -elimination resulting in the conjugated enamine **71**.¹³⁶

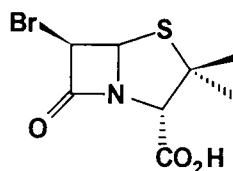


71

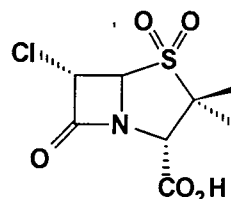
The discovery of the inhibitory action of clavulanic acid stimulated the search for other inhibitors, both from natural sources and through synthesis. As a result a number of such compounds have emerged that have powerful inhibitory properties towards β -lactamases, including penicillanic acid sulfone **72**, 6 β -bromopenicillanic acid **73** and 6 α -chloropenicillanic acid sulfone **74**. In general these compounds tend to be poor inhibitors of the transpeptidases but irreversible 'suicide' inhibitors of β -lactamases.



72

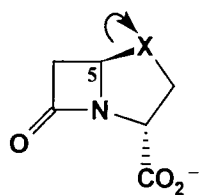


73

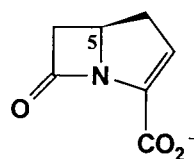


74

All of the mechanism-based inhibitors of the β -lactamases fall into two classes: those that contain a heteroatom at the 1-position, which may act as a leaving group from C-5, and those such as the carbapenams that do not (Fig. 3.5).



Class I



Class II

Fig. 3.5

3.3.1 Penicillanic acid sulfone 72

The nature of the interaction of penicillanic acid sulfone has been extensively studied and the detailed mechanism elucidated by Knowles using the RTM β -lactamase.¹²⁸

The pathways that account for the observed kinetics is illustrated in Fig. 3.6.

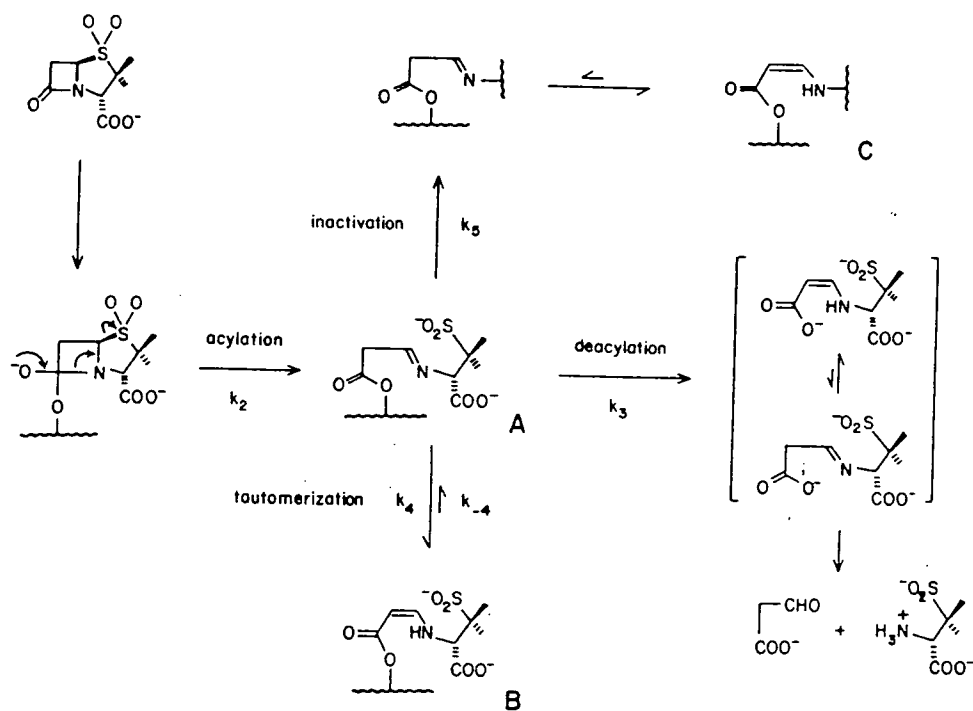


Fig. 3.6 Interaction of penicillanic acid sulfone with the β -lactamase

Following the formation of an acyl-enzyme intermediate (A) three separate processes can occur. Firstly, the penicillanic acid sulfone may act as a substrate for the enzyme and the β -lactam ring is hydrolytically cleaved, resulting in malonyl semialdehyde and the sulfinate of penicillamine. Secondly, the enzyme is transiently inhibited (B). Finally, the enzyme is irreversibly inactivated. The acyl-enzyme intermediate (A) is converted into a β -imino ester by an elimination reaction, which is followed by a transamination by an enzyme lysine residue. Such a reaction leads to a β -aminoacrylate crosslinked to two active site residues. Inhibition is slower than the rate of hydrolysis with *ca.* 7000 molecules of penicillanic acid sulfone being hydrolysed for each molecule of inactivated enzyme formed.

3.3.2 6 β -Bromopenicillanic acid 73

6 β -Bromopenicillanic acid (6-BPA) 73 has been shown to be a specific and potent irreversible inhibitor of a variety of β -lactamases.¹³⁷ The mechanism of the inactivation of *Bacillus cereus* β -lactamase by 6-BPA has been extensively studied and several reaction mechanisms have been postulated.

(i) Pratt and co-workers suggested that the formation of the acyl-enzyme complex is followed immediately by ring opening of the thiazolidine, with formation of a thiolate-immonium zwitterion 75, followed by rearrangement and cyclisation of the inhibitor to a 2,3-dihydro-1,4-thiazine-3,6-dicarboxylic acid derivative 76.¹³⁸ The final step involves the fast isomerisation of an imine to an enamine, which is facilitated by the acidity of the hydrogen atom on C-6 of the (6-BPA) (Fig. 3.7).

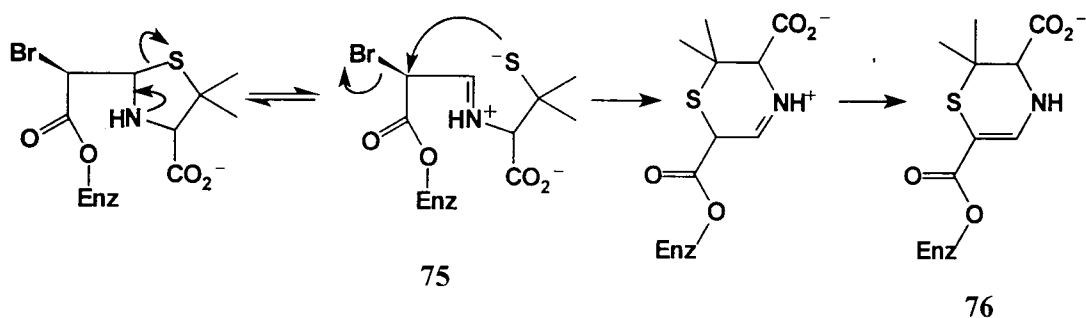


Fig. 3.7

(ii) A modified mechanism arose from the observation of the rapid loss of tritium from [³H]-6-BPA, which occurs on interaction with the enzyme.¹³⁸ Knowles suggested that a base is present that assists the removal of the 6 α proton in a stereospecific manner prior to the thiazolidine ring opening and that this is the driving force for a *trans* elimination across the C-5 and C-6 carbons, resulting in the direct formation of an enamine and ring opening.¹³⁹

(iii) More recently, Pratt and Cahn studied the kinetics and mechanism of the rearrangement of 6-BPA to 2,3-dihydro-1,4-thiazines.¹⁴⁰ They concluded that the most likely mechanism does not involve thiazolidine ring opening but direct intramolecular nucleophilic attack by the thiazolidine sulfur atom at C-6, displacing Br⁻ to give a bicyclic episulfonium ion intermediate. This then collapses to the dihydrothiazine 76 (Fig. 3.8).

For mechanisms (i) and (iii) the most important structural feature is the presence of a good leaving group at C-6, whereas for (ii) the presence of an acidic 6 α hydrogen is also essential for the rearrangement reactions leading to the dihydrothiazine formation.

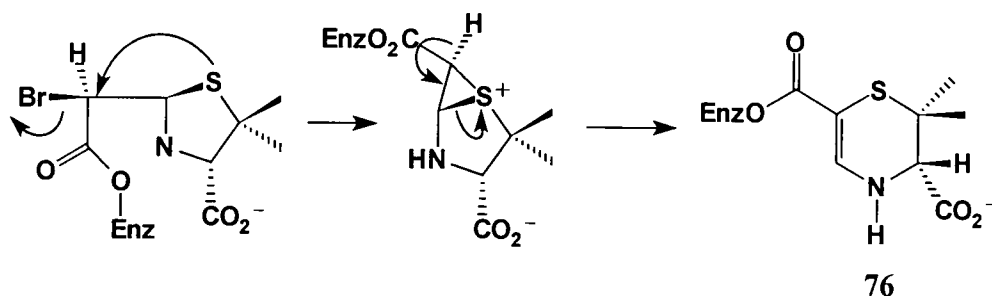
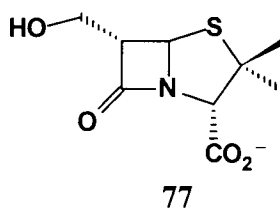


Fig. 3.8

Since the discovery of the potency of 6-BPA as a β -lactamase inhibitor there has been much interest in the synthesis of other 6-mono- and 6,6-di-halopenicillins, and in turn this lead to a synthesis of the 6-fluoropenicillins.¹⁴¹

3.3.3 6 α -(Hydroxymethyl)penicillanic acid 77

More recently the compound 6 α -(hydroxymethyl)penicillanic acid 77 has been shown to be a potent inhibitor for the TEM-1 β -lactamase.¹⁴²



This molecule was designed based on the minimal structure of penicillanic acid, which acylates the active site serine, but which would resist deacylation by being incorporated with a functionality that could displace an active-site water molecule responsible for the deacylation step of the hydrolytic reaction. Molecular modelling demonstrated that the hydroxy group of a 6 α -hydroxymethyl functionality would overlap with the space occupied by the structurally conserved water molecule (Wat-301).

After showing its potency as an inhibitor of the TEM-1 β -lactamase, a crystal structure of the complex of the β -lactamase inhibited by **77** was solved. Fig. 3.9 shows the 6 α -hydroxymethyl group acting as a hydrogen bond donor to the hydrolytic water molecule, preventing deacylation.¹⁴³

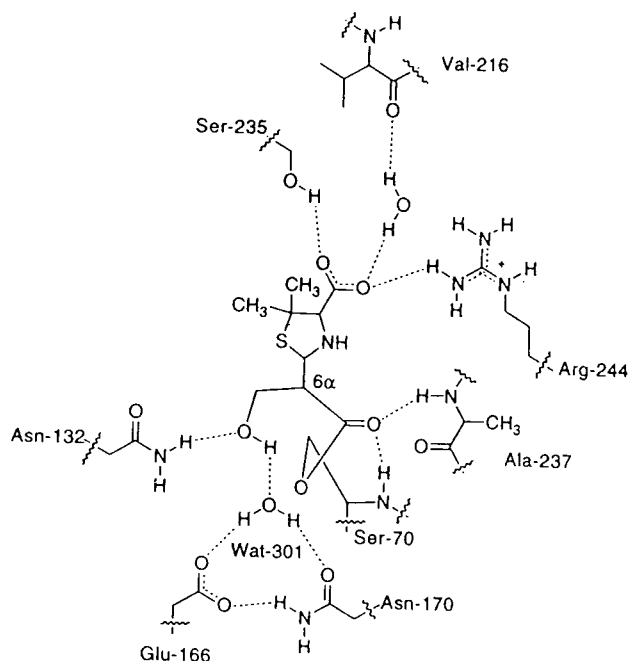


Fig. 3.9 Crystal structure of acyl-enzyme complex with **77**

3.4 Fluorinated penicillins and stereoelectronic effects

The introduction of a fluorine atom with either the α or β configuration at the C-6 position in the penam nucleus provided an attractive system with which to probe the stereoelectronic influence of fluorine.

As previously discussed the introduction of a fluorine atom at the C-6 position would be expected to cause little steric perturbation in the molecular geometry of the penam nucleus. However induced changes in the electronic character of the β -lactam can be expected with a fluorine at the C-6 position which may alter the mechanistic and inhibitory activity of the β -lactams.

A particular structural requirement for the ability of compounds such as penicillanic acid sulfone and 6-BPA to act as 'suicide' substrates for β -lactamases is the presence of a sufficiently acidic proton at C-6. The presence of a C-6 fluorine with its high electronegativity should alter the acidity of the C-6 proton allowing easier removal by a stereospecific base.

The introduction of a fluorine on the α carbon to a carbonyl functionality could be expected to induce a number of other effects. With the cyclohex-1-enylcarbonyl-CoA enoyl reductase discussed in Chapter 2 the introduction of a fluorine had a dramatic effect on the rate of the reaction. This was presumed to be due to the fluorine making the sp^2 centre more susceptible to hydride attack through an inductive effect. By direct analogy the fluorine at C-6 would be predicted to increase the susceptibility of the β -lactam carbonyl to attack by a serine residue and increase the acylating ability of the penicillin. The presence of the C-6 fluorine may also stabilise the tetrahedral transition state formed by attack of the serine residue (Fig. 3.10) onto the carbonyl which may subsequently slow the rate of further breakdown of the penicillin.

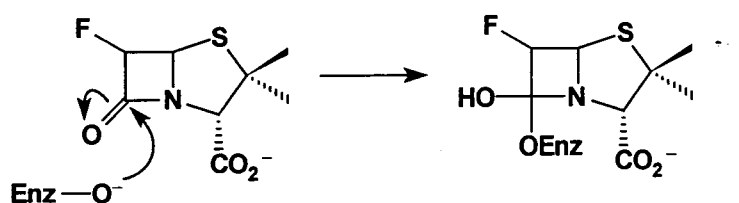


Fig. 3.10

A further consideration is the configuration of the fluorine atom at the C-6 position which may be α or β . The relative rates at which the β -lactam ring is hydrolysed by the enzyme may alter in each case. Studies into the aminolysis of penicillins by Page have demonstrated that attack of the nucleophile onto the carbonyl takes place from the least hindered α face of the β -lactam.¹⁴⁴ This result seems wholly reasonable with the thiazolidine ring and particularly the large sulfur atom hindering the approach of the nucleophile to the top β -face (Fig. 3.11).

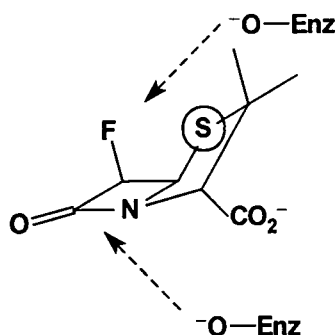


Fig. 3.11

With the attack of the nucleophile to one face and a fluorine on the α -carbon the system is suitable for analysis by the Anh–Eisenstein model, and may be used to predict whether a difference in the rate of hydrolysis between the two isomers may be expected to occur. The two distereoisomeric transition states for the hydrolysis of the β -lactam are illustrated in Fig. 3.12.

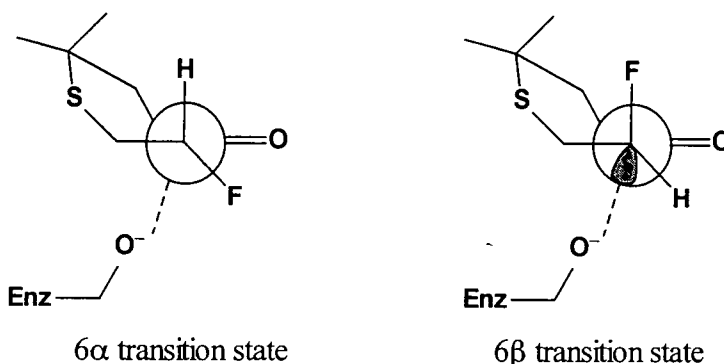


Fig. 3.12

The models show that the serine residue would be stabilised by an $n-\sigma^*$ interaction in the case of the β -isomer, and it could therefore be predicted that the β -isomer may be hydrolysed at a faster rate relative to the α isomer.

3.5 Biological activity of fluorinated penicillins

The inhibitory activity of a number of C-6 fluorinated penicillins against β -lactamase I of *Bacillus cereus* has been studied by Mascaretti (Table 3.1).¹⁴¹ The experiments showed that β -lactamase activity was instantaneously inhibited by the addition of 6β -fluoropenicillanic acid sulfone, 6β -fluoropenicillanic acid or 6α -fluoropenicillanic acid sulfone. The initial effect was followed by a progressive increase in the inhibition, but did not follow simple first order kinetics. The addition of 6α -fluoropenicillanic acid and 6β -bromo- 6α -fluoropenicillanic acid produced only a slight inhibition of enzyme activity. This lack of inhibition can be related to the lack of a 6α hydrogen which Knowles postulates as a requirement for inhibitory action.¹³⁹

Incubation of the β -lactam compounds with more enzyme was accompanied, except for 6β -fluoropenicillanic acid, by hydrolysis of the β -lactam ring, indicating that the compounds were also substrates for the enzyme.

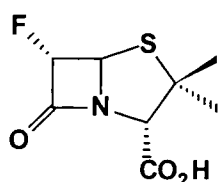
It was therefore concluded, based on the inhibitory action and their ability to behave as substrates, that these fluorinated penicillins not only bind to the enzyme but also acylate it.

Table 3.1 Inhibitory activity of 6-fluoropenicillins against β -lactamase I of *Bacillus cereus*.¹⁴¹

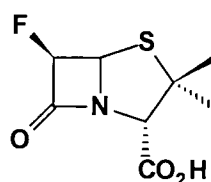
β -Lactam compound	IC ₅₀ /mM (without preincubation)	IC ₅₀ /mM (with 10 min preincubation)
6 β -Bromopenicillanic acid	1.0	0.5
6 β -Bromo-6 α -fluoropenicillanic acid	>5.0	>5.0
6 α -Fluoropenicillanic acid	>5.0	>5.0
6 β -Fluoropenicillanic acid	>2.5	0.4
Penicillanic acid sulfone	0.025	0.025
6 β -Fluoropenicillanic acid sulfone	1.0	0.25
6 α -Fluoropenicillanic acid sulfone	4.0	2.25

3.6 Synthesis of 6-fluoropenicillins

There have been a number of reports of the introduction of a fluorine atom into penicillins and cephalosporins. The recent developments in the chemistry and biochemistry of fluorinated β -lactams have been reviewed by Mascaretti, who has developed much of the synthetic chemistry towards the 6-fluoropenicillins **78** and **79**.¹⁴¹



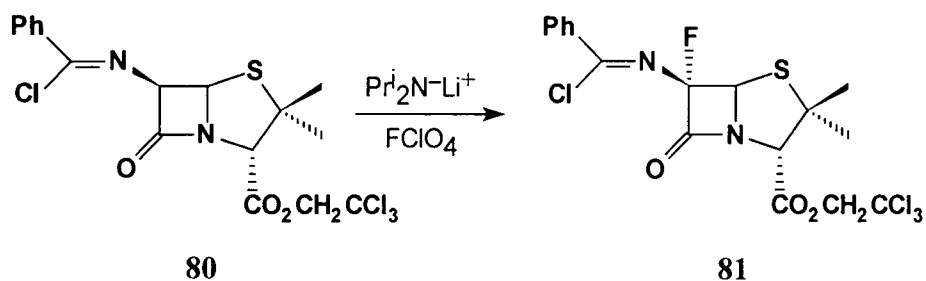
6 α -fluoropenicillanic acid **78**



6 β -fluoropenicillanic acid **79**

The first report of the introduction of a fluorine atom into a cephalosporin, at the C-7 position, was in 1973 by Slusarchyk.¹⁴⁵ The method involved the generation of a carbanion at C-7 from the benzaldehyde Schiff base, which was fluorinated by the

addition of electrophilic fluorine from perchloryl fluoride. A similar approach was used in 1974 to generate the C-6 carbanion of 6-imino chloride penicillin **80**, which was fluorinated with perchloryl fluoride to afford **81**.¹⁴⁶



The stereochemistry of the 6-fluoro substituent was presumed to be 6 α based on analogy with previous alkylation and acylation on the carbanion of the Schiff base of penicillins. No data was presented on the biological activity of these fluorinated penicillins.

In 1980 and 1983 two patents by the same authors were published claiming the synthesis of several 6 β -halopenicillanic acids and ester derivatives including **79**.¹⁴⁷ The merit of these patents is, however, difficult to judge, as no data on yield, characterisation, stereochemistry or biological activity of the compounds is reported. The synthetic route described in the patent for the synthesis of **79** is shown in Fig. 3.13.

Benzyl diazopenicillanate was treated with *N*-bromosuccinimide (NBS) and pyridinium poly(hydrogen fluoride) to give the geminal 6,6-bromofluoropenicillanate **82**. Removal of the C-6 bromine was achieved using tributyltin hydride, which was followed by ester hydrolysis with iodotrimethylsilane giving the fluoropenicillin **79**.

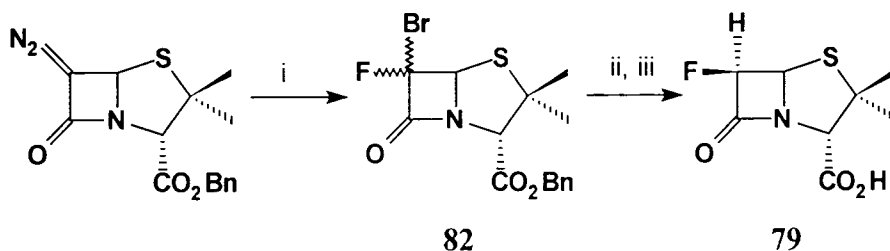


Fig. 3.13 Reagents and conditions: i, HF-pyridine, *N*-bromosuccinimide, Et₂O-THF; ii, Bu₃SnH, PhI; iii, Me₃SiI, CCl₄

The same authors also reported a second synthetic approach for the introduction of fluorine at C-6 with the β configuration, using DAST to convert a hydroxy group to the corresponding fluorine (Fig. 3.14).

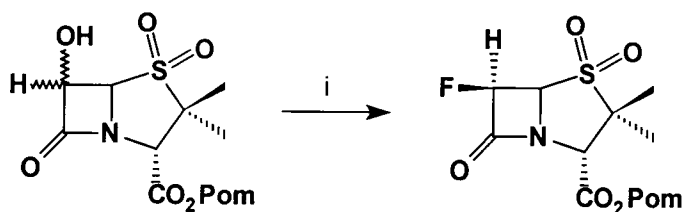


Fig. 3.14 Reagents and conditions: i, DAST, CH_2Cl_2 , $-78\text{ }^\circ\text{C}$; Pom = $\text{CH}_2\text{OCOBU}'$

3.6.1 Synthesis of Pom 6 α -fluoropenicillanate

The synthesis of the two 6-fluoropenicillins **78** and **79** required for this study exploited the extensive work of Mascaretti *et al.* Initial efforts were focused on the synthesis of the pivaloyloxymethyl (Pom) protected penicillins as they appeared to provide a suitable route to the desired compounds. The first stages in the synthesis of all of the penicillins was the esterification and subsequent diazotisation to afford the diazopenicillanate compound **84**.

Commercially available 6-APA **69** was protected as its pivaloyloxymethyl ester following the procedure of Daehne *et al.*¹⁴⁸ This involved the formation of the triethylammonium salt, which was reacted with chloromethyl pivalate in dry DMF. The free amino compound proved to be relatively unstable and was therefore isolated as its crystalline hydrochloride or toluene-*p*-sulfonate salt **83**, which was generally accomplished in 75% yield. The diazopenicillanate **84** was conveniently prepared following the method of Wiering and Wynberg,¹⁴⁹ which involved stirring **83** in a mixture of dichloromethane and water (1:1) with sodium nitrite. Although the diazopenicillanate could be isolated as an amber glass in high yield (90%), it was routinely used without purification as decomposition at room temperature was rapid.

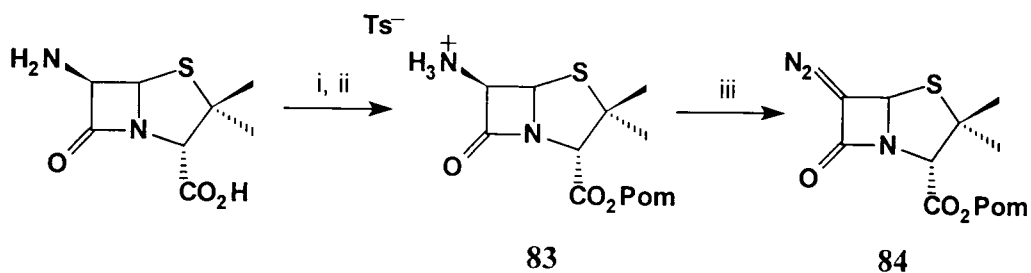


Fig. 3.15 Reagents and conditions: i, Et_3N , $\text{ClCH}_2\text{OCOC}(\text{CH}_3)_3$, DMF; ii, PTSA, EtOAc ; iii, NaNO_2 , CH_2Cl_2 , H_2O

Pom 6 α -fluoropenicillanate **86** was prepared from the corresponding Pom 6 α -hydroxy compound using DAST as the fluorinating reagent. Thus treatment of the diazopenicillanate **84** with a 1 M solution of perchloric acid in acetone at 5 °C following the method of Sheehan *et al.*¹⁵⁰ afforded **85** in 83% yield. Treatment with DAST then introduced fluorine and furnished exclusively the 6 α -fluoro stereoisomer **86** in 70% yield.

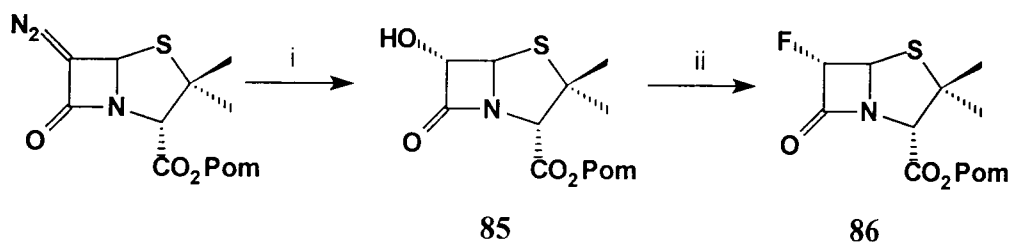
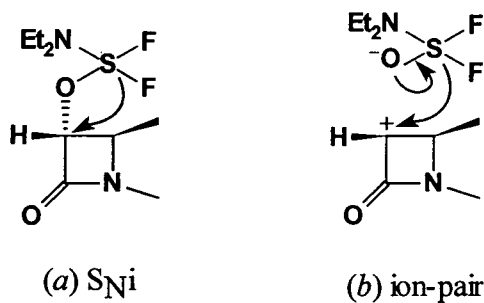


Fig. 3.16 Reagents and conditions: i, 1 M HClO_4 , acetone, 83%; ii, DAST, CH_2Cl_2 , 70%

An important feature of the fluorination is the retention of the α stereochemistry of the C-6 substituent, with none of the corresponding β -isomer being produced. The retention of stereochemistry in the DAST reaction can be rationalised by either an $\text{S}_{\text{N}}\text{i}$ (intramolecular) type mechanism or by the formation of an intimate ion pair. A key feature in the fluorination is clearly the shape of the penam nucleus, where the fluorine approaches the least hindered face, so retaining the stereochemistry at C-6.



3.6.2 Synthesis of 6 α -fluoropenicillanic acid

With **86** in hand, attempts were made to remove the Pom protecting group to release the desired penicillanic acid. It is well documented that the application of conventional methods of ester cleavage to deprotection of penicillin esters presents problems with hydrolysis of the β -lactam ring.¹⁵¹ However Mascaretti has developed a simple and effective method for the removal of Pom esters of penicillins using bis(tributyltin) oxide in non-hydroxylic solvents, where the ester cleavage is thought to proceed as outlined below (Fig. 3.17).¹⁵²

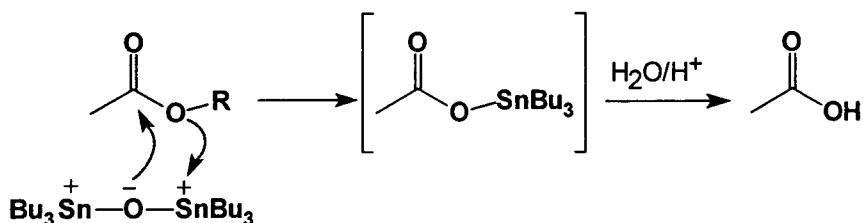


Fig. 3.17 Ester deprotection with bis(tributyltin) oxide; R = Me, Et, Ph, Pom

The proposed mechanism involves an organotin intermediate which is hydrolysed on work up to afford the free acid.

A deprotection reaction was attempted using bis(tributyltin) oxide. After acidic work-up the ¹⁹F NMR spectrum of the resultant residue was complex and showed a number of products with apparent β -lactam cleavage and none of the desired deprotected acid. Mascaretti and co-workers had observed similar problems in their attempts to deprotect Pom 6 β -bromo-6 α -fluoropenicillanate, which they attributed to a fluorodestannylation reaction as a result of the hard tin atom interacting with the hard fluorine.¹⁵³

The problems incurred using the Pom esters were overcome by using a benzyl ester, for which there was good literature precedence for removal, to afford the acids.¹⁵⁴ Indeed, Mascaretti published details of the synthesis of the two C-6 fluorinated penicillins using benzyl ester protecting groups.¹⁵⁵ Thus the modified synthesis to 6 α -fluoropenicillanic acid **78** is outlined in Fig. 3.18.

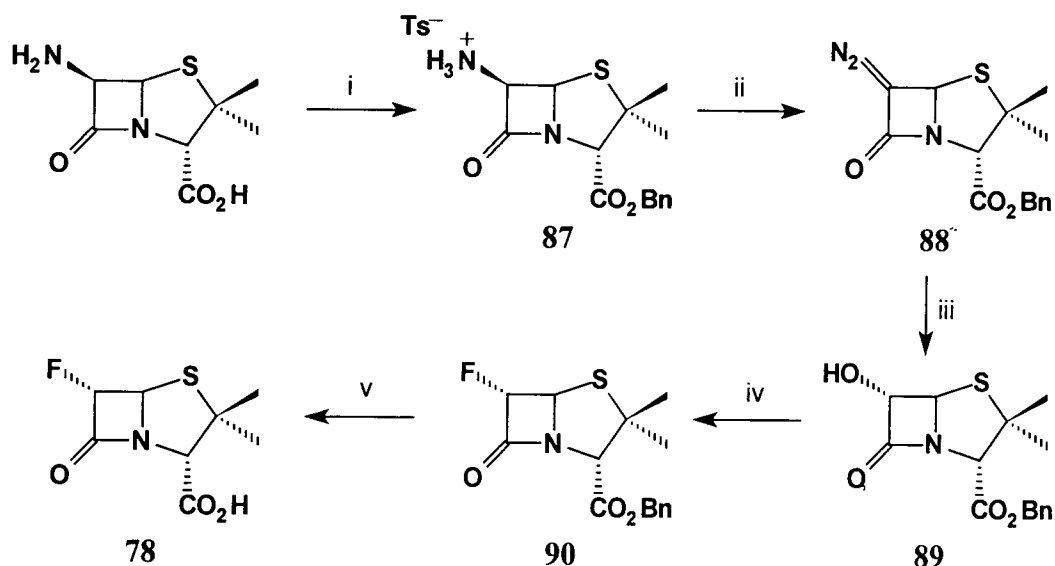


Fig. 3.18 Reagents and conditions: i, PhCHN₂, CH₂Cl₂, PTSA, EtOAc, 80%; ii, NaNO₂, PTSA, CH₂Cl₂-H₂O, 84%; iii, 0.2 M HClO₄, acetone, 75%; iv, DAST, CH₂Cl₂, 65%; v, AlCl₃, CH₃NO₂, 95%

Initial attempts to protect the carboxylic acid as a benzyl ester using benzyl bromide and benzyl chloroformate proved unsuccessful, however in the event, the benzylation was achieved in good yield using phenyldiazomethane (PhCHN₂) in MeOH-CH₂Cl₂.¹⁵⁶ Initial methods for the preparation of phenyldiazomethane involved the reaction of benzaldehyde tosyl hydrazone with sodium methoxide in pyridine.¹⁵⁷ This however proved to be an unreliable method, with the major difficulty being removal of residual pyridine, used as the reaction solvent. With repeated attempts this often meant the production of large amounts of pyridine tosylate when the salt of the penicillin was isolated, and this frustrated satisfactory purification.

A second, more reliable method for the preparation of phenyldiazomethane was evaluated involving the reaction of base (NaOMe) with *N*-nitroso-*N*-benzyltoluene-*p*-sulfonamide. This was conveniently synthesised in large quantities from benzylamine and toluene-*p*-sulfonyl chloride to afford *N*-benzyltoluene-*p*-sulfonamide which, in turn, was nitrosated using NaNO₂ in an acetic acid-acetic anhydride mix.¹⁵⁸ Finally, reaction

with sodium methoxide in MeOH-CH₂Cl₂ gave a solution of phenyldiazomethane, which was used directly to benzylate 6-APA (Fig. 3.19).

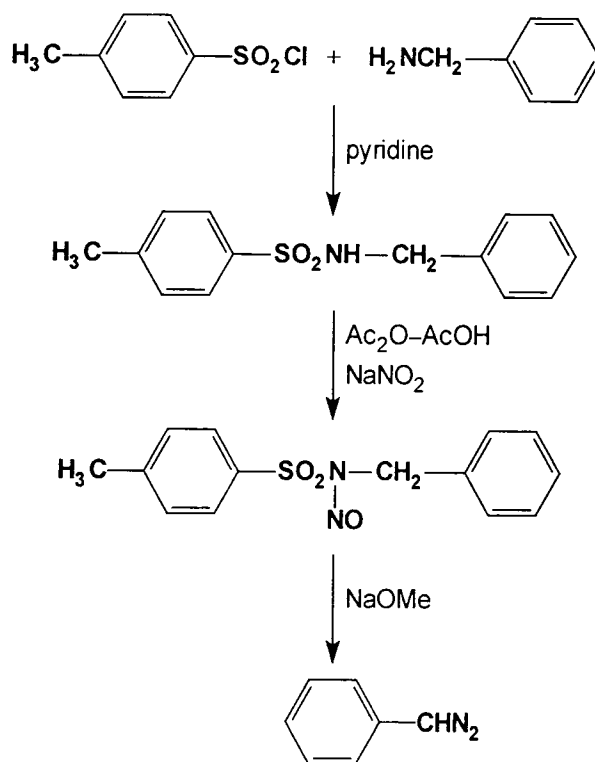


Fig. 3.19

Phenyldiazomethane is very toxic and potentially explosive; therefore at no time was any attempt made to purify or isolate it. However, successful benzylation was clear proof that it had been prepared. Unreacted 6-APA was removed from the reaction by filtration and in a similar manner to the Pom ester, the benzylated penicillin was isolated as the stable crystalline toluene-*p*-sulfonate salt **87**. Compound **87** was converted to **90** as previously described for the Pom derivative (Fig. 3.18). Thus diazotisation was followed by hydrolysis to afford the 6 α -hydroxy derivative **89**, which was fluorinated with DAST. The benzyl group was successfully removed by treatment of the ester with aluminium trichloride in nitromethane, following the conditions of Tsuji, which gave the desired carboxylic acid **78** in good yield.¹⁵⁹ Finally, **78** was secured as its cyclohexylammonium salt **91** by treatment of the free carboxylic acid with cyclohexylamine in EtOAc (Fig. 3.20).

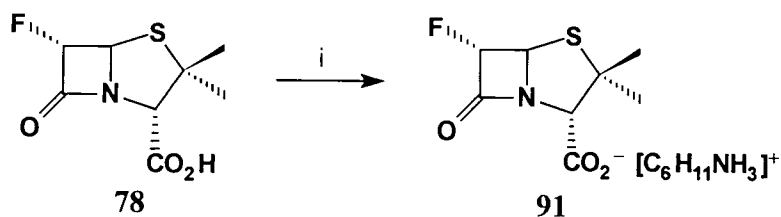


Fig. 3.20 Reagents and conditions: i, cyclohexylamine, EtOAc, 95%

3.6.3 Synthesis of benzyl 6β-fluoropenicillanate

The synthesis of 6β-fluoropenicillanic acid **79** was again reported by Mascaretti and is outlined below in Fig. 3.21.

The initial steps towards the synthesis of **93** follow those described previously for the α-epimer. In order to synthesise the benzyl 6β-bromo-6α-fluoropenicillanate **92** the diazopenicillanate was reacted formally with bromine monofluoride. Mascaretti reported that an earlier procedure using NBS and HF-pyridine had given rise to a complex mixture of products and had therefore investigated the use of NBS with a range of fluoride sources including TBAF, KF-18-crown-6 complex and CsF, all without success.¹⁶⁰ The most reliable source of fluoride was found to be tetrabutylammonium bifluoride in CH₂Cl₂. This fluorinating reagent was prepared by the method of Camps using an ionic exchange reaction between ammonium bifluoride and tetrabutylammonium chloride with a strongly basic Amberlite ion exchange resin.¹⁶¹ The salt, which is highly hygroscopic, was heated at 60 °C *in vacuo* prior to use, in order to remove all traces of moisture.

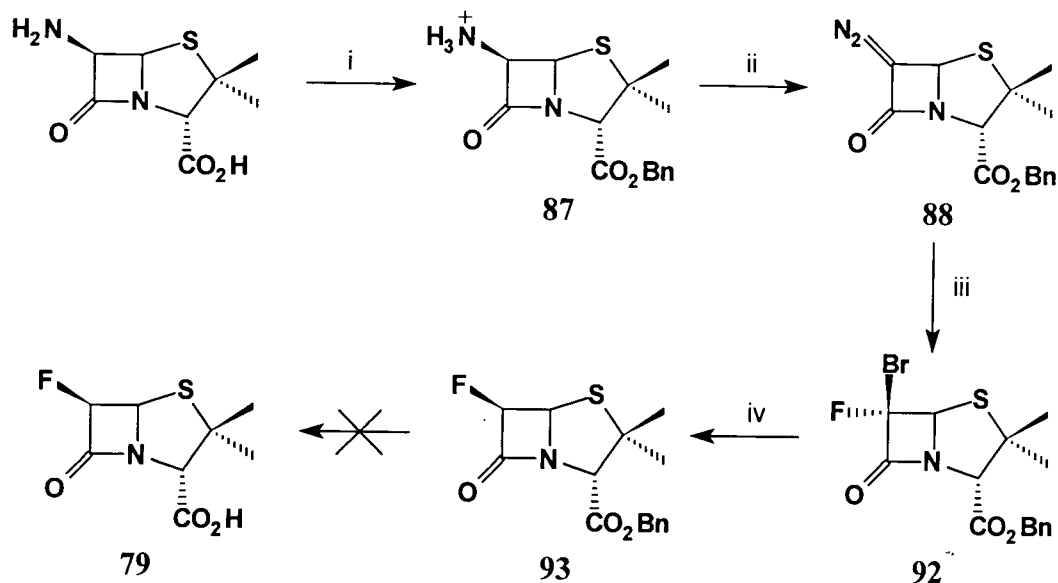


Fig. 3.21 *Reagents and conditions:* i, PhCHN₂, CH₂Cl₂, PTSA, EtOAc, 80%; ii, NaNO₂, PTSA, CH₂Cl₂-H₂O, 84%; iii, TBABF, NBS, CH₂Cl₂-CH₃CN, 45%; iv, (Me₂PhCCH₂)₃SnH, AIBN, Et₂O, 60%

Subsequent treatment of **88** with NBS and TBABF in CH₂Cl₂ at -40 °C resulted in a mixture of products. The major product from the reaction, identified by GC-MS, was the desired 6 β -bromo-6 α -fluoropenicillanate **92** and the minor product was 6,6-dibromopenicillanate. The reaction exploits an electrophilic bromine and nucleophilic HF₂⁻ and proceeds stereoselectively with the electrophilic bromine occupying the 6 β and the fluorine the 6 α configuration.

A third compound was occasionally identified as a component of the reaction mixture by GC-MS. This was the corresponding 6-bromo-6-chloro derivative (Fig. 3.22). This compound arises as chloride is present from unreacted tetrabutylammonium chloride from the ion exchange preparation of TBABF when a deficiency of resin was used. Thus this side reaction could be minimised by using sufficient quantities of resin.

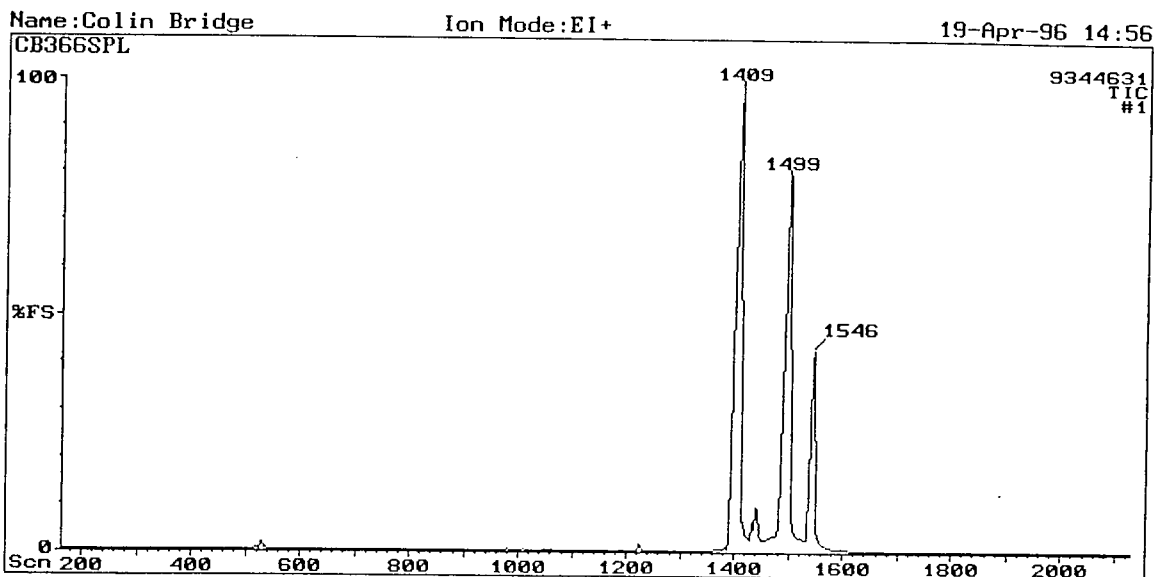


Fig. 3.22

1409; 6 β -bromo-6 α -fluoropenicillanate

1499; 6,6-dibromopenicillanate

1546; 6-bromo-6-chloropenicillanate

The mixture of **92** and the 6,6-dibromo compound was inseparable by column chromatography and was therefore progressed as a mixture to the next stage of the synthesis, the radical-induced reductive debromination using a tin hydride reagent. Initial attempts using tributyltin hydride afforded a mixture of the two epimers, **78** and **79**, in a 2:1 ratio of 6 β over 6 α . This was somewhat unsatisfactory and purification to remove the tributyltin products also caused difficulties. Mascaretti found that using a much more hindered tin hydride reagent tris(2-methyl-2-phenylpropyl)tin hydride (trineophyltin hydride) **96** had several advantages over alkyltin reagents.¹⁶² The reagent is a stable crystalline solid which is easy to handle, the reaction is rapid and clean, and the products are not contaminated with organotin residues. Most critically, the reduction proceeded with a much higher level of diastereofacial selectivity than with tributyltin hydride.

The synthesis of the (trineophyltin hydride)tin hydride reagent is outlined in Fig. 3.23. Reaction of tin tetrachloride with a filtered Grignard solution from neophyl chloride gave trineophyltin chloride **94** as a white crystalline solid in 86% yield.¹⁶³ Treatment of the chloride with a refluxing solution of sodium hydroxide in an ethanol-water mix afforded the trineophyltin hydroxide **95**, again in high yield and as a white

crystalline solid. Finally the tin hydroxide was reduced with borane in THF to give the required hindered tin hydride reagent.¹⁶⁴

Reductive debromination of **92** with trineophyltin hydride lead almost exclusively (>12:1) to the 6 β -fluoropenicillanate **93**.

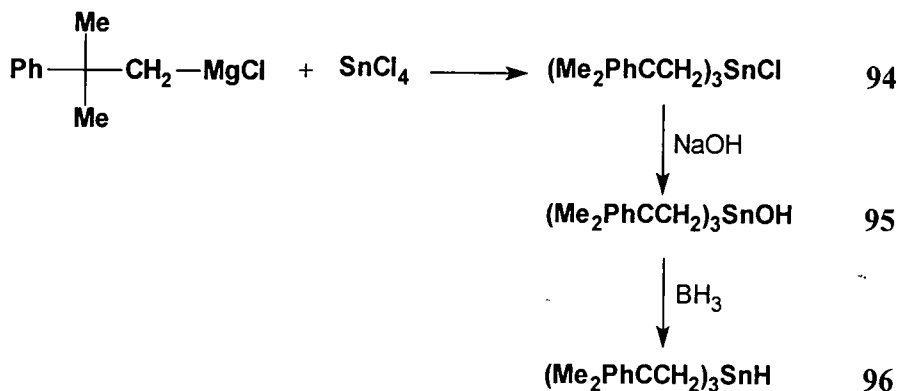


Fig. 3.23

The resultant diastereoisomeric ratio arises as the intermediate radical is assumed to have the conformation shown in Fig. 3.24, where the β -lactam ring is essentially planar and the thiazolidine ring has both the 2 β and 3 α substituents *pseudo*-axial with respect to the five-membered ring. Hydride delivery to the *si* face is then sterically preferred over delivery to the *re* face, thus giving the 6 β -halopenicillin as the predominant product. The much bulkier trineophyltin hydride reagent is sterically more demanding than tributyltin hydride, which could account for the observed increase in the diastereoisomeric ratio.

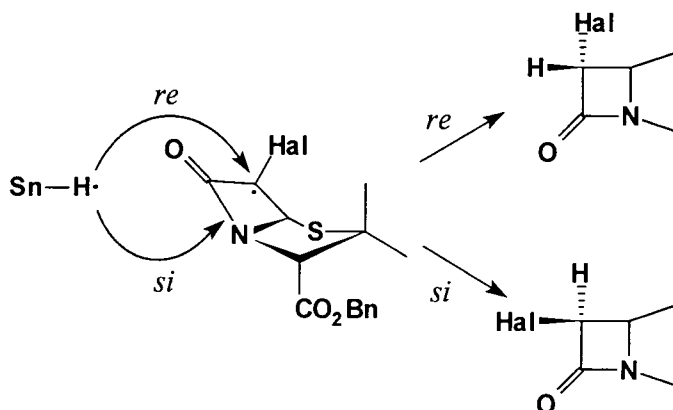


Fig 3.24 Radical-induced reductive debromination

With benzyl 6 β -fluoropenicillanate **93** in hand attempts were made to remove the benzyl protecting group to generate the free carboxylic acid required for the studies with the β -lactamase. However, despite literature precedence for such a conversion¹⁵⁵ by catalytic hydrogenation over Pd-C, removal of the benzyl group proved unsuccessful, with mixtures of products isolated. The use of AlCl₃ in nitromethane was also unsuccessful and the removal of the benzyl group frustrated the synthesis of the desired acid.

Mascaretti had observed a difference in the stability of the two isomers in that formation of the salt of the 6 β -fluoropenicillin had proven elusive, with hydrolysis products isolated from the reaction. With the benzyl esters **90** and **93** in hand a study of the methanolic hydrolysis was undertaken using both ¹⁹F NMR spectroscopic and spectrophotometric techniques to determine the relative rates of hydrolysis.

3.7 Enzymatic hydrolysis of 6 α -fluoropenicillanic acid

Having prepared 6 α -fluoropenicillanic acid **78**, the interaction with the β -lactamase I from *Bacillus cereus* was studied by ¹⁹F NMR spectroscopy and UV-VIS spectrometry. The hydrolysis of the β -lactam was conveniently monitored by following the decrease in the carbonyl absorption at 235 nm in buffer (pH 7) at room temperature. The observed spectrum (Fig. 3.25) shows that after hydrolysis the absorption of the β -lactam ring at 235 nm is absent and a new band at 340 nm is observed. Under the conditions used there was no detectable loss in enzyme activity, which was demonstrated by the enzyme's continuing ability to hydrolyse additional substrate.

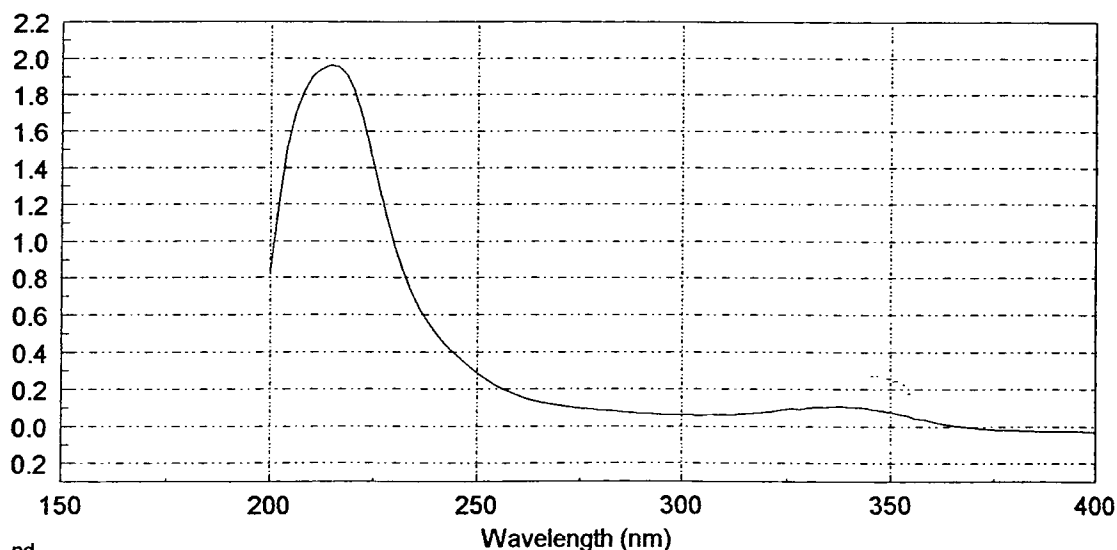


Fig 3.25

The enzyme reaction course was also followed by ^{19}F NMR spectroscopy in a buffer solution. The ^{19}F NMR spectra (Fig. 3.26) at an intermediate stage clearly shows that the fluorinated penicillin ($\delta -181.2$) is cleanly hydrolysed to a single new fluorinated product at $\delta -192.3$, which is presumably the hydrolysed β -lactam. Upon complete hydrolysis of the penicillin this product remained stable for an extensive period of time, with no apparent decomposition to further products.

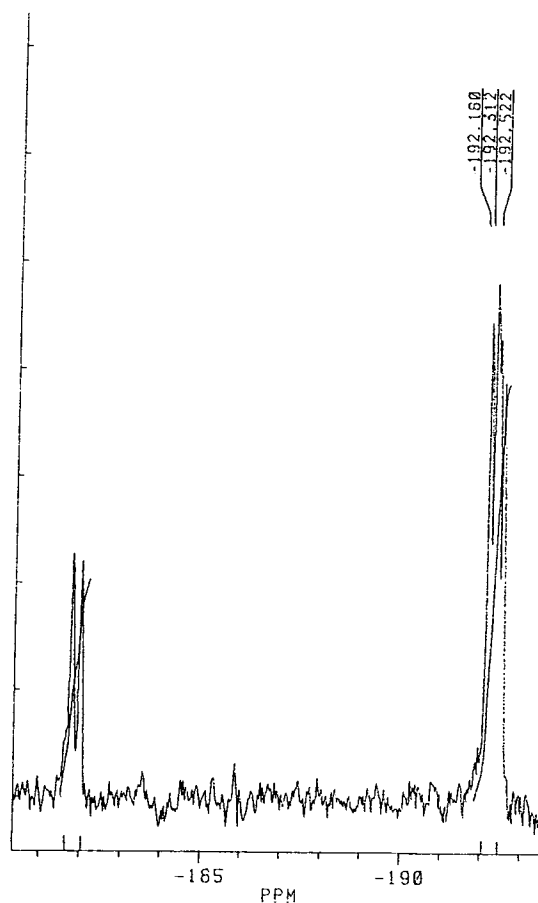


Fig. 3.26

These observations are consistent with the results reported by Mascaretti for the interaction of 6α -fluoropenicillanic acid with the β -lactamase I, which showed that the penicillin was a substrate for the β -lactamase but displayed only a slight inhibitory effect. Due to the lack of stability of the 6β carboxylate product this reaction could not be attempted with the other epimer.

3.8 Sodium methoxide mediated hydrolysis of 6 α - and 6 β -fluoropenicillanates

With the problems incurred in the synthesis of 6 β -fluoropenicillanic acid it was decided to undertake a comparative study of the chemical hydrolysis of the two fluorinated penicillin esters with sodium methoxide in MeOH. Using ^{19}F NMR spectroscopy and kinetic measurements, any difference in the rate of hydrolysis that existed between the two stereoisomers could be determined. The study was carried out under two sets of limiting conditions; firstly, where the methoxide was in excess of the penicillin, and secondly, the reverse with the penicillin in excess of the methoxide.

The chemical reactivity of β -lactams towards nucleophilic attack has been widely explored, with much of the work reviewed by P \ddot{a} ge.¹²⁶ The β -lactam ring is susceptible to nucleophilic attack because of the strain in the ring and the nonplanarity of the system inhibiting the usual amide resonance.

The action of oxygen-containing nucleophiles is of particular interest, as β -lactamases contain key serine residues which catalyse the hydrolysis of β -lactams, forming a penicillinoyl ester of the serine residue. Oxygen anions can catalyse the hydrolysis of penicillins by either acting as general bases or as nucleophiles. Basic anions act as nucleophilic catalysts, forming an intermediate penicilloyl ester *via* the tetrahedral intermediate **97**.

From the studies of the aminolysis of β -lactams the consensus is that the addition of the amine nucleophile is to the least hindered α -face of the carbonyl and it is a reversible process.¹⁴⁴ For uncatalysed reactions the rate limiting step of aminolysis is C–N bond fission.

The addition of an alkoxide ion to β -lactams will generate tetrahedral intermediate **97** (Fig. 3.27). The tetrahedral intermediate will breakdown *via* C–N bond fission at a rate k_2 to give the β -lactam ring-opened product which will then undergo rapid protonation from the solvent.

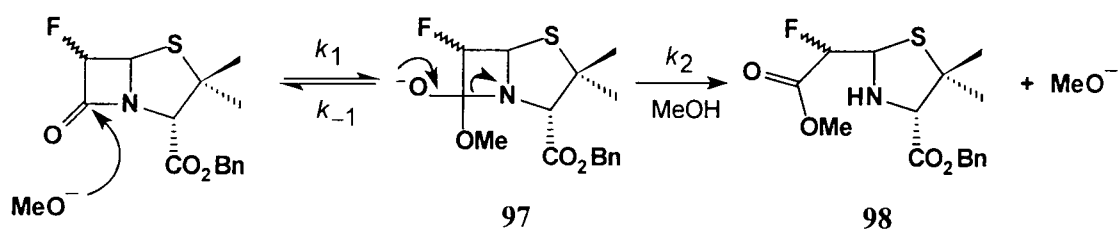


Fig. 3.27

Previous studies on the chemical hydrolysis of benzylpenicillin have shown that the nature of the nucleophile can alter the rate limiting step of the hydrolysis. With hydroxide ion catalysed hydrolysis attack of the nucleophile, *i.e.* k_1 , is rate limiting, whereas alkoxide ions react with rate limiting breakdown of the tetrahedral intermediate.¹²⁶

3.8.1 ^{19}F NMR spectroscopic study of hydrolysis

The hydrolyses of the two 6-fluoropenicillins using sodium methoxide were carried out separately in the first instance to determine the nature of the hydrolysis products. The penicillin ester was dissolved in $[\text{}^2\text{H}_4]$ methanol and an excess of sodium methoxide added to the mixture. The progress of the reaction was monitored by ^{19}F NMR spectroscopy. Both the 6α - and 6β -fluoropenicillanates were observed to form instantaneously (NMR time scale) an initial hydrolysis product, 6α at $\delta -195.5$ and 6β at $\delta -190.2$. These initial products of hydrolysis then reacted further, forming in the 6α case a second unidentified product at $\delta -190.0$. The 6β isomer was seen to give a much more complex spectrum. Notably, no fluoride ion elimination was detected, therefore fluorine was not being displaced from C-6 (*cf.* Br). The ^{19}F NMR spectrum also showed some evidence for the incorporation of deuterium at the C-6 position by a shift of 0.5 ppm and a loss of coupling in the fluorine signal of the first hydrolysed product. There was, however, no evidence for the epimerisation of the C-6 position in the starting compounds as has been previously observed with other penicillins.¹²⁶ The initial product observed in the ^{19}F NMR spectrum was assumed to be that of the ring opened ester **98** and is consistent with that observed in the enzymatic reaction. This was confirmed by isolation and characterisation of the initial products of hydrolysis by ^1H and ^{13}C NMR and IR spectroscopy, which were all consistent with the formation of **98**. However, in such a basic solution it is not unreasonable for this penicilloyl ester moiety to undergo further reaction and break down to other products *via* opening of the thiazolidine ring and formation of the enamine **99** (Fig. 3.28).

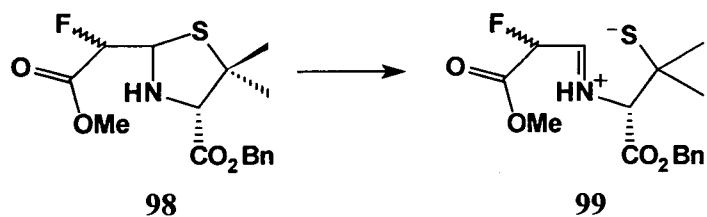


Fig. 3.28

3.8.2 Competitive hydrolysis study

With the initial products of hydrolysis of the two isomers identified in the ^{19}F NMR spectrum, the relative rates of hydrolysis of the two fluorinated penicillins with methanolic sodium methoxide was investigated. A 1:1 mixture of the two isomers was prepared in methanol (33 mM), this was treated with small quantities (5 μl) of a 0.03 M NaOMe solution and the ^{19}F NMR spectrum of the solution taken. The results of the competitive hydrolysis study are outlined in Table 3.1. The ratios of product and starting material were calculated by simple integration of the observed NMR spectra. An illustrative ^{19}F NMR spectrum from the competitive study is shown in Fig. 3.29.

Table 3.1 Competitive hydrolysis of fluoropenicillinates

α Substrate reacted (%)	β Substrate reacted (%)	Ratio $\alpha:\beta$ remaining
0	0	1:1
0	18	1.22:1
0	22	1.28:1
0	35	1.53:1
23	66	2.28:1
26	81	3.90:1
28	83	4.23:1
31	88	5.75:1

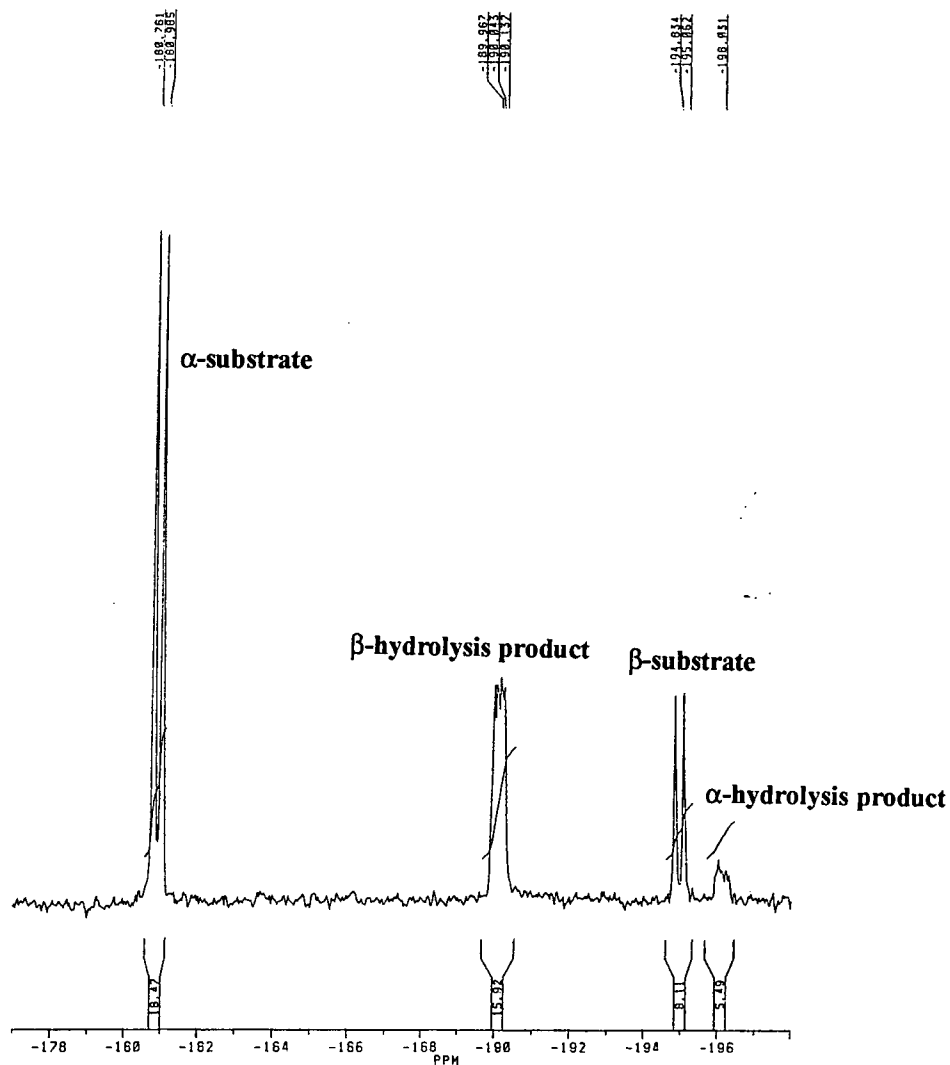


Fig. 3.29 ^{19}F NMR spectrum from competitive hydrolysis of 6α - and 6β -fluoropenicillanates

The competitive hydrolysis study by ^{19}F NMR spectroscopy demonstrates that the β -isomer of the fluorinated penicillin was hydrolysed preferentially over the α -isomer. Clearly the results from the initial stages of this study are the most significant because with time the relative concentration of the two epimers changes. The results show that greater than 35% of the β -isomer is hydrolysed before any reaction of the α -isomer has taken place. It is also apparent that the MeO^- is acting catalytically as much less than one equivalent was required to hydrolyse all the β -lactam present.

3.8.3 Kinetic analysis of hydrolysis

The competitive hydrolysis experiment by ^{19}F NMR spectroscopy demonstrated qualitatively that the β -isomer was preferentially hydrolysed with respect to the α -isomer. In order to obtain quantitative data a kinetic analysis of the hydrolysis reaction was undertaken. Initial reactions demonstrated that on addition of methanolic sodium methoxide to the substrate in methanol an increase in absorbance occurred at 310 nm, which corresponded to the formation of the penicilloyl ester moiety **98**. The rate constants of the reaction were therefore determined by following the rate of increase in absorbance at 310 nm (Fig. 3.30) under two sets of limiting conditions; (i) substrate in excess of methoxide, and (ii) methoxide in excess of substrate.

In the latter case, with methoxide in excess, the measurements were made using stopped-flow spectrometry (see Appendix 1) as the rates were too fast to measure by conventional methods. The software used to run the stopped flow apparatus calculated the observed rate constants (k_{obs}). The results were precisely fitted to a first order rate equation.

The reaction rates with the fluoropenicillanate in excess were assessed by conventional spectrophotometric methods. The reactions were initiated by the addition of substrate to a solution of methoxide in methanol of known concentration in a 2.5 cm³ cuvette. The changes in absorbance with time were entered into a software package to determine k_{obs} values. Again the data corresponded precisely to first order kinetics.

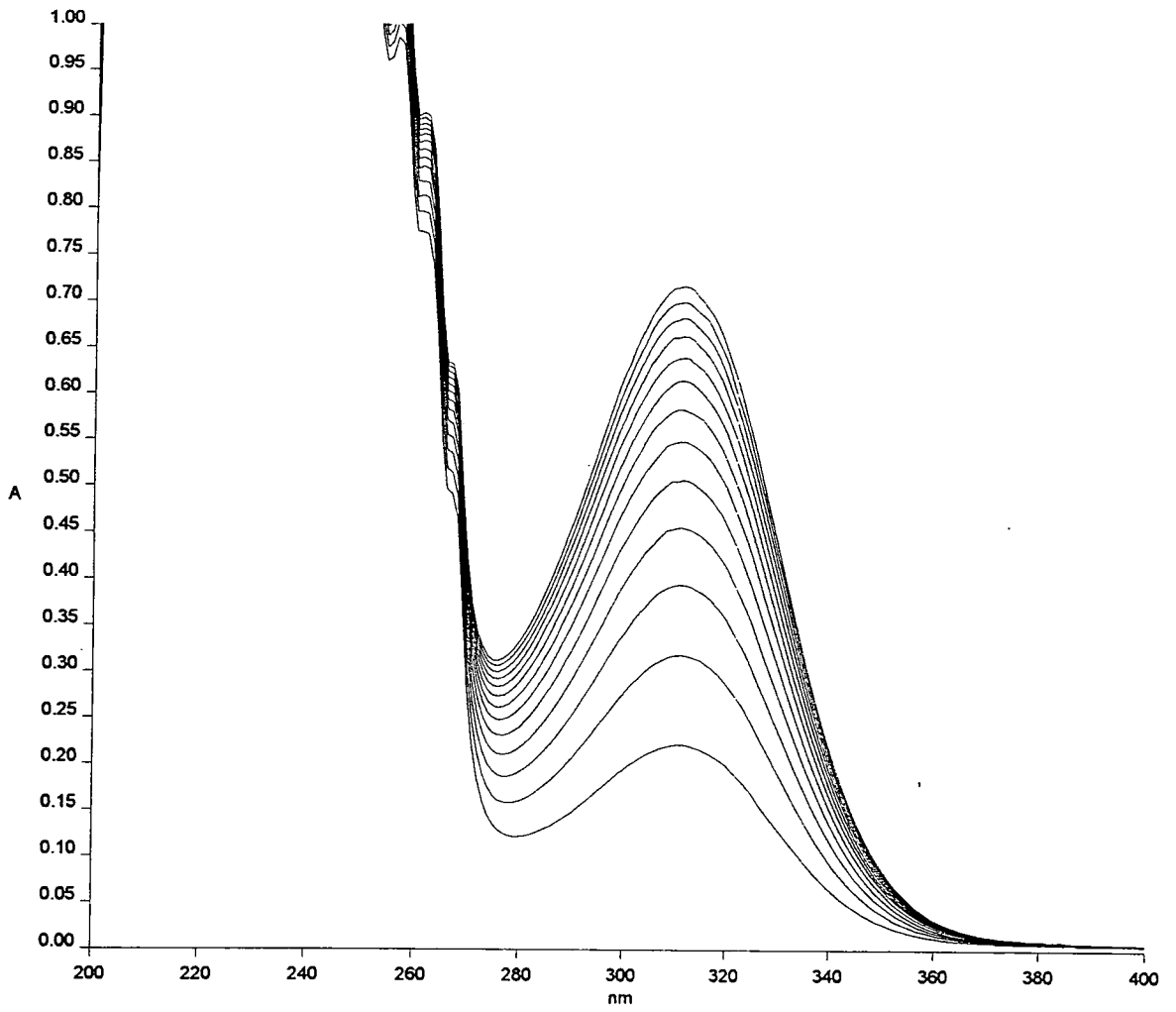


Fig. 3.30

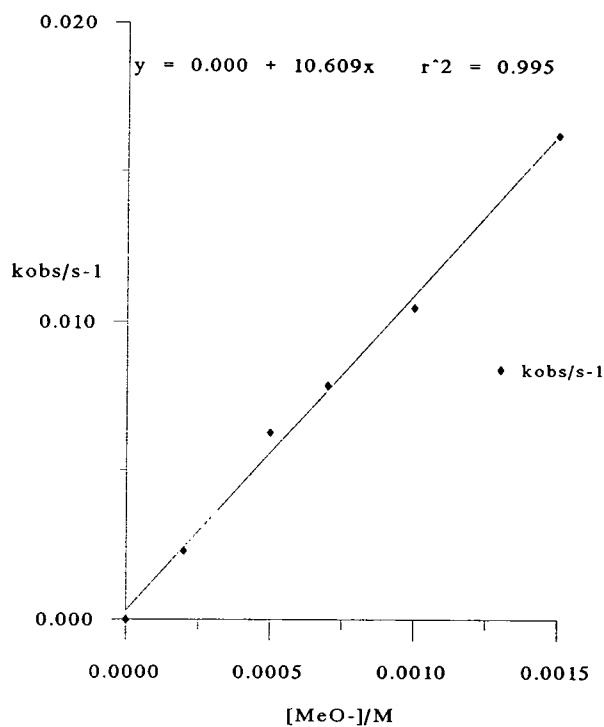
3.8.4 Kinetic results

(i) Substrate in excess of methoxide

The values obtained for k_{obs} of both the 6α and 6β fluorinated penicillanates are shown in Tables 3.2 and 3.3. In both cases the [sub] was 1.5 mM.

Table 3.2 6α -Fluoropenicillanate: Abs $_{\infty}$ 0.65

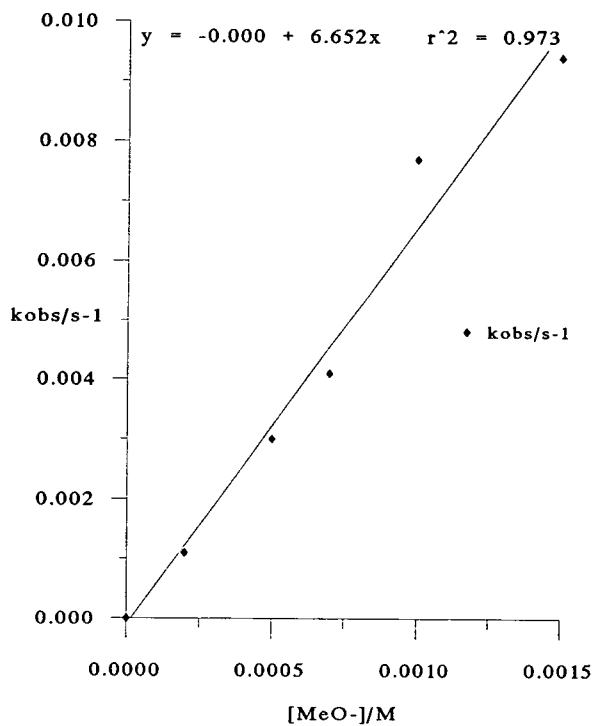
[MeO ⁻]/M	0.0002	0.0005	0.0007	0.0010	0.0015
$k_{\text{obs}}/\text{s}^{-1}$	2.3×10^{-3}	6.3×10^{-3}	7.9×10^{-3}	10.5×10^{-3}	16.2×10^{-3}



Second order rate constant for hydrolysis of 6α -fluoropenicillanate = $10.6 \text{ dm}^3 \text{ mol}^{-1} \text{ s}^{-1}$

Table 3.3 6 β -Fluoropenicillanate: Abs $_{\infty}$ 1.1

[MeO ⁻]/M	0.0002	0.0005	0.0007	0.0010	0.0015
k_{obs}/s^{-1}	0.0011	0.0030	0.0041	0.0077	0.0094



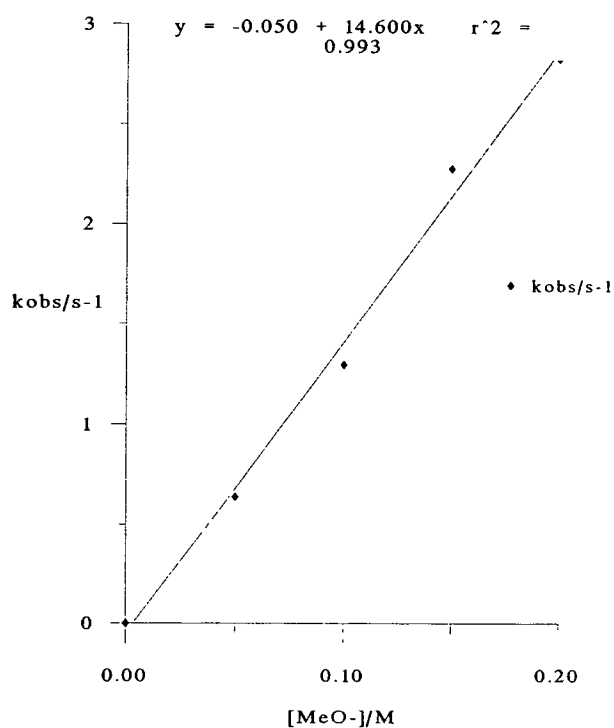
Second order rate constant for hydrolysis of 6 β -fluoropenicillanate = 6.6 dm³ mol⁻¹ s⁻¹

(ii) Methoxide in excess of substrate

The values obtained for k_{obs} of both the α and β fluorinated penicillanates are shown in Tables 3.4 and 3.5. In both cases the $[\text{sub}]$ was 0.15 mM.

Table 3.4 6 α -Fluoropenicillanate: Abs $_{\infty}$ 0.15

$[\text{MeO}^-]/\text{M}$	0.05	0.10	0.15	0.20
$k_{\text{obs}}/\text{s}^{-1}$	0.64	1.30	2.28	2.82

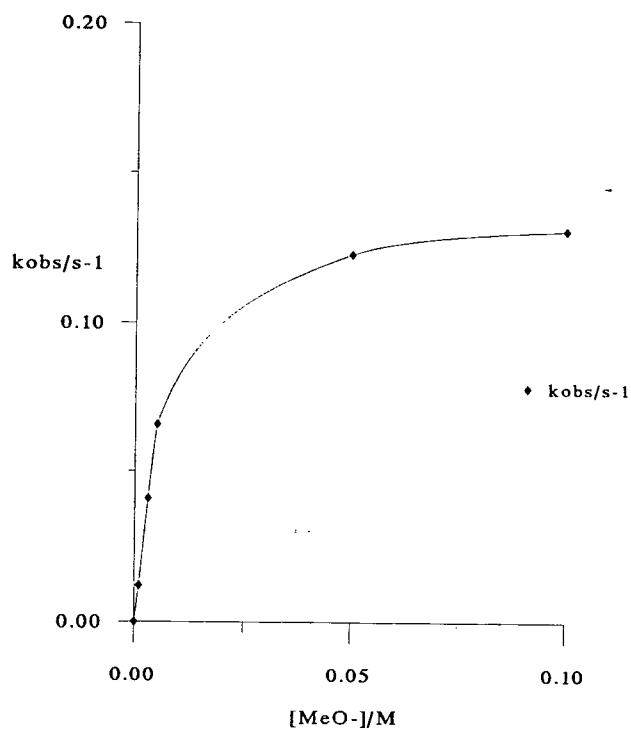


Second order rate constant for hydrolysis of 6 α -fluoropenicillanate = $14.6 \text{ dm}^3 \text{ mol}^{-1} \text{ s}^{-1}$



Table 3.5 6 β -Fluoropenicillanate: Abs_∞ 0.11

[MeO ⁻]/M	0.001	0.003	0.005	0.05	0.10
$k_{\text{obs}}/\text{s}^{-1}$	0.012	0.041	0.066	0.123	0.131



Rate of hydrolysis of 6 β -fluoropenicillanate

3.8.5 Discussion of kinetic analysis

Examination of the results obtained by kinetic analysis of the hydrolysis of the two isomers of benzyl 6-fluoropenicillanate with sodium methoxide gave a number of interesting results.

(i) The methoxide is acting catalytically as the hydrolysis is seen to go to completion with much less than an equivalence of methoxide added.

(ii) At low concentrations of methoxide, for both the 6 α and 6 β substrates the first order rate constants, k_{obs} , increase linearly with methoxide concentration.

(iii) At low concentrations of methoxide the observed rate, k_{obs} , is greater for the α -isomer.

(iv) At higher concentrations of methoxide, values of k_{obs} for the 6 α isomer continue to increase linearly with methoxide concentration. However, the 6 β -isomer is seen to behave differently and values of k_{obs} become independent of methoxide concentration at high concentrations of methoxide.

By consideration of the mechanism of the reaction (Fig. 3.27) of the methoxide with the penicillin, a suitable rate equation may be derived (Appendix 1) linking k_{obs} with the equilibrium constant K_1 , k_2 and $[\text{MeO}^-]$.

$$k_{\text{obs}} = \frac{k_2 K_1 [\text{MeO}^-]}{1 + K_1 [\text{MeO}^-]} \quad (3.1)$$

(i) β -Isomer

When the substrate was in excess of methoxide a linear dependence of k_{obs} on methoxide was observed. This indicates from eqn. (3.1) that $1 \gg K_1[\text{MeO}^-]$ and therefore:

$$k_{\text{obs}} = k_2 K_1 [\text{MeO}^-]$$
$$\therefore k_2 K_1 \approx 6.6 \text{ dm}^3 \text{ mol}^{-1} \text{ s}^{-1}$$

However, when methoxide was in excess a curvilinear dependence on methoxide concentration was found. The initial reaction slope was $13 \text{ dm}^3 \text{ mol}^{-1} \text{ s}^{-1}$. At higher

concentrations of methoxide the graph reaches a limit where $K_1[\text{MeO}^-] \gg 1$ and therefore:

$$k_{\text{obs}} = k_2 = 0.13 \text{ s}^{-1}$$

$$\text{Initial slope} = k_2 K_1 = 13 \text{ dm}^3 \text{ mol}^{-1} \text{ s}^{-1}$$

$$\therefore K_1 = 100 \text{ dm}^3 \text{ mol}^{-1}$$

If initial methoxide attack were the rate limiting step then a straight line graph with a first order dependence on methoxide would be expected.

(ii) α -Isomer

If the mechanism remains the same for the α -isomer then eqn. (3.1) is equally valid for this isomer. With the substrate in excess of the methoxide a linear dependence on methoxide is observed, indicating $1 \gg K_1[\text{MeO}^-]$. Therefore:

$$k_{\text{obs}} = k_2 K_1 [\text{MeO}^-]$$

$$\therefore k_2 K_1 = 10.6 \text{ dm}^3 \text{ mol}^{-1} \text{ s}^{-1}$$

When the methoxide is in excess, again k_{obs} increases linearly with methoxide concentration:

$$k_2 K_1 = 14.6 \text{ dm}^3 \text{ mol}^{-1} \text{ s}^{-1}$$

As a linear plot is obtained $1 \gg K_1[\text{MeO}^-]$:

$$K_1[\text{MeO}^-] < 1 \text{ when } [\text{MeO}^-] = 0.2 \text{ mol dm}^{-3}$$

$$\therefore K_1 < 5 \text{ dm}^3 \text{ mol}^{-1}$$

If $k_2 K_1 \approx 12 \pm 2 \text{ dm}^3 \text{ mol}^{-1} \text{ s}^{-1}$, k_2 must \therefore be $> 2.4 \text{ dm}^3 \text{ mol}^{-1} \text{ s}^{-1}$.

Therefore to summarise the results:

	$k_2/\text{dm}^3 \text{ mol}^{-1} \text{ s}^{-1}$	$K_1/\text{dm}^3 \text{ mol}^{-1}$
α	>2.4	<5
β	0.13	100

These results indicate that the tetrahedral intermediate formed between the β -isomer and methoxide is more stable than the corresponding intermediate for the α -isomer, but that the rate of C–N bond fission (k_2) is faster in the case of the α substrate.

The results of the kinetic experiments can also be used to explain the observations of the competitive hydrolysis experiment using ^{19}F NMR spectroscopy. If the systems were at equilibrium then it might be expected from the k_2K_1 values to observe similar reaction velocities and indeed this is the case.

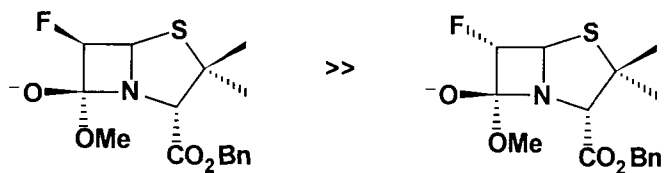
$$k_2K_1 \alpha = 12 \pm 2 \text{ dm}^3 \text{ mol}^{-1} \text{ s}^{-1}$$

$$k_2K_1 \beta = 10 \pm 3 \text{ dm}^3 \text{ mol}^{-1} \text{ s}^{-1}$$

However if k_{-1} is not very much greater than k_2 then the rate of initial attack of methoxide k_1 may determine the reaction pathway. To this end the observation that $K_1[\beta] \gg K_1[\alpha]$ would imply that $k_1\beta \gg k_1\alpha$. This would in turn account for the observation of the β -isomer being hydrolysed at a faster rate than the α -isomer in the competitive hydrolysis experiment.

3.9 Conclusions

The results from the ^{19}F NMR spectroscopic experiments show that the β -isomer is hydrolysed in a competitive experiment preferentially over the α -isomer. The kinetic analysis of the two substrates with methoxide gave absolute values for the rates of hydrolysis which were almost identical within experimental error. However, the much larger equilibrium constant for the β -isomer is consistent with the observations in the NMR experiment. This indicates that the tetrahedral intermediate formed with the β -isomer and the methoxide is much more stable than that of the α -substrate.



The reason for the increased stability of the β -isomer is not immediately obvious and no conclusions about this have yet been drawn.

The observed results are, however, in accordance with those predicted by applying an Anh–Eisenstein model to the hydrolysis, with the β -isomer being hydrolysed at a greater rate relative to the α isomer. However, it would be inappropriate to draw a conclusion that the observed differences are arising solely due to this type of interaction.

Chapter Four

The Synthesis of α -Fluoro Ketones by 1,4-Additions of Monofluorinated Enamines to Michael Acceptors

The Synthesis of α -Fluoro Ketones by 1,4-Additions of Monofluorinated Enamines to Michael Acceptors

4.1 Introduction

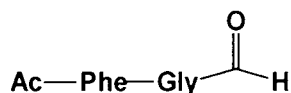
The inhibition of proteolytic activity by low-molecular weight synthetic inhibitors serves mainly to control undesirably high levels of proteases within biological systems. The mode of catalytic acceleration and inhibition of hydrolysis of a peptide bond by serine proteases has been studied intensively for more than 30 years.¹⁶⁵ More than 130 serine proteases have been classified which, despite mechanistic similarities, are involved in a broad range of important biological processes (Table 4.1).

Table 4.1 Some biological processes performed by serine proteases¹⁶⁵

Type of reaction	Enzyme(s)	Physiology	Pathology
Activation of zymogens	Trypsin, chymotrypsin	Coagulation of blood	Thrombosis, pancreatitis.
Fibrinolysis	Plasmin	Destruction of blood clots	Cell invasion
Degradation of highly cross-linked proteins	Elastases, caphepsin G	Proteolysis of elastins	Pulmonary emphysema, arthritis

Inhibition of the proteases is commonly achieved by a slow binding of the inhibitor to the enzyme, forming a tightly-bound enzyme-inhibitor complex [EI] which is slowly hydrolysed. The designs of synthetic inhibitors are based mainly on peptide aldehydes.

Peptide and amino acid analogues containing aldehydic functional groups have been shown to be good inhibitors of hydrolytic enzymes such as serine and cysteine proteases. For example, papain is inhibited by **100** ($K_i = 5 \times 10^{-8} \text{ M}$)¹⁶⁶ and elastase is inhibited by **101** ($K_i = 8 \times 10^{-7} \text{ M}$).¹⁶⁷

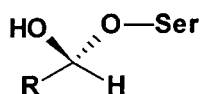


100



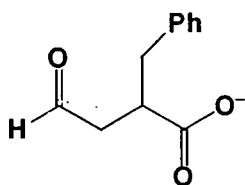
101

In aqueous solution aldehydes exist predominately as hydrates, and therefore it is likely that the aldehyde in the active site exists bound to the serine oxygen as a hemiacetal **102**. Indeed, NMR spectroscopy has provided evidence for the formation of a bound hemiacetal.^{168,169} Wolfenden suggested that the hemiacetal replaces the tetrahedral intermediate that is formed during the hydrolysis of peptide substrates and therefore the aldehydic peptides are transition-state analogue inhibitors.¹⁷⁰

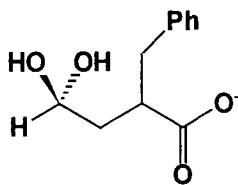


102

Aldehydes are also known to be efficient inhibitors of metalloproteases, *e.g.* **103**, which is an inhibitor of carboxypeptidase A.¹⁷¹ The inhibitory species is likely to be the hydrated form **104**, which resembles the tetrahedral adduct formed when H₂O adds to the carbonyl group of a peptide substrate.



103



104

Although efficient inhibitors, these aldehydic peptides have limitations, principally that the aldehyde functionality can be placed only on the carboxy-terminal side of peptides. Since proteases interact with groups on both sides of the scissile peptide bond, protease inhibitors that make use of these long-range interactions are likely to have a higher degree of specificity toward targeted proteases. Peptide derivatives that contain recognition structures on both sides of an internal ketone can be prepared, however, due to the low tendency of ketones to hydrate in solution or form a hemiketal with an active-site nucleophile, the utility of these compounds as inhibitors is limited. On the other hand, the introduction of an electronegative atom on the α -carbon increases the ketones susceptibility to hydration and attack by nucleophiles. Thus fluoro ketones have been extensively studied as potent inhibitors of hydrolytic enzymes.^{172,173} Both di- and tri-fluoromethyl ketones exist in water almost entirely in

the hydrated form, and inhibition is therefore probably due to the formation of a stable hemiketal with the active site serine residue. Fig. 4.1 shows how trifluoromethyl ketones, *e.g.* **105**, in aqueous solvents are 97–100% hydrated, which can be compared to <1% for the corresponding methyl ketones **106**.¹⁷⁴

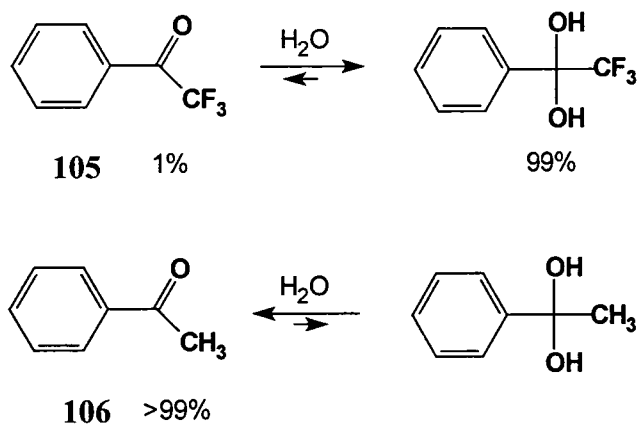
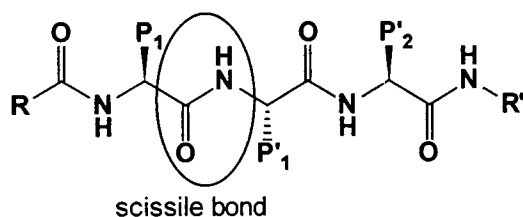
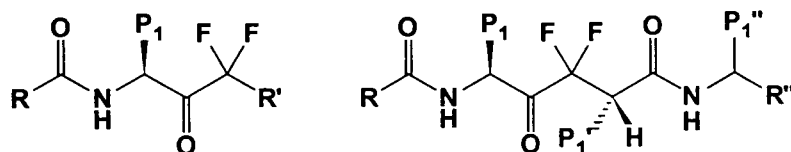


Fig. 4.1

Replacement in substrates of proteolytic enzymes of the scissile amide bond by perfluoromethyl or difluoromethylene ketones has generated a number of potent transition state type inhibitors (Fig. 4.2).¹⁷⁵



Difluoromethylene ketones have a potential advantage in terms of affinity and selectivity over C-terminal trifluoromethyl ketones (Type A inhibitors, Fig. 4.2) in that they may occupy additional binding sites on the leaving group side (S' subsites).¹⁷⁶ Much of the early work relied on the incorporation of difluorostatones **114** (Type B), which led to the discovery of efficient pepsin and renin inhibitors. The introduction of difluoromethylene ketones through incorporation of a spacer group (Type C) have been applied to the inactivation of α -chymotrypsin and elastase.¹⁷⁷ True dipeptide isosteres (Type D), though, are rare due to the difficulty of developing general and readily accessible chemistry along, with the potential reactivity of intermediates and final compounds.



Type A inhibitors: $R' = F$

Type B inhibitors: $R' = \text{CONHR}''$

Type C inhibitors: $R' = (\text{CH}_3)_2\text{CONHR}''$

Type D inhibitors

Fig. 4.2

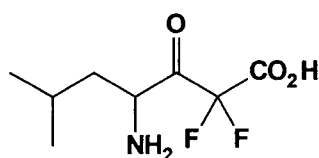
Fluoro ketone substrate analogues have been found to be inhibitors of acetylcholine esterase, zinc metaloproteases like carboxypeptidase A and angiotensin-converting enzyme¹⁷² (Table 4.2).

Table 4.2 Inhibitors of acetylcholinesterase¹⁷²

No.	Compound	K_i/nM	No.	Compound	K_i/nM
107		16	111		1.6
108		310 000	112		600
109		410 000	113		$>10^6$
110		8 000			

The trifluoromethyl ketone **107** is an effective, reversible inhibitor of acetylcholinesterase. The observed K_i value is 2×10^{-4} -fold lower than that for the corresponding methyl ketone **108**. The trifluoromethyl ketone **110**, which is shorter than **107** by a single methylene group, is a poorer inhibitor. However it is the difluoromethyl ketone **111** which in this study emerged as the best inhibitor of the enzyme.

Similarly aspartyl proteases like pepsin are inhibited by a synthetic analogue of pepstatin containing difluorostatone 114.



114

^{13}C NMR analysis of the difluorostatone containing peptide in $[\text{}^2\text{H}_6]\text{DMSO}-\text{D}_2\text{O}$ (4:1) demonstrated that it exists predominately in the hydrated form and is an extremely potent inhibitor of pepsin ($K_i = 6 \times 10^{-11} \text{ M}$).

In all the cases outlined, the fluoro ketones are seen to be much more effective inhibitors than their non-fluorinated analogues and display a strong affinity to remain associated with their target enzymes. The strong binding of fluoro ketones in the case of angiotensin-converting enzyme suggests their potential use as antihypertensives.

Brodbeck *et al.* reported the time-dependent inhibition of acetylcholine esterases from several sources using trifluoromethyl ketones.¹⁷⁸ It is noteworthy that the corresponding $-\text{CCH}_3$ analogues are simple reversible inhibitors with no irreversible features. An excellent example of inhibition is outlined in Fig. 4.3. *m*-Trimethylaminophenyl trifluoromethyl ketone forms a tremendously stable covalent enzyme tetrahedral adduct. The accumulating species is indeed very stable since dialysis for eight days resulted in regaining only 20% of the catalytic activity.

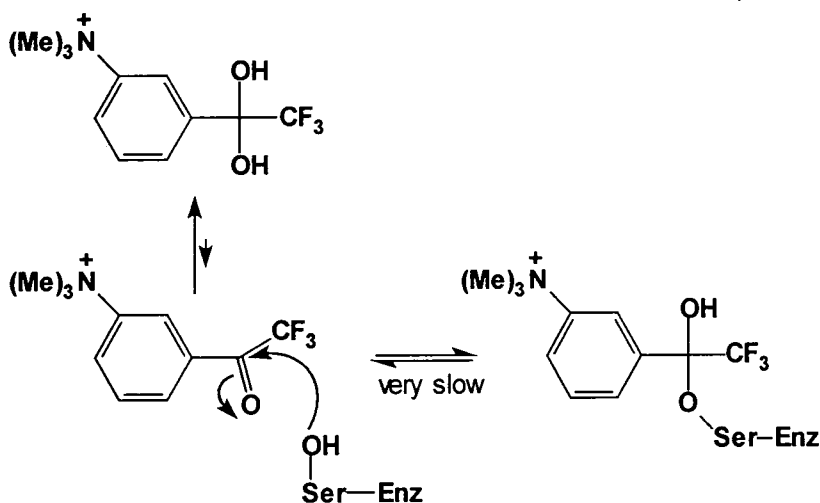


Fig. 4.3

4.2 Synthesis of fluorinated ketones

With the biological potential of α -fluorinated ketones as outlined in 4.1, it is not surprising that such compounds have received attention as key substances for the preparation of medicines and agrochemicals. As such, a number of synthetic methods have been established for the formation of α -fluoro ketones, many of which were reviewed by Rozen and Filler¹⁷⁹ and some of which are outlined below. The reactions are categorised as either nucleophilic or electrophilic fluorination, or the reaction of compounds which contain fluorine. However, new and efficient methods for the preparation of α -fluoro ketones are continually sought.

A common method widely employed for the synthesis of α -fluoro ketones involves reaction of diazo ketones with hydrogen fluoride–pyridine at 0 °C.⁷⁶ When the reaction is performed in the presence of added halide ions, *e.g.* by using *N*-halosuccinimides, the fluorohalo ketones **115** are obtained (Fig. 4.4).

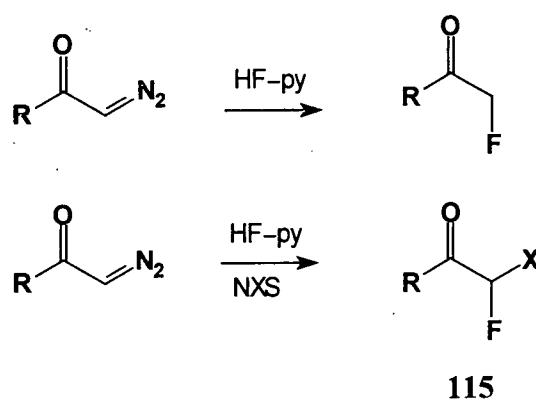


Fig. 4.4

Other nucleophilic sources of fluorine exploited in the synthesis of α -fluorocarbonyl compounds include metal and tetraalkylammonium fluorides,¹⁷⁹ nitrosyl fluoride (NOF), which converts double bonds to fluoro ketones in two steps,¹⁸⁰ and reagents that contain a P–F bond, *e.g.* PhPF_4 .¹⁸¹

The use of electrophilic fluorinating reagents by reaction with metal enolates has also proven an effective method in the production of α -fluoro ketones. Much recent work has focussed on improvements to the efficiency and stability of the electrophilic reagents. One of the earliest electrophilic fluorinating reagents, perchloryl fluoride (FCIO_3), is extremely hazardous, and regularly gave rise to mixtures of products.¹⁸²

Acetyl hypofluorite has also been employed as an electrophilic fluorinating reagent and reacts as outlined in Fig. 4.5 *via* the enolate **116**.¹⁸³

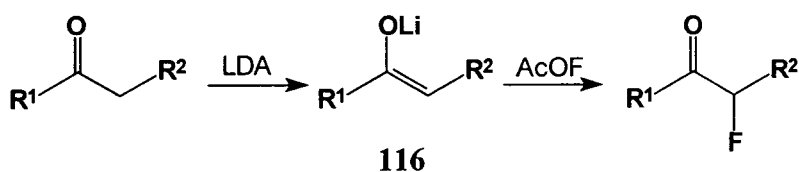
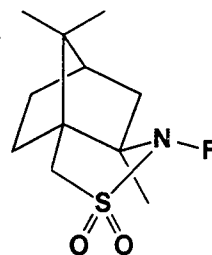
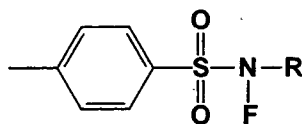
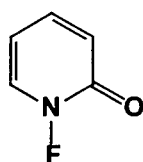
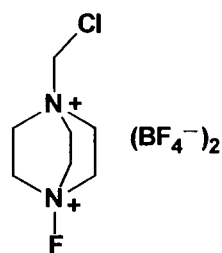


Fig. 4.5

More recently a number of new *N*-fluoro compounds have been developed which provide an easier to handle and more stable source of F^+ . These include *N*-fluoro-2-pyridone **117**,¹⁸⁴ various *N*-fluoro sulfonamides **118**¹⁸⁵ and enantioselective reagents like the *N*-fluoro sultam **119**.¹⁸⁶



Elemental fluorine has also been used in the synthesis of α -fluoro ketones, initially Purrington found success by reacting silyl enol ethers with 5% F_2 in N_2 to obtain the desired fluorinated products.¹⁸⁷ 2-Fluoro-1,3-dicarbonyl compounds **121** have aroused considerable interest as small molecules that provide building blocks for the preparation of larger biologically active compounds. The electrophilic fluorinating reagent F-TEDA-BF_4 (TEDA = triethylenediamine) **120** efficiently reacts with 1,3-dicarbonyl compounds at room temperature to give the α -fluoro derivatives in good yield.¹⁸⁸



120

More recently, Chambers *et. al.* have shown that fluorine gas can be used directly to prepare 2-fluoro 1,3-diketones **121** and keto esters,¹⁸⁹ giving a mixture of products shown in Fig. 4.6.

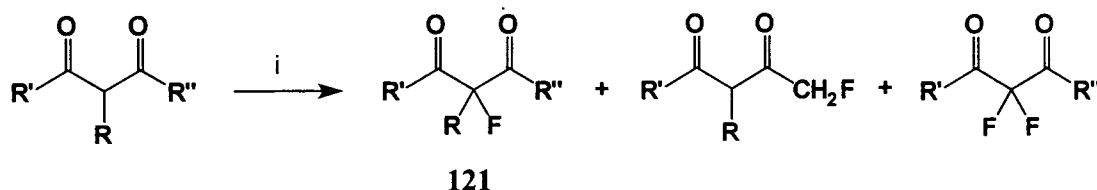


Fig. 4.6 Reagents and conditions: i, 0.05 mol F₂ (10% N₂), formic acid, 10–15 °C

The reaction of electrophiles with α -fluorinated enolate anions¹⁹⁰ or aza enolates, generated after deprotonation of imines of fluoroacetone¹⁹¹ (Fig. 4.7), has proven moderately successful. In their extensive study of fluorinated azaenolates, Welch and Eswarakrishnan demonstrated how variation in base and reaction temperature affected the regioselectivity of deprotonation of fluoroacetone and the subsequent product of alkylation (Table 4.3).¹⁹²

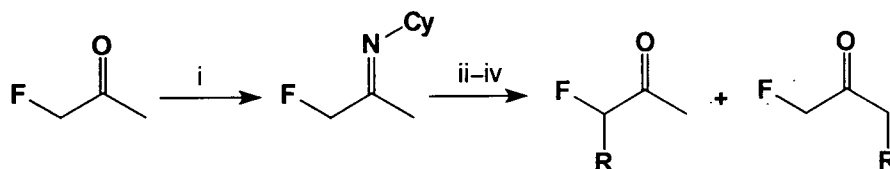


Fig. 4.7 Reagents and conditions: i, cyclohexylamine, K₂CO₃; ii, base; iii, RX; iv, H₃O⁺

Table 4.3

Alkyl halide	Base ^a	T/°C	RCHFCOCH ₃	CH ₂ FCOCH ₂ R	Yield (%)
CH ₃ I	A	-30	11	89	48
CH ₃ I	B	-80	96	4	43
CH ₂ =CHCH ₂ Br	A	-30	9	91	62
CH ₂ =CHCH ₂ Br	B	-80	97	3	69

^a A = LHMDS; B = LDA.

Finally, α -fluoro ketones have been successfully synthesised by hydrogen fluoride-mediated isomerisation of 2-fluorooxiranes, although this methodology is limited to appropriate systems (Fig. 4.8).¹⁹³

**Fig. 4.8** Isomerisation of 2-fluorooxiranes

It became attractive to investigate the application of Stork enamine type chemistry to develop a new method for the synthesis of α -fluoro ketones *via* the alkylation of fluoro enamines.¹⁹⁴ Such an approach would offer a neutral and mild method towards the formation of α -fluorinated ketone compounds. Stork enamine chemistry appears in most undergraduate textbooks, but interestingly no examples using 2-fluoro ketones have been reported in the literature. This aspect of the project aimed to assess if this particular application was problematic or if it had just been overlooked.

4.3 Stork enamine chemistry

The reactivity of enamines has been known since 1883, when first Collie, and then Benary and Robinson described the C-alkylation of aminocrotonic esters.¹⁹⁵ However, the wide-ranging applicability of the reaction of enamines with electrophiles was not realised until Stork's pioneering work in 1954. The Stork enamine reaction involves the C-alkylation or -acylation of carbonyl compounds *via* an enamine intermediate **122**, and

since 1954 it has become a common synthetic strategy.¹⁹⁶ In the definitive paper Stork considered factors affecting the structure and reactivity of enamines and their alkylation and acylation.¹⁹⁷ The Stork method generally leads almost exclusively to monoalkylated products with alkylation directed towards the less substituted side of the ketone **123** (Fig. 4.9).

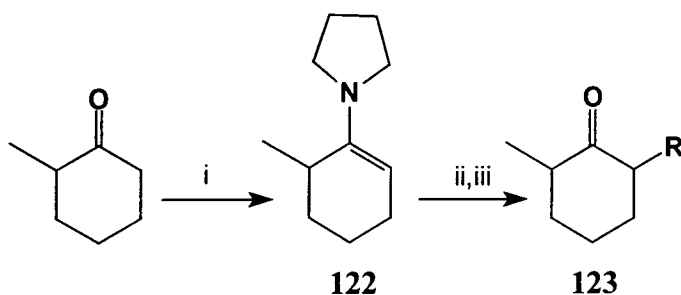
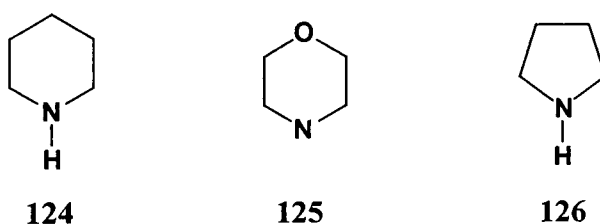


Fig. 4.9 Reagents and conditions: i, pyrrolidine, molecular sieves; ii, RX; iii, H_3O^+

The enamines of ketones are readily prepared in high yield by the condensation reaction of the appropriate ketones and amines in a suitable solvent such as benzene, toluene or xylene. The eliminated water is usually removed either by means of a Dean–Stark head or molecular sieves.¹⁹⁸ Alternatively, a chemically inert drying agent, *e.g.* K_2CO_3 or MgSO_4 , may be suspended in the reaction mixture. The most commonly used amines are the cyclic amines piperidine **124**, morpholine **125** and pyrrolidine **126**.



Using enamine methodology the reaction of α -fluoroacetophenones with various amines was explored along with the subsequent alkylation of the derived enamines to afford α -fluoro ketone compounds.

4.4 Synthesis of α -fluoroacetophenones and enamines

The required α -fluoroacetophenones **127**–**130** were readily prepared (Fig. 4.10) from the appropriately substituted acid chlorides, firstly by reaction with diazomethane to generate the corresponding diazo ketones. The diazo ketones were then treated *in situ* with hydrogen fluoride in pyridine to yield the desired α -fluoroacetophenones in relatively good yields. This one-pot procedure gave rise to a mixture of both the α -fluoro and α -chloro-acetophenones, which were readily separable by column chromatography. The desired α -fluoro compounds all gave satisfactory analytical data.

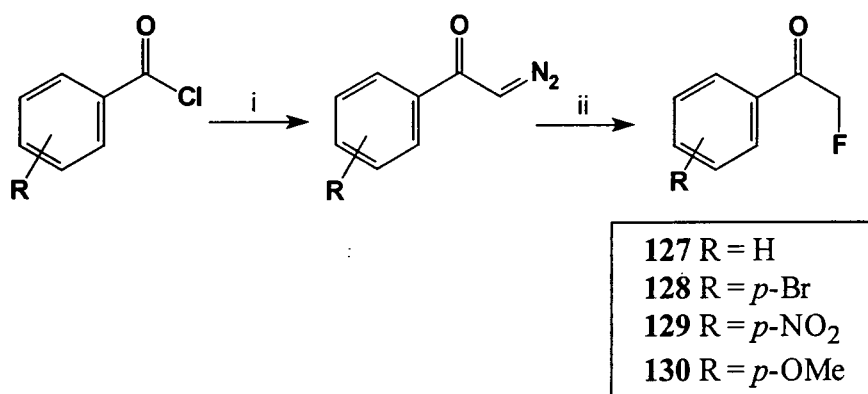


Fig 4.10 Reagents: i, CH₂N₂, Et₂O; ii, HF–pyridine, Et₂O, 45–63%

The α -fluoroacetophenones were heated under reflux with a number of amines including pyrrolidine **126**, diisopropylamine and diethylamine in a variety of solvents. In the reactions using the acyclic amines, no indication of enamine formation was detected by ¹⁹F NMR spectroscopy. Only with pyrrolidine was the formation of the enamine intermediates observed. The generated enamines were a mixture of *E* and *Z* isomers (Fig. 4.11) which were easily distinguishable by ¹⁹F NMR spectroscopy of the reaction mixture. This meant that the extent of conversion could be readily monitored.

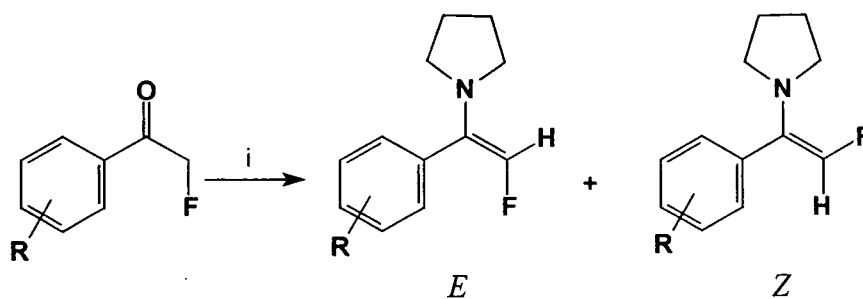


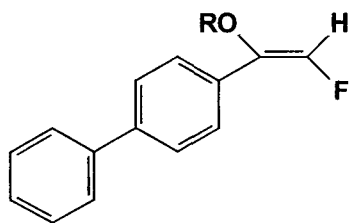
Fig 4.11 Reagents and conditions: i, **126**, 4 Å molecular sieves, benzene, heat, 95%

The enamine formation was assessed in a range of solvents and the relative ratio of the geometric isomers determined directly by integration of the observed signals in the ^{19}F NMR spectra of the reaction mixtures. The results, compiled in Table 4.4, show that in most cases conversion to the enamine intermediate was high. There was however only a limited effect on the isomer ratio by substitution of the aromatic ring, with the largest observed ratio occurring with substitution of a *p*-nitro group.

Table 4.4 *E/Z* ratios as determined by ^{19}F NMR spectroscopy

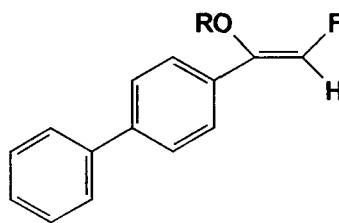
Substituent	Solvent	Conversion (%)	Ratio <i>E:Z</i>
H	Et ₂ O	100	1.22:1.0
H	CCl ₄	76	1.11:1.0
H	C ₆ H ₆	96	1.27:1.0
NO ₂	C ₆ H ₆	70	1.65:1.0
OMe	C ₆ H ₆	69	1.45:1.0
Br	C ₆ H ₆	95	1.44:1.0

In all the cases the predominant signals observed in the ^{19}F NMR spectra were to lower frequency (between δ -166.3 and -173.0) with those to higher frequency in the range δ -154.5 to -160.3. The signals to lower frequency were assigned to the *E* isomers, consistent with the previous assignment of the *E/Z* isomers of the structurally related enol ether systems **131** and **132**.^{199,200}



(*E*)-**131** R = MeOCH₂ (δ -162.9)

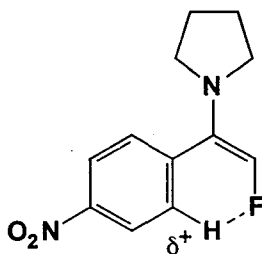
(*E*)-**132** R = SiMe₂Bu^t (δ -164.7)



(*Z*)-**131** R = MeOCH₂ (δ -154.0)

(*Z*)-**132** R = SiMe₂Bu^t (δ -157.2)

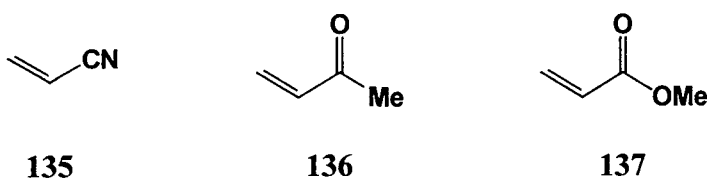
The reason for the preference towards the *E* isomer remains unclear and may arise from either electronic or steric factors. One possible explanation may be that the fluorine is interacting electrostatically with the *ortho* aromatic proton, thereby preferentially stabilising the *E* isomer. This interaction should increase with the introduction of a *p*-nitro group which would render the proton more δ^+ , increasing the observed ratio, consistent with the experimental result.



The polarity of the reaction solvent had little bearing on the observed ratio of geometric isomers. All attempts to isolate the enamine intermediates resulted in decomposition back to starting materials and as a result the enamine products were never isolated or purified.

4.5 Alkylation of fluoroenamines

The mixture of *E/Z* fluoroenamines derived from the reaction of pyrrolidine and the α -fluoroacetophenones **127–130** were treated *in situ*, under refluxing conditions, with a variety of potential Michael acceptors. The consumption of the enamine, presumably *via* an iminium species **133** (Fig. 4.12), lead to the generation of the new alkylated enamines **134** after treatment with acrylonitrile **135**, methyl vinyl ketone **136** and methyl acrylate **137**.



The accumulation of the alkylated enamines was again monitored directly by ¹⁹F NMR spectroscopy of the reaction mixture. There now appeared to be a significant stereochemical bias (*ca.* 8:1) in favour of one of the geometric isomers. The predominant signals were again to low frequency (up-field) (δ -145.5 to -164.0) and by correlation were assigned to the *E* isomer. This preference is again presumably due either to unfavourable steric interactions between the aromatic proton and the R group or an electronic effect between the fluorine and aromatic proton.

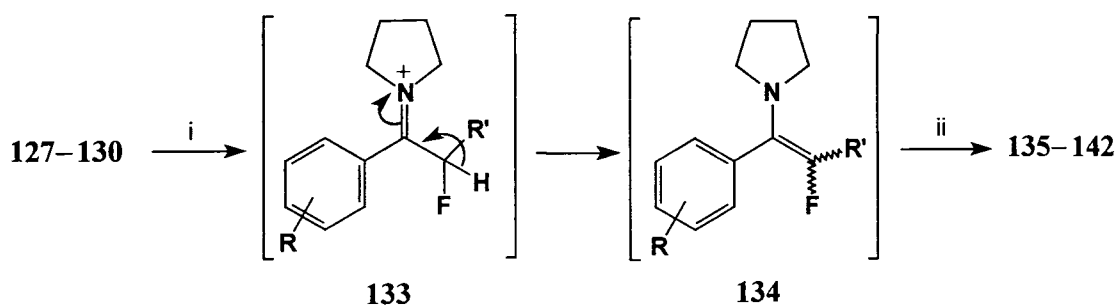


Fig 4.12 Reagents: i, Michael acceptor; ii, H₃O⁺

These reaction intermediates were, however, not isolated, but subjected to acidic work up to afford the desired ketones **138–143** in moderate overall yields (48–60%) (Fig. 4.13).

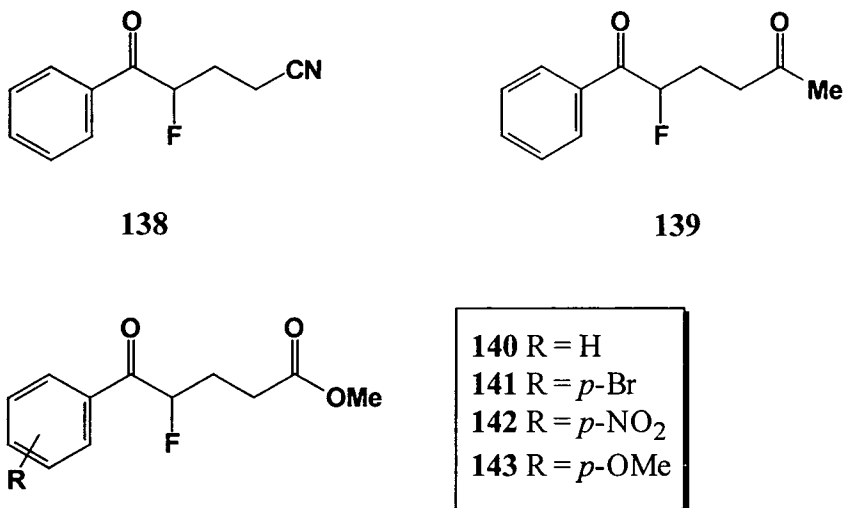


Fig. 4.13

Reaction of the enamine with cyclohexenone gave after work-up the α -fluoro ketone **144** as a 2:3 mixture of diastereoisomers, and the reaction with methyl methacrylate generated **145** as a 1:1.2 mixture of diastereoisomers (Fig. 4.14). The reaction of the enamine with methyl methacrylate was observed by ¹⁹F NMR spectroscopy to proceed at a significantly slower rate than with the other Michael acceptors, typically taking several days to react compared with just several hours in the other cases. This observation is consistent with the methyl group of the methylacrylate deactivating the double bond to attack by nucleophiles.

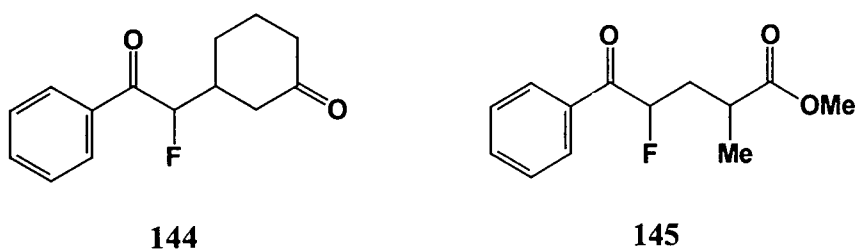
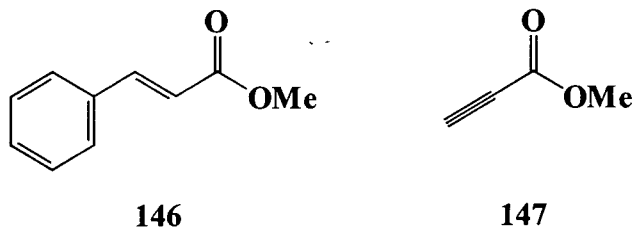


Fig. 4.15

The Michael acceptors used to generate these products provided a range of α -fluoro ketones with pendant functional groups which have the potential to be further elaborated. Problems, however, were encountered when the methodology was extended to other alkylating reagents. The enamine did not undergo reaction with methyl

cinnamate **146**, possibly due to steric hindrance of the phenyl group. Reaction with methyl propiolate **147** under similar conditions generated a complex mixture of fluorinated products which were not isolated.



Alkylation reactions with various alkyl halides including methyl iodide, allyl bromide and ethyl bromoacetate were unsuccessful, and no alkylated products were isolated using reagents of this type.

In conclusion we have demonstrated for the first time that a range of α -fluoro ketones can be prepared using Stork-enamine chemistry. The methodology worked well for Michael acceptors but did not extend to more straightforward alkylation reactions. It became appropriate at this stage to investigate if the Stork enamine reaction could be carried out asymmetrically, with a homochiral pyrrolidine base.

4.6 Asymmetric induction *via* Stork enamine methodology

Asymmetric induction was first observed by Yamada in the alkylation of chiral enamines derived from various esters of proline (Fig. 4.16).²⁰¹ The resultant 2-substituted cyclohexanones were shown to have the *S* configuration, with typical enantiomeric excesses of 10–30%, which could be increased by use of a bulky ester to 50–60% ee. The observed induction in the product arises from a kinetically controlled enantioselective alkylation of the enamine intermediate.

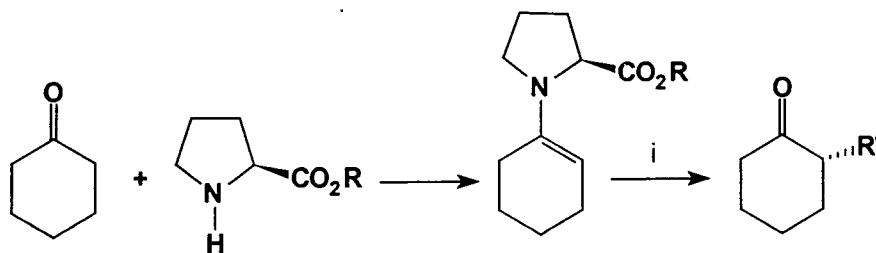
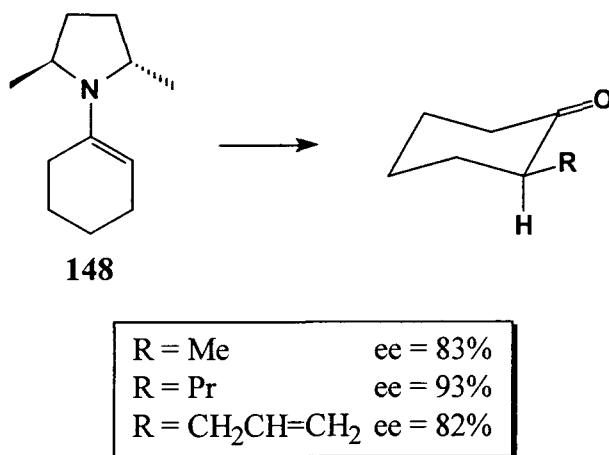


Fig. 4.16 Reagents: i, $\text{CH}_2=\text{CHCOCH}_3$

The degree of enantioselectivity was substantially increased by the use of an amine with a C_2 axis of symmetry. Using the cyclohexanone enamine **148** derived from (+)-*trans*-2,5-dimethylpyrrolidine, Whitesell and Felman achieved optical yields in excess of 80%, but with the opposite absolute configuration predominating.²⁰²



Of particular interest was the use of (2*S*)-(diphenylmethyl)pyrrolidine **151** as a potential chiral amine for the formation of the enamines. An efficient synthesis of this pyrrolidine derivative has been developed recently in Durham and is outlined in Fig. 4.17.²⁰³

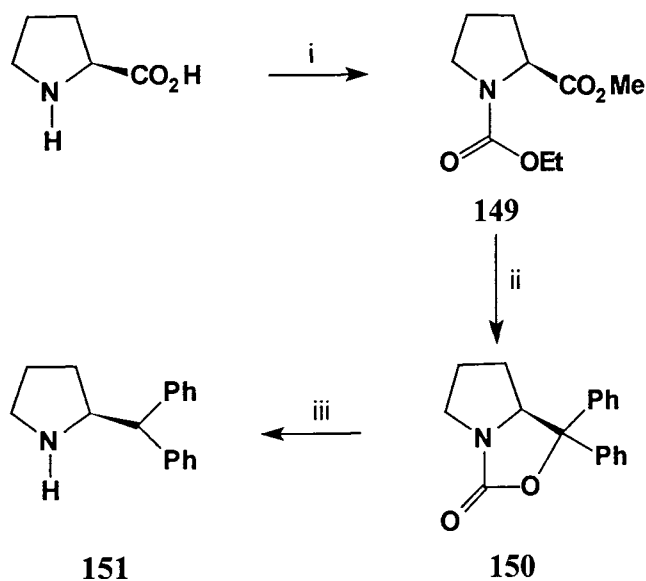


Fig. 4.17 Reagents: i, EtCOCl, MeOH, 91%; ii, PhMgBr, THF, 82%; iii, Pd-C, MeOH, H₂, 67%

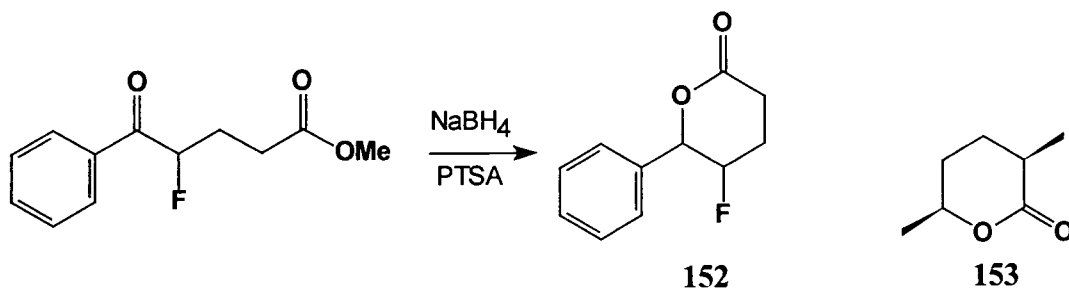
The amine (2*S*)-(diphenylmethyl)pyrrolidine was prepared in good overall yield from (*S*)-proline. (*S*)-Proline was firstly treated with ethyl chloroformate in methanol, affording **149** in 91%, and subsequent treatment with two equivalents of phenylmagnesium bromide in THF gave the cyclic carbamate **150**, which was recrystallised from diethyl ether in 82% yield. Finally, hydrogenation of the carbamate produced the desired product in an overall yield of 50% from (*S*)-proline.

The reaction of α -fluoroacetophenone **127** with the amine (2*S*)-(diphenylmethyl)pyrrolidine **151** was attempted under the same conditions as those previously employed. However, despite several attempts with varying conditions no reaction, as judged by ^{19}F NMR spectroscopy of the reaction mixture, was observed. It was therefore concluded that the diphenylmethyl group was sterically too demanding for successful reaction to occur and attempts at asymmetric induction were discontinued. Of course the potential exists to explore other homochiral pyrrolidine bases.

4.7 Potential uses of the methodology

4.7.1 Fluorinated lactones

With the range of compounds prepared, elaboration of the pendant functional group could be envisaged to produce a series of novel fluorinated lactones by reduction and cyclisation to give lactones such as **152**.



By refinement of the fluoro ketone precursor by, for example, the use of fluoroacetone to replace α -fluoroacetophenone, and using suitable Michael acceptors, a series of fluorinated lactones could be assessed that are fluorinated analogues of insect pheromones such as **153**.

Chapter Five

Preliminary Studies into the Effect of Fluorine with Transketolase and Glycerol-3-Phosphate Dehydrogenase

Preliminary Studies into the Effect of Fluorine with Transketolase and Glycerol-3-Phosphate Dehydrogenase

Part A. Preliminary Studies with Transketolase

A5.1 Introduction

The enzyme transketolase (E.C. 2.2.1.1) belongs to the group of enzymes known as the transferases that catalyse the transfer of a molecular group from one molecule to another. *In vivo* transketolase catalyses a vital step in the pentose phosphate pathway which oxidises glucose-6-phosphate to carbon dioxide and a five carbon sugar phosphate. The carbon atoms of the pentose are then rearranged by two enzymes—transaldolase and transketolase—which catalyse transfers of two or three carbon units between molecules. The major functions of the pentose phosphate pathway are the generation of NADPH and supply of ribose-5-phosphate. Transketolase catalyses the transfer of a two carbon ketol group from D-xylulose-5-phosphate to D-ribose-5-phosphate, generating D-sedoheptulose-7-phosphate (Fig. A5.1).²⁰⁴

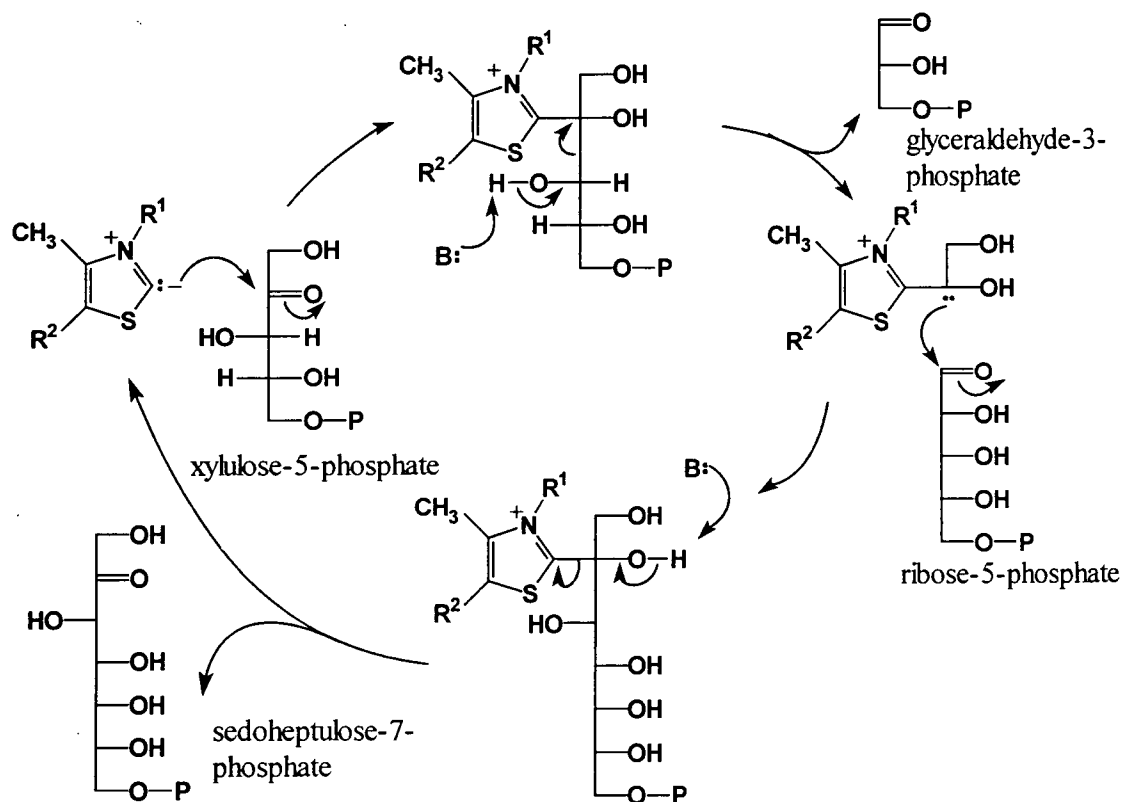


Fig. A5.1

Transketolase is one of several enzymes which catalyse reactions involving intermediates with a negative charge on what was initially a carbonyl carbon atom. The enzyme requires magnesium(II) ions and thiamine pyrophosphate (TPP) as co-factors. The transketolase reaction is initiated by addition of thiamine pyrophosphate anion to the carbonyl of a ketose phosphate (xylulose-5-phosphate). The adduct undergoes an aldol like cleavage, retaining C-1 and C-2 on the enzyme surface in the form of the glycoaldehyde derivative of TPP. This intermediate can exist as a resonance stabilised carbanion, and can condense with the carbonyl of another aldolase. The products of the reaction with ribose-5-phosphate are sedoheptulose-7-phosphate and 3-phosphate-glyceraldehyde (Fig. A5.1). The transketolase activity has also been shown to play an important role in the biosynthesis of aromatic amino acids like L-phenylalanine and related metabolites from D-glucose.²⁰⁵

In the last few years, an increasing number of papers dealing with enzymatic synthesis of monosaccharides by aldol reactions have demonstrated the usefulness of such enzymes.²⁰⁶ The isolated enzyme itself, however, has also been shown to have significant synthetic potential.²⁰⁷ The use of hydroxypyruvate **155** as the ketol makes the reaction more efficient and also, by the release of carbon dioxide, irreversible. The products of the reaction are the trihydroxylated compounds **156** with the *D-threo* configuration (Fig. A5.2).

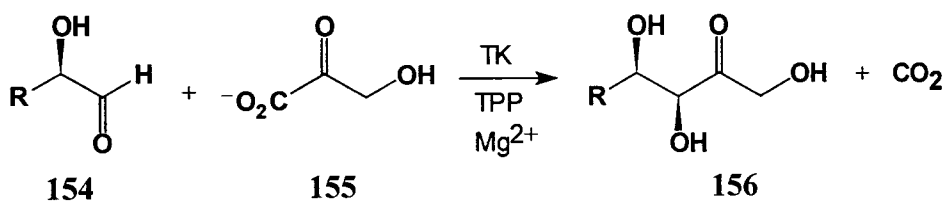


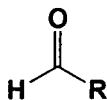
Fig. A5.2

It had initially been thought that only the α -hydroxy aldehydes of the *D*-configuration **154** were potential aldehyde acceptors, but a study by Demuyneck *et al.* has shown that some simple α -unsubstituted aldehydes are substrates for transketolase.²⁰⁷ This study demonstrated that aliphatic aldehydes were good substrates for the enzyme and that the presence of a hydroxy group or oxygen atom at the α and/or β position had a positive effect on the observed rate of reaction. For example, glycoaldehyde **157** was shown to be a better substrate than acetaldehyde **158**. Steric

hindrance near the aldehyde group also reduced the reactivity of the aldehyde (*c.f.* 159 and 160).

Table A5.1 Relative reactivities of aldehydes (RCHO) with hydroxypyruvate in yeast transketolase-catalysed carbon–carbon bond formation

Compound	R	V_{rel}
157	HOCH ₂ –	1
158	CH ₃ –	0.25
159	(<i>R,S</i>) CH ₃ CH(OH)CH ₂ –	0.29
160	(<i>R,S</i>) CH ₃ CH(OBz)CH ₂ –	0.14
161	(<i>R,S</i>) CH ₂ FCH(OH)–	0.47



Demuynck also demonstrated that transketolase displays enantioselectivity on reaction of racemic α -hydroxy aldehydes with hydroxypyruvate in that L-glyceraldehyde was not a suitable substrate for the enzyme.²⁰⁸ This contrasts with fructose 1,6-diphosphate aldolase, which accepts both isomers as substrates.

In a similar study, using transketolase obtained from an over expressed *E. coli* transformant carrying the transketolase gene, the aldehyde specificity was again shown to be relatively low.²⁰⁹ α -Hydroxy aldehydes were again the best substrates, however aldehydes such as propionaldehyde and pyruvaldehyde were also converted into the corresponding products. The low substrate specificity for the aldehyde component together with the high stereoselectivity for the carbon–carbon bond formation make the enzyme a potentially useful catalyst for asymmetric synthesis.

A5.2 Reaction of an α -fluoro aldehyde with transketolase

The previous studies with racemic α -hydroxy aldehydes demonstrated the enzyme's ability to show diastereoselectivity between the isomers of the aldehyde. The results of the studies also indicated that the presence of an α -D-hydroxy group enhanced the rate of reaction, and that the reaction was subject to steric effects. The introduction,

therefore, of an α -fluorine atom would be predicted to induce several effects on the reactivity of the aldehyde. If the increased rate observed in the α -D-hydroxy compounds arose due to the electronegativity of the hydroxy group then the introduction of the fluorine atom would serve to increase this effect. Indeed, as discussed previously in Chapter 4, the presence of an α -fluorine would be expected to stabilise the tetrahedral intermediate formed in the reaction between the carbanion equivalent and the fluorinated aldehyde. Clearly, as discussed previously, the introduction of an α -fluorine would not introduce a significant steric effect compared to an α -hydroxy aldehyde, however with the introduction of an α -fluorine atom there exists the possibility of a stabilising stereoelectronic effect which may control the diastereoselectivity of the enzymic transformation. In the previous analyses an Anh–Eisenstein type stabilisation between the σ^* orbital of the C–F bond and the attacking carbon nucleophile is predicted to favour one diastereoisomeric transition state over the other (Fig A5.3).

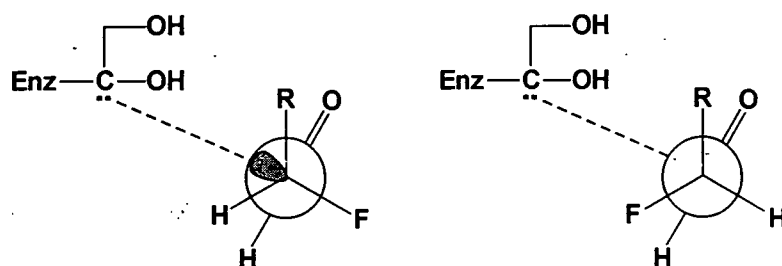


Fig. A5.3

A5.3 Aims of investigation

The aim of the initial investigation was to determine whether the transketolase activity would process an α -fluorinated aldehyde substrate with any diastereoselectivity. The α -fluoro aldehyde chosen for investigation was 2-fluorohexanal. Previous studies have shown that butyraldehyde is a substrate for the enzyme and that increasing the length of the carbon chain lowered the reactivity of the enzymatic transformation.²⁰⁹ However, in order to obtain a material that was relatively easy to handle, a compromise between chain length and volatility was reached with 2-fluorohexanal **165**.

The anticipated products of the reaction of 2-fluorohexanal with hydroxypyruvate and transketolase are shown below in Fig. A5.4. It was envisaged that any

diastereoselectivity could be analysed directly by ^{19}F NMR analysis of the product mixture.

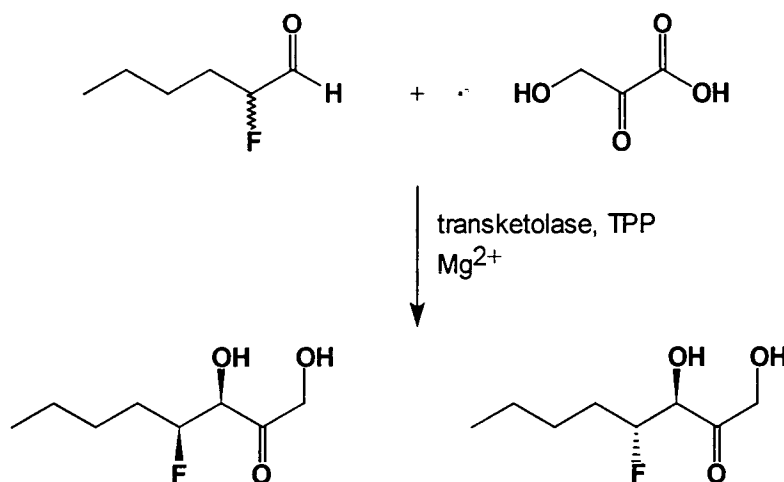


Fig. A5.4

A5.4 Synthesis of 2-fluorohexanal

The synthetic route established for the synthesis of 2-fluorohexanal is outlined below (Fig. A5.5). The synthesis began with commercially available methyl hexanoate, which was conveniently brominated at the α position following the procedure of Pogany.¹⁰⁹ Thus methyl hexanoate was heated at 80 °C with a mixture of bromine and red phosphorus for 16 h to afford **162** in high yield as a colourless oil after distillation. Fluorination to give **163** was achieved by nucleophilic halogen replacement of bromide using silver(I) fluoride in wet acetonitrile.¹⁰⁹ This transformation was the limiting step in the synthetic sequence due to the amount of silver fluoride required to achieve synthetically useful yields and the high cost (£35 for 5 g) of the silver fluoride. After removal of the silver salts and purification by column chromatography, the product **163** was isolated in 80% yield. The fluorinated ester was then reduced to 2-fluorohexanol **164** by reaction with lithium aluminium hydride in diethyl ether. This product was obtained in 77% yield after purification by column chromatography. Finally, the alcohol was oxidised to the target aldehyde **165** by stirring with pyridinium chlorochromate and 3 Å molecular sieves in CH_2Cl_2 .²¹⁰

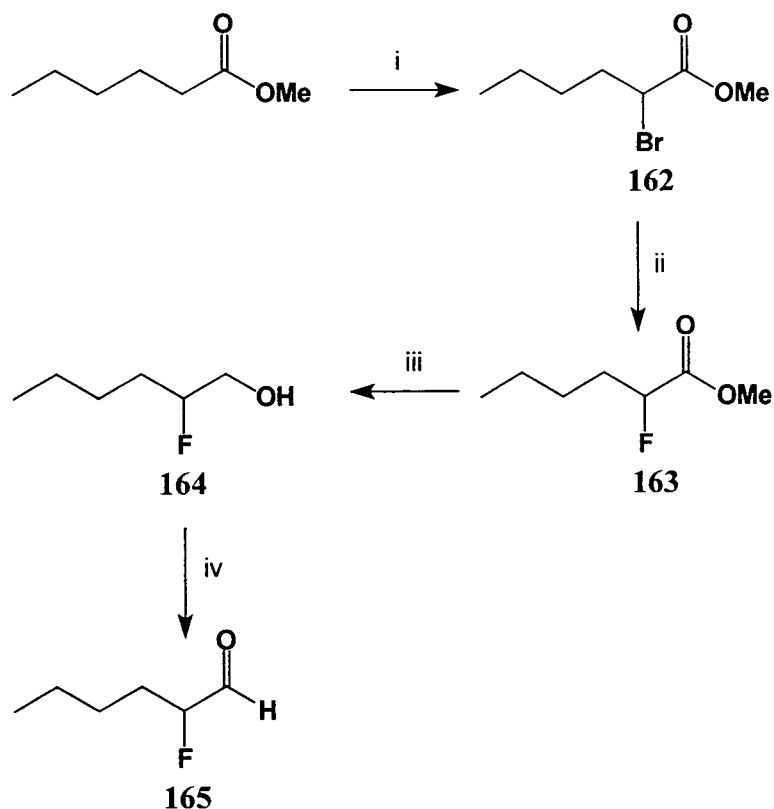
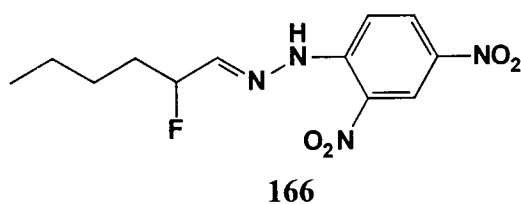


Fig. A5.5 Reagents: i, Br_2 , red phosphorus, MeOH , 86%; ii, AgF (4.5 equiv.), $\text{MeCN-H}_2\text{O}$, 80%; iii, LiAlH_4 , Et_2O , 77%; iv, PCC , 3 \AA molecular sieves, CH_2Cl_2 , 64%

Aldehyde **165** was characterised by formation of its 2,4-dinitrophenylhydrazone derivative **166** after treatment with an acidic solution of 2,4-dinitrophenylhydrazine.



A5.5 Results and discussion

The enzyme reactions were initiated by the addition of a solution of hydroxypruvic acid and aldehyde **165** in glycylglycine buffer to a solution of magnesium chloride, thiamine pyrophosphate and transketolase in glycylglycine buffer adjusted to pH 7.6. The reaction was placed in on orbital shaker at 29 °C and was monitored by ^{19}F NMR spectroscopy. Control reactions were also undertaken with identical solutions prepared but without the addition of enzyme.

A5.5.1 Results from NMR data for enzyme and control reaction

The enzyme reaction was repeated twice, varying the amount of TPP used in the reactions; however, both runs gave similar overall results. Importantly, the controls showed that no reaction took place in the absence of transketolase. The only observable change in the ^{19}F NMR spectra of the controls was the formation of a peak at $\delta -120$, which was assigned to the elimination of fluoride from the aldehyde.

On the other hand, the enzyme reactions *did* generate a number of novel fluorinated products. The resultant ^{19}F NMR spectrum (250 MHz) after 15 h at 29 °C clearly shows five peaks. The reaction was frozen at this point to arrest further reaction and a high field ^{19}F NMR spectrum (470 MHz) was recorded (Fig. A5.6). This again showed the five peaks observed previously along with a number of smaller, previously unobserved, signals which could either have formed in the time between the reaction and observation of the high field NMR spectrum or were just not visible at lower field.

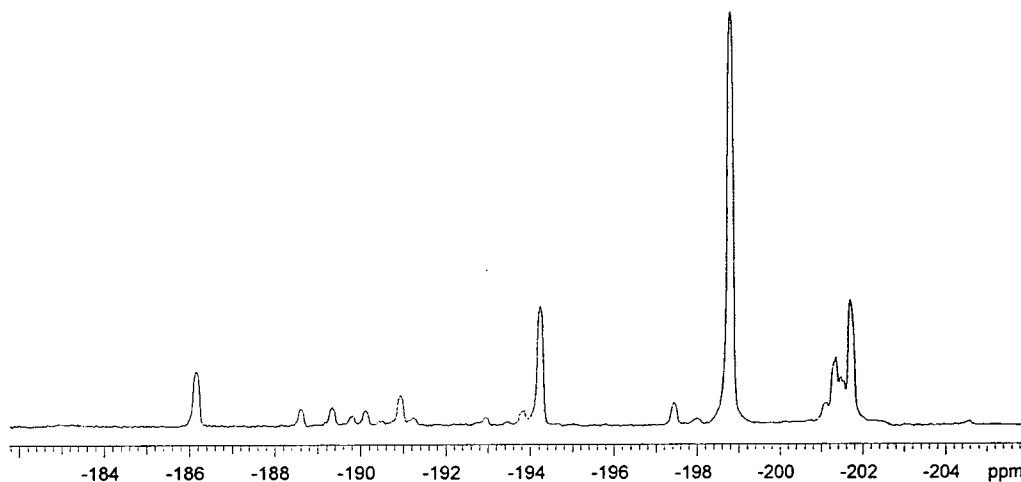


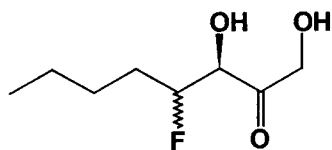
Fig. A5.6 ^{19}F NMR spectrum of the reaction solution of 2-fluorohexanal with transketolase after 15 h at 29 °C

The observed ^{19}F NMR spectrum is clearly complex, with the formation of a number of fluorinated compounds. The major signals were tentatively assigned as outlined in Table A5.2.

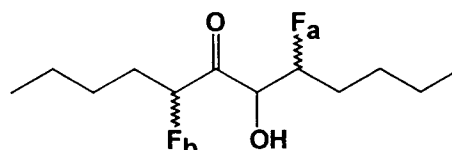
Table A5.2 ^{19}F NMR data for the reaction of 2-fluorohexanal with transketolase

δ (ppm)	Assignment
-201.7	F _a Condensation product 168
-201.3	Residual 2-fluorohexanal 165
-198.8	Diastereoisomeric product 167
-194.2	F _b Condensation product 168
-186.2	Diastereoisomeric product 167
-120.0	Fluoride

The results from the NMR experiments appear to indicate the formation of three major products, the two diastereoisomeric products **167** arising from the addition of hydroxypyruvate to the aldehyde and a self-condensation product from the aldehyde **168**.



167



168

The observed ratio between the two diastereoisomeric products from the ^{19}F NMR spectrum appears to be as high as 9:1. The fluoride content is also much greater in the presence of the enzyme than in the control reactions, indicating a much more facile fluoride elimination.

When the reaction was left to proceed for a longer period of time (90 h) the observed ratio (250 MHz) between the two diastereoisomers fell to approximately 2:1. Such an observation is indicative of an enzymatic kinetic resolution whereby one enantiomer of the α -fluoro aldehyde is processed more rapidly than the other.

A5.6 The chemistry of the enzyme reactions

A5.6.1 Formation of diastereoisomeric products

A mechanism for the formation of the two diastereoisomers by the addition of hydroxypyruvate to 2-fluorohexanal is outlined below (Fig. A5.7). The diastereoselectivity will depend on the relative energies of the diastereoisomeric transition states in the condensation

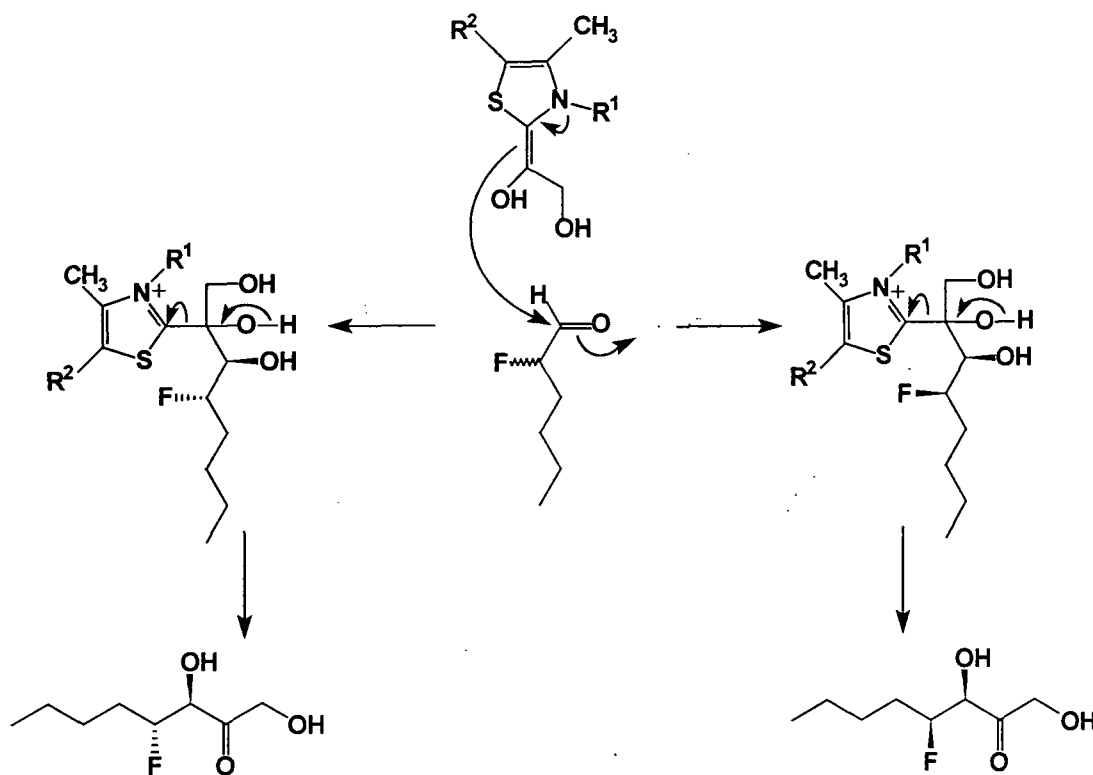


Fig. A5.7

A5.6.2 Formation of the self-condensation product

The formation of the observed self-condensation product **168** can be accounted for by the mechanism outlined below. The TPP anion, instead of reacting with hydroxy-pyruvate, condenses directly with the α -fluoro aldehyde. This adduct may then react with a second molecule of the α -fluoro aldehyde to generate the proposed self-condensation product **168** (Fig. A5.8).

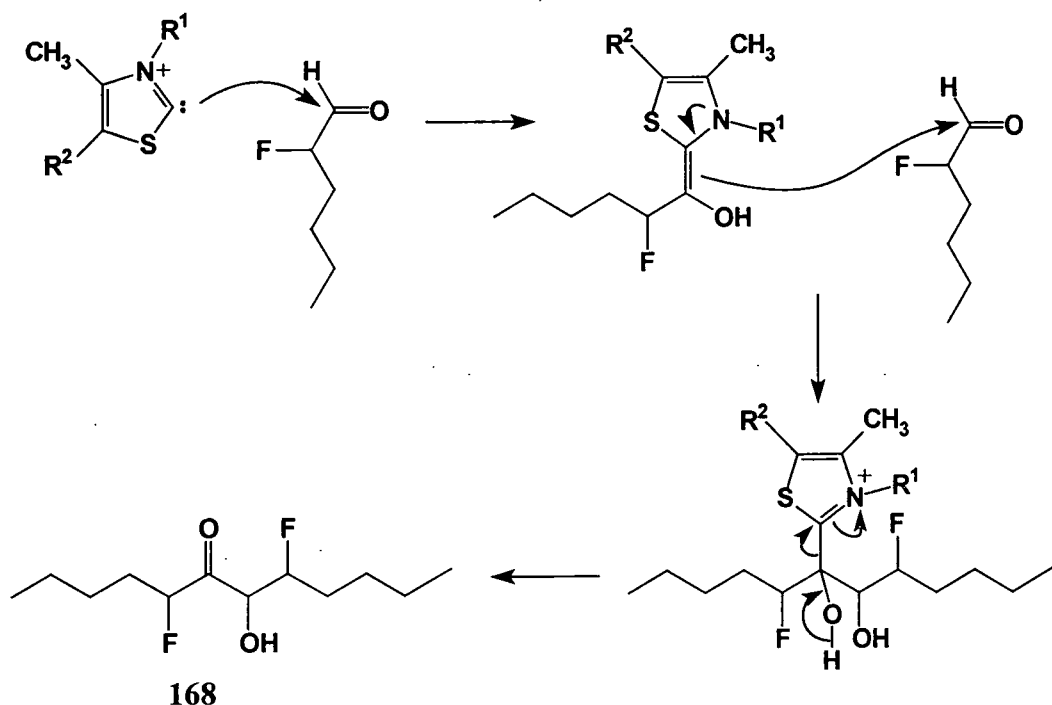


Fig. A5.8

A5.6.3 Elimination of fluoride

In both the enzyme and the control reactions the elimination of fluoride was observed. The amount of fluoride increased with time, which suggests the formation is either due to instability of the product or as a consequence of TPP chemistry. There exist three possible mechanisms by which fluoride elimination may be induced.

(i) Fluoride is generated in the control reactions, which must come from decomposition of 2-fluorohexanal. A non-enzymatic reaction between TPP and 2-fluorohexanal may generate the adduct **169** shown below (Fig. A5.9), which would then be able to eliminate fluoride.

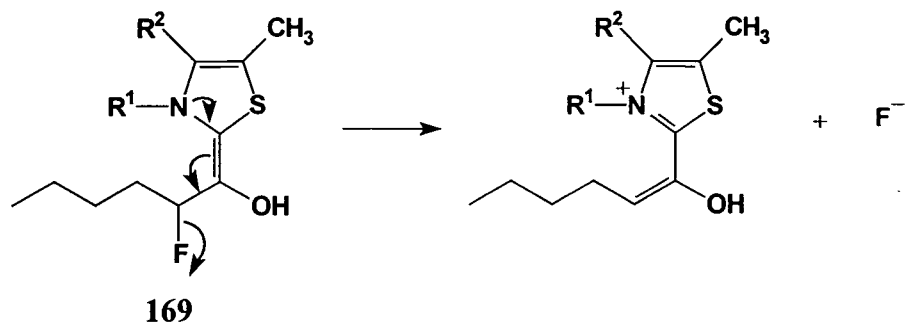


Fig. A5.9

(ii) In the enzymatic reaction, fluoride elimination may occur from the diastereoisomeric products of hydroxypyruvate addition to 2-fluorohexanal (Fig. A5.10). It may also be the case that the diastereoisomers have differing stability towards F^- elimination.

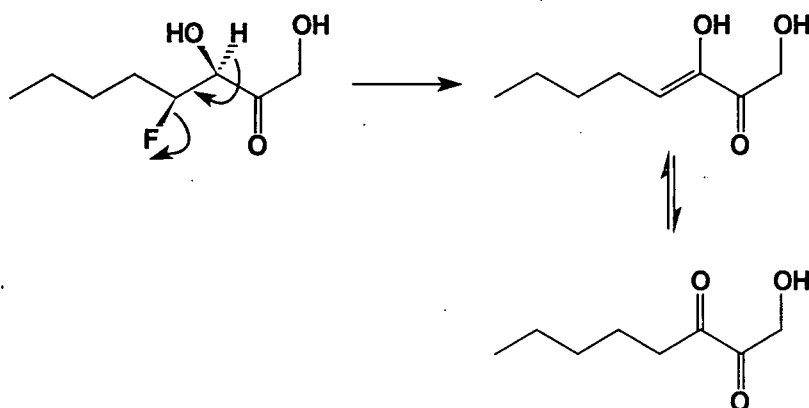


Fig. A5.10

(iii) The proposed difluoro condensation product 168 may also undergo fluoride elimination (Fig. A5.11)

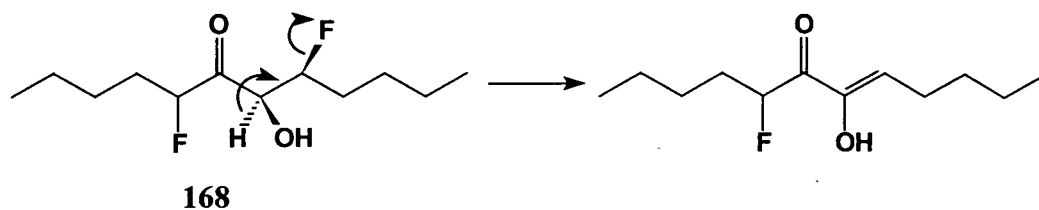


Fig. A5.11

A5.7 Conclusions and future work

The enzymatic reaction between 2-fluorohexanal and transketolase has been studied. The resultant high field ^{19}F NMR spectrum of the enzymatic reaction indicated the formation of a number of novel fluorinated compounds. Importantly, no reaction products were seen in the absence of enzyme. The anticipated diastereoisomeric products have been tentatively assigned in the ^{19}F NMR spectrum in a 9:1 ratio. It was, however, not possible to assess the rates of reaction or levels of conversion attained. There was also apparent a second major product, which was considered to arise from the self-condensation of two aldehyde molecules.

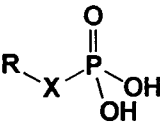
The work performed here on the interaction of α -fluorinated aldehydes with transketolase forms a basic introduction to the use of fluorinated substrates with the transketolase enzyme. This preliminary study was conducted towards the end of the research programme with the assistance of a final year undergraduate student. No compounds were isolated or purified. Further work is currently being undertaken to extend this study.

Part B. The enzymatic oxidation of mono- and di-fluoromethylenephosphonate analogues of glycerol-3-phosphate

B5.1 Introduction

Phosphonates have been widely studied as phosphate mimics for many years.²¹¹ The replacement of the bridging oxygen by a CH₂ moiety renders the phosphonate resistant to phosphatase hydrolysis. While the substitution maintains a similar conformation, which is important for protein binding, the electronic consequences can prove detrimental as the electronegativity of oxygen is not matched by the CH₂. This is clearly demonstrated by analysis of the pK_a values for the second deprotonation of the phosphate, which has a value of 6.4 compared to 7.6 for the phosphonate.²¹² The acidity of the phosphonate can be increased by the introduction of fluorine onto the methylene group (Table B5.1).

Table B5.1 Various pK_a values for second deprotonation

	
X	pK _a
O	6.4
CH ₂	7.6
CHF	6.5
CF ₂	5.4

The introduction of a single fluorine (CHF) increases the acidity of the phosphonate, generating a pK_a which is essentially identical to that of the phosphate (6.5),²¹³ without greatly altering the geometry of the molecule. This modification gives rise to compounds that are much closer analogues to the parent phosphonate. Indeed, a recent theoretical analysis predicted a close relationship between the electrostatic profiles of the CHF phosphonate and the phosphate groups.²¹⁴

The geometry of the phosphonates has been studied by X-ray analysis of suitable compounds. A particularly interesting correlation can be found with the C–X–P bond angles as one and two fluorine atoms are introduced (Table B5.2).²¹⁵

Table B5.2 C–X–P angles of the phosphate and phosphonates as determined by X-ray crystallography^a

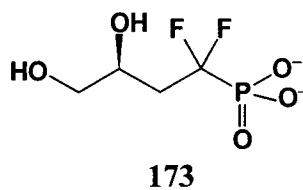
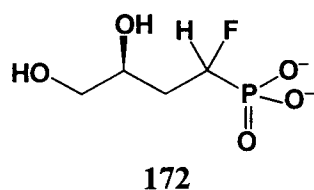
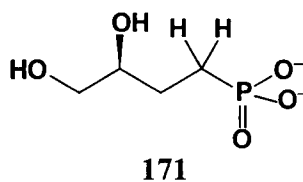
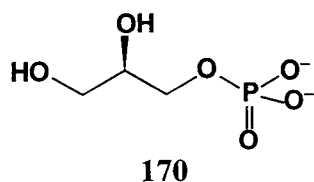
The diagram shows a phosphorus atom (P) double-bonded to an oxygen atom (O) above it. The phosphorus atom is also single-bonded to a negatively charged oxygen atom (O⁻) to its right, a hydroxyl group (OH) below it, and an X atom to its left. The X atom is further bonded to a CH₂ group, which is then bonded to an R group.

X	C–X–P (°)
O	118.7
CH ₂	112.1
CHF	113.3
CF ₂	116.5

^a R = NH₃⁺ in all cases except when X = O, where R = CH₂NH₃⁺.

The data obtained from the X-ray structure analyses of aminophosphonates shows that, in the case of the CHF phosphonate, the observed C–X–P angle is similar to that for the parent phosphonate but that the introduction of a CF₂ group results in significant angle widening. Despite the obvious advantages of the CHF-phosphonate in terms of its steric and electrostatic profile these compounds have received surprisingly little attention as potential phosphonate mimics.

The synthesis and evaluation of fluorinated phosphonates as mimics for monophosphonates in the glycolytic pathway has been studied previously.^{216,217} Initially, a racemic sample of the CF₂-phosphonate **173**, an analogue of *sn*-glycerol-3-phosphate **170**, was demonstrated to be a substrate for NADH-linked glycerol-3-phosphate dehydrogenase.²¹⁶ Perhaps surprisingly, these studies suggested that **173** was in fact a poorer substrate than both *sn*-glycerol-3-phosphate **170** and the CH₂-phosphate analogue **171**. The difluorophosphonate was apparently turned over by the enzyme at one-sixth the rate of that of the natural substrate.



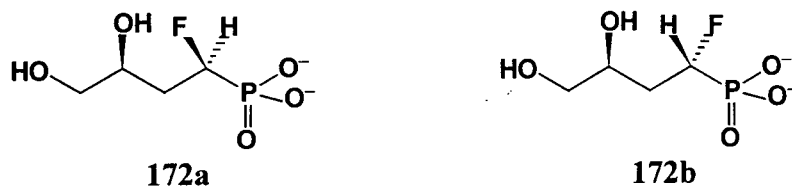
In a more recent study, the CHF-phosphonate **172** was synthesised along with a homochiral sample of **173** and both were assessed as substrates for the enzyme glycerol-3-phosphate dehydrogenase (G-3-P).²¹⁵ The results are summarised below in Table B5.3.

Table B5.3 Values of K_m and V_{rel} for the oxidation of **170** and phosphonates **171–173** by G-3-P dehydrogenase.²¹⁵

X	K_m /mM	V_{rel}
O	0.20	1.0
CH ₂	0.18	0.8
CHF	0.17	0.9
CF ₂	0.73	0.8

The results show that both of the fluorinated phosphonates analogues are good substrates for the enzyme, however the CHF-phosphonate was a significantly better substrate than the CF₂ phosphonate (K_m **172** = 0.17 mM, K_m **173** = 0.73 mM). All of the substrates had similar maximal rates (V_{rel}) relative to **170** at substrate saturation levels, however the CF₂-phosphonate emerged uniquely as a poorer substrate by K_m . This was argued to be due to an adverse electrostatic interaction with the enzyme surface caused by the second fluorine atom.

Within this study a comparison of the rates of enzymatic oxidation of the diastereoisomers of the CHF-phosphonate **172** was also undertaken.



The ^{19}F NMR signals for **172a** and **172b** are resolved in the ^{19}F NMR spectrum of the mixture of the diastereoisomers, although no assignment of the signals has been made. Analysis of the change in ratio of the integrals of the signals associated with each diastereoisomer, over time, showed that one of the isomers apparently decreased relative to the other by 20% over a period of 65 min (Fig. B5.1).

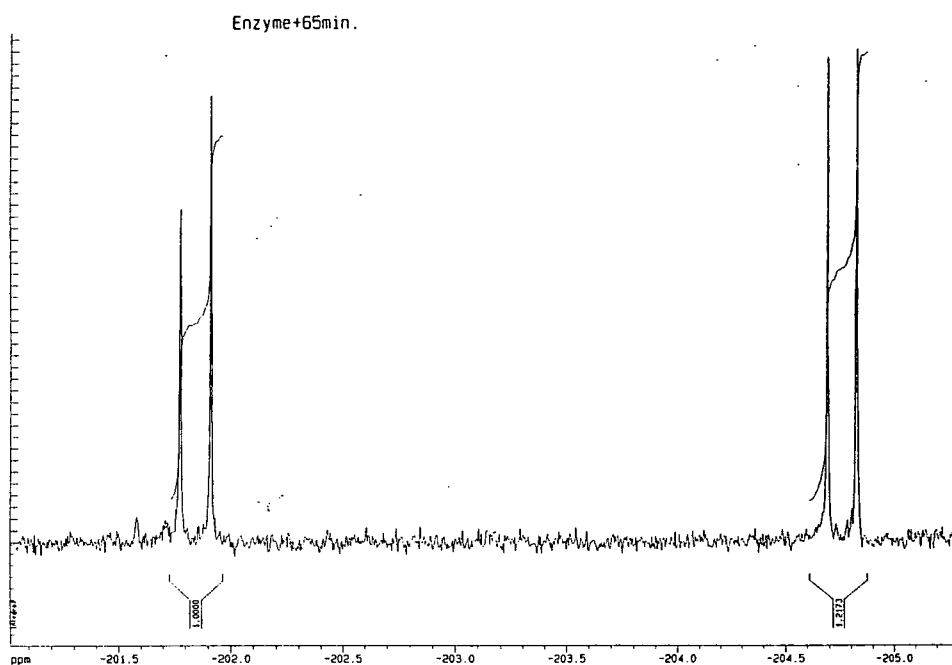
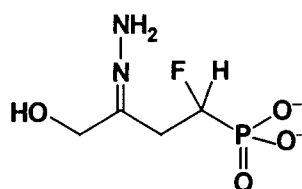


Fig. B5.1

It was, however, not possible within the study to accurately calculate the extent of conversion. The oxidised product of the reaction, which under the conditions of the assay is the hydrazone **174** (hydrazine pH 9.5), did not appear to accumulate as it was not apparent by ^{19}F NMR spectroscopy. One possibility is that the product decomposed under the basic conditions of the assay. The ^{19}F NMR profile of the reaction indicated

that the dehydrogenase could distinguish between the diastereoisomers of **172** and that this discrimination arose from a kinetic preference by the enzyme for one of the diastereoisomers.



174

A short study was initiated using samples previously prepared (by Dr Jens Nieschalk)²¹⁵ to investigate the reaction of the CHF and CF₂ phosphonate analogues of glycerol-3-phosphate with G-3-P dehydrogenase. The key issue here was to monitor the reactions at neutral pH to try to arrest decomposition of the reaction products. Thus hydrazine was removed and a co-factor recycling protocol was established.

B5.1.1 Coupled enzyme co-factor recycling

As previously described in Chapter 2, the major practical problem associated with the use of enzymes in organic synthesis is the expense of co-enzymes like NADH. This can be overcome by using catalytic quantities of the co-enzyme and recycling it *in situ* to the active form in a coupled enzyme system. Whitesides demonstrated that NAD(P)H could be recycled on up to a mole scale using several enzymes, each with differing catalytic activities, in the same vessel without one interfering with the others.^{91,92} Thus, in coupled enzyme recycling protocols an auxiliary enzyme system, which may be a single or multiple enzyme system, is used to regenerate the co-enzyme. In Fig. B5.2 the HLADH-catalysed reduction of 2-methylcyclohexanone is shown. The co-enzyme is recycled by a glyceraldehyde-3-phosphate dehydrogenase (GAPDH) catalysed oxidation of glyceraldehyde-3-phosphate. This auxiliary substrate is formed from an aldolase-catalysed cleavage of fructose-1,6-diphosphate.²¹⁸

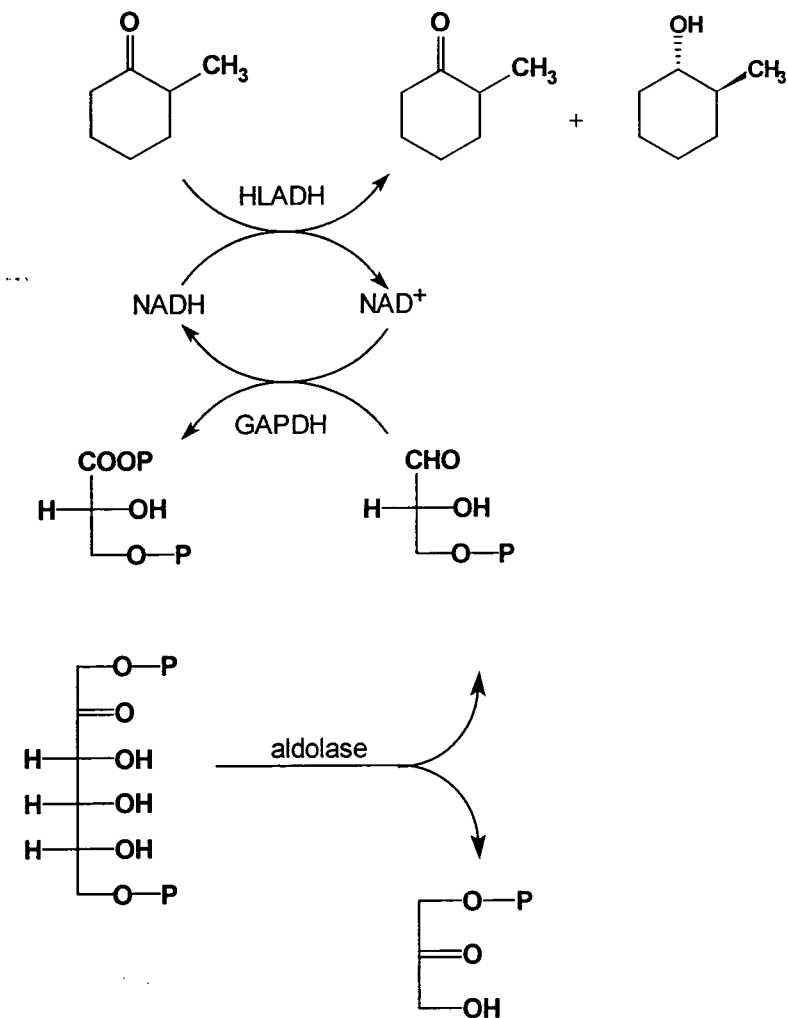


Fig. B5.2 Coupled enzyme recycling of NADH co-factor²¹⁸

B5.2 Enzymatic oxidation of CF₂-phosphonate 173

With a sample of the CF₂-phosphonate analogue **173** of *sn*-glycerol-3-phosphate in hand a study of its oxidation with G-3-P dehydrogenase was undertaken at neutral pH. ¹⁹F NMR spectroscopy was used to follow the reaction course and to determine the nature of the products. The application of enzyme coupled co-factor recycling was also investigated using fluoropyruvate **175** with lactate dehydrogenase (LDH). Fluoropyruvate is a good substrate for LDH and the introduction of a fluorine atom gave a convenient handle with which to calculate the extent of conversion by ¹⁹F NMR spectroscopy (Fig. B5.3).

Initial control reactions with *sn*-glycerol-3-phosphate and NAD⁺ using fluoropyruvate demonstrated that the conversion could be followed by ¹⁹F NMR

spectroscopy *via* integration of the signals for fluoropyruvate (triplet, δ -228.5) and fluorolactate (doublet of triplets, δ -229.5).

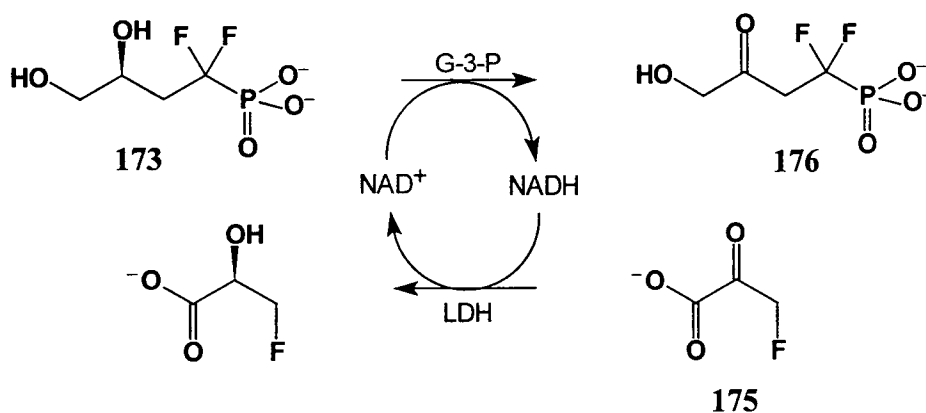


Fig. B5.3

Glycerol-3-phosphate dehydrogenase was added to a solution of pH 7 buffer containing the difluorophosphonate 173 and fluoropyruvate 175 in a 1:1 ratio, with NAD⁺ and lactate dehydrogenase. The reaction was maintained at 30 °C and the progress was monitored by removal of aliquots for ¹⁹F NMR analysis (Fig. B5.4).

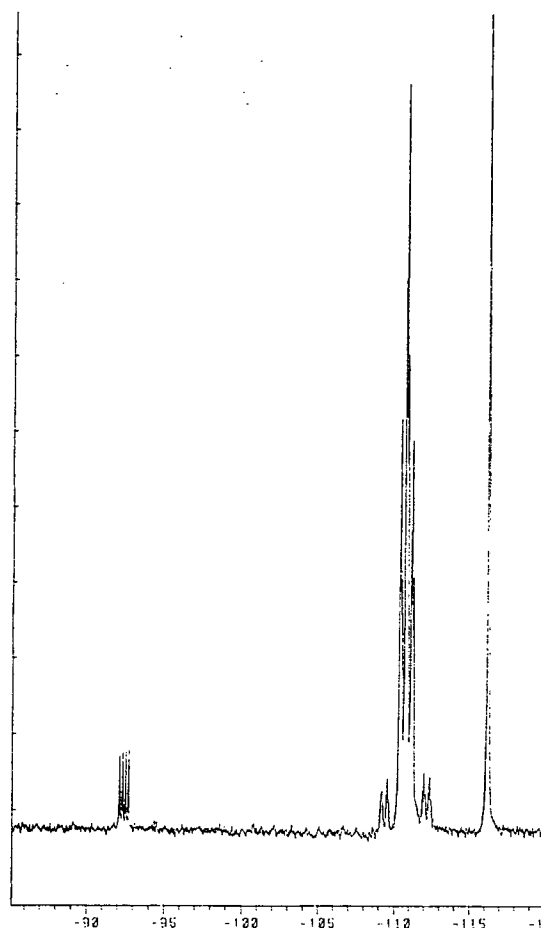


Fig. B.5.4

At neutral pH the reaction was extremely slow but stable, turning over the phosphonate for several days. ^{19}F NMR spectroscopy enabled analysis of the products formed on enzymatic oxidation. Clearly the expected product from the oxidation was the ketone **176**. It was not however apparent that this product was accumulating, but a new peak (doublet of doublets) emerged at $\delta -93$ in the ^{19}F NMR spectrum, which was assigned to the fluorovinylmethylenephosphonate **177**,²¹⁷ and also a large singlet became apparent at $\delta -117$ which was assigned to the accumulation of fluoride (Fig. B5.4). However, closer analysis of the ^{19}F NMR spectrum showed that there was a change in the coupling pattern of the signal associated with the starting material. Further analysis of the ^{19}F NMR spectrum revealed that the ketone **176** was indeed being generated but that its ^{19}F NMR signal was coincident with the signal of the starting CF_2 -phosphonate **173**. This oxidised product was then breaking down *via* the elimination of hydrogen fluoride, giving **177** and fluoride ion in solution. That this was indeed the case was confirmed by the addition of base to the reaction solution, after which the observed coupling pattern for the CF_2 -phosphonate was restored, along with an increase in the fluoride concentration. Thus in basic conditions hydrogen fluoride elimination is induced and all of the ketone **176** decomposed to reveal unreacted starting material at $\delta -108.5$. It is not clear, however, why **177** did not accumulate to any extent, and we have to deduce that it is also labile to fluoride elimination. A Michael-type addition of water to **177** could result in fluoride release, as shown below in Fig. B5.5.

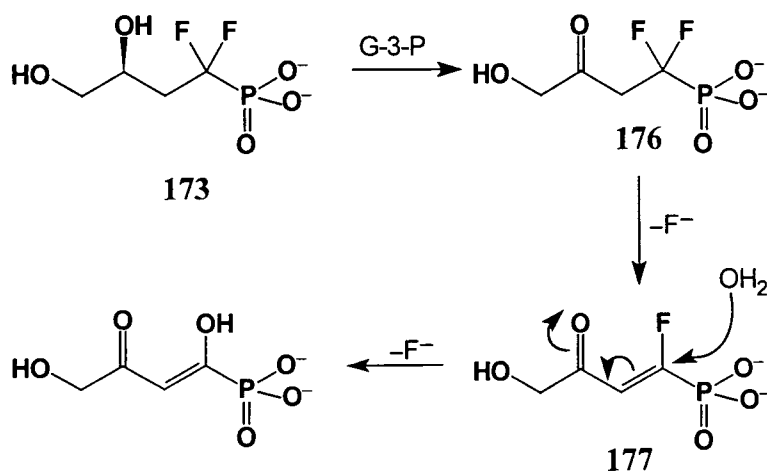


Fig. B5.5

B5.3 Enzymatic oxidation of CHF-phosphonate

Using the same protocol as described for the CF₂-phosphonate, the enzymatic oxidation of the CHF-phosphonate **172** analogue of *sn*-glycerol-3-phosphate was investigated. The reaction, although again slow, was quicker than that observed with **173** and the reaction took typically 24 h to go to completion. The reaction progress was again monitored by ¹⁹F NMR spectroscopy, and as the reaction proceeded the predominant signal was again that assigned to fluoride generated by elimination, however the anticipated ketone product **178** was not apparent. It was therefore postulated that the ketone was forming but was subsequently undergoing rapid elimination in solution (Fig. B5.6).

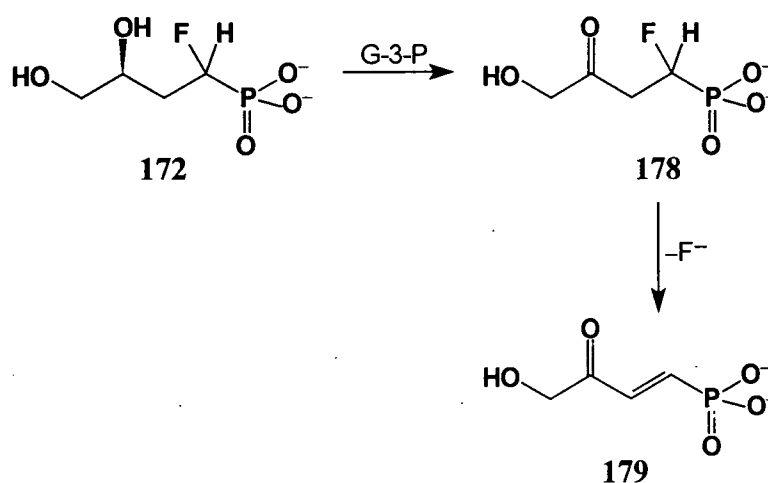


Fig. B5.6

The depletion of both diastereoisomers of **172** was apparent, however it initially appeared that the enzyme was showing a significant level of discrimination between the two diastereoisomers. Fig. B5.7 shows the high field ¹H-decoupled ¹⁹F NMR spectrum of the oxidation of **172**.

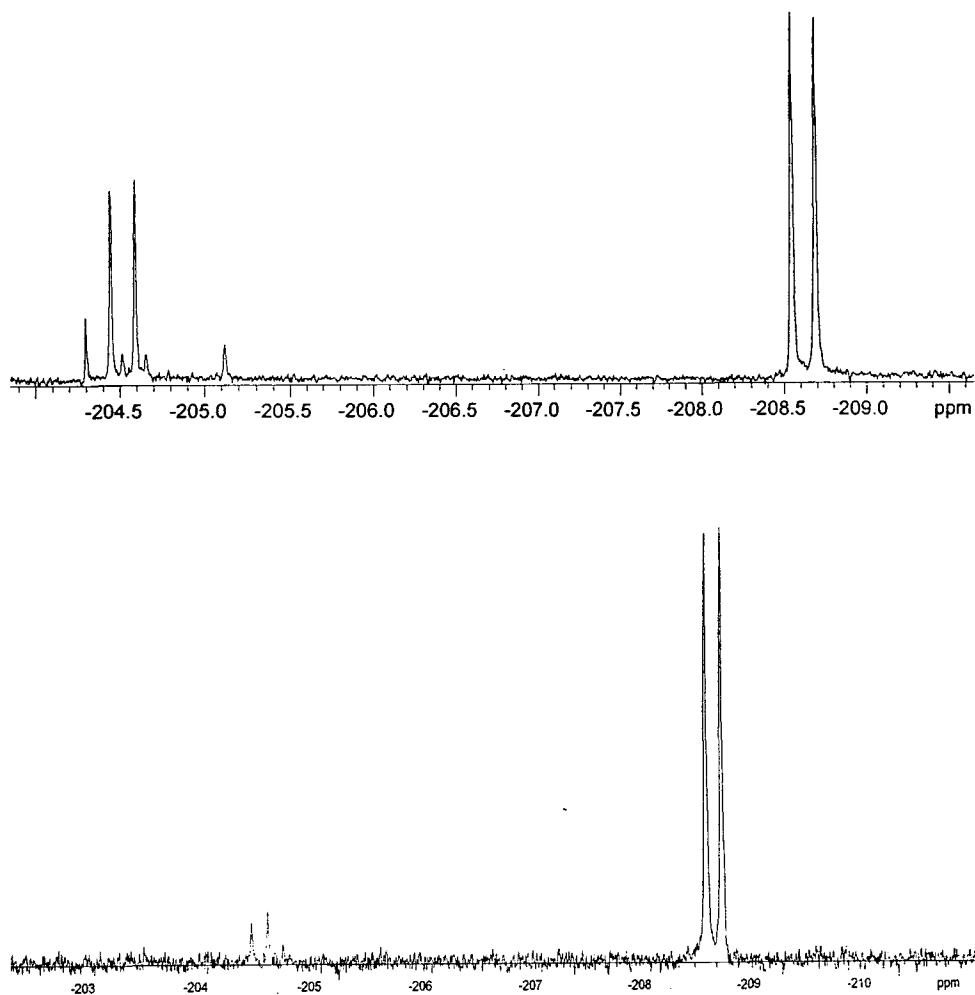


Fig. B5.7 ^{19}F NMR spectra of the reaction solution of **172** with G-3-P dehydrogenase

After several runs it became apparent, by careful integration of the observed ^{19}F NMR spectra, that the expected oxidation product was again coincident with one of the diastereoisomers of the starting CHF-phosphonate. This made it impossible therefore to quantitatively evaluate any diastereoisomeric discrimination during the oxidation of the CHF phosphonate.

B5.4 Conclusions

The enzymatic oxidations of the fluorinated glycerol-3-phosphate analogues **172** and **173** were successfully carried out at neutral pH employing a coupled enzyme co-factor recycling protocol. By this study and for the first time, a number of the secondary products of the enzymatic oxidation of the fluorinated glycerol-3-phosphate analogues

172 and 173 have been identified. This is the first case where the behaviour and products of any CF₂-phosphonate analogue has been studied, and it emerges that in this situation, although good substrates, the fluorine is metabolically labile.

Chapter Six

Experimental

Experimental

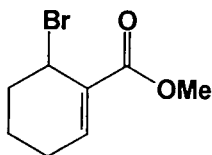
6.1 General

Nuclear magnetic resonance (NMR) spectra were obtained on Varian Gemini 200 (^1H at 199.975 MHz, ^{13}C at 50.289 MHz), Varian XL-200 (^1H at 200.057 MHz), Bruker AC-250 (^1H at 250.133 MHz, ^{13}C at 62.257 MHz, ^{19}F at 235.342 MHz), Varian VXR-400(S) (^1H at 399.952 MHz, ^{13}C at 100.577 MHz, ^{19}F at 376.291 MHz) and Bruker AMX-500 (^{19}F at 470.528 MHz) spectrometers with deuteriochloroform as solvent, unless otherwise stated (residual CHCl_3 : δ_{H} 7.26, δ_{C} 77.0). Chemical shifts are recorded in ppm (δ units). ^{19}F NMR spectra are referenced to an external standard of CFCl_3 (δ 0). Signal splitting patterns are described as singlet (s), doublet (d), triplet (t), quartet (q) or multiplet (m). Infrared (IR.) spectra were recorded on a Perkin-Elmer FT-IR 1720X spectrometer using conventional techniques in four scans. Low resolution mass spectra were recorded on a VG Analytical 7070E Organic Mass Spectrometer, and gas chromatography–mass spectra (GC–MS) recorded using a Hewlett-Packard 5890 Series II gas chromatograph, equipped with a 25 m SE30 column, connected to a VG Mass Lab Trio 1000. High resolution mass spectra were performed by the EPSRC service at the University of Swansea. Flash Column Chromatography was performed using silica gel (60–240 mesh). Melting points were determined using a Gallenkamp melting point apparatus and are uncorrected.

All non-aqueous reactions were carried out under an atmosphere of dry nitrogen in pre-dried glassware. All solvents were distilled prior to use. Light petroleum refers to the fraction boiling in the range 40–60 °C. Solvents were dried from the following reagents under a nitrogen atmosphere: tetrahydrofuran and ether (sodium and benzophenone); benzene, hexane and dichloromethane (calcium hydride); chloroform and carbon tetrachloride (phosphorus pentoxide); methanol (magnesium methoxide); ethanol (magnesium ethoxide). All other reagents were reagent grade and used as supplied unless otherwise stated.

6.2 Experimental to Chapter Two

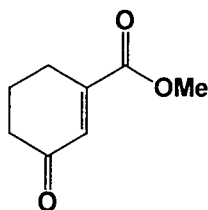
Methyl 3- and 6-bromocyclohex-1-enecarboxylates **45,46**^{107,108}



N-Bromosuccinimide (1.99 g, 11.2 mmol) was added to a solution of methyl cyclohex-1-enecarboxylate (1.52 g, 10.9 mmol) in carbon tetrachloride (30 ml). AIBN (0.21 g, 1.3 mmol) was added and the solution stirred under the light of two 100 W bulbs. Stirring was continued until succinimide was observed floating on the top of the solution. The reaction mixture was diluted with water (50 ml), extracted into diethyl ether (3 × 50 ml) and washed with water (50 ml), 5% aqueous sodium sulfite (50 ml), water (50 ml) and brine (50 ml). The organic layer was dried (MgSO₄) and the solvent removed under reduced pressure. The crude residue was purified over silica gel eluting with light petroleum–diethyl ether (90:10). Active fractions were combined to give **45** (0.19 g, 16.2%) and **46** (0.24 g, 20.4%) as colourless oils.

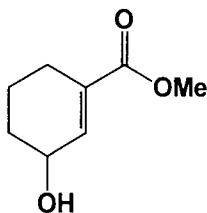
6-Bromocyclohex-1-enecarboxylate **46**: $\delta_{\text{H}}(\text{CDCl}_3)$ 7.04 (1H, dd, CH), 5.20 (1H, d, CHBr), 3.75 (3H, s, CH₃), 1.70–2.60 (6H, m, CH₂); $\delta_{\text{C}}(\text{CDCl}_3)$ 165.5 (CO), 142.6 (CH), 131.9 (C), 51.8 (MeO), 45.0 (CHBr), 31.7 (CH₂), 25.4 (CH₂), 16.5 (CH₂); $\nu_{\text{max}}(\text{neat})/\text{cm}^{-1}$ 2952, 1718, 1649, 1436; m/z (EI+) 220.9 (M⁺, 37.3%), 218.9 (M⁺, 39.1%), 139.0 (M⁺–Br 100%). C₈H₁₂O₂Br (MH⁺) requires 219.002066. Found: 219.00207.

Methyl 3-oxocyclohex-1-enecarboxylate **50**^{110,111}



A solution of chromium trioxide (4.46 g, 44.7 mmol) in acetic anhydride (25 ml) and glacial acetic acid (50 ml) was added dropwise over 35 min to a stirred solution of methyl 1-cyclohexenecarboxylate (2.03 g, 14.5 mmol) in benzene (50 ml) at 18–20 °C. Stirring was continued at this temperature for an additional 10 min and then benzene (50 ml) was added and the reaction cooled in an ice bath. The reaction was cautiously neutralised with concentrated KOH (100 ml). The two phase mixture was poured into water (200 ml) and extracted into diethyl ether (3 × 100 ml). The diethyl ether extracts were washed with saturated sodium hydrogen carbonate (3 × 100 ml) and brine (2 × 100 ml) and dried (MgSO₄). The solvent was removed under reduced pressure to yield crude product as a yellow oil. Purification over silica gel, eluting with CH₂Cl₂, gave the title compound as a colourless oil (1.25 g, 56%): $\delta_{\text{H}}(\text{CDCl}_3)$ 6.70 (1H, s, CH), 3.80 (3H, s, OMe), 2.56 (2H, dt, CH₂), 2.43 (2H, t, CH₂), 2.03 (2H, p, CH₂); $\delta_{\text{C}}(\text{CDCl}_3)$ 200.2 (CO), 167.2 (CO), 149.2 (C), 133.3 (CH), 52.9 (MeO), 38.0 (CH₂), 25.2 (CH₂), 22.5 (CH₂); $\nu_{\text{max}}(\text{neat})/\text{cm}^{-1}$ 2950, 1724, 1686, 1616, 1437, 1256, 1229; m/z (EI⁺) 154 (M⁺, 61.5%), 126 (M⁺-28, 100%).

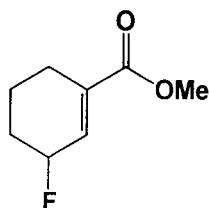
Methyl 3-hydroxycyclohex-1-enecarboxylate **51**¹¹²



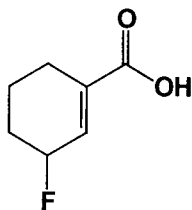
NaBH₄ (0.36 g, 9.5 mmol) was added to a solution of methyl 3-oxocyclohex-1-enecarboxylate (1.37 g, 8.9 mmol) and CeCl₃·7H₂O (9.95 g, 26.7 mmol) dissolved in methanol (66 ml). There was an initial effervescence accompanied by an increase in

temperature. Stirring was continued for 30 min, at which time the methanol was removed under reduced pressure and the mixture extracted into diethyl ether (3 × 50 ml). The ethereal extracts were combined, dried (MgSO₄) and the solvent removed under reduced pressure to give a yellow oil. Purification over silica gel (70:30 diethyl ether–light petroleum) gave the title compound as a colourless oil (1.11 g, 80%): $\delta_{\text{H}}(\text{CDCl}_3)$ 6.86 (1H, d, CH), 4.32 (1H, br m, CHOH), 3.72 (3H, s, OMe), 1.45–2.30 (6H, m, CH₂); $\delta_{\text{C}}(\text{CDCl}_3)$ 167.7 (CO), 140.0 (CH), 132.1 (C), 65.8 (CHOH), 51.8 (OMe), 31.0 (CH₂), 24.1 (CH₂), 19.0 (CH₂); $\nu_{\text{max}}(\text{neat})/\text{cm}^{-1}$ 3413, 2945, 1717, 1649, 1437, 1263, 1239; m/z (CI⁺) 156.0 (M⁺, 100%), 174.0 (M⁺+18, 77.1%). C₈H₁₂O₃ (M⁺) requires 156.07864. Found: 156.0786.

Methyl 3-fluorocyclohex-1-enecarboxylate **48**⁷²

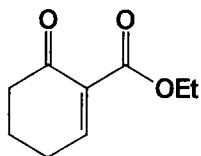


A solution of methyl 3-hydroxycyclohex-1-enecarboxylate (0.92 g, 5.9 mmol) in CH₂Cl₂ (5 ml) was added dropwise to a stirred solution of diethylaminosulfur trifluoride (DAST) (1.00 g, 6.2 mmol) in CH₂Cl₂ (5 ml) at –78 °C under nitrogen. The reaction was then allowed to warm to room temperature, and water (20 ml) was added. The organic layer was separated, washed with water and then dried (MgSO₄). The crude material was purified over silica gel (90:10 light petroleum–diethyl ether) to give **48** as a colourless oil (0.65 g, 69%); $\delta_{\text{H}}(\text{CDCl}_3)$ 6.88 (1H, dm, CH), 5.13 (1H, dm, J 48 Hz, CHF), 3.76 (3H, s, OMe), 1.50–2.50 (6H, m, CH₂); δ_{C} 166.2 (CO), 134.2 (C), 133.9 (d, J 19.3 Hz, CH), 85.1 (d, J 164 Hz CHF), 51.3 (OMe), 27.7 (d, J 19.3 Hz, CH₂), 23.5 (CH₂), 17.5 (CH₂); $\delta_{\text{F}}(\text{CDCl}_3)$ –172.04 (br d, J 45.6 Hz); $\nu_{\text{max}}(\text{neat})/\text{cm}^{-1}$ 2951, 1716, 1649, 1263, 1246, 1246; m/z (EI⁺) 158.1 (M⁺, 40.2%); (CI⁺) 176.1 (M⁺+18, 22.2%), 139.1 (M⁺–HF, 100%). C₈H₁₁O₂F (M⁺) requires 158.07430. Found: 158.0743.



Methyl 3-fluorocyclohex-1-enecarboxylate (1.19 g, 7.5 mmol) was added to a solution of KOH (1 g) in methanol (20 ml) and stirred at room temperature. The reaction was monitored by TLC (80:20 light petroleum–diethyl ether). When the starting material had disappeared the reaction was acidified with dilute aqueous HCl and extracted into diethyl ether (3 × 50 ml). The ethereal layers were combined, dried (MgSO₄) and the solvent removed under reduced pressure to give a white solid, which was recrystallised from diethyl ether with light petroleum (0.83 g, 77%); mp 62–64 °C; $\delta_{\text{H}}(\text{CDCl}_3)$ 11.05 (1H, br s, CO₂H), 7.04 (1H, dm, CH), 5.15 (1H, dm, *J* 47 Hz, CHF), 1.55–2.5 (6H, m, CH₂); $\delta_{\text{C}}(\text{CDCl}_3)$ 172.3 (CO), 137.0 (d, *J* 19.55 Hz, CH), 134.5 (d, *J* 9.3 Hz, C), 85.7 (d, *J* 164.82 Hz, CHF), 28.2 (d, *J* 19.3 Hz, CH₂), 23.8 (d, *J* 2.7 Hz, CH₂), 18.1 (d, *J* 2.6 Hz, CH₂); $\delta_{\text{F}}(\text{CDCl}_3)$ -173.27 (d, *J* 44.7 Hz); $\nu_{\text{max}}(\text{CHCl}_3)/\text{cm}^{-1}$ 3029, 2951, 1697, 1651, 1276, broad acid region; *m/z* (EI⁺) 144.1 (M⁺, 29.5%), 99.1 (M⁺-CO₂H, 100%). C₇H₉O₂F requires C, 58.31; H, 6.30. Found: C, 57.97; H, 6.15%.

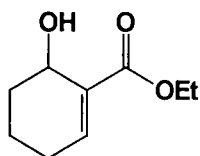
Ethyl 6-oxocyclohex-1-enecarboxylate **52**¹¹⁵



Dry pyridine (1.20 g, 15.2 mmol) was added to a solution of phenylselenium chloride (2.68 g, 14.0 mmol) in CH₂Cl₂ (25 ml), cooled to 0 °C and stirred for 15 min. A

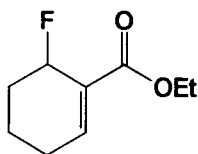
solution of ethyl 2-oxocyclohexanecarboxylate (2.02 g, 11.5 mmol) in CH_2Cl_2 (5 ml) was added and the reaction complex allowed to stir for an additional 15 min. The organic layer was washed with a 10% aqueous HCl (2×10 ml), re-cooled to 0°C and then H_2O_2 (30%, 0.1 ml) was added. After 10 min an additional aliquot of H_2O_2 (0.1 ml) was added and again after another 10 min. After a further 10 min, water (10 ml) was added and the organic layer separated and washed with NaHCO_3 (10 ml). The organic extracts were dried (MgSO_4) and the solvent removed under reduced pressure to afford the title compound. Purification over silica gel (60:40 light petroleum–diethyl ether) gave the product as a clear colourless oil (1.83 g, 95%); $\delta_{\text{H}}(\text{CDCl}_3)$ 7.59 (1H, t, CH), 4.19 (2H, q, J 7.1 Hz, CH_2), 2.43 (4H, m, CH_2), 1.99 (2H, p, CH_2), 1.24 (3H, t, J 7.1 Hz, CH_3); $\delta_{\text{C}}(\text{CDCl}_3)$ 195.2 (CO), 165.1 (CO), 156.3 (CH), 133.6 (C), 61.5 (OCH_2), 39.2 (CH_3), 26.5 (CH_2), 22.6 (CH_2), 14.6 (CH_2); $\nu_{\text{max}}(\text{neat})/\text{cm}^{-1}$ 1738, 1684, 1619, 1374, 1270, 1224; m/z (EI+) 169.0 ($\text{M}^+ + 1$, 100%).

Ethyl 6-hydroxycyclohex-1-enecarboxylate **53**¹¹⁶



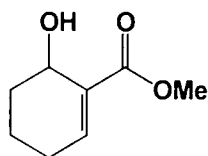
A small quantity (0.5 ml) of saturated potassium carbonate (31 g, in 35 ml water) was added to 25% aqueous glutaraldehyde (61.72 g, 0.2 M). Triethyl phosphonoacetate (22.43 g, 0.1 M) was then added slowly over 2 h with simultaneous slow addition of aqueous potassium carbonate (1.6 ml, 0.1 equiv.) at 20°C . The remaining aqueous basic solution was then added slowly (2 h) and the solution was stirred for 48 h at room temperature. The solution was then extracted into diethyl ether (4×100 ml), washed with brine (100 ml) and dried (MgSO_4). Removal of the solvent under reduced pressure gave a yellow oil which was purified over silica gel (50:50 light petroleum–diethyl ether) to afford the title compound (3.57 g, 21%); $\delta_{\text{H}}(\text{CDCl}_3)$ 7.06 (1H, t, CH), 4.51 (1H, br m, CHOH), 4.20 (2H, q, J 7.1 Hz, CH_2), 1.5–2.5 (6H, m, CH_2), 1.28 (3H, t, J 7.1 Hz, CH_3); $\delta_{\text{C}}(\text{CDCl}_3)$ 167.6 (CO), 143.0 (CH), 132.8 (C), 63.3 (CHOH), 60.8 (OCH_2), 30.4 (CH_2), 26.4 (CH_2), 17.6 (CH_2), 14.6 (CH_3); $\nu_{\text{max}}(\text{neat})/\text{cm}^{-1}$ 3474, 1714, 1647; m/z (CI+) 170.0 (M^+ , 100%); (EI+) 153.0 ($\text{M}^+ - \text{OH}$, 100%).

*Ethyl 6-fluorocyclohex-1-enecarboxylate 55*⁷²



A solution of ethyl 6-hydroxycyclohex-1-enecarboxylate (0.79 g, 4.6 mmol) in CH_2Cl_2 (5 ml) was added dropwise to a stirred solution of diethylaminosulfur trifluoride (DAST) (0.97 g, 6.0 mmol) in CH_2Cl_2 (5 ml) at $-78\text{ }^\circ\text{C}$ under nitrogen. The reaction was then allowed to warm to room temperature, and water (20 ml) was added. The organic layer was separated, washed with water and dried (MgSO_4), and the crude material purified over silica gel (90:10 light petroleum–diethyl ether) to give **55** as a colourless oil (0.45 g, 2.6 mmol, 57%); $\delta_{\text{H}}(\text{CDCl}_3)$ 7.30 (1H, m, CH), 5.41 (1H, dm, J 46.8 Hz, CHF), 4.24 (2H, q, J 7.1 Hz, CH_2), 1.5–2.5 (6H, m, CH_2), 1.31 (3H, t, J 7.1 Hz, CH_3); $\delta_{\text{C}}(\text{CDCl}_3)$ 165.8 (CO), 146.4 (d, J 6.4 Hz, CH), 128.7 (d, J 17 Hz, C), 82.2 (d, J 165 Hz, CHF), 60.6 (OCH_2), 28.4 (d, J 22 Hz, CH_2), 25.8 (d, J 3 Hz, CH_2), 15.8 (CH_2), 14.2 (CH_3); $\delta_{\text{F}}(\text{CDCl}_3)$ -165.98 (t, J 44 Hz); $\nu_{\text{max}}(\text{neat})/\text{cm}^{-1}$ 1720, 1654, 1437, 1266, 1243, 1090; m/z (EI+) 173.1 ($\text{M}^+ + 1$, 29, 4%), 153.1 ($\text{M}^+ - \text{HF}$, 100%). $\text{C}_9\text{H}_{17}\text{O}_2\text{FN}$ (MNH_4^+) requires 190.1243. Found: 190.1243.

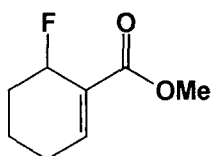
*Methyl 6-hydroxycyclohex-1-enecarboxylate 49*¹¹⁶



A small quantity (0.5 ml) of aqueous potassium carbonate (31 g, 0.23 M in 35 ml) was added to 25% aqueous glutaraldehyde (60.99 g, 0.15 M). Trimethyl phosphonoacetate (18.21 g, 0.1 M) was then added slowly over 2 h with simultaneous slow addition of aqueous potassium carbonate (1.6 ml, 0.1 equiv.) at $20\text{ }^\circ\text{C}$. The remaining aqueous basic solution was then added slowly (2 h) and the solution was stirred for 48 h at room

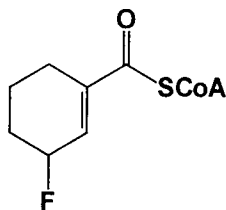
temperature. The solution was then extracted into diethyl ether (4 × 100 ml), washed with brine (100 ml) and dried (MgSO₄). Removal of the solvent gave a yellow oil which was purified by distillation (66 °C, 0.2 mmHg) to afford the title compound (3.14 g, 20%); bp 64–66 °C (0.2 mmHg); δ_H(CDCl₃) 7.09 (1H, t, CH), 4.52 (1H, br m, CHOH), 3.76 (3H, s, OMe), 1.5–2.5 (6H, m, CH₂); δ_C(CDCl₃) 166.5 (CO), 143.7 (CH), 132.9 (C), 63.9 (CHOH), 52.2 (OMe), 30.4 (CH₂), 26.6 (CH₂), 17.9 (CH₂); ν_{max}(neat)/cm⁻¹ 3480, 2947, 1716, 1647, 1437; *m/z* (EI+) 157.0 (M⁺+1, 100%), 139 (M⁺-OH, 82.7%). C₈H₁₃O₃ (MH⁺) requires 157.0864. Found: 157.0865.

*Methyl 6-fluorocyclohex-1-enecarboxylate 47*⁷²



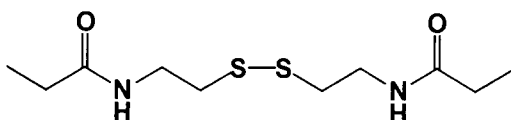
A solution of methyl 6-hydroxy-1-cyclohexenecarboxylate (0.97 g, 6.2 mmol) in CH₂Cl₂ (5 ml) was added dropwise to a stirred solution of diethylaminosulfur trifluoride (DAST) (1.12 g, 6.95 mmol) in CH₂Cl₂ (5 ml) at -78 °C under nitrogen. The reaction was then allowed to warm to room temperature, and water (20 ml) was added. The organic layer was separated, washed with water and dried (MgSO₄). The crude product was purified over silica gel (80:20 light petroleum–diethyl ether) to give **47** as a colourless oil (0.46 g, 47%); δ_H(CDCl₃) 7.32 (1H, m, CH), 5.40 (1H, dt, *J* 47.8 Hz, CHF), 3.79 (3H, s, OMe), 1.45–2.50 (6H, m, CH₂); δ_C 166.8 (CO), 147.3 (d, *J* 6.5 Hz, CH), 129.0 (d, *J* 17.1 Hz, C), 82.7 (d, *J* 165.8 Hz, CHF), 52.3 (OMe), 28.9 (d, *J* 21.9 Hz, CH₂), 26.4 (d, *J* 2.9 Hz, CH₂), 16.2 (CH₂); δ_F(CDCl₃) -166.00 (t, *J* 45 Hz); ν_{max}(neat)/cm⁻¹ 2952, 1720, 1649, 1436; *m/z* (EI+) 158.2 (M⁺, 15.6%); (CI+) 176.2 (M⁺+18, 100%). C₈H₁₅O₂FN (MNH₄⁺) requires 176.10867. Found: 176.1087.

3-Fluorocyclohex-1-enecarbonyl-CoA **41**¹¹⁷



3-Fluoro-1-cyclohexenecarboxylic acid (10 mg, 0.07 mmol) was added to a solution of triethylamine (10 μ l) in THF (2 ml) and stirred for 5 min. Ethyl chloroformate (8 μ l) was added and a precipitate formed. The reaction was stirred under nitrogen for 10 min (solution 1). In a separate flask, co-enzyme A (13 mg, 0.016 mmol) was added to a solution of NaHCO_3 in water (2 ml) (solution 2). Solution 1 was filtered through glass wool and added to solution 2, and the reaction stirred for 45 min. The pH was then decreased to 2 and the THF evaporated under reduced pressure. The aqueous phase was extracted into an equal volume of diethyl ether (3 \times 4 ml) and then the pH of the aqueous phase was raised to 4–5 and then freeze dried to give a white powder; $\delta_{\text{F}}(\text{D}_2\text{O})$ -170.25, -123.64 (F^-). No further analysis was carried out and this preparation was used directly in enzyme assays.

N,N'-Dipropionylcystamine **57**²¹⁹

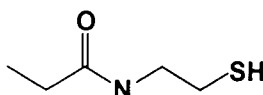


Propionyl chloride (20.34 g, 220 mmol) was added dropwise to an ice cooled solution of cystamine dihydrochloride (22.5 g, 100 mmol) in water (20 ml). The pH of the reaction was kept above pH 8.2 throughout the addition of the propionyl chloride by addition of aqueous KOH (12.5 M, 35 g of KOH and 50 ml). The resulting white precipitate was collected by filtration and washed thoroughly with cold water. Upon drying, the white solid of *N,N'*dipropionylcystamine (9.52 g, 36%) was stored in a desiccator; mp 92–93 $^{\circ}\text{C}$ (lit.,²¹⁸ 92–94.2 $^{\circ}\text{C}$); $\delta_{\text{H}}(\text{CDCl}_3)$ 6.60 (2H, br s, NH), 3.53 (4H, dt, J 6.3 Hz and 5.8 Hz, CH_2), 2.81 (4H, t, J 6.5 Hz, CH_2), 2.24 (4H, q, J 7.6 Hz, CH_2), 1.13 (3H, t, J 7.6 Hz, CH_3); $\delta_{\text{C}}(\text{CDCl}_3)$ 175.0 (CO), 38.9 (CH_2), 38.3 (CH_2), 30.0 (CH_2), 10.3 (CH_3), $\nu_{\text{max}}(\text{Nujol})/\text{cm}^{-1}$ 3260, 3060, 1625, 1545; m/z (CI+) 265 ($\text{M}^+ + 1$, 2.64%).

3% Sodium amalgam

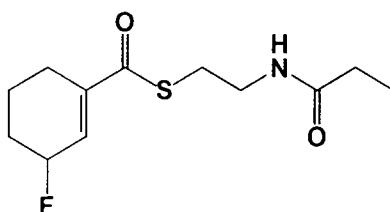
Distilled mercury (430 g, 2.1 mol) was carefully dropped onto small pieces of sodium (13 g, 0.6 mol) under an inert atmosphere of nitrogen. The reaction was kept hot with the aid of a Bunsen burner to ensure continuous reaction. The hot liquid was poured into a glass dish and cut up into small pieces before the sodium amalgam cooled and solidified as a block.

N-Propionylcystamine **58**²¹⁹



3% Sodium amalgam (13 g) was added to a solution of *N,N'*-dipropionylcystamine (1.32 g, 5 mmol) in dry methanol (50 ml) under nitrogen, and the reaction mixture stirred for 90 min at room temperature. The remaining mercury was removed by filtration, and the solution added to dilute HCl (50 ml). The product was extracted into CH₂Cl₂ (3 × 50 ml), dried (MgSO₄) and the solvent removed under reduced pressure to afford *N*-propionylcystamine (0.66 g, 49%) as a colourless oil; $\delta_{\text{H}}(\text{CDCl}_3)$ 6.05 (1H, br s, NH), 3.36 (2H, dt, *J* 7.9 and 6.6 Hz, CH₂), 2.66 (2H, dt, *J* 8.1 and 6.6 Hz, CH₂), 2.18 (2H, q, *J* 7.6 Hz, CH₂), 1.35 (1H, t, *J* 8.5 Hz, SH), 1.10 (3H, t, *J* 7.6 Hz, CH₃); $\delta_{\text{C}}(\text{CDCl}_3)$ 174.7 (CO), 42.9 (CH₂), 30.0 (CH₂), 25.0 (CH₂), 10.4 (CH₃); $\nu_{\text{max}}(\text{neat})/\text{cm}^{-1}$ 3293, 3077, 2976, 2938, 2547, 1650, 1548; *m/z* (EI+) 134 (M⁺+1, 28.29).

S-(*N*-propionamidoethyl) 3-fluorocyclohex-1-enethiocarboxylate **59**

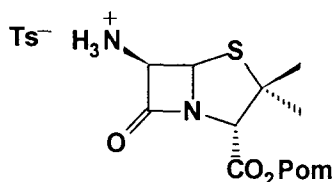


Carbonyldiimidazole (67 mg, 0.41 mmol) suspended in THF (2 ml) was added to a solution of 3-fluorocyclohex-1-enecarboxylic acid (50 mg, 0.34 mmol) dissolved in

THF (2 ml) and the mixture stirred under N₂ for 30 min. A solution of *N*-propionylcystamine (68 mg, 0.51 mmol) in THF (2 ml) was added and the mixture was stirred overnight under N₂. Removal of the THF under reduced pressure gave an oil that was purified over silica gel (80:20 CH₂Cl₂-EtOAc). The active fractions were combined and the solvent removed under reduced pressure to give the product as a colourless oil (53 mg, 59%); $\delta_{\text{H}}(\text{CDCl}_3)$ 6.85 (1H, m, CH), 5.85 (1H, br s, NH), 5.15 (1H, dm, *J* 47 Hz, CHF), 3.47 (2H, q, *J* 6.2 Hz, CH₂), 3.10 (2H, t, *J* 6.5 Hz, CH₂), 1.50–2.50 (6H, m, CH₂), 2.20 (2H, q, *J* 7.6 Hz, CH₂), 1.14 (3H, t, *J* 7.6 Hz, CH₃); $\delta_{\text{C}}(\text{CDCl}_3)$ 193.2 (CO), 173.9 (CO), 142.2 (d, *J* 9 Hz, C), 132.9 (d, *J* 20 Hz, CH), 85.6 (d, *J* 165 Hz, CHF), 39.4 (CH₂), 29.6 (CH₂), 28.4 (d, *J* 20 Hz, CH₂), 28.4 (CH₂), 24.0 (d, *J* 2.6 Hz, CH₂), 18.0 (d, *J* 4.9 Hz, CH₂), 9.73 (CH₃); $\delta_{\text{F}}(\text{CDCl}_3)$ -172.22 (dm, *J* 45.2 Hz); $\nu_{\text{max}}(\text{neat})/\text{cm}^{-1}$ 3290, 2938, 1654, 1647, 1543, 1147; *m/z* (CI⁺) 260.5 (MH⁺, 32%), 240 (M⁺-19, 23%). C₁₂H₁₉O₂SNF (MH⁺) requires 260.11205. Found: 260.1121.

6.3 Experimental to Chapter Three

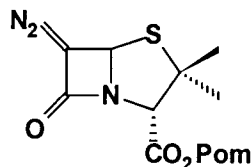
*Pivaloyloxymethyl 6-aminopenicillanate hydrotosylate 83*¹⁴⁸



Triethylamine (3.5 ml, 24.9 mmol) was added to a suspension of 6-aminopenicillanic acid (3.52 g, 16.6 mmol) in dry DMF (30 ml), and the reaction stirred for 30 min. Chloromethyl pivalate (4.8 ml, 33.2 mmol) was added and the solution was stirred for 4 h at room temperature. The mixture was diluted with EtOAc and the precipitated Et₃N·HCl removed by filtration. The filtrate was washed with water (4 × 100 ml) and then the organic layer was dried (MgSO₄) and the volume concentrated to approximately half under reduced pressure. Treatment of the stirred solution of the crude ester with TsOH in EtOAc (0.5 M, 40 ml) at room temperature precipitated the crystalline toluene-*p*-sulfonate, which was filtered, washed with EtOAc and Et₂O and dried to afford **83** as a white crystalline solid (6.25 g, 75%); mp 154–155 °C (decomp.) [lit.,¹⁴⁸ 150–151 °C

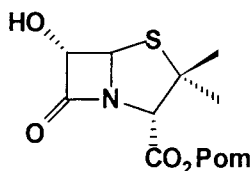
(decomp.); $\delta_{\text{H}}(\text{CDCl}_3)$ 7.45 (4H, AB, J 7.9 Hz, Ph), 5.76 (2H, AB, J 5.4 and 13.4 Hz, OCH₂O), 5.39 (1H, d, J 4.0 Hz, CH), 4.96 (1H, d, J 4.0 Hz, CH), 4.44 (1H, s, CHCO₂), 2.33 (3H, s, Me), 1.44 (3H, s, Me), 1.37 (3H, s, Me), 1.19 (9H, s, Me); $\nu_{\text{max}}(\text{KBr})/\text{cm}^{-1}$ 3250, 2950, 1760, 1730, 1480, 1215. C₂₁H₃₀N₂O₈S₂ requires C, 50.19; H, 6.02; N, 5.57. Found: C, 50.24; H, 6.13; N, 5.58%.

Pivaloyloxymethyl 6-diazopenicillanate **84**¹⁴⁹



Sodium nitrite (1.73 g, 25.1 mmol) was added to an ice cooled solution of **83** (0.65 g, 1.38 mmol) in a mixture of water (60 ml) and CH₂Cl₂ (60 ml). The solution was stirred vigorously for 5 min, after which time toluene-*p*-sulfonic acid (0.37 g, 1.93 mmol) was added in portions over a 20 min period. Stirring was continued for an additional 10 min, and the solution transferred into an ice cold separating funnel. The organic layer was removed, washed with brine, dried (MgSO₄) and the solvent removed under reduced pressure to afford the product as an amber glass (0.37 g, 79%); $\delta_{\text{H}}(\text{CDCl}_3)$ 6.15 (1H, s, CH), 5.79 (2H, AB, J 5.6 Hz, OCH₂O), 4.36 (1H, s, CHCO₂), 1.61 (3H, s, Me), 1.42 (3H, s, Me), 1.18 (9H, s, Me); $\delta_{\text{C}}(\text{CDCl}_3)$ 176.6 (CO), 166.7 (CO), 166.2 (CON), 79.7 (CH₂), 70.1 (C), 68.5 (CH), 63.6 (C), 38.7 (C), 33.7 (Me), 26.8 (Me), 25.7 (Me), 20.7 (CN₂); $\nu_{\text{max}}(\text{neat})/\text{cm}^{-1}$ 2970, 2083 (N=N=C), 1800, 1760, 1480, 1450, 1215.

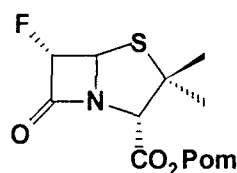
Pivaloyloxymethyl 6 α -hydroxypenicillanate **85**²²⁰



A solution of perchloric acid (1 M, 10 ml) in water (40 ml) was added with swirling to an ice cold solution of pivaloyloxymethyl 6-diazopenicillanate (0.53 g, 1.55 mmol) in

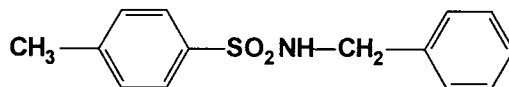
acetone (50 ml). The solution was kept at 5 °C for 12 h and was then extracted into CH₂Cl₂ (3 × 50 ml). The organic extracts were combined and washed with saturated aqueous sodium hydrogen carbonate (2 × 30 ml) and water (2 × 50 ml), dried (MgSO₄) and the solvent removed under reduced pressure. Purification over silica gel, eluting with CH₂Cl₂–EtOAc (90:10) afforded the title compound as a yellow oil (0.42 g, 82%); δ_H(CDCl₃) 5.83 (2H, AB system, *J* 5.6 Hz, OCH₂O), 5.25 (1H, d, *J* 1.4 Hz, CH), 4.82 (1H, d, *J* 1.4 Hz, CH), 4.47 (1H, s, CHCO₂), 1.55 (3H, s, Me), 1.47 (3H, s, Me), 1.21 (9H, s, Me); δ_C(CDCl₃) 176.9 (CO), 171.1 (CO), 166.2 (CO), 85.1 (COH), 79.7 (CH₂), 71.1 (CHS), 68.5 (C), 63.9 (C), 38.8 (C), 33.2 (Me), 26.8 (Me), 25.6 (Me); ν_{max}(neat)/cm⁻¹ 3420 (OH), 2979, 1760 (broad C=O), 1479, 1450, 1215; *m/z* (EI+) 331 (M⁺, 1.4%), 274 (5.3%).

Pivaloyloxymethyl 6α-fluoropenicillanate **86**²²⁰



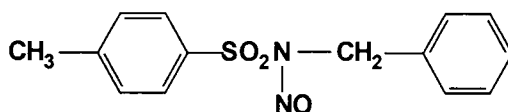
A solution of pivaloyloxymethyl 6α-hydroxypenicillanate (0.45 g, 1.35 mmol) in dry CH₂Cl₂ (5 ml) was added to a solution of DAST (0.27 ml, 2.03 mmol) in dry CH₂Cl₂ (5 ml) cooled to -78 °C under nitrogen. The reaction was allowed to warm to room temperature and was stirred overnight. The reaction was quenched by the addition of water (10 ml) and the organic layer was separated, washed with water (3 × 20 ml), dried (MgSO₄) and the solvent removed under reduced pressure. Purification over silica gel afforded the title compound as a colourless oil (0.37 g, 82%); δ_H(CDCl₃) 5.80 (2H, AB system, *J* 5.6 Hz, OCH₂O), 5.45 (1H, dd, *J* 1.2 and 5.2 Hz, CH), 5.34 (1H, dd, *J* 1.2 and 5.3 Hz, CHF), 4.52 (1H, s, CH), 1.53 (3H, s, Me), 1.46 (3H, s, Me), 1.19 (9H, s, Me); δ_C(CDCl₃) 176.5 (CO), 165.7 (CO), 165.2 (d, *J* 22 Hz, CO), 98.2 (d, *J* 235 Hz, CHF), 79.7 (OCH₂O), 68.7 (d, *J* 24 Hz, CHS), 68.7 (CH), 64.1 (C), 38.7 (CMe₃), 33.6 (Me), 26.8 (Me), 25.3 (Me); δ_F(CDCl₃) -181.7 (dd, *J* 53 and 5.1 Hz); ν_{max}(neat)/cm⁻¹ 2960, 1800, 1760 (broad), 1480, 1215; *m/z* (CI+) 334 (M⁺+1, 8.2%), 276 (M⁺+1–Bu^t, 45%).

N-Benzyltoluene-*p*-sulfonamide¹⁵⁹



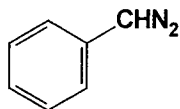
Toluene-*p*-sulfonyl chloride (40 g, 0.21 M) was added cautiously to a solution of benzylamine (20 g, 0.19 M) in dry pyridine (50 ml). The addition was accompanied by an increase in temperature and a change in colour. The solution was stirred for 1 h and poured into ice water. The oily precipitate, which solidified on agitation, was removed by filtration and washed with copious amounts of water. Purification by recrystallisation from methanol gave the product as clear colourless crystals (14.65 g, 69%); mp 114–115 °C (lit.,¹⁵⁹ 114 °C); $\nu_{\max}(\text{KBr})/\text{cm}^{-1}$ 3268 (NH), 3100, 2950, 1598, 1495, 1454, 1422. $\text{C}_{14}\text{H}_{15}\text{NO}_2\text{S}$ requires C, 64.34; H, 5.79; N, 5.36. Found: C, 64.16; H, 5.80; N, 5.13%.

N-Nitroso-*N*-benzyltoluene-*p*-sulfonamide¹⁵⁹



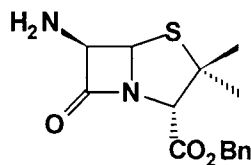
Sodium nitrite (60 g, 0.85 M) was added in portions over 6 h to a solution of *N*-benzyltoluene-*p*-sulfonamide (10.5 g, 0.04 M) in glacial acetic acid (50 ml) and acetic anhydride (200 ml) cooled to 0 °C. The reaction temperature was kept below 10 °C throughout the addition, and the mixture became green in colour. After the addition of sodium nitrite was completed the reaction was stirred overnight at room temperature. The mixture was poured into ice water and cooled for 1 h. The pale yellow precipitate was filtered, washed several times with water and dried *in vacuo*. The crude product was recrystallised from ethanol to afford the title compound as a yellow crystalline solid (10.1 g, 85%); mp 88–89 °C (lit.,¹⁵⁹ 90–92 °C); $\nu_{\max}(\text{KBr})/\text{cm}^{-1}$ 3110, 2950, 1594, 1496, 1383 (N-NO). $\text{C}_{14}\text{H}_{14}\text{N}_2\text{O}_3\text{S}$ requires C, 57.92; H, 4.86; N, 9.65. Found: C, 58.01; H, 4.98; N, 9.54%.

Phenyldiazomethane



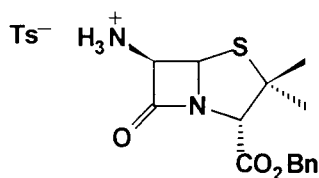
N-Nitroso-*N*-benzyltoluene-*p*-sulfonamide (3.43 g, 11.8 mmol) was added in portions over a period of 1 h to a stirred solution of sodium methoxide (0.64 g, 11.8 mmol) in CH₂Cl₂-MeOH (6:1) at room temperature. The mixture was stirred under reflux for 20 min, allowed to cool, transferred to a separating funnel and water (100 ml) was added to dissolve the salts. The organic solution was repeatedly washed with water (3 × 100 ml), dried (MgSO₄) and was then used directly.

Benzyl 6β-aminopenicillanate



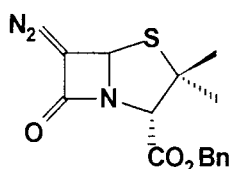
A solution of phenyldiazomethane in CH₂Cl₂ (50 ml) was added to a suspension of 6-aminopenicillanic acid (6-APA) (1.14 g, 5.2 mmol) in methanol (20 ml) at room temperature, and the reaction was stirred vigorously. The disappearance of the red colour of the phenyldiazomethane was accompanied by effervescence due to the evolution of nitrogen. After 1 h the solution was filtered to remove unreacted 6-APA (0.37 g, 1.7 mmol), the filtrate was then washed with water (3 × 100 ml), dried (MgSO₄) and the solvent removed under reduced pressure to afford the product as a yellow oil; δ_H(CDCl₃) 7.33 (5H, s, Ph), 5.46 (1H, d, *J* 4.3 Hz, CH), 5.14 (2H, s, CH₂), 4.51 (1H, d, *J* 4.3 Hz, CH), 4.39 (1H, s, CH), 1.85 (2H, br s, NH₂), 1.57 (3H, s, CH₃), 1.38 (3H, s, CH₃); δ_C(CDCl₃) 177.6 (CO), 167.8 (CO), 134.6, 128.5, 128.4, 69.8, 69.8, 67.2, 63.8, 62.7, 31.6 (CH₃), 26.8 (CH₃); ν_{max}(neat)/cm⁻¹ 3388, 3329, 3033, 2966, 2931, 1778, 1745.

Benzyl 6β-aminopenicillanate hydrotosylate 87



A solution of toluene-*p*-sulfonic acid in EtOAc (0.5 M, 40 ml) was added to a solution of benzyl 6β-aminopenicillanate in EtOAc (10 ml) and the reaction stirred at room temperature. After a short time a precipitate formed which was collected by filtration and washed successively with EtOAc and diethyl ether, and dried *in vacuo*. The product was recovered as an amorphous white solid (0.91 g, 45%); mp 154–155 °C (lit.,²²¹ 155–158 °C); $\delta_{\text{H}}(\text{CDCl}_3)$ 7.42 (4H, AB system, J 8.0 Hz, Ts), 7.34 (5H, s, Ph), 5.43 (1H, d, J 4.3 Hz, CH), 5.14 (2H, s, CH₂), 4.95 (1H, d, J 4.3 Hz, CH), 4.45 (1H, s, CH), 2.30 (3H, s, CH₃), 1.43 (3H, s, CH₃), 1.28 (3H, s, CH₃); C₂₂H₂₆N₂O₆S₂ requires C, 55.21; H, 5.48; N, 5.85. Found: C, 55.05; H, 5.55; N, 5.63%.

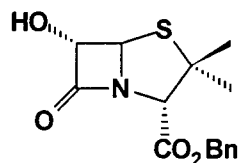
*Benzyl 6-diazopenicillanate 88*¹⁴⁹



Sodium nitrite (2.15 g, 31.2 mmol) was added to an ice cooled solution of benzyl 6-aminopenicillanate tosylate (0.39 g, 0.83 mmol) in a mixture of water (60 ml) and CH₂Cl₂ (60 ml). The solution was stirred vigorously for 5 min, after which time toluene-*p*-sulfonic acid (0.24 g, 1.24 mmol) was added in portions over a 20 min period. Stirring was continued for an additional 10 min, and the solution transferred into an ice cold separating funnel. The organic layer was removed, washed with brine, dried (MgSO₄) and the solvent removed under reduced pressure to afford the product as an amber glass (0.21 g, 84%); $\delta_{\text{H}}(\text{CDCl}_3)$ 7.36 (5H, s, Ph), 6.15 (1H, s, CH), 5.16 (2H, s, CH₂), 4.39 (1H, s, CH), 1.60 (3H, s, CH₃), 1.35 (3H, s, CH₃); $\delta_{\text{C}}(\text{CDCl}_3)$ 167.9 (CO), 166.3 (CO), 134.8, 134.7, 128.6, 128.5, 70.0 (CH₂), 68.8 (C), 67.3 (CH), 63.9 (C), 33.8

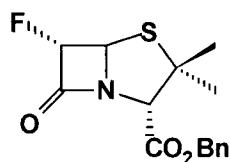
(CH₃), 25.7 (CH₃), 21.4 (C); $\nu_{\max}(\text{neat})/\text{cm}^{-1}$ 3064, 3033, 2970, 2083 (C=N=N), 1746 (broad, C=O), 1455, 1390.

*Benzyl 6 α -hydroxypenicillanate 89*¹⁵⁰



A solution of perchloric acid (1 M, 10 ml) in water (40 ml) was added with swirling to an ice cold solution of benzyl 6-diazopenicillanate (0.51 g, 1.6 mmol) in acetone (50 ml). The solution was kept at 5 °C for 12 h and was then extracted into CH₂Cl₂ (3 × 50 ml). The organic extracts were combined and washed with saturated aqueous sodium hydrogen carbonate (2 × 30 ml) and water (2 × 50 ml), dried (MgSO₄) and the solvent removed under reduced pressure. Purification over silica gel, eluting with CH₂Cl₂-EtOAc (90:10) afforded the title compound as a yellow solid (0.37 g, 75%); mp 161–162 °C (lit.,¹⁵⁰ 162–163 °C); $\delta_{\text{H}}(\text{CDCl}_3)$ 7.37 (5H, s, Ph), 5.28 (1H, d, *J* 1.2 Hz, CH), 5.18 (2H, s, CH₂), 4.82 (1H, d, *J* 1.3 Hz, CH), 4.50 (1H, s, CH), 1.52 (3H, s, CH₃), 1.37 (3H, s, CH₃); $\delta_{\text{C}}(\text{CDCl}_3)$ 172.1 (CO), 168.1 (CO), 135.3, 129.3, 129.2, 85.7 (COH), 71.7, 69.4, 68.1, 64.6 (C), 33.9 (CH₃), 26.2 (CH₃); $\nu_{\max}(\text{neat})/\text{cm}^{-1}$ 3420, 3019, 2980, 1775, 1745, 1457, 1381, 1215; *m/z* (CI⁺) 325 (NH₄M⁺, 1.7%), 308 (MH⁺, 6.9%).

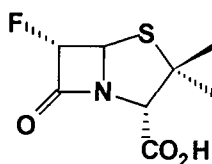
*Benzyl 6 α -fluoropenicillanate 90*¹⁵⁵



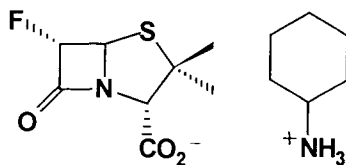
A solution of benzyl 6 α -hydroxypenicillanate (0.25 g, 0.81 mmol) in dry CH₂Cl₂ (5 ml) was added to a solution of DAST (0.22 ml, 1.62 mmol) in dry CH₂Cl₂ (5 ml) cooled to –78 °C under nitrogen. The reaction was allowed to warm to room temperature, was stirred overnight and was then quenched by the addition of water (10 ml). The organic

layer was separated and washed with water (3 × 20 ml), dried (MgSO₄) and the solvent removed under reduced pressure. Purification over silica gel afforded the title compound as a colourless oil (0.16 g, 65%); $\delta_{\text{H}}(\text{CDCl}_3)$ 7.37 (5H, s, Ph), 5.46 (1H, dd, *J* 5.2 and 1.6 Hz, CH), 5.33 (1H, dd, *J* 5.3 and 1.6 Hz, CHF), 5.19 (2H, s, CH₂), 4.54 (1H, s, CH), 1.53 (3H, s, CH₃), 1.39 (3H, s, CH₃); $\delta_{\text{C}}(\text{CDCl}_3)$ 166.7 (CO), 165.5 (d, *J* 20.6 Hz, CO), 134.5, 128.7, 128.7, 128.6, 98.2 (d, *J* 237 Hz, CHF), 68.9 (d, *J* 24.7 Hz, CH), 67.5 (CH), 64.2 (C), 33.9 (CH₃), 25.3 (CH₃); $\delta_{\text{F}}(\text{CDCl}_3)$ -181.6 (dd, *J* 53.0 and 5.2 Hz); $\nu_{\text{max}}(\text{neat})/\text{cm}^{-1}$ 3110, 3010, 2950, 1790, 1745; *m/z* (CI+) 327 (MNH₄⁺, 100%); (EI+) 309 (M⁺, 10%). C₁₅H₁₆FNO₃S (M⁺) requires 309.0835. Found: 309.0835.

6 α -Fluoropenicillanic acid **78**¹⁵⁵



A solution of aluminium trichloride (100 mg, 0.75 mmol) in anhydrous nitromethane (1 ml) was added to a solution of benzyl 6 α -fluoropenicillanate (52 mg, 0.17 mmol) in CH₂Cl₂ (4 ml) cooled to 0 °C and the reaction stirred for 1 h. The reaction solution was diluted with EtOAc (5 ml), washed with hydrochloric acid (0.5 M, 5 ml) and the aqueous phase extracted with EtOAc (3 × 10 ml). The combined organic extracts were dried (MgSO₄) and the solvent removed under reduced pressure to afford the title compound as a yellow oil (43 mg, 82%); $\delta_{\text{H}}(\text{CD}_3\text{OD})$ 8.20 (1H, br s, CO₂H), 5.46 (1H, dd, *J* 1.6 and 4.9 Hz, CH), 5.38 (1H, dd, *J* 5.3 and 1.6 Hz, CHF), 4.59 (1H, s, CH), 1.60 (3H, s, CH₃), 1.57 (3H, s, CH₃); $\delta_{\text{C}}(\text{CD}_3\text{OD})$ 170.4 (CO), 167.8 (d, *J* 21 Hz, CO), 99.2 (d, *J* 237 Hz, CHF), 70.6 (CH), 70.0 (d, *J* 24.4 Hz, CH), 65.0 (C), 33.5 (CH₃), 26.0 (CH₃); $\delta_{\text{F}}(\text{CD}_3\text{OD})$ -182.40 (dd, *J* 53.2 and 5.3 Hz).

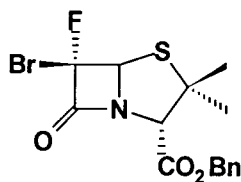


A solution of cyclohexylamine (53 mg, 0.55 mmol) in EtOAc (5 ml) was added to a stirred solution of 6 α -fluoropenicillanic acid (98 mg, 0.45 mmol) in EtOAc (5 ml). Upon addition a white precipitate formed which was removed by filtration, washed repeatedly with EtOAc and dried *in vacuo* to afford the title compound as a white amorphous solid (88 mg, 62%); mp 165–166 °C; $\delta_{\text{H}}(\text{D}_2\text{O})$ 5.38 (1H, dd, J 50.8 and 1.6 Hz, CHF), 5.37 (1H, dd, J 4.8 and 1.6 Hz), 4.19 (1H, s, CH), 4.00 (1H, m, CH), 1.83 (2H, m, CH₂), 1.65 (2H, m, CH₂), 1.50 (2H, m, CH₂), 1.37 (3H, s, CH₃), 1.35 (3H, s, CH₃); $\delta_{\text{C}}(\text{D}_2\text{O})$ 173.5 (CO), 168.3 (d, J 20.2 Hz, CO), 96.1 (d, J 233 Hz, CHF), 71.4 (CH), 67.9 (d, J 24.4 Hz, CH), 63.5 (C), 50.1 (C), 31.9 (CH₂), 30.1 (CH₃), 25.0 (CH₂), 24.1 (CH₂), 23.6 (CH₃); $\delta_{\text{F}}(\text{D}_2\text{O})$ -184.16 (dd, J 52.7 and 4.5 Hz); $\nu_{\text{max}}(\text{neat})/\text{cm}^{-1}$ 3420, 2933, 2860, 1790, 1610, 1450. C₁₄H₂₃FN₂O₃S requires C, 52.81; H, 7.28; N, 8.80. Found: C, 52.79; H, 7.54; N, 8.55%.

*Tetrabutylammonium bifluoride (TBABF)*¹⁶¹

A 0.7 M solution of ammonium bifluoride was slowly passed through Amberlite IRA-140 ion exchange resin (40 g). The process was continued until the eluent gave a negative test for chloride ions with silver nitrate. The resin was sequentially washed with distilled water (150 ml) and acetonitrile (150 ml) and was then dried under vacuum (18 mmHg). A solution of tetrabutylammonium chloride (1 g) in acetonitrile (20 ml) was then passed through the resin and the operation repeated three times. The resin was then washed with acetonitrile (20 ml), all the organic extracts were combined and the solvent was removed under reduced pressure to give the title compound as a viscous oil which solidified on cooling; $\delta_{\text{H}}(\text{CDCl}_3)$ 3.28 (8H, m, CH₂), 1.60 (8H, m, CH₂), 1.38 (8H, m, CH₂), 0.93 (12H, t, J 7.2 Hz, CH₃); δ_{F} -156.5 (br s).

*Benzyl 6β-bromo-6α-fluoropenicillanate 92*¹⁵⁵



A solution of *N*-bromosuccinimide (0.17 g, 0.94 mmol) in CH_2Cl_2 – CH_3CN (5 ml, 4:1) and a solution of TBABF (0.34 g, 1.18 mmol) in CH_2Cl_2 (5 ml) were added dropwise simultaneously to a solution of benzyl 6-diazopenicillanate (0.25 g, 0.78 mmol) in anhydrous CH_2Cl_2 (5 ml) cooled to -40°C . The reaction was allowed to warm to room temperature and stirring was continued for 2 h, after which time the reaction was quenched by the addition of water (10 ml). The organic layer was separated, washed with water (3×10 ml), dried (MgSO_4) and the solvent removed under reduced pressure to give a dark oil. The crude residue was purified over silica gel eluting with CH_2Cl_2 –light petroleum (60:40) to afford the product as a yellow oil (0.13 g, 43%). The product was identified as a mixture of the title compound and the corresponding benzyl 6,6-dibromopenicillanate.

Benzyl 6β-bromo-6α-fluoropenicillanate: $\delta_{\text{H}}(\text{CDCl}_3)$ 7.38 (5H, s, Ph), 5.62 (1H, d, J 5.6 Hz, CH), 5.20 (2H, s, CH_2), 4.55 (1H, s, CH), 1.56 (3H, s, CH_3), 1.39 (3H, s, CH_3); $\delta_{\text{C}}(\text{CDCl}_3)$ 166.3 (CO), 162.3 (d, J 22.4 Hz, CO), 134.4, 128.6, 128.5, 107.9 (d, J 305 Hz, CBrF), 77.1 (d, J 26.8 Hz, CH), 69.0 (CH), 67.5 (CH_2), 64.1 (C), 33.3 (CH_3), 25.5 (CH_3); $\nu_{\text{max}}(\text{neat})/\text{cm}^{-1}$ 3030, 2966, 2930, 1790, 1745, 1460; m/z (GC–MS) (EI+) 387 (M^+ , 3.3%), 389 (M^++2 , 3.3%), 296 (M^+-91 , 0.5%), 298 (M^++2-91 , 0.5%).

Benzyl 6,6-dibromopenicillanate: $\delta_{\text{H}}(\text{CDCl}_3)$ 7.33 (5H, s, Ph), 5.76 (1H, s, CH), 5.16 (2H, s, CH_2), 4.53 (1H, s, CH), 1.60 (3H, s, CH_3), 1.36 (3H, s, CH_3); m/z (GC–MS) 447 (M^+ , 1.3%), 449 (M^++2 , 2.8%), 451 (M^++4 , 0.9%).

*Trineophyllin chloride 94*¹⁶³



A solution of stannic chloride (16.3 g, 62.4 mmol) in diethyl ether (100 ml) was added to a filtered Grignard solution prepared from neophyl chloride (43 g, 0.26 mol) and

magnesium turnings (23.5 g, 0.98 g atom) in dry diethyl ether (300 ml). The reaction was heated under reflux for 1 h and left standing overnight. Benzene (200 ml) was added to the slurry and the excess Grignard was decomposed by the addition of methanol. The material was filtered and the residue was washed twice with benzene. The solvent was then removed under reduced pressure to give a white solid which was purified by recrystallisation from hexane–benzene (7:3) to afford the title compound as a white crystalline solid (19.6 g, 41%); mp 117.5–118.2 °C (lit.,¹⁶³ 117.5–118.5 °C). C₃₀H₃₉SnCl requires C, 65.07; H, 7.10. Found: C, 65.07; H, 6.82%.

*Trineophyltin hydroxide 95*¹⁶³



Trineophyltin chloride (6.5 g, 11.8 mmol) was added to a solution of NaOH (3.5 g, 87.5 mmol) in ethanol–water (250 ml. of 95% ethanol) and the reaction was heated under reflux for 15 h. The volatiles were removed under reduced pressure and the residue was washed with water until neutral. The dry solid was recrystallised from hot heptane to afford the title compound as a white crystalline solid (4.1 g, 67%); mp 145.5–146.6 °C (lit.,¹⁶³ 145–146 °C). C₃₀H₄₀SnO requires C, 67.31; H, 7.53. Found: C, 67.54; H, 7.41%.

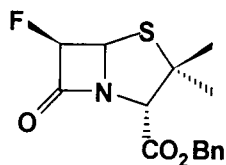
*Trineophyltin hydride 96*¹⁶⁴



A solution of borane in THF (1.0 M, 7.6 ml, 7.6 mmol) was added to a solution of trineophyltin hydroxide (4.1 g, 7.6 mmol) in THF (30 ml) and the reaction heated under reflux for 1 h. The solvent was removed under reduced pressure, then diethyl ether (30 ml) and water (10 ml) were added and the mixture stirred for 10 min. The aqueous layer was removed and the process repeated three times to remove inorganic boron compounds. The diethyl ether layer was then dried (MgSO₄) and the solvent removed to give a white solid. Recrystallisation from diethyl ether afforded the title compound as a white crystalline solid (3.7 g, 93%); mp 49.5–50.5 °C (lit.,¹⁶⁴ 50–51 °C); $\delta_{\text{H}}(\text{CDCl}_3)$ 7.22 (15H, m, Ph), 4.54 (1H, m, H), 1.31 (18H, s, CH₃), 1.04 (6H, d, *J* 49 Hz, CH₂);

$\delta_{\text{C}}(\text{CDCl}_3)$ 151.0 (d, J 34.2 Hz), 128.0, 125.4, 125.3, 37.5 (d, J 20.3 Hz), 32.1 (d, J 34.2 Hz), 30.4 (d, J 34.3 Hz). $\text{C}_{30}\text{H}_{40}\text{Sn}$ requires C, 69.37; H, 7.76. Found: C, 69.55; H, 7.81%.

*Benzyl 6 β -fluoropenicillanate 93*¹⁵⁵



A solution of trineophyllin hydride (0.48 g, 0.92 mmol) in diethyl ether (5 ml) was added to a solution of benzyl 6 β -bromo-6 α -fluoropenicillanate (178 mg, 0.45 mmol) and AIBN (10 mg) in diethyl ether (5 ml) and the reaction stirred at room temperature for 3 h. The solvent was removed under reduced pressure and the crude product purified over silica gel eluting with CH_2Cl_2 –light petroleum (75:25). The active fractions were combined and the solvent was removed under reduced pressure to afford the title compound as a clear oil (83 mg, 60%); $\delta_{\text{H}}(\text{CDCl}_3)$ 7.26 (5H, s, Ph), 5.74 (1H, dd, J 5.4 and 3.4 Hz, CHF), 5.50 (1H, dd, J 3.6 and 3.5 Hz, CH), 5.20 (2H, s, CH_2), 4.54 (1H, s, CH), 1.64 (3H, s, CH_3), 1.43 (3H, s, CH_3); $\delta_{\text{C}}(\text{CDCl}_3)$ 169.2 (d, J 21 Hz, CO), 167.1 (CO), 134.5, 128.8, 128.7, 91.9 (d, J 225 Hz, CHF), 70.8 (CH), 67.5 (CH_2), 66.5 (d, J 21.5 Hz, CH), 64.1 (C), 31.6 (CH_3), 26.3 (CH_3); $\delta_{\text{F}}(\text{CDCl}_3)$ -196.2 (dd, J 54.8 and 3.6 Hz); $\nu_{\text{max}}(\text{neat})/\text{cm}^{-1}$ 3110, 3030, 2965, 1790, 1745; m/z (GC–MS) (EI+) 309 (M^+ , 10%). $\text{C}_{15}\text{H}_{16}\text{FNO}_3\text{S}$ (M^+) requires 309.0835. Found: 309.0835.

6.4 Experimental to Chapter Four

Preparation of Diazomethane

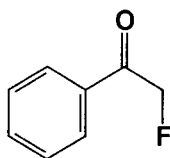
A solution of *N*-methyl-*N*-nitrosotoluene-*p*-sulfonamide (18.77 g, 87.6 mmol) in diethyl ether (200 ml) was added dropwise to a solution of 2-(2-ethoxyethoxy)ethanol (20 ml) containing KOH (5.38 g, 96 mmol), H_2O (10 ml) and diethyl ether (10 ml) at 70°C. The vapours from the reaction were collected by bubbling through two diethyl ether traps

maintained at 0 °C. When the reaction mixture had become colourless, the solutions in the traps were combined and used immediately.

General procedure for the synthesis of α -fluoroacetophenones

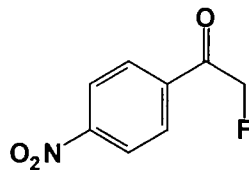
A solution of pyridinium poly(hydrogen fluoride) was added to an ethereal solution at -15 °C containing the desired diazoacetophenone, prepared *in situ* from benzoyl chloride and diazomethane. The reaction was allowed to warm to room temperature and was stirred for 4 h under an atmosphere of N₂. The product was extracted into hexane (3 × 100 ml) and hydrogen fluoride removed by treatment of the extract with anhydrous KF until neutral. The combined extracts were dried (MgSO₄), and the solvent removed under reduced pressure. Purification over silica gel, eluting with CH₂Cl₂-light petroleum (40:60), afforded the α -fluoroacetophenones.

*α -Fluoroacetophenone 127*⁷⁶



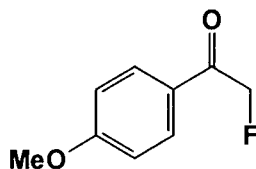
The product was recovered as a clear oil (2.20 g, 45%); $\delta_{\text{H}}(\text{CDCl}_3)$ 7.45–7.95 (5H, m, Ph), 5.53 (2H, d, J 46.8 Hz, CH₂F); $\delta_{\text{C}}(\text{CDCl}_3)$ 193.3 (d, J 15.3 Hz, CO), 134.0, 133.5, 128.8, 127.7, 83.4 (d, J 182 Hz, CH₂F); $\delta_{\text{F}}(\text{CDCl}_3)$ -231.8 (t, J 46 Hz), $\nu_{\text{max}}(\text{neat})/\text{cm}^{-1}$ 3063, 2935, 1706, 1597; m/z (GC-MS) (EI⁺) 138 (M⁺, 6.8%), 105 (M⁺-CH₂F, 100%).

α-Fluoro-*p*-nitroacetophenone 129



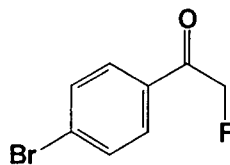
The product was recovered as an orange solid, (3.63 g, 63%); mp 90–92 °C; $\delta_{\text{H}}(\text{CDCl}_3)$ 8.35 (2H, d, J 8.8 Hz, Ph), 8.09 (2H, d, J 8.9 Hz, Ph), 5.54 (2H, d, J 46.7 Hz, CH_2F); $\delta_{\text{C}}(\text{CDCl}_3)$ 192.5 (d, J 8.5 Hz, CO), 138.1, 129.8, 129.2, 124.0, 83.7 (d, J 184.7 Hz, CH_2F); $\delta_{\text{F}}(\text{CDCl}_3)$ -229.9 (t, J 47.0 Hz); $\nu_{\text{max}}(\text{CHCl}_3)/\text{cm}^{-1}$ 3111, 2937, 2111, 1709, 1598, 1524, 1345; m/z (EI+) 183 (M^+ , 0.65%), 164 ($\text{M}^+ - \text{HF}$, 1.9%), 149 ($\text{M}^+ - \text{CH}_2\text{F}$, 100%). $\text{C}_8\text{H}_6\text{O}_3\text{NF}$ requires C, 52.47; H, 3.30; N, 7.65. Found: C, 52.12; H, 3.27; N, 7.43%.

α-Fluoro-*p*-methoxyacetophenone 130



The product was recovered as a white solid (2.45 g, 54%); mp 78–79 °C (lit.,²²² 78.5–79.4 °C); $\delta_{\text{H}}(\text{CDCl}_3)$ 7.85 (2H, d, J 8.9 Hz, Ph), 6.92 (2H, d, J 8.9 Hz, Ph), 5.44 (2H, d, J 47.0 Hz, CH_2F), 3.83 (3H, s, OMe); $\delta_{\text{C}}(\text{CDCl}_3)$ 192.6 (d, J 15.5 Hz, CO), 164.7, 130.7, 127.1, 114.6, 83.9 (d, J 183 Hz, CH_2F), 56.0 (OMe); $\delta_{\text{F}}(\text{CDCl}_3)$ -228.9 (t, J 46.8 Hz); $\nu_{\text{max}}(\text{CHCl}_3)/\text{cm}^{-1}$ 3110, 2935, 1695, 1598; m/z (CI+) 169 ($\text{M}^+ + 1$), 186 ($\text{M}^+ + 18$); (EI+) 168 (M^+), 135 ($\text{M}^+ - \text{CH}_2\text{F}$). $\text{C}_9\text{H}_9\text{O}_2\text{F}$ requires C, 64.28; H, 5.39. Found: C, 64.35; H, 5.52%.

p-Bromo- α -fluoroacetophenone **128**

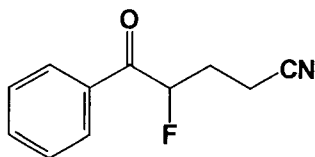


The product was recovered as a white solid (2.04 g, 47%); mp 71–72 °C (lit.,²²³ 70–72 °C); δ_{H} (CDCl₃) 7.76 (2H, d, *J* 8.6 Hz, Ph), 7.63 (2H, d, *J* 8.6 Hz, Ph), 5.47 (2H, d, *J* 46.9 Hz, CH₂F); δ_{C} (CDCl₃) 192.6 (d, *J* 15.9 Hz, CO), 132.3, 132.2, 129.3, 129.3, 83.5 (d, *J* 186 Hz, CH₂F); δ_{F} (CDCl₃) –230.49 (t, *J* 46.1 Hz); ν_{max} (CHCl₃)/cm^{–1} 3115, 2945, 1687, 1588; *m/z* (EI⁺) 216, 218 (M⁺), 183, 185 (M⁺–CH₂F). C₈H₆BrFO requires C, 44.27; H, 2.79. Found: C, 44.38; H, 2.80%.

General procedure for formation of Michael adducts

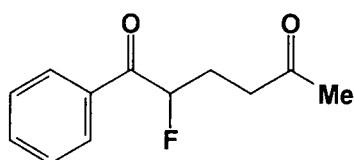
Pyrrolidine (1.5 mmol) was added to a solution of α -fluoroacetophenone (1 mmol) in benzene over 4 Å molecular sieves (5 g). The solution was heated under reflux and the progress of the reaction monitored by ¹⁹F NMR spectroscopy. Upon consumption of the ketone, the appropriate Michael acceptor (10 mmol) was added and the solution heated under reflux for 12h. Water (10 ml) was added and the solution heated for a further 1h. After cooling, the reaction was filtered through Celite and the product extracted into diethyl ether. The ethereal extracts were combined and washed successively with dilute HCl (25 ml), NaHCO₃ (25 ml) and water (25 ml), dried (MgSO₄) and the solvent removed under reduced pressure. Purification over silica gel eluting with CH₂Cl₂–light petroleum (40:60) afforded the desired α -fluoro ketones **138–145** as clear oils (45–63%).

4-Fluoro-5-oxo-5-phenylpentanenitrile 138



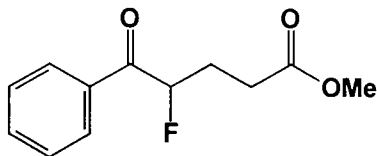
The product was recovered as a clear oil (103 mg, 55%); $\delta_{\text{H}}(\text{CDCl}_3)$ 2.30 (2H, m, CH_2), 2.62 (2H, m, CH_2), 5.74 (1H, ddd, J 48.4, 8.9, 3.6 Hz, CHF), 7.49-7.98 (5H, m, Ph); $\delta_{\text{C}}(\text{CDCl}_3)$ 13.0 (d, J 5.0 Hz, CH_2), 28.0 (d, J 21.8 Hz, CH_2), 90.7 (d, J 185 Hz, CHF), 118.4 (CN), 128.9, 129.0, 133.7, 134.4, 194.6 (d, J 20.1 Hz, CO); $\delta_{\text{F}}(\text{CDCl}_3)$ -190.95 (ddd, J 48.5 and 29.0 Hz); $\nu_{\text{max}}(\text{neat})/\text{cm}^{-1}$ 3110, 2985, 2248, 1698, 1597; m/z (CI+) 191 (M^+ , 9.5%), 209 ($\text{M}^+ + 18$, 100%). $\text{C}_{11}\text{H}_{11}\text{NOF}$ (MH^+) requires 192.0825. Found: 192.0827.

5-Fluoro-6-oxo-6-phenylhexan-2-one 139



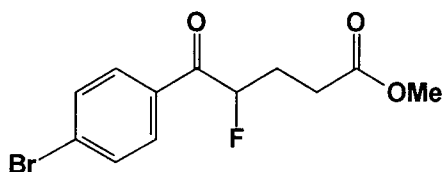
The product was recovered as a clear oil (127 mg, 52%); $\delta_{\text{H}}(\text{CDCl}_3)$ 2.13 (3H, s, Me), 2.20 (2H, m, CH_2), 2.67 (2H, m, CH_2), 5.68 (1H, ddd, J 49.6, 9.0 and 3.6 Hz, CHF), 7.42-7.99 (5H, m, Ph); $\delta_{\text{C}}(\text{CDCl}_3)$ 26.4 (d, J 21.3 Hz, CH_2), 29.9 (Me), 37.6 (d, J 3.4 Hz, CH_2), 91.7 (d, J 181.6 Hz, CHF), 128.6, 128.7, 128.7, 133.9, 195.9 (d, J 18.3 Hz, CO); $\delta_{\text{F}}(\text{CDCl}_3)$ -193.46 (ddd, J 50.0 and 19.2 Hz); $\nu_{\text{max}}(\text{neat})/\text{cm}^{-1}$ 2923, 1710, 1702, 1597; m/z (CI+) 209 ($\text{M}^+ + 1$, 100%), 226 ($\text{M}^+ + 18$, 82.8%). $\text{C}_{12}\text{H}_{14}\text{O}_2\text{F}$ (MH^+) requires 209.0978. Found: 209.0975.

Methyl 4-fluoro-5-oxo-5-phenylpentanoate **140**



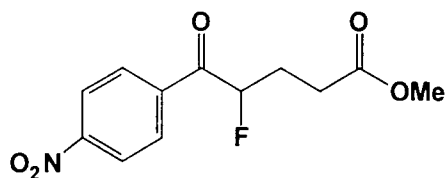
The product was recovered as a clear oil (137 mg, 60%); $\delta_{\text{H}}(\text{CDCl}_3)$ 2.25 (2H, m, CH_2), 2.58 (2H, m, CH_2), 3.69 (3H, s, OMe), 5.75 (1H, ddd, J 49.2, 9.2 and 3.2 Hz, CHF), 7.45–8.01 (5H, m, Ph); $\delta_{\text{C}}(\text{CDCl}_3)$ 27.6 (d, J 21.4 Hz, CH_2), 28.6 (d, J 3.4 Hz, CH_2), 51.8 (OMe), 91.8 (d, J 182.8 Hz, CHF), 128.8, 128.8, 128.8, 133.9, 173.0 (CO_2Me), 195.7 (d, J 18.7 Hz, CO); $\delta_{\text{F}}(\text{CDCl}_3)$ -193.02 (ddd, J 50.8 and 19.2 Hz); $\nu_{\text{max}}(\text{neat})/\text{cm}^{-1}$ 2953, 1737, 1700, 1597; m/z (CI⁺) 225 ($\text{M}^+ + 1$, 100%), 242 ($\text{M}^+ + 18$, 72.4%). $\text{C}_{12}\text{H}_{14}\text{O}_3\text{F}$ (MH^+) requires 225.092697. Found: 225.092700.

Methyl 5-(4-bromophenyl)-4-fluoro-5-oxopentanoate **141**



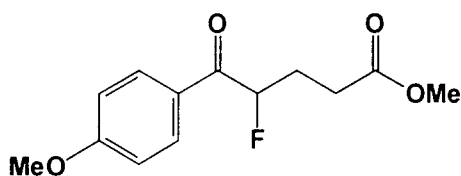
The product was recovered as a clear oil (79 mg, 57%); $\delta_{\text{H}}(\text{CDCl}_3)$ 2.18 (2H, m, CH_2), 2.54 (2H, m, CH_2), 3.72 (3H, s, OMe), 5.70 (1H, ddd, J 49.2, 8.9 and 3.7 Hz, CHF), 7.65 (2H, d, J 8.6 Hz, Ph), 7.90 (2H, d, J 8.6 Hz, Ph); $\delta_{\text{C}}(\text{CDCl}_3)$ 195.0 (d, J 19.1 Hz, CO), 173.0 (CO_2Me), 132.6, 132.2, 130.4, 129.3, 92.0 (d, J 183.2 Hz, CHF), 51.9 (OMe), 28.5 (d, J 3.4 Hz, CH_2), 27.6 (d, J 21.3 Hz, CH_2); $\delta_{\text{F}}(\text{CDCl}_3)$ -192.3 (ddd, J 50.0 and 32.3 Hz); $\nu_{\text{max}}(\text{neat})/\text{cm}^{-1}$ 2950, 1735, 1700, 1585, 1437, 1399, 1219, 1175; m/z (CI⁺) 303, 305 ($\text{M}^+ + 1$, 63%), 320, 322 ($\text{M}^+ + 18$, 100%). $\text{C}_{12}\text{H}_{16}\text{O}_3\text{BrFN}$ ($\text{M} + \text{NH}_4^+$) requires 320.0298. Found: 320.0298.

Methyl 4-fluoro-5-(4-nitrophenyl)-5-oxopentanoate **142**



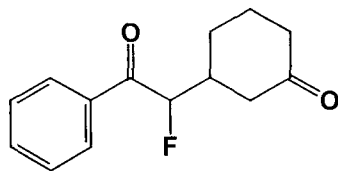
The product was recovered as a clear oil (85 mg, 45%); $\delta_{\text{H}}(\text{CDCl}_3)$ 2.21 (2H, m, CH_2), 2.57 (2H, m, CH_2), 3.66 (3H, s, OMe), 5.67 (1H, ddd, J 49.0, 8.9 and 3.6 Hz, CHF), 8.21 (2H, d, J 8.8 Hz, Ph), 8.35 (2H, d, J 8.8 Hz, Ph); $\delta_{\text{C}}(\text{CDCl}_3)$ 194.8 (d, J 10 Hz, CO), 172.9 (CO_2Me), 150.6, 138.4, 130.1, 123.9, 92.4 (d, J 183.6 Hz, CHF), 51.9 (OMe), 28.4 (d, J 3.4 Hz, CH_2), 27.3 (d, J 21.4 Hz, CH_2); $\delta_{\text{F}}(\text{CDCl}_3)$ -192.0 (ddd, J 50.0 and 32.7 Hz); $\nu_{\text{max}}(\text{neat})/\text{cm}^{-1}$ 2952, 1733, 1706, 1603, 1525, 1438, 1347, 1218, 1173; m/z (GC-MS) (EI+) 269 (M^+ , 6%), 238 (M^+-31 , 15%); (CI+) 287 (M^++18 , 82%). $\text{C}_{12}\text{H}_{12}\text{O}_5\text{FN}$ (M^+) requires 269.0699. Found: 269.0700.

Methyl 4-fluoro-5-(4-methoxyphenyl)-5-oxopentanoate **143**



The product was recovered as a clear oil (75 mg, 51%); $\delta_{\text{H}}(\text{CDCl}_3)$ 2.19 (2H, m, CH_2), 2.53 (2H, m, CH_2), 3.65 (3H, s, OMe), 3.81 (3H, s, OMe), 5.64 (1H, ddd, J 49.5, 9.6 and 3.6 Hz, CHF), 6.90 (2H, d, J 9.2 Hz, Ph), 7.96 (2H, d, J 9.2 Hz, Ph); $\delta_{\text{C}}(\text{CDCl}_3)$ 194.1 (d, J 18.3 Hz, CO), 173.2 (CO_2Me), 164.1, 131.3, 126.8, 114.0, 91.8 (d, J 182.0 Hz, CHF), 55.5 (OMe), 51.8 (OMe), 28.7 (d, J 3.8 Hz, CH_2), 27.8 (d, J 21.4 Hz, CH_2); $\delta_{\text{F}}(\text{CDCl}_3)$ -192.4 (ddd, J 50.0 and 32.3 Hz); $\nu_{\text{max}}(\text{neat})/\text{cm}^{-1}$ 2955, 1735, 1700, 1685, 1601, 1261, 1174; m/z (EI+) 254 (M^+ , 2%); (CI+) 255 (M^++1 , 12%). $\text{C}_{13}\text{H}_{16}\text{O}_4\text{F}$ (MH^+) requires 255.1033. Found: 255.1033.

3-(1-Fluoro-2-oxo-2-phenylethyl)cyclohexanone **144**



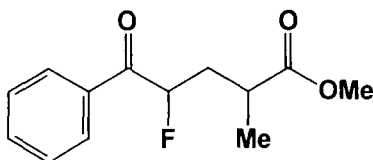
The product was recovered as a clear oil (125 mg, 48%) and as an inseparable mixture of diastereoisomers (62:38).

Major diastereoisomer: $\delta_{\text{H}}(\text{CDCl}_3)$ 5.53 (1H, dd, J 48.8 and 3.6 Hz, CHF); $\delta_{\text{C}}(\text{CDCl}_3)$ 209.6 (CO), 195.4 (d, J 19.8 Hz, COCHF), 95.6 (d, J 188.4 Hz, CHF); $\delta_{\text{F}}(\text{CDCl}_3)$ -199.27 (dd, J 48.5 and 24.1 Hz).

Minor diastereoisomer: $\delta_{\text{H}}(\text{CDCl}_3)$ 5.42 (1H, dd, J 48.6 and 3.2 Hz, CHF); $\delta_{\text{C}}(\text{CDCl}_3)$ 209.7 (CO), 195.5 (d, J 19.5 Hz, COCHF), 95.6 (d, J 188.4 Hz, CHF); $\delta_{\text{F}}(\text{CDCl}_3)$ -199.6 (dd, J 48.5 and 24.8 Hz).

$\nu_{\text{max}}(\text{neat})/\text{cm}^{-1}$ 3115, 2942, 1709, 1597; m/z (CI⁺) 235 (M^+ +1, 19.3%), 252 (M^+ +18, 100%). $\text{C}_{14}\text{H}_{16}\text{O}_2\text{F}$ ($M\text{H}^+$) requires 235.1134. Found: 235.1137.

Methyl 4-fluoro-2-methyl-5-oxo-5-phenylpentanoate **145**



The product was recovered as a clear oil (95 mg, 40%) and as an inseparable mixture of diastereoisomers (52:48).

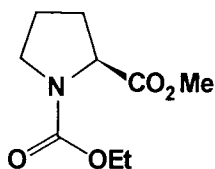
Major diastereoisomer: $\delta_{\text{H}}(\text{CDCl}_3)$ 1.25 (3H, d, J 7.2 Hz, Me), 3.67 (3H, s, OMe), 5.65 (1H, ddd, J 46.6, 9.0 and 3.4 Hz, CHF); $\delta_{\text{C}}(\text{CDCl}_3)$ 195.6 (d, J 17.9 Hz, COCHF), 175.9 (CO₂Me), 91.6 (d, J 183.9 Hz, CHF); $\delta_{\text{F}}(\text{CDCl}_3)$ -189.2 (ddd, J 50.0, 33.9 and 16.6 Hz).

Minor diastereoisomer: $\delta_{\text{H}}(\text{CDCl}_3)$ 1.30 (3H, dd, J 7.2 and 0.8 Hz, Me), 3.75 (3H, s, OMe), 5.77 (1H, ddd, J 49.8, 10.8 and 2.4 Hz, CHF); $\delta_{\text{C}}(\text{CDCl}_3)$ 196.0 (d, J 19.4

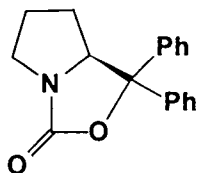
Hz, COCHF), 176.2 (CO₂Me), 91.3 (d, *J* 181.2 Hz, CHF); δ_F(CDCl₃) -193.4 (ddd, *J* 50.0, 38.0 and 15.1 Hz).

ν_{max}(neat)/cm⁻¹ 3110, 2985, 1732, 1701, 1597; *m/z* (CI+) 239 (M⁺+1, 100%), 256 (M⁺+18, 78%). C₁₃H₁₅O₃F (MH⁺) requires 239.1083. Found: 239.1084.

Methyl (2S)-N-ethoxycarbonylpyrrolidine-2-carboxylate **149**²⁰³

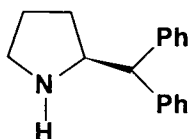


A solution of (*S*)-(-)-proline (25.0 g, 217.0 mmol) in dry methanol (150 ml) was added to anhydrous K₂CO₃ (28.6 g, 217 mmol) followed by the addition of ethyl chloroformate (49.0 g, 434 mmol) over 5 min at 25 °C. The reaction mixture was stirred for 12 h at 0 °C and then the excess MeOH was removed under reduced pressure and water (100 ml) was added. The reaction was extracted into chloroform (3 × 50 ml) and the combined organic extracts were washed with brine (2 × 30 ml) and then dried over MgSO₄. Removal of the solvent under reduced pressure gave the title compound (as a 1:1 mixture of two conformers by NMR analysis) (39.5 g, 91%) as a colourless oil; δ_H(CDCl₃) 4.12 (2H, m, CH₂), 3.92 (2H, m, CH₂), 3.49 (3H, s, OMe), 3.33 (1H, m, CH), 1.9 (4H, m, CH₂), 1.03 (3H, m, CH₃); δ_C(CDCl₃) (two conformers 1:1) 172.7, 172.6, 154.5, 154.0, 60.7, 58.5, 58.2, 51.5, 46.1, 45.7, 30.3, 29.3, 23.7, 22.9, 14.1, 14.0; ν_{max}(neat)/cm⁻¹ 2980, 2881, 1748, 1704, 1414, 1381, 1348, 1277; *m/z* (CI+) 202 (M+H, 100%), 142 (12%); (EI+) 201 (M⁺, 1.3%).



A solution of phenylmagnesium bromide in THF (1.0 M, 386 ml, 386 mmol) was added to a solution of methyl (2*S*)-*N*-ethoxycarbonylpyrrolidine-2-carboxylate (39.0g, 193 mmol) in THF (100 ml) under an inert atmosphere of N₂ at 0 °C. The solution was warmed to room temperature and heated under reflux for 3 h. The reaction was then added to an ice cold solution of NH₄Cl, and the aqueous layer extracted into ethyl acetate (4 × 100 ml). The combined organic extracts were dried over MgSO₄ and the solvent removed to afford the title compound (44.0g, 82%) as a white solid, which was recrystallised from diethyl ether; mp 148–149 °C (lit.,²²⁴ 147–148 °C); δ_H(CDCl₃) 7.53–7.21 (10H, m, Ph), 4.53 (1H, m, CH), 3.64, 3.31 (2H, AB, CH₂N), 1.83 (4H, m, CH₂), 1.15 (1H, m, CH); δ_C(CDCl₃) 160.3, 143.1, 140.1, 128.4, 126.6, 125.0, 85.7, 69.0, 45.9, 28.8, 24.7; ν_{max}(KBr)/cm⁻¹ 2969, 2863, 1976, 1757, 1583, 1492, 1447, 1374, 1255; *m/z* (EI) 279.1 (M⁺, 27%), 105.0 (100%). C₁₈H₁₇NO₂ requires C, 77.38; H, 6.14; N, 5.02. Found: C, 77.55; H, 6.15; N, 5.10%.

(2*S*)-2-(Diphenylmethyl)pyrrolidine 151

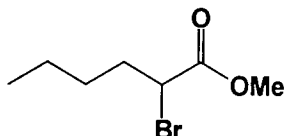


A mixture of 1,1-Diphenyl-5,6,7,7a-tetrahydro-1H,3H-pyrrolo[1,2-c][1,3]oxazol-3-one (5.0 g, 17.9 mmol) and Pd/C (1.0 g) (10%) in methanol (100 ml) was hydrogenated at ambient temperature for 48 h. The catalyst was filtered off and the methanol removed under reduced pressure. Purification, firstly over silica gel eluting with ethyl acetate and then methanol, followed by distillation, gave the title compound (2.8 g, 67%) as a colourless oil; [α]_D -7.84 (*c* 2.05, CHCl₃) [lit., -7.8 (*c* 2.11, CHCl₃)]; δ_H(CDCl₃) 7.28 (10H, m, Ph), 3.89 (2H, m, CH), 2.93; 2.85 (2H, AB, CH₂N), 1.69 (4H, m, CH₂), 1.37

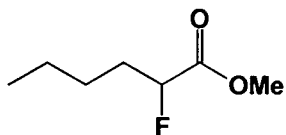
(1H, m, CH₂); $\delta_{\text{C}}(\text{CDCl}_3)$ 142.9, 142.8, 128.6, 128.4, 128.0, 126.4, 62.1, 57.2, 45.6, 30.5, 24.3; $\nu_{\text{max}}(\text{neat})/\text{cm}^{-1}$ 3405, 2962, 1596, 1494, 1450, 1399, 1348; m/z (CI) 238.4 (M^+ , 39%).

6.5 Experimental to Chapter Five

Methyl 2-bromohexanoate 162

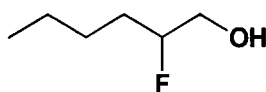


Bromine (17.06 g, 5.5 ml, 0.11 mmol) was added dropwise to a mixture of methyl hexanoate (3.5 g, 27.0 mmol) and red phosphorus (1.25 g, 40.5 mmol) at 80 °C. The reaction was kept at 80 °C for 16 h and was then cooled to 0 °C. Methanol (50 ml) was added dropwise over 1 h, the reaction was allowed to warm to room temperature and was then heated to 80 °C until the evolution of HBr ceased. The mixture was poured into light petroleum (200 ml), and NaHSO₃ (2 g) in water (150 ml) was added. The aqueous layer was separated and washed with water until neutral (4 × 100 ml). The organic extracts were dried (MgSO₄) and the solvent removed under reduced pressure, giving a yellow oil. Purification by distillation (53 °C, 0.1 mmHg) afforded the title compound as a colourless oil (4.8 g, 86%); $\delta_{\text{H}}(\text{CDCl}_3)$ 4.22 (1H, t, J 7.4 Hz, CHBr), 3.78 (3H, s, OMe), 2.04 (2H, m, CH₂), 1.36 (4H, m, CH₂), 0.91 (3H, t, J 7.0 Hz, CH₃); $\delta_{\text{C}}(\text{CDCl}_3)$ 170.4 (CO), 52.9 (OMe), 45.7 (CHBr), 34.6 (CH₂), 29.4 (CH₂), 21.9 (CH₂), 13.8 (CH₃); $\nu_{\text{max}}(\text{neat})/\text{cm}^{-1}$ 2956, 2932, 2872, 1745, 1436, 1154; m/z (GC-MS) (EI+) 208 (M^+ , 0.25%) 210 ($\text{M}^+ + 2$, 0.25%), 152 ($\text{M}^+ - 56$, 100%), 154 ($\text{M}^+ + 2 - 56$, 100%).



Silver(I) fluoride (2.5 g, 19.7 mmol) was added to a solution of methyl 2-bromohexanoate (0.96 g, 4.6 mmol) in acetonitrile (20 ml) containing water (0.5 ml), and the slurry was stirred vigorously for 24 h at 80 °C. The reaction was allowed to cool and was then filtered through Celite to remove the remaining silver salts. The filtrate was washed with water and extracted into CH₂Cl₂ (3 × 50 ml). The organic extracts were combined, dried (MgSO₄) and the solvent removed under reduced pressure to give a yellow oil. Purification over silica gel, eluting with light petroleum–diethyl ether (90:10), afforded the title compound as a colourless oil (0.55 g, 80%); $\delta_{\text{H}}(\text{CDCl}_3)$ 4.90 (1H, dt, J 48 and 6.5 Hz, CHF), 3.78 (3H, s, OMe). 1.87 (2H, m, CH₂), 1.38 (4H, m, CH₂), 0.91 (3H, t, J 6.9 Hz, CH₃); $\delta_{\text{C}}(\text{CDCl}_3)$ 170.5 (d, J 23.7 Hz, CO), 89.0 (d, 183 Hz, CHF), 52.2 (OMe), 32.1 (d, J 20.8 Hz, CH₂), 26.4 (d, J 3 Hz, CH₂), 22.1 (CH₂), 13.7 (CH₃); δ_{F} –192.6 (dt, J 46.5 and 24.0 Hz); $\nu_{\text{max}}(\text{neat})/\text{cm}^{-1}$ 2960, 2932, 2870, 1757, 1197; m/z (GC–MS) (EI⁺) 149 (MH⁺, 1%), 92 (M⁺–56, 100%).

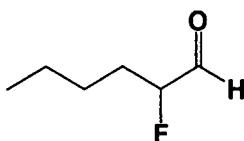
2-Fluorohexanol 164



A solution of methyl 2-fluorohexanoate (0.65 g, 4.4 mmol) in diethyl ether (10 ml) was added dropwise to a solution of LiAlH₄ (0.33 g, 8.7 mmol) in diethyl ether (25 ml). The reaction was stirred at room temperature until the starting material was consumed (TLC) and then it was cooled to 0 °C and water cautiously added. The alkaline solution was neutralised with hydrochloric acid and the aqueous phase extracted into diethyl ether (3 × 50 ml). The ethereal extracts were combined, dried (MgSO₄), and the solvent removed under reduced pressure. Purification over silica gel eluting, with light petroleum–diethyl ether (70:30), afforded the title compound as a clear oil (0.41 g,

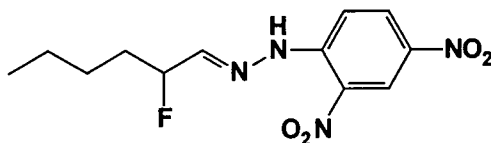
77%); $\delta_{\text{H}}(\text{CDCl}_3)$ 4.57 (1H, dm, J 48 Hz, CHF), 3.68 (2H, dd, J 21 and 6 Hz, CH_2OH), 2.20 (1H, br s, OH), 1.24–1.75 (6H, m, CH_2), 0.90 (3H, t, J 6 Hz, CH_3); δ_{C} 94.7 (d, J 167 Hz, CHF), 64.7 (d, J 21.7 Hz, CH_2OH), 30.6 (d, J 20.2 Hz, CH_2), 26.9 (d, J 4.7 Hz, CH_2), 22.4 (CH_2), 13.8 (CH_3); δ_{F} (CDCl_3) -190.0 (septet, J 46.6 and 22.2 Hz); $\nu_{\text{max}}(\text{neat})/\text{cm}^{-1}$ 3354, 2956, 2932, 2872, 2862, 1466, 1058; m/z (GC-MS) (EI+) 102 (M^+-18 , 0.3%), 88 (3.3%), 69 (28%).

2-Fluorohexanal 165



A solution of 2-fluorohexanol (0.35 g, 2.9 mmol) in CH_2Cl_2 (5 ml) was added to a suspension of pyridinium chlorochromate (1.24 g, 5.8 mmol) and dry powdered 3 Å molecular sieves (4 g) in CH_2Cl_2 (40 ml), and the reaction stirred under N_2 at room temperature for 2 h. The reaction mixture was filtered through a silica gel pad and was washed with CH_2Cl_2 (250 ml) to remove chromium salts. The solvent was removed under reduced pressure to give the title compound as a clear oil (0.22 g, 64%); $\delta_{\text{H}}(\text{CDCl}_3)$ 9.75 (1H, d, J 6.4 Hz, CHO), 4.95 (1H, dt, J 48.5 and 6.7 Hz, CHF), 1.10–1.75 (6H, m, CH_2), 0.90 (3H, t, J 6.8 Hz, CH_3); δ_{F} -200.0 (dt, J 48.5 and 24.7 Hz); $\nu_{\text{max}}(\text{neat})/\text{cm}^{-1}$ 2957, 2925, 2850, 1735, 1436, 1340.

2-Fluorohexanal 1-(2,4-dinitrophenyl)hydrazone 166



A solution of 2,4-dinitrophenylhydrazine in 2 M hydrochloric acid (10 ml) was added to 2-fluorohexanal (100 mg, 0.85 mmol) and the mixture shaken to coagulate and left to stand for 15 min. An orange precipitate formed, which was collected by filtration, washed with water and dried *in vacuo* to afford the title product as an orange solid (125

mg, 49%); mp 69.5–70.5 °C (lit.,²²⁵ 70–71 °C); $\delta_{\text{H}}(\text{CDCl}_3)$ 11.10 (1H, s, NH), 9.13 (1H, dd, J 21 Hz, CH), 8.31 (1H, m, Ph), 7.92 (1H, d, J 9 Hz, Ph), 7.53 (1H, m, Ph), 5.15 (1H, dm, J 48 Hz, CHF), 1.25–2.05 (6H, m, CH₂), 0.95 (3H, t, J 6.9 Hz, CH₃); $\delta_{\text{C}}(\text{CDCl}_3)$ 152.7, 147.4 (d, J 27 Hz, CH), 137.6, 129.8, 128.6, 123.4, 116.5, 91.3 (d, J 167 Hz, CHF), 33.0 (d, J 22.0 Hz, CH₂), 26.4 (d, J 4 Hz, CH₂), 22.4 (CH₂), 13.9 (CH₃); δ_{F} -182.9 (dm, J 47.6 and 20 Hz); $\nu_{\text{max}}(\text{CHCl}_3)/\text{cm}^{-1}$ 3290, 3019, 2960, 1793, 1617, 1594, 1467, 1381, 1216; m/z (EI+) 298 (M⁺, 0.81%), 279 (M⁺-19, 5%). C₁₂H₁₅FN₄O₄ (M⁺) requires 298.1077. Found: 298.1077.

6.6 General protocol for enzyme assays

Cyclohex-1-enylcarbonyl-CoA reductase

A solution of cyclohex-1-enylcarbonyl-CoA (10 μl , 10 mM stock) was added to a solution containing NADPH (10 μl , 10 mM stock), cyclohex-1-enylcarbonyl-CoA reductase (CHCR) (2 μ) and a phosphate buffer (978 μl , 50 mM potassium phosphate buffer at pH 7.3 containing 10% glycerol). The reaction was followed by monitoring the depletion of NADPH spectrophotomerically at 340 nm. Initial rates were determined from the obtained plots.

β -Lactamase 1

A solution of β -lactamase 1 from *Bacillus cereus* (100 μl , 10 units) was added to a solution of cyclohexylammonium 6 α -fluoropenicillanate (1 ml, 1 mM stock) in phosphate buffer (pH 7) in a cuvette. The hydrolysis reaction was monitored spectrophotomerically at 240 nm.

Methanolic hydrolysis of 90 and 93

A solution of methanolic sodium methoxide (125 μl , 0.5 mM) was added to a solution of benzyl 6 α -fluoropenicillanate (170.5 μl , 1.5 mM) in methanol (2.2045 ml) in a cuvette. The hydrolysis reaction was monitored spectrophotomerically at 310 nm and the rates calculated from the obtained plots.

Transketolase

A solution of hydroxypyruvic acid (110 mg, 1 mmol) and 2-fluorohexanal (50mg, 0.4 mmol) in glycylglycine buffer (20 ml, 100 mmol dm⁻³, pH 7.6) was added to a solution of magnesium chloride (1 mg, 6 mmol), thiamine pyrophosphate (11.25 mg, 0.025mmol) and transketolase (50 U) in glycylglycine buffer (0.5 ml, 100 mmol dm⁻³, pH 7.6). The pH of the solution was then adjusted to 7.6 with NaOH (0.1 mol dm⁻³). The reaction was allowed to proceed at 29 °C on an orbital shaker and was monitored by ¹⁹F NMR spectroscopy.

Glycerol-3-phosphate dehydrogenase

A solution of glycerol-3-phosphate (290 µl, 100 U) was added to a solution containing monofluorophosphonate **172** (11.4 mg, 29.5 µmol), β-fluoropyruvic acid (5.7 mg, 44.3 µmol), NAD⁺ (18.5 mg, 25 µmol) and lactate dehydrogenase (400 µl, 2000 U) in phosphate buffer (pH 7, 500 µl). The reaction was allowed to proceed at 30 °C and the reaction was monitored by ¹⁹F NMR spectroscopy.

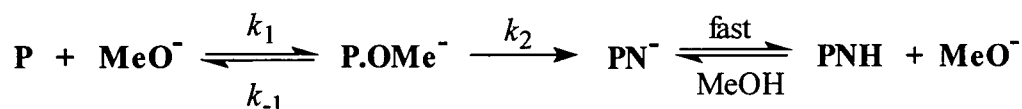
Chapter Seven

Appendices

Appendices

7.1 Appendix 1

7.1.1 Derivation of equation (3.1)



If we assume that the C-N bond breaking is rate limiting then,

$$\frac{d[\text{PNH}]}{dt} = k_2 [\text{P.OMe}^-] \quad (\text{A1})$$

$$[\text{P}] + [\text{P.OMe}^-] + [\text{PNH}] = \text{constant}$$

$$\frac{d[\text{P}]}{dt} + \frac{d[\text{P.OMe}^-]}{dt} + \frac{d[\text{PNH}]}{dt} = 0 \quad (\text{A2})$$

$$K_1 = \frac{[\text{P.OMe}^-]}{[\text{P}][\text{MeO}^-]} \Rightarrow [\text{P}] = \frac{[\text{P.OMe}^-]}{K_1[\text{MeO}^-]}$$

$$\therefore \frac{d[\text{P}]}{dt} = \frac{1}{K_1[\text{MeO}^-]} \cdot \frac{d[\text{P.OMe}^-]}{dt} \quad (\text{A3})$$

Substituting eqns. (A1) and (A3) into eqn. (A2) gives

$$\frac{1}{K_1[\text{MeO}^-]} \cdot \frac{d[\text{P.OMe}^-]}{dt} + \frac{d[\text{P.OMe}^-]}{dt} + k_2 [\text{P.OMe}^-] = 0$$

$$\frac{d[\text{P.OMe}^-]}{dt} \cdot \left(1 + \frac{1}{K_1[\text{MeO}^-]} \right) + k_2 [\text{P.OMe}^-] = 0$$

$$\frac{-d[\text{P.OMe}^-]}{dt} = k_{\text{obs}}[\text{P.OMe}^-]$$

$$k_{\text{obs}} \left(1 + \frac{1}{K_1[\text{MeO}^-]} \right) - k_2 = 0$$

$$k_{\text{obs}} = \frac{k_2 K_1 [\text{MeO}^-]}{1 + K_1 [\text{MeO}^-]} \quad (3.1)$$

7.1.2 Stopped-flow spectrometry

For measurement of rate constants too fast to measure by conventional methods, a High-Tech SF-3 series stopped-flow spectrometer was used. This is shown schematically in Fig. 7.1.

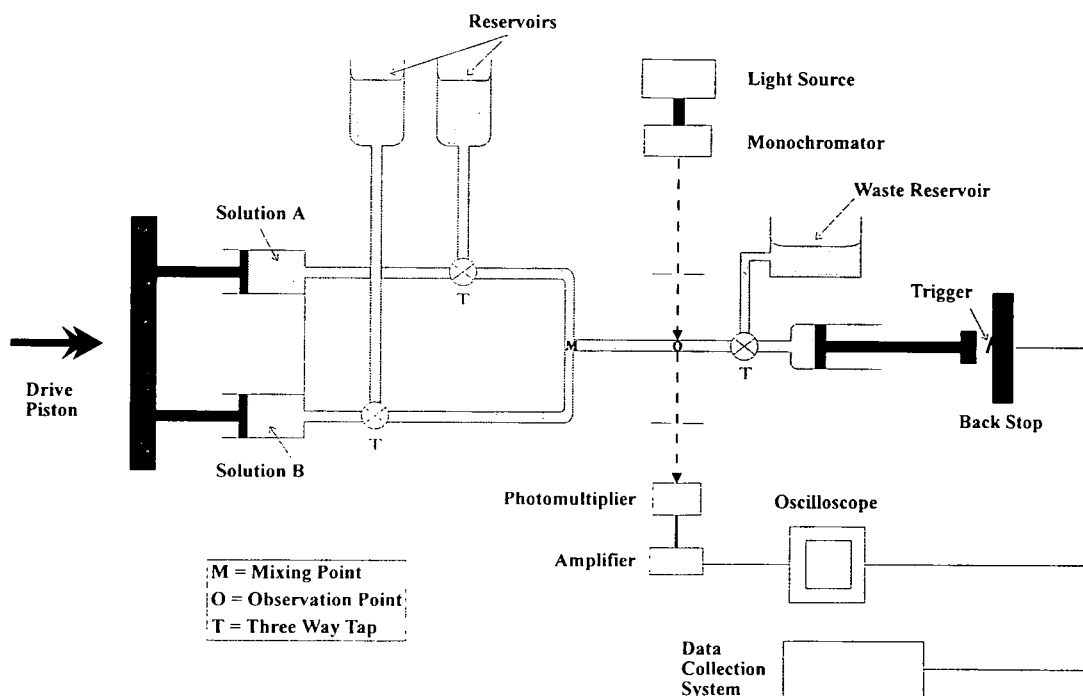


Fig. 7.1

The two solutions to be reacted, A and B, are stored in reservoirs and are drawn into two identical syringes so that equal volumes are mixed. The syringes are compressed simultaneously, and mixing occurs at point M extremely rapidly. The dead time of this machine is estimated to be 2 ms so reactions with half-lives smaller than

this cannot be measured by stopped-flow techniques. The mixture flows into a thermostatted 2 mm path length quartz cell at point O. The plunger of the third syringe will hit a stop and the flow of solution will be stopped. Hitting the stop also triggers the acquisition of data from the reaction. The reaction is observed by passing a beam of monochromatic light of an appropriate wavelength through the cell by fibre-optic cable. The light is passed through a photomultiplier and the change in voltage measured due to a change in absorbance of the solution is observed. The software used to run the stopped-flow machines also transforms voltage/time data into absorbance/time data. It also calculates the observed rate constants.

7.2 Appendix 2

7.2.1 Requirements for the Board of Studies

The Board of Studies in Chemistry requires that each postgraduate research thesis contains an appendix listing:-

- (i) All research colloquia, seminars and lectures arranged by the Department of Chemistry during the period of the author's residence as a postgraduate student.
- (ii) Lectures organised by Durham University Chemical Society.
- (iii) Details of the Postgraduate induction course.
- (iv) All research conferences attended and papers presented by the author during the period when research for the thesis was carried out.

7.2.2 Colloquia, lectures and seminars from invited speakers

1993–1994 (August 1–July 31)

September 13 Prof. Dr. A. D. Schlüter, Freie Universität Berlin, Germany

Synthesis and Characterisation of Molecular Rods and Ribbons

September 13 Dr. K. J. Wynne, Office of Naval Research, Washington, USA

Polymer Surface Design for Minimal Adhesion

September 14 Prof. J. M. DeSimone, University of North Carolina, Chapel Hill, USA

Homogeneous and Heterogeneous Polymerisations in Environmentally Responsible Carbon Dioxide

September 28 Prof. H. Ila, North Eastern Hill University, India

Synthetic Strategies for Cyclopentanoids via Oxoketene Dithioacetals

October 4 Prof. F. J. Feher,[†] University of California, Irvine, USA

Bridging the Gap between Surfaces and Solution with Sessilquioxanes

- October 14 Dr. P. Hubberstey, University of Nottingham
**Alkali Metals: Alchemist's Nightmare, Biochemist's Puzzle and Technologist's Dream*
- October 20 Dr. P. Quayle,† University of Manchester
**Aspects of Aqueous ROMP Chemistry*
- October 21 Prof. R. Adams,† University of South Carolina, USA
**Chemistry of Metal Carbonyl Cluster Complexes: Development of Cluster Based Alkyne Hydrogenation Catalysts*
- October 27 Dr. R. A. L. Jones,† Cavendish Laboratory, Cambridge
Perambulating Polymers
- November 10 Prof. M. N. R. Ashfold,† University of Bristol
High Resolution Photofragment Translational Spectroscopy : A New Way to Watch Photodissociation
- November 17 Dr. A. Parker,† Rutherford Appleton Laboratory, Didcot
Applications of Time Resolved Resonance Raman Spectroscopy to Chemical and Biochemical Problems
- November 24 Dr. P. G. Bruce,† University of St. Andrews
Structure and Properties of Inorganic Solids and Polymers
- November 25 Dr. R. P. Wayne, University of Oxford
**The Origin and Evolution of the Atmosphere*
- December 1 Prof. M. A. McKervey,† Queen's University, Belfast
**Synthesis and Applications of Chemically Modified Calixarenes*
- December 8 Prof. O. Meth-Cohn,† University of Sunderland
**Friedel's Folly Revisited—A Super Way to Fused Pyridines*

- December 16 Prof. R. F. Hudson, University of Kent
Close Encounters of the Second Kind
- January 26 Prof. J. Evans,† University of Southampton
Shining Light on Catalysts
- February 2 Dr. A. Masters,† University of Manchester
Modelling Water Without Using Pair Potentials
- February 9 Prof. D. Young,† University of Sussex
**Chemical and Biological Studies on the Coenzyme Tetrahydrofolic Acid*
- February 16 Prof. K. H. Theopold, University of Delaware, USA
Paramagnetic Chromium Alkyls : Synthesis and Reactivity
- February 23 Prof. P. M. Maitlis,† University of Sheffield
**Across the Border: From Homogeneous to Heterogeneous Catalysis*
- March 2 Dr. C. Hunter,† University of Sheffield
**Noncovalent Interactions between Aromatic Molecules*
- March 9 Prof. F. Wilkinson, Loughborough University of Technology
Nanosecond and Picosecond Laser Flash Photolysis
- March 10 Prof. S.V. Ley, University of Cambridge
**New Methods for Organic Synthesis*
- March 25 Dr. J. Dilworth, University of Essex
Technetium and Rhenium Compounds with Applications as Imaging Agents

- April 28 Prof. R. J. Gillespie, McMaster University, Canada
The Molecular Structure of some Metal Fluorides and Oxofluorides: Apparent Exceptions to the VSEPR Model.
- May 12 Prof. D. A. Humphreys, McMaster University, Canada
**Bringing Knowledge to Life*
- May 27 Prof. J.-M. Lehn, (Musgrave Lecture), University of Strasbourg, France.
**Perspectives in Supramolecular Chemistry from molecular recognition towards self-organisation.*

1994–1995 (August 1–July 31)

- October 5 Prof. N. L. Owen, Brigham Young University, Utah, USA
**Determining Molecular Structure—the INADEQUATE NMR way*
- October 19 Prof. N. Bartlett, University of California
**Some Aspects of Ag^{II} and Ag^{III} Chemistry*
- November 2 Dr. P. G. Edwards, University of Wales, Cardiff
The Manipulation of Electronic and Structural Diversity in Metal Complexes—New Ligands
- November 3 Prof. B. F. G. Johnson, Edinburgh University
Arene–metal Clusters
- November 9 Dr. G. Hogarth, University College, London
New Vistas in Metal-imido Chemistry
- November 10 Dr. M. Block, Zeneca Pharmaceuticals, Macclesfield
**Large-scale Manufacture of ZD 1542, a Thromboxane Antagonist Synthase Inhibitor*

- November 16 Prof. M. Page, University of Huddersfield
**Four-membered Rings and β -Lactamase*
- November 23 Dr. J. M. J. Williams, University of Loughborough
**New Approaches to Asymmetric Catalysis*
- December 7 Prof. D. Briggs, ICI and University of Durham
Surface Mass Spectrometry
- January 11 Prof. P. Parsons, University of Reading
**Applications of Tandem Reactions in Organic Synthesis*
- January 18 Dr. G. Rumbles, Imperial College, London
Real or Imaginary Third Order Non-linear Optical Materials
- January 25 Dr. D. A. Roberts, Zeneca Pharmaceuticals
**The Design and Synthesis of Inhibitors of the Renin-angiotensin System*
- February 1 Dr. T. Cosgrove, Bristol University
**Polymers do it at Interfaces*
- February 8 Dr. D. O'Hare, Oxford University
Synthesis and Solid-state Properties of Poly-, Oligo- and Multi-decker Metallocenes
- February 22 Prof. E. Schaumann, University of Clausthal
**Silicon- and Sulfur-mediated Ring-opening Reactions of Epoxide*
- March 1 Dr. M. Rosseinsky, Oxford University
Fullerene Intercalation Chemistry
- March 22 Dr. M. Taylor, University of Auckland, New Zealand
Structural Methods in Main-group Chemistry

April 26 Dr. M. Schroder, University of Edinburgh
Redox-active Macrocyclic Complexes : Rings, Stacks and Liquid Crystals

May 4 Prof. A. J. Kresge, University of Toronto
The Ingold Lecture: Reactive Intermediates: Carboxylic acid Enols and Other Unstable Species

1995–1996 (August 1–July 31)

October 11 Prof. P. Lugar, Frei Univ Berlin, FRG
Low Temperature Crystallography

October 13 Prof. R. Schmutzler, Univ Braunschweig, FRG.
Calixarene–Phosphorus Chemistry: A New Dimension in Phosphorus Chemistry

October 18 Prof. A. Alexakis, Univ. Pierre et Marie Curie, Paris,
**Synthetic and Analytical Uses of Chiral Diamines*

October 25 Dr. D. Martin Davies, University of Northumbria
Chemical Reactions in Organised Systems.

November 1 Prof. W. Motherwell, University College, London
**New Reactions for Organic Synthesis*

November 3 Dr B. Langlois, University Claude Bernard-Lyon
**Radical Anionic and Pseudo-Cationic Trifluoromethylation*

November 8 Dr. D. Craig, Imperial College, London
**New Strategies for the Assembly of Heterocyclic Systems*

November 15 Dr. Andrea Sella, UCL, London
Chemistry of Lanthanides with Polypyrazoylborate Ligands

November 17 Prof. David Bergbreiter, Texas A&M, USA

Design of Smart Catalysts, Substrates and Surfaces from Simple Polymers

- November 22 Prof. I. Soutar, Lancaster University
**A Water of Glass? Luminescence Studies of Water-Soluble Polymers.*
- November 29 Prof. Dennis Tuck, University of Windsor, Ontario, Canada
New Indium Coordination Chemistry
- December 8 Prof. M. T. Reetz, Max Planck Institut, Mulheim
**Perkin Regional Meeting*
- January 10 Dr. Bill Henderson, Waikato University, NZ
Electrospray Mass Spectrometry - a new sporting technique
- January 17 Prof. J. W. Emsley, Southampton University
Liquid Crystals: More than Meets the Eye
- January 24 Dr. Alan Armstrong, Nottingham University
**Alkene Oxidation and Natural Product Synthesis*
- January 31 Dr. J. Penfold, Rutherford Appleton Laboratory,
Soft Soap and Surfaces
- February 7 Dr. R. B. Moody, Exeter University
Nitrosations, Nitrations and Oxidations with Nitrous Acid
- February 12 Dr. Paul Pringle, University of Bristol
Catalytic Self-Replication of Phosphines on Platinum(O)
- February 14 Dr. J. Rohr, University of Gottingen, FRG
Goals and Aspects of Biosynthetic Studies on Low Molecular Weight Natural Products
- February 21 Dr C. R. Pulham, University of Edinburgh

*Heavy Metal Hydrides—An Exploration of the Chemistry of Stannanes
and Plumbanes*

- February 28 Prof. E. W. Randall, Queen Mary & Westfield College
New Perspectives in NMR Imaging
- March 6 Dr. Richard Whitby, University of Southampton
*New Approaches to Chiral Catalysts: Induction of Planar and Metal
Centred Asymmetry*
- March 7 Dr. D. S. Wright, University of Cambridge
Synthetic Applications of Me₂N-p-Block Metal Reagents
- March 12 Prof. V. Balzani, University of Bologna
RSC Endowed Lecture: **Supramolecular Photochemistry*
- March 13 Prof. Dave Garner, Manchester University
Mushrooming in Chemistry
- April 30 Dr. L. D. Pettit, Chairman, IUPAC Commission of Equilibrium Data
pH-Metric Studies using Very Small Quantities of Uncertain Purity

† Invited specially for the graduate training programme.

* Attended by the author.

7.2.3 First year induction courses

This course consisted of a series of one hour lectures on the services available in the department.

Departmental Organisation	Dr. E. J. F. Ross
Safety Matters	Dr. G. M. Brooke
Electrical Appliances	Mr. B. T. Barker
Chromatography and Microanalysis	Mr. T. F. Holmes
Absorptiometry and Inorganic Analysis	Mr. R. Coult
Library Facilities	Mr. R. B. Woodward
Mass Spectroscopy	Dr. M. Jones
Nuclear Magnetic Resonance Spectroscopy	Dr. R. S. Matthews
Glass Blowing Techniques	Mr. R. Hart and Mr. G. Haswell

7.2.4 Research conferences attended

December 1993	RSC Postgraduate Symposium on Bio-organic Chemistry, Exeter University.
December 1994	RSC Postgraduate Symposium on Bio-organic Chemistry, Durham University.
December 1994	Modern Aspects of Stereochemistry, Sheffield University.
September 1995	The 11th European Symposium on Fluorine Chemistry, Bled, Slovenia.
December 1995	RSC Postgraduate Symposium on Bioorganic Chemistry, Southampton University.

7.2.5 Seminars, colloquia and poster presentations

September 1995	¥	The 11th European Symposium on Fluorine Chemistry, Bled, Slovenia.
December 1995	□	RSC Postgraduate Symposium on Bioorganic Chemistry, Southampton University.
December 1995	¥	ICI Poster Competition, University of Durham.
June 1995	□	University of Durham Graduate Colloquia.

□ Oral presentation by the author.

¥ Poster presentation by the author.

7.2.6 Papers published

Kinetic and Stereoelectronic Effects of a Fluorine Substituent on the Reaction Catalysed by an NADPH-Dependent Cyclohex-1-enylcarbonyl-CoA Reductase

C. F. Bridge, D. O'Hagan, K. A. Reynolds and K. K. Wallace, *J. Chem. Soc., Chem. Commun.*, 1995, 2329.

The Synthesis of α -Fluoroketones by 1,4-Additions of Mono-Fluorinated enamines to Michael Acceptors

C. F. Bridge and D. O'Hagan, *J. Fluorine Chem.*, 1997, **82**, 21.

References

References

- 1 G. C. Finger, *Adv. Fluorine Chem.*, 1961, **2**, 35.
- 2 M. M. Meyer and D. O'Hagan, *Chem. Br.*, 1992, 785.
- 3 D. B. Harper, J. T. G. Hamilton and D. O'Hagan, *Tetrahedron Lett.*, 1990, **31**, 7661.
- 4 (a) P. Goldman, *Science*, 1969, **164**, 90; (b) F. A. Smith, *Chem. Tech.*, 1973, 422; (c) R. Filler, *Chem. Tech.*, 1974, 752; (d) J. Mann, *Chem. Soc. Rev.*, 1987, **16**, 381; (e) Ciba Foundation Symposium, Carbon-Fluorine Compounds, *Chemistry, Biochemistry and Biological Activities*, Elsevier Biomedical, Amsterdam, 1972; (f) J. T. Welch, *Tetrahedron*, 1987, **43**, 3123; (g) R. Filler, *Organofluorine Chemicals and their Industrial Applications*, E. Harwood, Chichester, 1979; (h) M. R. C. Gerstenberger and A. Haas, *Angew. Chem., Int. Ed. Engl.*, 1981, **20**, 64; (i) I. Kumadaki, *J. Synth. Org. Chem. Jpn.*, 1984, **42**, 786; (j) K. Bannai and S. Kurozumi, *J. Synth. Org. Chem. Jpn.*, 1984, **42**, 794; (k) M. Fujita and T. Hiyama, *J. Synth. Org. Chem. Jpn.*, 1987, **45**, 664; (l) T. Kitazume and T. Yamazaki, *J. Synth. Org. Chem. Jpn.*, 1987, **45**, 888.
- 5 R. D. Chambers, *Fluorine in Organic Chemistry*, Wiley, New York, 1973; W. A. Sheppard and C. M. Sharts, *Organic Fluorine Chemistry*, Benjamin, New York, 1968.
- 6 M. Hudlicky, *Chemistry of Organic Fluorine Compounds*, 2nd edn., E. Horwood, Chichester, 1976.
- 7 H. Moissan, *Compt. Rend.*, 1886, **102**, 1543.
- 8 (a) F. Swarts, *Bull. Acad. R. Belg.*, 1892, **24**, 474; (b) F. Swarts, *Bull. Soc. Chim. Belg.*, 1896, **15**, 1134.
- 9 T. Midgley and A. L. Henne, *Ind. Eng. Chem.*, 1930, **22**, 542.
- 10 B. C. Saunders, *Some Aspects of the Chemistry and Toxic Action of Organic Compounds Containing Phosphorus and Fluorine*, Cambridge University Press, Cambridge, 1957.
- 11 J. S. C. Marais, *Onderstepoort J. Vet. Sci. Anim. Ind.*, 1943, **18**, 203.
- 12 J. Fried and E. F. Sabo, *J. Am. Chem. Soc.*, 1954, **76**, 1455.
- 13 A. L. Pogolotti, K. M. Ivanetich, H. Sommer and D. V. Santi, *Biochim. Biophys. Res. Commun.*, 1976, **70**, 972.
- 14 A. Bondi, *J. Phys. Chem.*, 1964, **68**, 441.

- 15 C. Walsh, *Adv. Enzymol.*, 1982, **55**, 197.
- 16 D. Seebach, *Angew. Chem., Int. Ed. Engl.*, 1990, **29**, 1320.
- 17 L. Dasaradhi and D. O'Hagan, *Biomed. Chem. Lett.*, 1993, **3**, 1655.
- 18 D. T. W. Chu and P. B. Fernandes, *Antimicrob. Agents Chemother.*, 1989, **33**, 131.
- 19 L. Dasaradhi, D. O'Hagan, M. C. Petty and C. Pearson, *J. Chem. Soc., Perkin Trans. 2.*, 1995, 221.
- 20 B. McDonough, P. M. MacDonald, B. D. Sykes and R. N. McElhaney, *Biochemistry*, 1983, **22**, 5097
- 21 J. T. Welch and S. Eswarakrishnan, *Fluorine in Bioorganic Chemistry*, Wiley, New York, 1990.
- 22 C. Walsh, *Tetrahedron*, 1982, **38**, 871.
- 23 E. Wang and C. Walsh, *Biochemistry*, 1978, **17**, 1313.
- 24 S. E. Chambers, E. Y. Lau and J. T. Gerig, *J. Am. Chem. Soc.*, 1994, **116**, 3603.
- 25 P. J. Card, *Carbohydr. Chem.*, 1985, **4**, 451.
- 26 A. A. E. Penglis, *Adv. Carbohydr. Chem. Biochem.*, 1981, **38**, 195.
- 27 W. E. Barnette, *Crit. Rev. Biochem.*, 1984, **15**, 201.
- 28 D. A. Dixon and B. E. Smart, *J. Phys. Chem.*, 1991, **95**, 1602.
- 29 A. Warshel, A. Papazyan and P. A. Kollman, *Science*, 1995, **269**, 102.
- 30 H. S. Rzepa, M. H. Smith and M. L. Webb, *J. Chem. Soc., Perkin Trans. 2.*, 1994, 703.
- 31 D. O'Hagan and H. S. Rzepa, *Chem. Commun.*, 1997, 645.
- 32 (a) L. Shimoni and J. P. Glusker, *Struct. Chem.*, 1994, **5**, 383; (b) J. A. K. Howard, V. J. Hoy, D. O'Hagan and G. T. Smith, *Tetrahedron*, 1996, **52**, 12 613.
- 33 M. E. Phelps, E. J. Hoffman, C. Stirlin, S. C. Huang, G. Robinson, N. McDonald, H. Schelbert and D. E. Kuhl, *J. Nucl. Med.*, 1978, **19**, 1311.
- 34 M.-C. Chapeau and P. A. Frey, *J. Org. Chem.*, 1994, **59**, 6994.
- 35 J. D. McCarter, M. J. Adams and S. G. Withers, *J. Biochem.*, 1992, **3**, 149.
- 36 P. Guédat, M. Poitras, B. Spiess, G. Guillemette and G. Schlewer, *Biorg. Med. Chem. Lett.*, 1996, **6**, 1175.
- 37 J. P. Guthrie and R. Kluger, *J. Am. Chem. Soc.*, 1993, **115**, 11569.
- 38 S. Wolfe, *Acc. Chem. Res.*, 1972, **5**, 102.
- 39 R. D. Amos, N. C. Handy, P. G. Jones, A. J. Kirby, J. K. Parker, J. M. Percy and M. D. Su, *J. Chem. Soc., Perkin Trans. 2*, 1992, 549.

- 40 (a) N. C. Craig, L. G. Piper and V. L. Wheeler, *J. Phys. Chem.*, 1971, **75**, 1453; (b) N.C. Craig and E. A. Entemann, *J. Am. Chem. Soc.*, 1961, **83**, 3047.
- 41 H. Friesen, *J. Am. Chem. Soc.*, 1980, **102**, 3978.
- 42 N. D. Epiotis, *J. Am. Chem. Soc.*, 1973, **95**, 3087.
- 43 R. Keck, H. Haas and J. Retey, *FEBS Lett.*, 1980, **114**, 287.
- 44 M. A. Marletta, P. A. Srere and C. Walsh, *Biochemistry*, 1981, **20**, 3719.
- 45 H. Lenz, W. Buckel, P. Wunderwald, G. Biedermann, V. Buschmeier, H. Eggerer, J. W. Cornforth, J. W. Redmond and R. Mallaby, *Eur. J. Biochem.*, 1971, **24**, 207.
- 46 H. Lenz and E. Eggerer, *Eur. J. Biochem.*, 1976, **65**, 237.
- 47 D. O'Hagan and H. S. Rzepa, *J. Chem.Soc., Chem. Commun.*, 1994, 2029.
- 48 (a) A. J. Kirby, *The Anomeric Effect and related Stereoelectronic Effects at Oxygen*, Springer Verlag, Berlin, 1983; (b) P. Deslongchamps, *Stereoelectronic Effects in Organic Chemistry*, Pergamon, Oxford, 1983.
- 49 H. Senderowitz, P. Aped and B. Fuchs, *Tetrahedron*, 1993, **49**, 3879.
- 50 S. David, O. Eisenstein, W. J. Hehre, L. Salem and R. Hoffmann, *J. Am. Chem. Soc.*, 1973, **95**, 3806.
- 51 G. A. Geffrey and J. H. Yates, *J. Am. Chem. Soc.*, 1979, **101**, 820.
- 52 M. Hayashi and H. Kato, *Bull. Chem. Soc. Jpn.*, 1980, **53**, 2701.
- 53 J. J. Irwin, T-K. Ha and J. Dunitz, *Helv. Chim. Acta.*, 1990, **73**, 1805.
- 54 (a) M. Chérest, H. Felkin and N. Prudent, *Tetrahedron Lett.*, 1968, 2199; (b) M. Chérest and H. Felkin, *Tetrahedron Lett.*, 1968, 2205.
- 55 N. T. Anh and O. Eisenstein, *Nouv. J. Chim.*, 1977, **1**, 61.
- 56 (a) H. B. Bürgi, J. D. Dunitz, J. M. Lehn and G. Wipff, *Tetrahedron*, 1974, **30**, 1563; (b) H. B. Bürgi, J. D. Dunitz and E. Shefter, *J. Am. Chem. Soc.*, 1973, **95**, 5065.
- 57 A. S. Cieplak, *J. Am. Chem. Soc.*, 1981, **103**, 4540.
- 58 S. S. Wong and M. N. Paddon-Row, *J. Chem. Soc., Chem. Commun.*, 1990, 456.
- 59 A. Sattler and G. Haufe, *Tetrahedron: Asymmetry*, 1995, **6**, 2841.
- 60 L. K. P. Lam, R. A. H. F. Hui and J. B. Jones, *J. Org. Chem.*, 1986, **51**, 2047.
- 61 L. Provencher, H. Wynn, J. B. Jones and A. R. Krawczyk, *Tetrahedron: Asymmetry*, 1993, **4**, 2025.
- 62 E. J. Toone, M. J. Werth and J. B. Jones, *J. Am. Chem. Soc.*, 1990, **112**, 4946.

- 63 P. Kalaritis, R. W. Regenye, J. J. Partridge and D. L. Coffen, *J. Org. Chem.*, 1990, **55**, 812.
- 64 T. Kitazume, K. Murata and T. Ikeya, *J. Fluorine Chem.*, 1986, **31**, 143.
- 65 D. O'Hagan and H. S. Rzepa, *J. Chem. Soc. Perkin Trans. 2*, 1994, 3.
- 66 C. J. Gorter and L. J. F. Broer, *Physics*, 1942, **9**, 591.
- 67 W. Kemp, *NMR in Chemistry*, Macmillan, Basingstoke, 1986.
- 68 A. Haas and M. Lieb, *Chimica*, 1985, **39**, 134.
- 69 S. Rozen and R. Filler, *Tetrahedron*, 1985, **41**, 1111.
- 70 G. A. Boswell, W. C. Ripka, R. M. Schribner and C. W. Tullock, *Org. React. (N.Y.)*, 1974, **21**, 1.
- 71 W. Dmowski, *J. Fluorine Chem.*, 1986, **32**, 255.
- 72 W. J. Middleton, *J. Org. Chem.*, 1975, **40**, 574.
- 73 M. Hudlicky, *Org. React. (N.Y.)*, 1988, **35**, 515.
- 74 R. D. Westland, R. A. Cooley, J. L. Holmes, J. S. Hong, M. H. Lin, M. L. Zwiesler and M. M. Grenan, *J. Med. Chem.*, 1973, **16**, 319.
- 75 G. A. Olah, M. Nojima and I. Kerekes, *Synthesis*, 1973, 779 and 785.
- 76 G. A. Olah, J. T. Welch, Y. D. Vankar, M. Nojima, I. Kerekes and J. A. Olah, *J. Org. Chem.*, 1979, **44**, 3872.
- 77 P. Bosch, F. Camps, E. Chamorro, V. Gasol and A. Guerrero, *Tetrahedron Lett.*, 1987, **28**, 4733.
- 78 F. Camps, E. Chamorro, V. Gasol and A. Guerrero, *J. Org. Chem.*, 1989, **54**, 4294.
- 79 G. Zubay, *Biochemistry*, 2nd edn., Maxwell Macmillan, New York, 1989, p. 264
- 80 C. J. Suckling, *Enzyme Chemistry, Impact and applications.*, Chapman and Hall, 1984.
- 81 (a) J. P. Klinman, *Biochemistry*, 1976, **15**, 2018; (b) W. W. Cleland, *Methods Enzymol.*, 1980, **64**, 104.
- 82 F. H. Westheimer, H. Fischer, E. E. Conn and B. Vennesland, *J. Am. Chem. Soc.*, 1951, **73**, 2043.
- 83 H. Fischer, E. E. Conn, B. Vennesland and F. H. Westheimer, *J. Biol. Chem.*, 1953, **202**, 687.
- 84 A. M. Gronenborn and G. M. Clore, *J. Mol. Biol.*, 1982, **157**, 155.
- 85 A. Fersht, *Enzyme Structure and Mechanism*, 2nd edn., Freeman, New York, 1985.
- 86 J. B. Jones and J. F. Beck, *Tech. Chem. (NY)*, 1976, **10**, 107.

- 87 V. Prelog, *Pure Appl. Chem.*, 1964, **9**, 119.
- 88 A. J. Irwin and J. B. Jones, *J. Am. Chem. Soc.*, 1976, **98**, 8476.
- 89 A. R. Battersby, J. Staunton and H. R. Wiltshire, *J. Chem. Soc., Perkin Trans. 1*, 1975, 1156.
- 90 A. R. Battersby, M. Nicoletti, J. Staunton and R. Vleggaar, *J. Chem. Soc., Chem. Commun.*, 1980, 43.
- 91 D. R. Walt, M. A. Findies, V. M. Rios-Mercadillo, J. Auges and G. M. Whiteside, *J. Am. Chem. Soc.*, 1984, **106**, 243.
- 92 C. H. Wong, S. L. Haynie and G. M. Whiteside, *J. Am. Chem. Soc.*, 1983, **105**, 115.
- 93 U. G. Wagner, H. Bergler, S. Fuchsbichler, F. Turnowsky, G. Hogenauer and C. Kratky, *J. Mol. Biol.*, 1994, **234**, 126.
- 94 B. Sedgwick and C. Morris, *J. Chem. Soc., Chem. Commun.*, 1980, 96.
- 95 D. O'Hagan, *The Polyketide Metabolites*, Ellis Horwood, New York, 1991.
- 96 M. Damberg, P. Russ and A. Zeeck., *Tetrahedron Lett.*, 1982, 59.
- 97 (a) M. Sugita, Y. Natori, T. Sasaki, K. Furihata, A. Shimazu, H. Seto and N. Otake, *J. Antibiot.*, 1982, **35**, 1460; (b) M. Sugita, T. Sasaki, K. Furihata, H. Seto and N. Otake, *J. Antibiot.*, 1982, **35**, 1467.
- 98 T. S. Wu, J. M. Beale and H. G. Floss, *J. Nat. Prod.*, 1987, **50**, 108.
- 99 R. Casati, J. M. Beale and H. G. Floss, *J. Am. Chem. Soc.*, 1987, **109**, 8102.
- 100 K. A. Reynolds, K. M. Fox, Z. Yuan and Y. Lam, *J. Am. Chem. Soc.*, 1991, **113**, 4339.
- 101 K. A. Reynolds, P. Wang, K. M. Fox, M. K. Speedie, Y. Lam and H. G. Floss, *J. Bacteriol.*, 1992, **174**, 3850.
- 102 K. A. Reynolds and K. K. Wallace, unpublished results.
- 103 J. D. Roberts, *Chem. Br.*, 1966, 529.
- 104 J. Cantacuzène and R. Jantzen, *Tetrahedron Lett.*, 1970, 3281.
- 105 M. Hudlicky, *J. Fluorine Chem.*, 1986, **32**, 441.
- 106 J. J. Delany and G. A. Berchtold, *J. Org. Chem.*, 1988, **53**, 3262.
- 107 C. Djerassi, *Chem. Rev.*, 1948, **43**, 271.
- 108 D. L. Anton, L. Hedstrom, S. M. Fish and R. H. Abeles, *Biochemistry*, 1983, **22**, 5903.
- 109 S. A. Pogany, G. M. Zentner and C. D. Ringeisen, *Synthesis*, 1987, 718.
- 110 G. L. Lange and J. A. Otulakowski, *J. Org. Chem.*, 1982, **47**, 5093.

- 111 M. Nakayama, S. Shinke, Y. Matsusita, S. Ohira and S. Hayashi, *Bull. Chem. Soc. Jpn.*, 1979, **52**, 184.
- 112 A. L. Gemal and J.-L. Luche, *J. Am. Chem. Soc.*, 1981, **103**, 5454.
- 113 M. E. Jung and M. A. Lyster, *J. Am. Chem. Soc.*, 1977, **99**, 968.
- 114 G. Olah and S. C. Narang, *Tetrahedron*, 1982, **38**, 2225.
- 115 D. Liotta, C. Barnum, R. Puleo, G. Zima, C. Bayer and H. S. Kezar, *J. Org. Chem.*, 1981, **46**, 2920.
- 116 J. Villieras, M. Rambaud and M. Graff, *Synth. Commun.*, 1986, **16**, 149.
- 117 M. Lai, D. Li, E. Oh and H. Liu, *J. Am. Chem. Soc.*, 1993, **115**, 1620.
- 118 G. Ottolina, S. Riva, G. Carrea, B. Daneli and B. F. Buckman, *Biochim. Biophys. Acta*, 1989, **998**, 173.
- 119 J. P. Klinman, *J. Biol. Chem.*, 1972, **247**, 7977.
- 120 K. E. Stremmer and C. D. Poulter, *J. Am. Chem. Soc.*, 1987, **109**, 5542.
- 121 (a) K. Dalziel, *J. Biol. Chem.*, 1963, **263**, 2850; (b) C. C. Wratten and W. W. Cleland, *Biochemistry*, 1963, **2**, 935.
- 122 E. P. Abraham, E. Chain, W. Baker and R. Robinson, *Pen. Report No. 103*, 1943.
- 123 D. C. Hodgkinson, C. W. Bunn, B. W. Rogers-Low and A. Turner-Jones, in *The Chemistry of Penicillin*, Princeton University Press, New Jersey, 1949.
- 124 J. C. Sheehan, K. R. Hénerly-Logan and D. A. Johnson, *J. Am. Chem. Soc.*, 1953, **75**, 3292.
- 125 R. Nagarajan, L. D. Boeck, M. Gorman, R. L. Hamill, C. E. Higgins, M. M. Hoehn, W. M. Stark and J. G. Whitney, *J. Am. Chem. Soc.*, 1971, **93**, 2308.
- 126 M. I. Page, *Adv. Phys. Org. Chem.*, 1987, **23**, 165.
- 127 B. G. Spratt, *Philos. Trans. R. Soc. London*, 1980, **289**, 27.
- 128 J. R. Knowles, *Acc. Chem. Res.*, 1985, **18**, 97.
- 129 A. Tomasz, *Annu. Rev. Microbiol.*, 1979, **33**, 113.
- 130 D. J. Tipper and J. L. Strominger, *Proc. Natl. Acad. Sci. USA*, 1965, **54**, 1133.
- 131 R. R. Yocum, H. Amanuma, T. A. O'Brien, D. J. Waxman and J. L. Strominger, *J. Bacteriol.*, 1982, **149**, 1150.
- 132 J.-M. Frere, J.-M. Ghuysen, J. Degelaen, A. Loffet and H. R. Perkins, *Nature (London)*, 1975, **258**, 168.
- 133 F. R. Batchelor, F. P. Doyle, J. H. C. Nayler and G. N. Robinson, *Nature (London)*, 1959, **183**, 257.

- 134 J. C. Sheehan and K. R. Hénerly-Logan, *J. Am. Chem. Soc.*, 1959, **81**, 5838.
- 135 A. G. Brown, D. Butterworth, M. Cole, G. Hanscomb, J. D. Hood, C. Reading and G. N. Robinson, *J. Antibiot.*, 1976, **29**, 668.
- 136 (a) J. F. Fisher, R. L. Charnas and J. R. Knowles, *Biochemistry*, 1978, **17**, 2180; (b) R. L. Charnas, J. F. Fisher and J. R. Knowles, *Biochemistry*, 1978, **17**, 2185.
- 137 R. F. Pratt and M. J. Loosemore, *Proc. Natl. Acad. Sci. USA.*, 1978, **75**, 4145.
- 138 (a) M. J. Loosemore and R. F. Pratt, *J. Org. Chem.*, 1978, **43**, 3611; (b) M. J. Loosemore, S. A. Cohen and R. F. Pratt, *Biochemistry*, 1980, **19**, 3990; (c) S. A. Cohen and R. F. Pratt, *Biochemistry*, 1980, **19**, 3996.
- 139 J. F. Fisher, J. G. Belasco, R. L. Charnas, S. Khosla and J. R. Knowles, *Philos. Trans. R. Soc. London, Ser. B*, 1980, **289**, 309.
- 140 R. F. Pratt and D. J. Cahn, *J. Am. Chem. Soc.*, 1988, **110**, 5096.
- 141 G. O. Danelon and O. A. Mascaretti, *J. Fluorine Chem.*, 1992, **56**, 109.
- 142 K. Miyashita, I. Massova, P. Taibi and S. Mobashery, *J. Am. Chem. Soc.*, 1995, **117**, 11055.
- 143 L. Maveyraud, I. Massova, C. Birck, K. Miyashita, J-P. Samama and S. Mobashery, *J. Am. Chem. Soc.*, 1996, **118**, 7435.
- 144 J. J. Morris and M. I. Page, *J. Chem. Soc., Perkin Trans. 2*, 1980, 212.
- 145 W. A. Slusarchyk, H. E. Applegate, P. Funke, W. Koster, M. S. Puar, M. Young and J. E. Dolfini, *J. Org. Chem.*, 1973, **38**, 943.
- 146 W. A. Spitzer, T. Goodson, M. O. Chaney and N. D. Jones, *Tetrahedron Lett.*, 1974, 4311.
- 147 (a) M. S. Kellog and E. S. Hamanka (Pfizer Inc.), *Ger. Offen*, 3 008 316, 1980 (*Chem. Abstr.*, 1981, **94**, 84113r); (b) M. S. Kellog and E. S. Hamanka (Pfizer Inc.), *US Pat.* 4 397 783, 1983 (*Chem. Abstr.*, 1983, **99**, 175473c).
- 148 W. V. Daehne, E. Frederiksen, E. Gundersen, F. Lund, P. Morch, H. J. Petersen, K. Roholt, L. Tybring and W. O. Godtfredsen, *J. Med. Chem.*, 1970, **13**, 607.
- 149 J. S. Wiering and H. Wynberg, *J. Org. Chem.*, 1976, **41**, 1574.
- 150 J. C. Sheehan, Y. S. Lo, J. Lölliger and C.C. Podewell, *J. Org. Chem.*, 1974, **39**, 1444.
- 151 S. Torri, H. Tanaka, M. Taniguchi and Y. Kamayama, *J. Org. Chem.*, 1991, **56**, 3633.
- 152 E. G. Mata and O. A. Mascaretti, *Tetrahedron Lett.*, 1991, **32**, 4239.

- 153 C. J. Salomon, E. G. Mata and O. A. Mascaretti, *J. Org. Chem.*, 1994, **59**, 7259.
- 154 J. E. Baldwin, J. E. Cobb and L. N. Sheppard, *Tetrahedron*, 1987, **52**, 915.
- 155 G. O. Danelon, M. Laborde, O. A. Mascaretti, S. B. Boggio and O. A. Roveri, *Bioorg. Med. Chem.*, 1993, **1**, 447.
- 156 A. A. Patchett, E. F. Rogers and W. J. Leanza, *Belg. Patent*, 634 374, 1963 (*Chem. Abstr.*, 1964, **61**, 1869c).
- 157 D. G. Farnum, *J. Org. Chem.*, 1963, **28**, 870.
- 158 C. G. Overberger and J.-P. Anselme, *J. Org. Chem.*, 1963, **28**, 592.
- 159 T. Tsuji, T. Kataoka, M. Yoshioka, K. Sendo, Y. Nishitani, S. Hirai, T. Maeda and W. Nagata, *Tetrahedron Lett.*, 1979, 2793.
- 160 E. G. Mata, E. L. Setti and O. A. Mascaretti, *J. Org. Chem.*, 1990, **55**, 3674.
- 161 F. Camps, E. Chamorro, V. Gasol and A. Guerreo, *J. Org. Chem.*, 1989, **54**, 4294.
- 162 E. G. Mata and O. A. Mascaretti, *Tetrahedron Lett.*, 1989, **30**, 3905.
- 163 W. T. Reichle, *Inorg. Chem.*, 1966, **5**, 87.
- 164 A. B. Chopa, A. E. Zúñiga and J. C. Podestá, *J. Chem. Res. (S)*, 1989, 234.
- 165 G. Fischer, *Nat. Prod. Rep.*, 1988, 465.
- 166 J. O. Westerik and R. Wolfenden, *J. Biol. Chem.* 1971, **247**, 8195.
- 167 R. C. Thompson, *Biochemistry*, 1973, **12**, 47.
- 168 G. Lowe and D. Nurse, *J. Chem. Soc., Chem. Commun.*, 1977, 815.
- 169 D. O. Shah, K. Lai and D. G. Gorenstein, *J. Am. Chem. Soc.*, 1984, **106**, 4272.
- 170 R. Wolfenden, *Annu. Rev. Biophys. Bioeng.*, 1976, **5**, 271.
- 171 R. E. Galardy and Z. P. Kortylewicz, *Biochemistry*, 1984, **23**, 2083.
- 172 M. H. Gelb, J. P. Svaren and R. H. Abeles, *Biochemistry*, 1985, **24**, 1813.
- 173 B. Imperiali and R. H. Abeles, *Biochemistry*, 1986, **25**, 3760.
- 174 C. Walsh, *Adv. Enzymol.*, 1982, **55**, 197.
- 175 R. H. Abeles and T. A. Alston, *J. Biol. Chem.*, 1990, **256**, 16705.
- 176 D. Schirlin, S. Baltzer, J. M. Altenburger, C. Tarnus and J. M. Remy, *Tetrahedron*, 1996, **52**, 305.
- 177 B. Imperiali and R. H. Abeles, *Biochemistry*, 1987, **26**, 4474.
- 178 U. Brodbeck, K. Schweikert, R. Gentinetta and M. Rottenberg, *Biochem. Biophys. Acta*, 1980, **199**, 473.
- 179 S. Rozen and R. Filler, *Tetrahedron*, 1985, **41**, 1111.
- 180 G. A. Boswell, A. L. Johnson and J. P. McDevitt, *J. Org. Chem.*, 1971, **36**, 575.

- 181 D. J. Costa, N. E. Boutin and J. G. Riess, *Tetrahedron*, 1974, **30**, 3793.
- 182 Y. Osawa and N. Neeman, *J. Org. Chem.*, 1967, **32**, 3055.
- 183 S. Rozen and O. Lerman, *J. Org. Chem.*, 1983, **48**, 724.
- 184 S. T. Purrington and W. A. Jones, *J. Org. Chem.*, 1983, **48**, 761.
- 185 W. E. Barnette, *J. Am. Chem. Soc.*, 1984, **106**, 452.
- 186 E. Differding and R. W. Lang, *Tetrahedron Lett.*, 1988, **29**, 6087.
- 187 S. T. Purrington, N. V. Lazaradis and C. L. Bumgardner, *Tetrahedron Lett.*, 1986, **27**, 2715.
- 188 R. E. Banks, N. J. Lawrence and A. L. Popplewell, *J. Chem. Soc., Chem. Commun.*, 1994, 343.
- 189 R. D. Chambers, M. P. Greenhall and J. Hutchinson, *Tetrahedron*, 1996, **52**, 1.
- 190 J. T. Welch and K. W. Seper, *Tetrahedron Lett.*, 1984, 5247.
- 191 K. N. Houk, R. W. Stozier, N. G. Rondon, R. R. Fraser and N. Chaqui-Offermanns, *J. Am. Chem. Soc.*, 1963, **85**, 207.
- 192 J. T. Welch and S. Eswarakrishnan, *Mol. Struct. Energ.*, 1988, **8**, 123.
- 193 D. Michel and M. Sclosser, *Tetrahedron*, 1996, **52**, 2429.
- 194 C. F. Bridge and D. O'Hagan, *J. Fluorine Chem.*, in the press.
- 195 P. W. Hickmott, *Tetrahedron*, 1982, **38**, 1975.
- 196 G. Stork, R. Terrell and J. Szmuszkovicz, *J. Am. Chem. Soc.*, 1954, **76**, 2029.
- 197 G. Stork, A. Brizzolara, H. Landesman, J. Szmuszkovicz and R. Terrell, *J. Am. Chem. Soc.*, 1963, **85**, 207.
- 198 K. Taguchi and F. H. Westheimer, *J. Org. Chem.*, 1971, **36**, 1570.
- 199 H. Uno, K. Samamoto, F. Semba and H. Suzuki, *Bull. Chem. Soc. Jpn.*, 1992, **65**, 210.
- 200 H. Uno, K. Samamoto and H. Suzuki, *Bull. Chem. Soc. Jpn.*, 1992, **65**, 218.
- 201 S. Yamada, K. Hiroi and K. Achiwa, *Tetrahedron Lett.*, 1969, 4233.
- 202 J. K. Whitesell and S. W. Felman, *J. Org. Chem.*, 1977, **42**, 1663.
- 203 D. Bailey, D. O'Hagan and M. Tavasli, *Tetrahedron: Asymmetry*, 1997, **8**, 149.
- 204 G. Zubay, in *Biochemistry*, 2nd edn., Macmillan, New York, 1988, p. 475.
- 205 K. M. Draths, D. L. Pompliano, D. L. Conley, J. W. Frost, A. Berry, G. L. Disbrow, R. J. Staversky and J. C. Lievens, *J. Am. Chem. Soc.*, 1992, **114**, 3956.
- 206 E. J. Toone, E. S. Simon, M. D. Bednarski and G. M. Whitesides, *Tetrahedron*, 1989, **45**, 5365.

- 207 C. Demuynck, J. Bolte, L. Hecquet and V. Dalmas, *Tetrahedron Lett.*, 1991, **32**, 5085.
- 208 J. Bolte, C. Demuynck and H. Samaki, *Tetrahedron Lett.*, 1987, **28**, 5525.
- 209 G. R. Hobbs, M. D. Lilly, N. J. Turner, J. M. Ward, A. J. Willets and J. M. Woodley, *J. Chem. Soc. Perkin Trans. 1*, 1993, 165.
- 210 N. C. J. E. Chesters, D. O'Hagan and R. J. Robins, *J. Chem. Soc. Perkin Trans. 1*, 1994, 1159.
- 211 R. Engel, *Chem. Rev.*, 1977, **77**, 349.
- 212 R. Adams and R. Harrison, *J. Biochem.*, 1974, **141**, 729.
- 213 G. M. Blackburn and D. E. Kent, *J. Chem. Soc., Perkin Trans. 1*, 1986, 913.
- 214 G. R. Thatcher and A. S. Campbell, *J. Org. Chem.*, 1993, **58**, 2272.
- 215 J. Nieschalk, A. S. Batsanov, D. O'Hagan and J. A. K. Howard, *Tetrahedron*, 1996, **52**, 165.
- 216 R. D. Chambers, R. Jaouhari and D. O'Hagan, *J. Chem. Soc., Chem. Commun.*, 1988, 1169.
- 217 R. D. Chambers, R. Jaouhari and D. O'Hagan, *Tetrahedron*, 1989, **45**, 5101.
- 218 G. L. Lemièrè, *Enzymes as Catalysts in Organic Synthesis*, ed. M. P. Schneider, Reidel, 1986, pp. 19–34.
- 219 S. Rogers, Ph.D. Thesis, University of Durham, 1994.
- 220 E. G. Mata, E. L. Setti and O. A. Mascaretti, *J. Org. Chem.*, 1990, **55**, 3674.
- 221 E. G. Brain, I. McMillan, J. H. C. Naylor, R. Southgate and P. Tolliday, *J. Chem. Soc., Perkin Trans. 1*, 1975, 562.
- 222 T. Eguchi, T. Aoyama and K. Katsumi, *Tetrahedron Lett.*, 1992, **33**, 5545.
- 223 D. D. Tanner, J. J. Chen, L. Chen and C. Luelo, *J. Am. Chem. Soc.*, 1991, **113**, 8074.
- 224 D. Delauney and M. L. Corre, *J. Chem. Soc., Perkin Trans. 1*, 1994, 3041.
- 225 E. Elkik and H. Assadi-Far, *C.R. Hebd. Seances Acad. Sci., Ser. C*, 1966, **262**, 763.

